Bureau of Mines
Report of Investigations 5225

FUNDAMENTAL FLASHBACK, BLOWOFF, AND YELLOW-TIP LIMITS OF FUEL GAS-AIR MIXTURES

BY JOSEPH GRUMER, MARGARET E. HARRIS, AND VALERIA R. ROWE

United States Department of the Interior — July 1956

FUNDAMENTAL FLASHBACK, BLOWOFF, AND YELLOW-TIP LIMITS OF FUEL GAS-AIR MIXTURES

BY JOSEPH GRUMER, MARGARET E. HARRIS,
AND VALERIA R. ROWE

* * * * * * * * * **Report of Investigations 5225**

UNITED STATES DEPARTMENT OF THE INTERIOR
Fred A. Seaton, Secretary
BUREAU OF MINES
Thos. H. Miller, Acting Director

Work on manuscript completed December 1955. The Bureau of Mines will welcome reprinting of this paper, provided the following footnote acknowledgment is made: "Reprinted from Bureau of Mines Report of Investigations 5225."

The work on which this report is based was done under a cooperative agreement between the Bureau of Mines, United States Department of the Interior, and the American Gas Association.

July 1956

FUNDAMENTAL FLASHBACK, BLOWOFF, AND YELLOW-TIP LIMITS OF FUEL GAS-AIR MIXTURES

by

Joseph Grumer,[1] Margaret E. Harris,[2] and Valeria R. Rowe[3]

CONTENTS

Page

Introduction and summary 1
Acknowledgments 2
Equipment and experimental procedure 2
Chapter I. - Flashback, blowoff, and flame-stability diagrams ... 3
A. Flashback and blowoff 3
B. Explanation of flame-stability diagrams 7
C. Some uses of flame-stability diagrams 11
D. Limitations of flame-stability diagrams 16
Chapter II. - Flame-stability data of fuels, calculation of flame-stability diagrams 22
A. Flame-stability diagrams of natural gases, liquid petroleum gases, and single-component fuels 22
B. Flame-stability diagrams of two-component fuels 24
C. Flame-stability diagrams of multicomponent fuels 47
1. Coke-oven gases 48
2. Oil gases 50
3. High-ethylene fuels containing hydrogen (more than about 50 percent ethylene) 56
4. Fuels containing nitrogen and carbon dioxide 56
Chapter III. - Yellow tipping and constant yellow-tip limits 59
Theory 60
Further consideration of the constant yellow-tip limit 63
Chapter IV. - Calculation of nonconstant yellow-tip limits of fuel gases 66

1/ Physical chemist; chief, Flame Research Section, Division of Explosives Technology, Bureau of Mines, Pittsburgh, Pa.
2/ Physical chemist, Flame Research Section, Division of Explosives Technology, Bureau of Mines, Pittsburgh, Pa.
3/ Chemist, Flame Research Section, Division of Explosives Technology, Bureau of Mines, Pittsburgh, Pa.

CONTENTS (Con.)

Page

Chapter V. - Flashback, blowoff, and yellow tipping on burners with short ports (drill ports) or noncircular channels (square, rectangular, and triangular channels) 90
A. Flashback and blowoff 90
Application of equation 13 to Poiseuille flow 92
Application of equation 13 to turbulent flow 92
Application of equation 13 to sharp-edged short ports (drill ports) 92
Application of equation 13 to noncircular channels with steady laminar flow 94
B. Constant and nonconstant yellow-tip limits 98
1. Sharp-edged short ports 98
2. Noncircular channels 98
3. Multiport burners 100
Chapter VI. - Temperature dependence of flame-stability and yellow-tip limits 100
Flashback 102
Blowoff 105
Yellow tipping 113
Closing comments 114
Definitions and nomenclature 115
Definitions 115
Nomenclature 117
Special bibliography of Bureau of Mines publications on fundamental combustion characteristics of fuel gases 118
Appendix. - Tables 120
Bibliography 197

TEXT TABLES

1. Converting the flame-stability diagram of methane to limit curves for a 0.25-inch port burner with steady laminar flow 16
2. Flashback and blowoff gradients for a two-component fuel, taken from composite flame-stability diagrams 47
3a. Calculation of flashback curve for fuel No. 43 by linear mixture rule 49
3b. Calculation of blowoff curve for fuel No. 43 by linear mixture rule.. 49
4a. Calculation of flashback curve for fuel No. 55 by linear mixture rule 53
4b. Calculation of blowoff curve for fuel No. 55 by linear mixture rule 53
5. Constant yellow-tip limits for single-component fuels 63
6. Comparison of experimental and calculated values of F_c for two-component and multicomponent fuels 65
7. Curves of constant yellow-tip fractions for fuel No. 68 80
8. Sample calculations of yellow-tip curves for fuel No. 71 ... 81
9. Sample calculations of yellow-tip curves for fuel No. 57 ... 83
10. Sample calculations of yellow-tip curves in units of L and M 84

TEXT TABLES (Con.)

Page

11. Calculation of ignition temperatures versus initial temperatures for methane-air flames 112
12. Calculation of ignition temperatures versus initial temperatures for propane-air flames 113

APPENDIX TABLES

1a. Critical boundary velocity gradients for flashback of single-component fuels 120
1b. Critical boundary velocity gradients for blowoff of single-component fuels 121
2a. Critical boundary velocity gradients for flashback of two-component fuels:
Methane-hydrogen mixtures 123
Carbon monoxide-hydrogen mixtures 124
Methane-carbon monoxide mixtures 126
Propane-hydrogen mixtures 127
Ethylene-hydrogen mixtures 128
Nitrogen-hydrogen mixtures 129
Other mixtures 129
2b. Critical boundary velocity gradients for blowoff of two-component fuels:
Methane-hydrogen mixtures 130
Carbon monoxide-hydrogen mixtures 131
Methane-carbon monoxide mixtures 132
Propane-hydrogen mixtures 133
Ethylene-hydrogen mixtures 134
Nitrogen-hydrogen mixtures 135
Other mixtures 135
3a. Critical boundary velocity gradients for flashback of multicomponent fuels:
Mixtures of coke-oven-gas type 136
Mixtures of oil-gas type 138
Other mixtures 138
3b. Critical boundary velocity gradients for blowoff of multicomponent fuels:
Mixtures of coke-oven-gas type 140
Mixtures of oil-gas type 142
Other mixtures 143
4. Calculation of flame-stability diagram by linear mixture rule:
Two-component mixture 145
Mixture of coke-oven-gas type 148
Mixture of oil-gas type 160
Other mixture 163
5. Yellow-tip limits of fuel gases; methane-propane group - ethylene 173
6. Yellow-tip limits of fuel gases; methane-ethylene 180
7. Yellow-tip limits of fuel gases; other fuels 182
8a. Calculation of coefficients of friction, λ , for sharp-edged short ports 185
8b. Critical boundary velocity gradients using λ for sharp-edged short ports 187

APPENDIX TABLES (Con.)

Page

9. Critical boundary velocity gradients for long cylindrical tubes at 348° and 423° K. 188
10a. Calculation of coefficients of friction, λ , for long square channels 189
10b. Critical boundary velocity gradients using λ for long square channels 190
11a. Calculation of coefficients of friction, λ , for long rectangular channels 191
11b. Critical boundary velocity gradients using λ for long rectangular channels 191
12a. Calculation of coefficients of friction, λ , for long triangular channels 192
12b. Critical boundary velocity gradients using λ for long triangular channels 192
13. Critical boundary velocity gradients for sharp-edged short ports at various initial temperatures 193
14. Yellow-tip limits for propylene at various initial temperatures 196

ILLUSTRATIONS

Fig.

1. Diagrammatic description of burning velocity, stream velocity, and flame position near flashback limit 5
2. Diagrammatic description of burning velocity, stream velocity, and flame position near blowoff limit 5
3. Parabolic velocity profile of a stream at a burner port .. 8
4. Critical flows for flashback of natural gas-air flames ... 8
5. Critical flows for blowoff of natural gas-air flames 9
6. Critical flows in gas-industry units for flashback of natural gas-air flames 9
7. Critical boundary velocity gradients for flashback and blowoff of natural gas-air flames 10
8. Critical boundary velocity gradients for flashback and blowoff of paraffin-air mixtures 10
9. Flame-stability diagrams for paraffin-air mixtures 12
10. Average flame-stability diagram for paraffin-air mixtures. 12
11. Use of average flame-stability diagram for paraffin-air mixtures to show performance of burners 15
12. Gas-industry type of flashback and blowoff limit curves for methane for 0.25-inch port with steady laminar flow. 15
13. Effect of nature of surrounding atmosphere on blowoff of natural gas-air flames 18
14. Critical boundary velocity gradients for flashback of methane-air and methane-oxygen mixtures 18
15. Critical boundary velocity gradients for flashback of propane-air and propane-oxygen mixtures 19
16. Critical boundary velocity gradients for blowoff of methane-air and methane-oxygen mixtures 19

ILLUSTRATIONS (Con.)

Fig. Page

17. Critical boundary velocity gradients for blowoff of propane-air and propane-oxygen mixtures 20
18. Quenching distances of tubes, slots, and plates for mixtures of several fuels with air 20
19. Flame-stability diagram for fuel No. 1 (91.5% CH_4, 5.2% C_2H_6, 1.3% C_3H_8, 0.2% C_3H_6, 0.2% C_4H_{10}, 0.1% C_4H_8, 0.9% CO_2, 0.6% N_2) 23
20. Flame-stability diagram for fuel No. 2 (100% CH_4) 25
21. Flame-stability diagram for fuel No. 3 (98.6% C_3H_8, 1.4% C_3H_6) 26
22. Flame-stability diagram for fuel No. 4 (99.7% C_2H_4, 0.2% C_4H_8, 0.1% C_3H_6) 27
23. Flame-stability diagram for fuel No. 5 (99.2% C_3H_6, 0.4% C_2H_6, 0.4% C_3H_8) 28
24. Flame-stability diagram for fuel No. 6 (100% C_6H_6) 29
25. Flame-stability diagram for fuel No. 7 (99.7% H_2, 0.3% O_2) 30
26. Flame-stability diagram for fuel No. 8 (88.9% CO, 9.7% CH_4, 1.3% H_2, 0.1% CO_2) 31
27. Flame-stability diagram for fuel No. 41 (79.4% CH_4, 20.6% C_2H_4); comparison of calculated curves and experimental points 32
28. Critical boundary velocity gradients for flashback of methane-hydrogen fuels 34
29. Critical boundary velocity gradients for blowoff of methane-hydrogen fuels 35
30. Critical boundary velocity gradients for flashback of carbon monoxide-hydrogen fuels 36
31. Critical boundary velocity gradients for blowoff of carbon monoxide-hydrogen fuels 37
32. Critical boundary velocity gradients for flashback of methane-carbon monoxide fuels 38
33. Critical boundary velocity gradients for blowoff of methane-carbon monoxide fuels 39
34. Critical boundary velocity gradients for flashback of propane-hydrogen fuels 40
35. Critical boundary velocity gradients for blowoff of propane-hydrogen fuels 41
36. Critical boundary velocity gradients for flashback of ethylene-hydrogen fuels 42
37. Critical boundary velocity gradients for blowoff of ethylene-hydrogen fuels 43
38. Critical boundary velocity gradients for flashback of nitrogen-hydrogen fuels 44
39. Critical boundary velocity gradients for blowoff of nitrogen-hydrogen fuels 45
40. Flame-stability diagram for 83.3% CO, 16.7% H_2 46

ILLUSTRATIONS (Con.)

Fig. Page

41. Flame-stability diagram for fuel No. 43 (58.4% H_2, 26.3% CH_4, 10.6% CO, 4.6% N_2, 0.1% CO_2); comparison of calculated curves and experimental points 51
42. Flame-stability diagram for fuel No. 65 (36.4% H_2, 22.6% CO, 13.3% CH_4, 7.2% C_2H_6, 5.8% C_2H_4, 1.9% C_3H_8, 0.1% C_3H_6, 9.8% N_2, 2.9% CO_2); comparison of calculated curves and experimental points 52
43. Flame-stability diagram for fuel No. 55 (37.4% CH_4, 33.4% C_2H_4, 15.2% H_2, 14.0% N_2); comparison of calculated curves and experimental points 54
44. Flame-stability diagram for fuel No. 67 (37.5% CH_4, 20.4% C_2H_4, 17.5% H_2, 3.9% CO, 13.3% N_2, 7.4% CO_2); comparison of calculated curves and experimental points 55
45. Flame-stability diagram for fuel No. 63 (56.5% C_2H_4, 15.8% H_2, 13.8% CH_4, 0.1% C_3H_6, 13.8% N_2); comparison of calculated curves and experimental points 57
46. Flame-stability diagram for fuel No. 58 (62.5% CH_4, 22.2% H_2, 15.3% N_2); comparison of calculated curves and experimental points 58
47. A schematic yellow-tip limit flame for the critical port radius, R* 61
48. Yellow-tipped aerated flames 64
49. Flame-characteristics diagram for fuel No. 2 (100% CH_4) .. 67
50. Flame-characteristics diagram for fuel No. 68 (89.5% CH_4, 6.7% C_2H_6, 2.7% C_3H_8, 0.4% C_3H_6, 0.4% C_4H_{10}, 0.3% CO_2) . 68
51. Flame-characteristics diagram for fuel No. 3 (98.6% C_3H_8, 1.4% C_3H_6) 69
52. Yellow-tip fractions for methane-propane group-ethylene fuels for g_y = 300 71
53. Yellow-tip fractions for methane-propane group-ethylene fuels for g_y = 800 72
54. Yellow-tip fractions for methane-propane group-ethylene fuels for g_y = 3,000 73
55. Yellow-tip fractions for methane-propane group-ethylene fuels for g_y = 10,000 74
56. Yellow-tip fractions for methane-propane group-ethylene fuels for g_y = 20,000 and above 75
57. Yellow-tip fractions for methane-ethylene fuels for g_y = 300 76
58. Yellow-tip fractions for methane-ethylene fuels for g_y = 800 and 3,000 77
59. Yellow-tip fractions for methane-ethylene fuels for g_y = 10,000, 20,000 and above 78

ILLUSTRATIONS (Con.)

Fig. Page

60. Curves of constant yellow-tip fractions for fuel No. 68 (89.5% CH_4, 6.7% C_2H_6, 2.7% C_3H_8, 0.4% C_3H_6, 0.4% C_4H_{10}, 0.3% CO_2) 79
61. Flame-characteristics diagram for fuel No. 71 (62.1% CH_4, 35.5% C_3H_8, 2.4% C_2H_6); comparison of experimental points and calculated curves 82
62. Flame-characteristics diagram for fuel No. 57 (32.1% CH_4, 28.4% C_2H_4, 12.5% H_2, 27.0% N_2); comparison of experimental points and calculated curves 82
63. A, Yellow-tip limit curves for burners in free air; natural gas; B, comparison of predicted yellow-tip limits for burners in free air and observed limits on multiports; natural gas 85
64. Flame-characteristics diagram for fuel No. 6 (100% C_6H_6) .. 87
65. Yellow-tip limits for fuel No. 84 (100% C_7H_8).......... 87
66. Yellow-tip limits for fuel No. 85 (97.3% C_2H_2, 2.7% CH_3COCH_3) 88
67. Yellow-tip limits for fuel No. 86 (84.2% CH_4, 7.6% C_2H_2, 5.3% C_2H_6, 1.6% C_3H_6, 0.6% C_4H_{10}, 0.3% C_3H_6, 0.4% CO_2) .. 88
68. Flame-characteristics diagram for fuel No. 87 (91.6% CH_4, 4.0% C_7H_8, 3.2% C_2H_6, 0.7% C_3H_8, 0.2% C_3H_6, 0.3% CO_2) ... 89
69. Flame-stability diagram for fuel No. 17 (79.3% CO, 19.7% H_2, 0.6% N_2, 0.3% CO_2, 0.1% O_2) 93
70. Coefficients of friction for sharp-edged short ports (data obtained with a CO-H_2 fuel with port depths of 0.635 and 0.318 cm.) 93
71. Flame-stability diagram for fuel No. 17 (79.7% CO, 20.1% H_2, 0.2% CO_2); comparison of points for sharp-edged short ports and curves for long cylindrical tubes 95
72. Flame-stability diagram for fuel No. 2 (100% CH_4) at 348° and 423° K. for long cylindrical tubes 95
73. Top and front views of methane flames near flashback on noncircular channels 97
74. A, Comparison of experimental and calculated velocity pressures; square channel, 1.068 x 1.075 cm.; B, effect of flame on flow profile in square channel, 1.068 x 1.075 cm.; theoretical flame pressure, 0.010 cm. 97
75. λ coefficients for several flow profiles (equations 13a-h). 99
76. Venturi burner with exchangeable sharp-edged short hot ports 101
77. Flame-stability diagram for fuel No. 2 (100% CH_4) at 473° K. for sharp-edged short ports 101
78. Critical boundary velocity gradients for flashback of methane-air flames at various initial temperatures 103
79. Critical boundary velocity gradients for blowoff of methane-air flames at various initial temperatures 103

ILLUSTRATIONS (Con.)

Fig.		Page
80.	Critical boundary velocity gradients for blowoff of propane-air flames at various initial temperatures	104
81.	Flame temperatures for methane-air	107
82.	Flame temperatures for propane-air	107
83.	Schematic temperature profiles for a flame	109
84.	Comparison of experimental points and calculated curves for flashback of methane-air flames at various initial temperatures	110
85.	Comparison of experimental and calculated curves for blowoff of methane-air flames at various initial temperatures	110
86.	Comparison of experimental and calculated curves for blowoff of propane-air flames at various initial temperatures	111
87.	A, Influence of initial temperature on yellow tipping of propylene; B, ambient air temperatures above a 7.95-cm. O.D. plate, 0.346-cm. I.D. drill port; no flame	111

INTRODUCTION AND SUMMARY

About a century ago Bunsen and his associates invented the famous burner that bears his name and was to become the ancestor of today's gas appliances. Over the years, Bunsen's invention became the starting point of a highly developed, practical technology that culminated in the gas industry as we now know it. However, it did not occur to the early workers to investigate the scientific potentialities of the new device, and as a result the science of gas-burner performance did not keep pace with the growing industry. It was with the objective of closing the rapidly widening gap between science and technology that the present research was undertaken Its immediate purpose was to provide basic information on the combustion characteristics of fuel gases, in particular as they affect flashback, blowoff, and yellow tipping.

Information obtained in the present research and contained within this report consists of the following:

(1) Fundamental flashback and blowoff characteristics have been determined, it is believed, for all fuel-gas mixtures in which the gas industry may be interested. These are critical boundary velocity gradients for flames in free air, on burners with ports at room temperature and pressure. Burner aeration is characterized by the parameter, fraction of stoichiometric. These basic limits are explained, values are presented, and calculation procedure is given for deriving corresponding values of port loading and percent primary air (chs. I and II).

(2) Fundamental yellow-tipping characteristics of fuel gases have been discovered and measured for burners in free air, with ports at room temperature and pressure. These constant yellow-tip limits, which occur on rather large ports only, are the foundation of a graphical method of correlating yellow tipping over the range of practical port diameters (chs. III and IV).

(3) The influence of different port shapes, depths, and temperatures on the basic flashback, blowoff, and yellow-tip characteristics of fuel gases has been studied to establish the fundamental relationships and to provide needed data for some fuels (chs. V and VI).

The above is the extent of the subject matter of this report. However, the research has brought forth other matters that are reserved for a subsequent writing. Information has been obtained on the nature of flashback on turndown. Also a method of predicting exchangeability of fuel gases has been developed. Most of this information has appeared in the journal articles that are listed in the special bibliography at the close of this report (Bureau of Mines Publications on Fundamental Combustion Characteristics of Fuel Gases). The method of predicting exchangeability that is based on theory pertaining to upright ports in free air at room temperature and pressure appears to be applicable to burners operating in homes and industry.

However, it is planned to investigate the effect of nonideal conditions on the method before it is recommended for widespread use. To date, the method has been successful in every trial in which it has been tested against the known experience of gas utilities.

Although the fundamental studies of many aspects of burner and appliance design are still lacking, presentation of the current material at this date offers advantages to the gas industry and correspondingly to the public in that it is a compilation of generally applicable data that may become a part of the academic training of future gas engineers and that can stimulate and guide further applied research.

ACKNOWLEDGMENTS

The authors are grateful to their colleagues in the Bureau of Mines and to the members of the American Gas Association Supervising Committee for Project PDC-3-GU, the Domestic Gas Research Committee, and the Technical Advisory Group for General Utilization Research for the interest and advice received in the course of these investigations and in the preparation of the report. Particular acknowledgment for valuable assistance in preparing this report is offered to Dr. Robert W. Van Dolah, chief, and Mrs. Ruth Brinkley, technical assistant, of the Division of Explosives Technology, Bureau of Mines. Acknowledgment is extended to the American Gas Association for funds contributed to this research; Dr. Guenther von Elbe, formerly with the Bureau of Mines and now with Combustion and Explosives Research, Inc.; Dr. David S. Burgess, chief, Branch of Physical Sciences, Bureau of Mines; Dr. Channing W. Wilson, research chemist, Consolidated Gas Electric Light & Power Co. of Baltimore; Thomas Lee Robey, coordinator of research, and Roy A. Siskin, utilization research engineer, American Gas Association; John Corsiglia, chief utilization engineer, Surface Combustion Corp.; Earl J. Weber, research engineer, American Gas Association Laboratories; Lyman M. Van der Pyl, chief chemist, Rockwell Manufacturing Co.; John F. Anthes, assistant chief chemist, The Brooklyn Union Gas Co.; and C. C. Winterstein, special assistant, The Philadelphia Gas Works Co., for many helpful discussions. Much of the data on flame stability was obtained by Harold Schultz, chemical engineer, a former member of the Bureau of Mines staff.

EQUIPMENT AND EXPERIMENTAL PROCEDURE[4]

Only premixed streams of fuel gas and air, flowing through single upright ports in free air, at room temperature and pressure, were used in these studies. Data obtained apply to both premix and air-entraining burners because the flame port cannot respond to the manner in which the mixture flowing through it was prepared. In general, the burners used were long cylindrical glass and, in some instances, metal tubes of constant cross section, 40 to 100 diameters long. The special burners used to study flame stability and yellow tipping on short ports and hot ports are described in chapter VI. The burners used in tests with noncircular ports consisted of long metal channels of constant, triangular, square, or rectangular cross section. Flame-port dimensions were varied to provide cross checks among burners and to permit measurements over a wide range of fuels and fuel-air mixtures. Except when otherwise noted, all burners were single ports in free, still air at room temperature (around 78° F.) and atmospheric pressure (around 730-750 mm. pressure) and in an upright position.

Fuel-air mixtures were prepared by flowmetering and mixing fuel and air from compressed-gas cylinders. Flows were regulated and maintained steady by very fine

---

4/ Definitions and nomenclature are given on pp. 115-118.

needle valves. The mixing chambers were equipped with right-angled, high-velocity jets. Calibrated glass-wool flowmeters (13, 16, 21)[5] held at constant temperature and accurate to within ± 1 percent of the instantaneous flow were used. Since the flow through the glass-wool flowmetering element depends upon the viscosity of the gas, corrections for the effect of fluctuating barometric pressure were unnecessary. The perfect gas law was used to correct flowmeter readings to burner-port conditions when the pressures or temperatures at the two stations differed. This difference, except where noted, was always small or nonexistent.

Fuel mixtures were prepared by mixing gases in a compressed-gas cylinder. After standing for at least 2 weeks, the fuels were analyzed with the mass spectrometer.

In the conduct of a particular test the air and fuel flows were so adjusted that a stable flame was formed. The fuel flow was then varied until flashback, blowoff, or yellow tipping was just observed. This flow rate was taken as the blowoff, flashback or yellow-tip limit, as the case might be. The transition from stable flame to complete blowoff was usually very sharp; partly lifted flames were unusual or occurred only over a negligible range of flows. The flashback limits were usually sharp, tilted flames being either absent or appearing only over a very short range. Moreover, care was taken to select port diameters so that tilted flames[6] seldom occurred. The yellow-tip limit was sharp, except for large flames of methane and natural gas. Before each run the port was checked to make certain that it was at room temperature. Enough determinations were made to delineate curves of flashback, blowoff, and yellow tipping for each fuel by varying total flow, fuel-air composition, and burner diameter.

In running these tests certain elections were made. Premixed streams of gas and air were used instead of air-entraining burners to eliminate uncertainties about complete mixing. Flowmeters were used rather than wet-test meters to obtain steady and instantaneous readings of flows. Long ports with steady laminar flow were used in preference to short ones with unsteady laminar flow, so that the flow profile was known with certainty. Single-port burners eliminated uncertainties regarding distribution of the total flow among multiports and the possible interaction of flames on adjacent ports. The ports were held upright to exclude changes in the flow profile due to buoyancy. In all, the equipment was designed to yield experimental data as universally applicable and unambiguous as possible.

CHAPTER I. - FLASHBACK, BLOWOFF, AND FLAME-STABILITY DIAGRAMS

A. Flashback and Blowoff

It is of interest to inquire into the mechanism of stabilization of a stationary flame on a burner port. The answer requires introduction of the concept of the critical boundary velocity gradient, a fundamental physical parameter for representing flashback and blowoff characteristics of a fuel gas. This concept, first proposed by Lewis and von Elbe (19), describes the circumstances that cause a flame to flash back into the port or blow off from the port.

We can reason that a flame will remain stationary in space when the rate of consumption of unburned combustible mixture equals the rate at which combustible

---

5/ Underlined numbers in parentheses refer to items in the bibliography at the end of this report.

6/ See p. 21.

mixture is fed to the flame. Correspondingly, a flame is expected to stabilize on a burner port at a point in the approach stream where equality exists between the burning velocity and the stream velocity. This equality is generally found near the boundary of the stream where the stream velocity is reduced by friction with the wall. It is therefore at the boundary of the stream, that is, near the port wall, that we must look for relations describing flame-stability limits.

Let us first consider the phenomenon of flashback, taking for example an explosive gas-air mixture in a tube with a diameter large enough to allow flame to propagate. The combustion wave cannot come closer to the wall of the tube than the quenching distance at flashback as the burning velocity is zero within virtually the entire space defined by the quenching distance, and thus no flame exists here. At greater distances from the wall of the tube the burning velocity rises rather sharply to almost its standard value, as shown schematically by the heavy curves in figure 1. This figure gives only conditions near the edge of the stream. The other lines (a, b, and c) in the figure are lines of stream velocity for three different approach flows. The stream velocity is zero at the wall; over a short distance from the wall (boundary of the stream) it increases in virtually a linear fashion; toward the axis it rises to its maximum. If the flow corresponds to line a of figure 1, the stream velocity falls in part below the burning velocity. Here the flame will move upstream against the flow; that is, it flashes back because the burning velocity exceeds the stream velocity at some point over the stream cross section. At that point the combustible mixture can be consumed faster by the flame than mixture is being fed to the flame. Therefore the flame moves against the flow. If the flow increases (line b), the combustion wave remains stationary in an unstable equilibrium position within the mouth of the port. This is the condition at the flashback limit. The point of balance between the standard burning velocity and the stream velocity is at the point of tangency of line b with curve A. The tangent or slope of line b at this point is approximately the quotient of the standard burning velocity and the quenching distance at flashback of the gas-air mixture under consideration, that is, the ratio of ordinate to abscissa. This quotient of standard burning velocity and quenching distance equals the critical boundary velocity gradient for flashback for the gas-air mixture under consideration. If the flow corresponds to line c, the stream velocity is everywhere larger than the burning velocity, and the flame is swept out of the tube. A stable flame can form on top of the burner for the flow of line c.

Therefore, considerations of the nature of flashback lead to the conclusion that the critical boundary velocity gradient for flashback equals the quotient of two parameters - the burning velocity and the quenching distance at flashback. The burning velocity must be a fundamental parameter of the fuel-oxidant mixture, because, as defined, it is the manifestation of the chemical reaction rate. The quenching distance at flashback must also be a fundamental characteristic of the mixture, since it reflects the ability of a heat sink of large capacity to extract energy from the system rapidly enough to prevent flammation. The gradient, being a quotient of two fundamental parameters, must itself be a fundamental parameter and should be independent of port diameter (see pp. 17 and 21). This last conclusion may be used to test the validity of the proposed mechanism. In the course of their pioneering work (19) on the stability of Bunsen-burner flames, Lewis and von Elbe proposed this mechanism and showed the gradient to be independent of port diameter within explainable limits. Much corroborating evidence has come since then (1943) from many laboratories.

Let us now consider blowoff. When the flame moves out of the mouth of the port to a position atop the port, the combustion wave propagates in the free stream

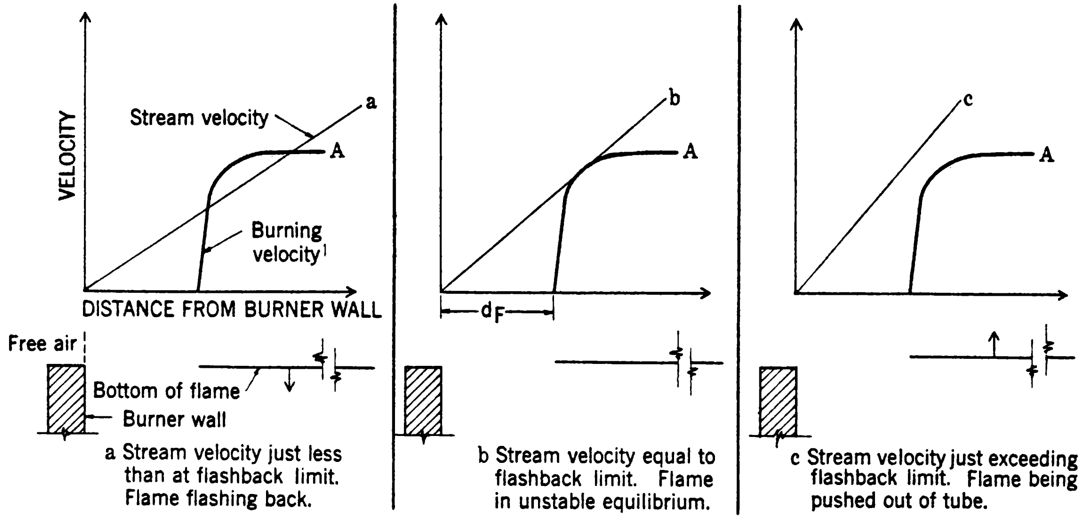

Figure 1. - Diagrammatic description of burning velocity, stream velocity, and flame position near flashback limit.

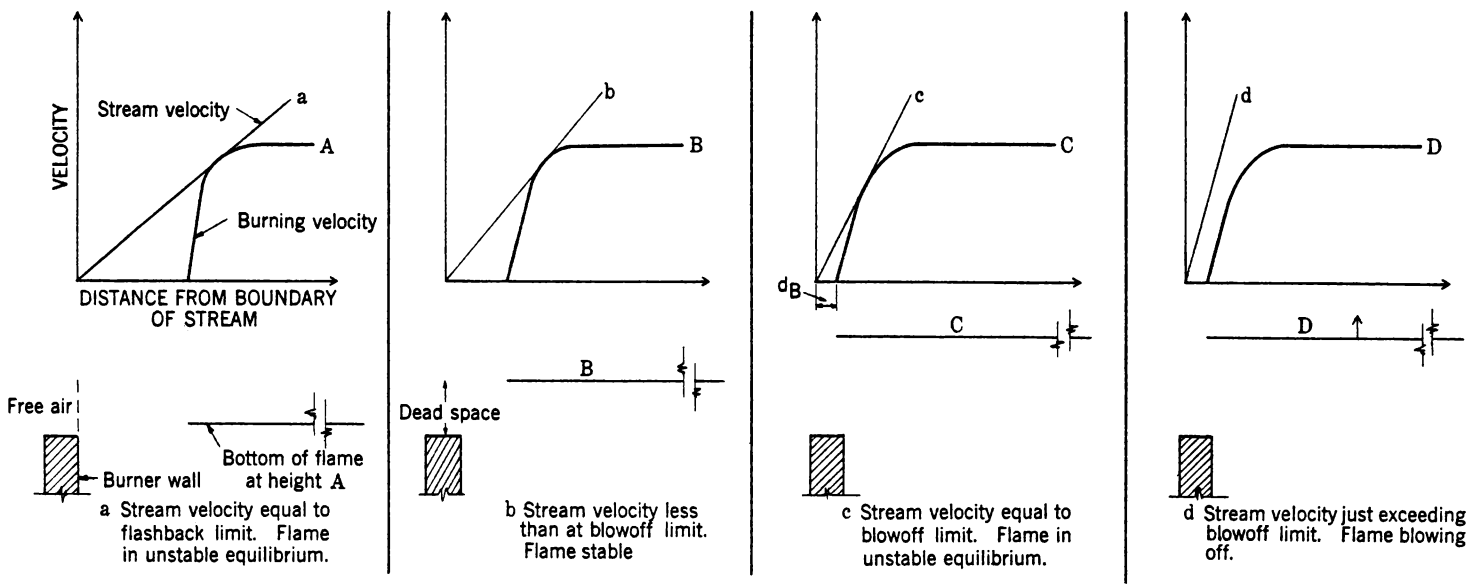

Figure 2. - Diagrammatic description of burning velocity, stream velocity, and flame position near blowoff limit.

above the rim of the tube, and correspondingly the quenching effect of the tube rim is reduced. Consequently, the curve of burning velocity shifts closer toward the stream boundary. This is illustrated in figure 2, which will be used to explain the phenomenon of blowoff. Four burning-velocity curves are shown, corresponding to four heights, A, B, C and D, of the flame base above the rim. At height A, close to the rim, the burning-velocity curve is about the same as in figure 1. The slope of line a in figure 2 is the same as that of line b in figure 1. At height B the burning-velocity curve has shifted toward the boundary of the stream. The shift toward the boundary continues up to height C. Here the quenching effect of the tube rim is very small, but the burning-velocity curve drops to zero near the stream boundary because an outermost layer of nonexplosive gas is formed by interdiffusion with secondary air and transfer of momentum. At heights exceeding C the nonexplosive boundary layer broadens, and correspondingly the burning-velocity curve recedes from the boundary. Hence, if the approach velocity is large (line d), it exceeds the burning velocity everywhere, and the flame blows off the tube because it can find no point where a balance exists between the burning velocity and the stream velocity. The condition shown by curve C and line c of figure 2 is the blowoff limit. The critical slope of stream velocity in this instance is known as the critical boundary velocity gradient for blowoff, g_B. It is approximately the quotient of the standard burning velocity and the quenching distance at blowoff of the gas-air mixture under consideration (again, the ratio of ordinate to abscissa).

However, the quenching distance at flashback differs from the quenching distance at blowoff. The quenching distance at flashback results from the loss of heat and active radicals to the wall of the port. On the other hand, the quenching distance at blowoff comes about largely through dilution with ambient air whereby a noncombustible fuel-air mixture is formed at the boundary of the stream and, to a small extent, by the loss of heat and chemical enthalpy downward toward the rim of the port.7/

We note that the blowoff gradient is the quotient of two terms that depend on the identity of the fuel-oxidant mixture. These are the standard burning velocity and the quenching distance at blowoff. Accordingly, the blowoff gradient is also a fundamental quantity of the mixture. Evidence for this was first presented by Lewis and von Elbe (19), who showed that blowoff gradients are independent of tube diameter within wide limits. Again, as with regard to flashback, corroborating evidence has come from many laboratories since then.

If now we consider stable flames, we find that, at any flow between the limiting lines a and c of figure 2, the flame settles down to a height above the rim such that the stream-velocity curve and the burning-velocity curve meet each other tangentially. For example, let us suppose that the approach flow is adjusted to correspond to the stream-velocity line b. If the combustion wave drops below the height B, the burning-velocity curve shifts to the right, the stream velocity is larger everywhere than the burning velocity, and the combustion wave is forced to lift up again toward the height B. If it should exceed this height, the burning-velocity curve shifts to the left, the stream velocity falls below the burning velocity at some distance from the boundary, and the combustion wave moves back to its equilibrium position at height B. Thus the flame remains stable between a critical lower and upper gradient of the stream velocity at the stream boundary,

7/ Dead space is still another quantity and is not identical with quenching distances at flashback and blowoff. It is the distance between the base of a stable flame and the rim of the port beneath the flame. Dead space depends on the flow and varies between heights A and C of figure 2, for the reasons given on pp. 6 and 7.

corresponding to the slopes of lines a and c and to the flashback and blowoff limits, respectively. For a flame burning in air the blowoff gradient increases sharply when the mixture is enriched with fuel gas, because in this case the inter-diffusing air at first increases the burning velocity at the boundary. Therefore rich flames are much more stable than lean flames. However, if the surrounding atmosphere does not consist of air but of some inert gas, rich flames blow off readily, the blowoff gradient decreasing with increasing fuel concentration.

It can be seen from these considerations that the critical boundary velocity gradients g_F and g_B (for flashback and blowoff, respectively) are based on properties of the gas-air mixture and are therefore essentially dissociated from burner characteristics. They depend upon the burning velocity of the combustible mixture, on its quenching distance at flashback, and on its quenching distance at blowoff in free air. Such factors as port diameter, shape, depth, and inclination should not, within definable limits, affect the critical boundary velocity gradients of flashback and blowoff. Therefore we may expect that, for a given fuel-oxidant system, there will be 1 flashback curve and 1 blowoff curve, independent of the port factors. We will see, as this discussion develops, that this is the case within certain limitations, some of which will be explained; others must await further study.

We may next consider the techniques of experimentally determining values of the critical boundary velocity gradients. It is generally more difficult to measure the standard burning velocity and the distance from the boundary of the stream over which the flame is quenched than it is to determine the slope of line b in figure 1 (for the flashback limit) or that of line c of figure 2 (for the blowoff limit). For example, the slope of such curves can be determined as follows: There are sketched in figure 3 a burner port and the velocity profile of a stream of combustible mixture flowing through it. When the velocity profile of the stream at the burner port is known, it is possible to calculate the slope of the curve of stream velocity versus distance from the axis of the port. The slope of this curve near the wall of the port is the boundary velocity gradient. For steady laminar flow the boundary velocity gradient, which is denoted by g, is calculated to be

$$g = 4\, V/\pi R^3, \tag{1}$$

where V is the volume rate of flow through a burner port of radius R. If the value assigned to V is the flow at which the flame just flashes back into the burner, equation 1 gives the critical boundary velocity gradient for flashback, g_F. If V is the flow at which the flame just blows off from the burner, we obtain the critical boundary velocity gradient for blowoff, g_B. Any flow through a burner port can be expressed in units of g, the boundary velocity gradient, but the critical boundary velocity gradient refers only to the limiting condition, either for flashback or for blowoff. Equations for calculating g for other port shapes and types of flow are discussed later (ch. V).

B. Explanation of Flame-Stability Diagrams

The practical advantage of the above theoretical treatment of flame stability can be seen by examining figures 4-7,[8/] based on data in reference (19). The critical flows of natural gas-air mixtures at which flashback and blowoff were

8/ Data presented in figs. 4-11 and 13-18 were obtained with less accurate flowmeters than those employed to obtain data in subsequent chapters. However, the agreement between the 2 sets of data where they overlap is entirely adequate for the purpose of presenting theory.

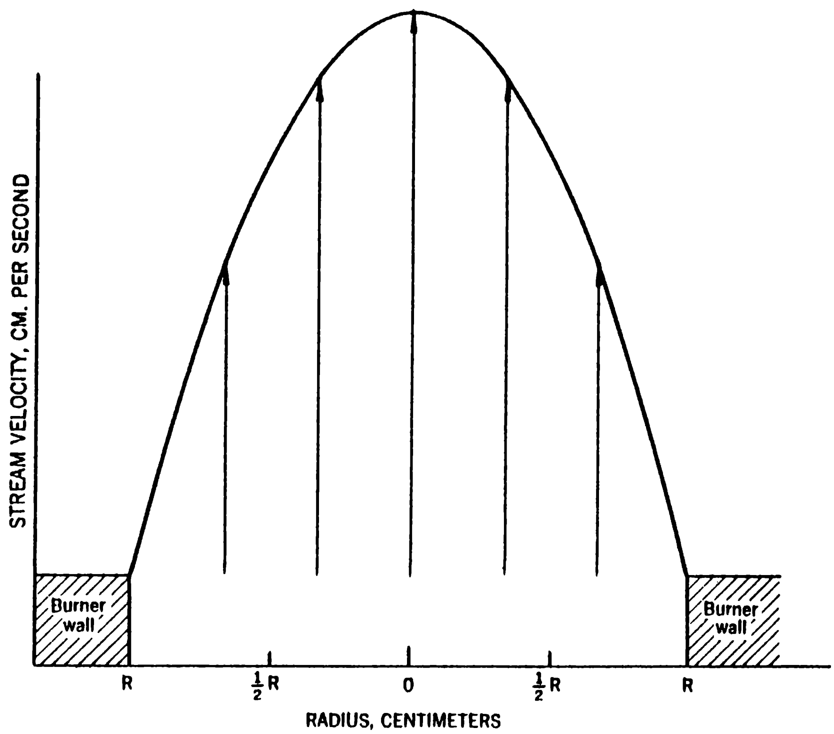

Figure 3. - Parabolic velocity profile of a stream at a burner port.

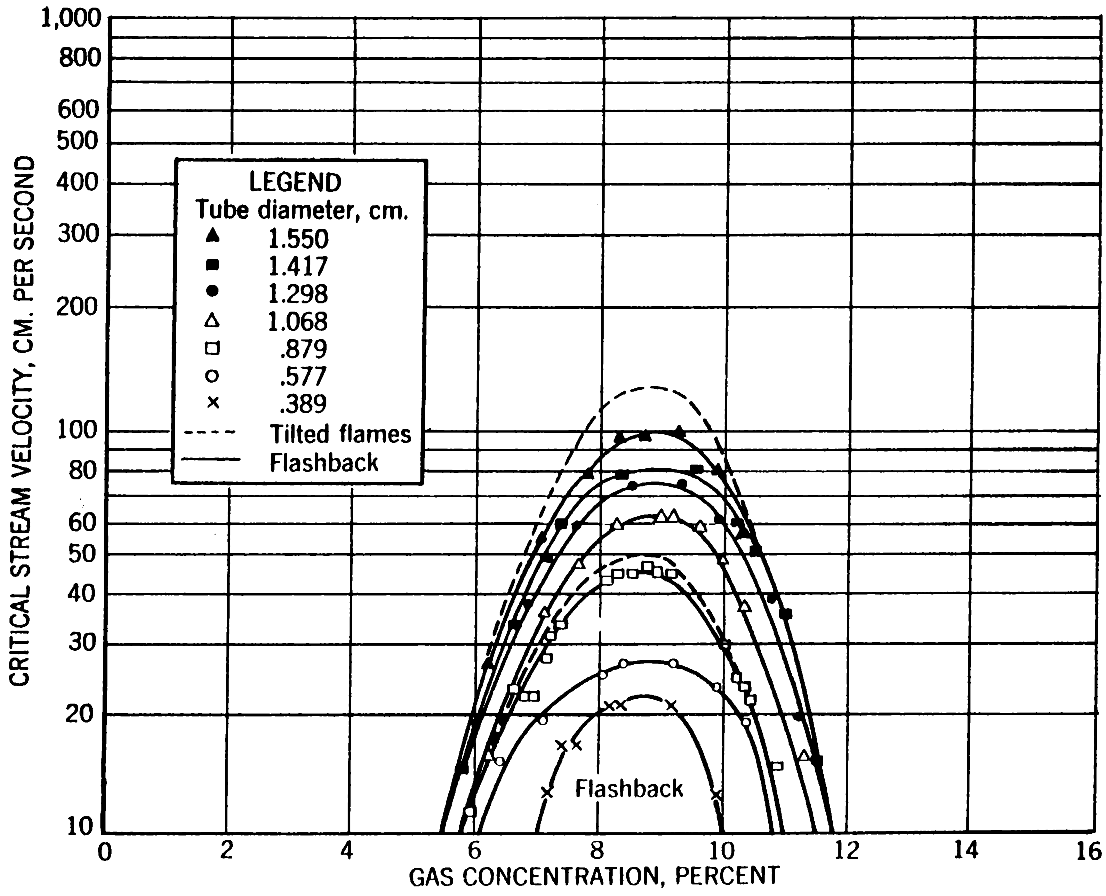

Figure 4. - Critical flows for flashback of natural gas-air flames (Lewis and von Elbe).

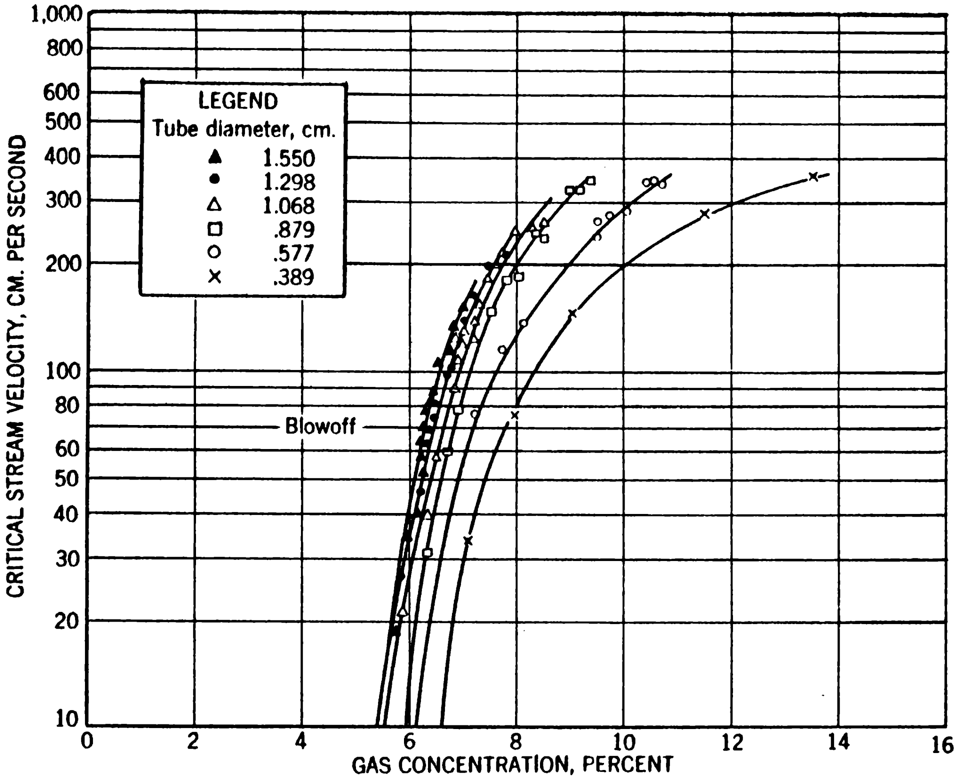

Figure 5. - Critical flows for blowoff of natural gas-air flames (Lewis and von Elbe).

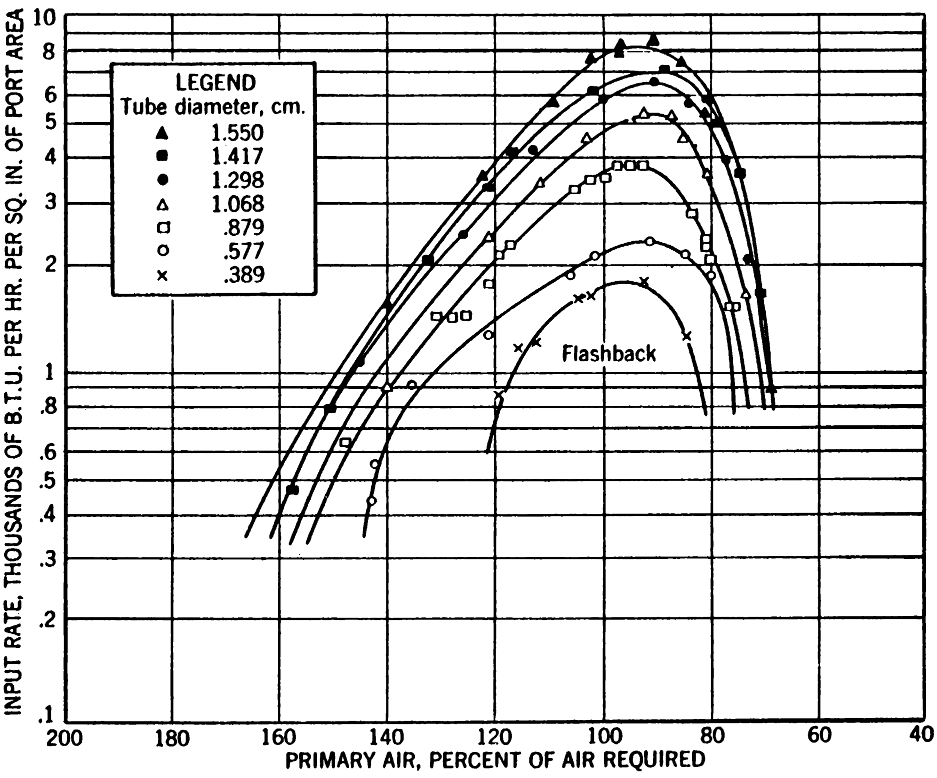

Figure 6. - Critical flows in gas-industry units for flashback of natural gas-air flames (Lewis and von Elbe).

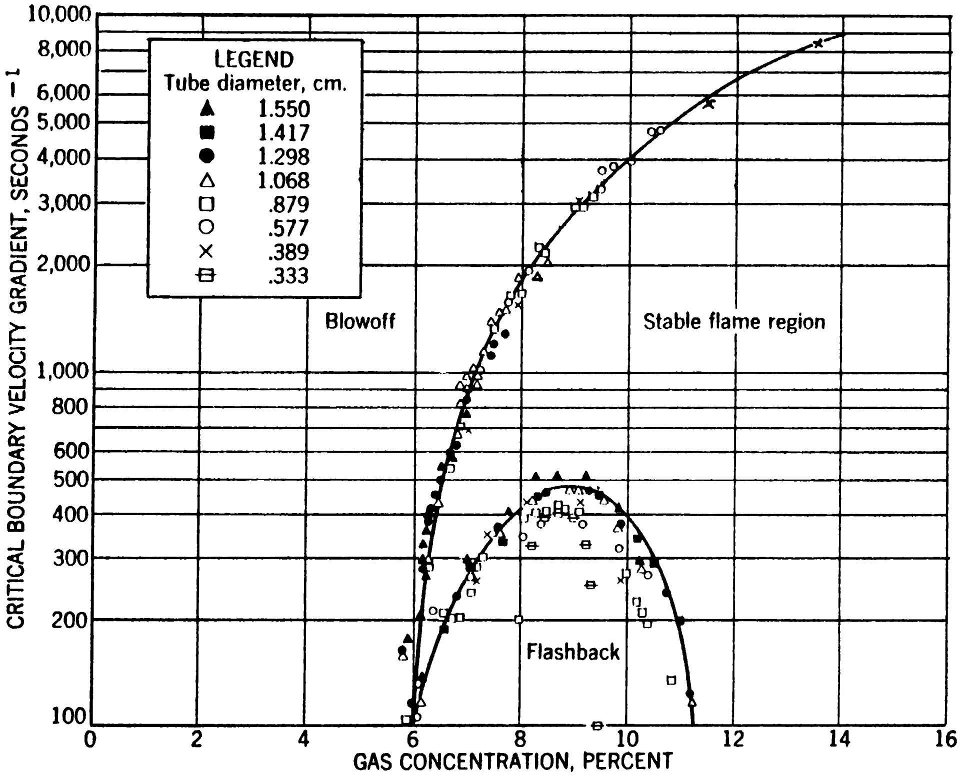

Figure 7. - Critical boundary velocity gradients for flashback and blowoff of natural gas-air flames (Lewis and von Elbe).

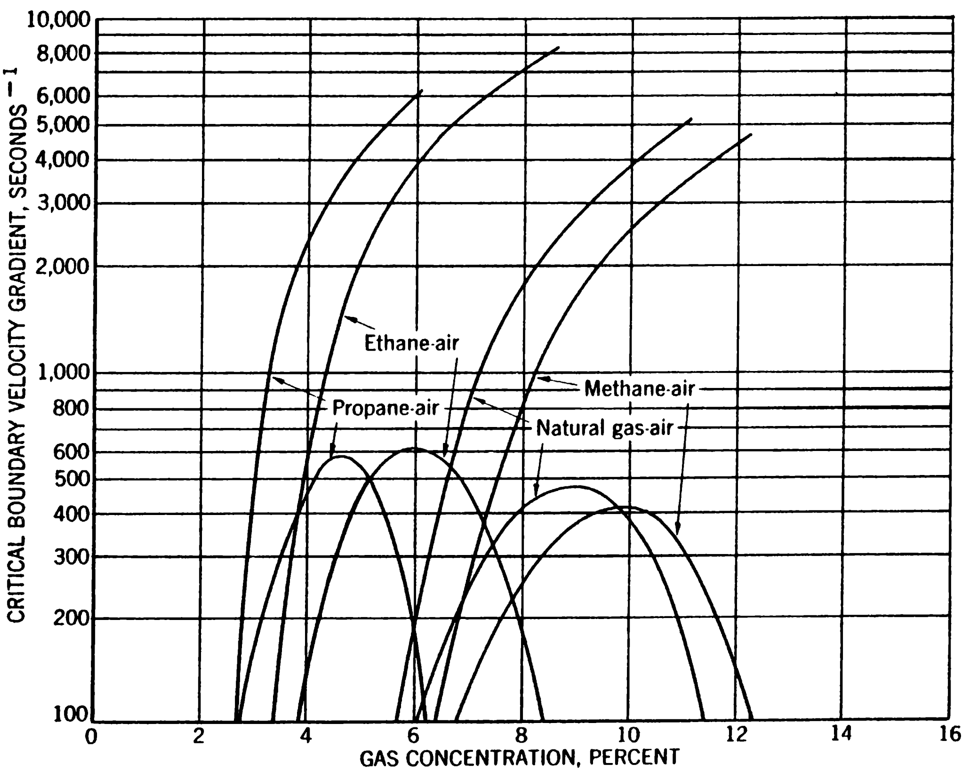

Figure 8. - Critical boundary velocity gradients for flashback and blowoff of paraffin-air mixtures.

observed with various burners are presented in figures 4[9/] and 5. There is a different set of curves for each size burner port, regardless of whether flow is in volumetric units (V) (19), linear units ($V/\pi R^2$), or (B.t.u./hr.in.^{2}). (See, for example, figure 6, in which the data of figure 4 are replotted in B.t.u./hr.in.^{2} versus percent of primary air.) However, by plotting the data of figures 4 and 5 against critical boundary velocity gradients instead of $V/\pi R^2$, or V, or B.t.u./hr.in.^{2}, substantially a single curve is obtained for flashback and another for blowoff for ports of various sizes. This has been done in figure 7, in which both g_F and g_B are plotted and which defines the flame-stability region of natural gas-air mixtures. Similar diagrams may be obtained for all combustible constituents of commercial fuel gases, among which are hydrogen, carbon monoxide, methane, ethane, ethylene, propane, propylene, and butane. The same is true for mixtures of these constituents with one another and with noncombustibles, such as oxygen, nitrogen, and carbon dioxide.

An additional simplification can be made in representing flame-stability limits. If critical boundary velocity gradients for flashback and blowoff are plotted against percent gas for several gases, the curves will lie apart from each other if the stoichiometric fuel percentages are different, as illustrated in figure 8 for several hydrocarbons. When the fuel percentage is divided by the stoichiometric fuel percentage, the function "fraction of stoichiometric," F, is obtained. The higher the value of this ratio, the richer the mixture will be. The stoichiometric fuel percentage for methane is 9.46, for this natural gas 8.49, for ethane 5.64, and for propane 4.02. A methane-air mixture containing 12 percent methane has an F value of 12.0/9.46 = 1.27.

When the ratio fraction of stoichiometric is used, flashback and blowoff data for all fuels center around the value of F = 1.0, as is illustrated in figure 9.

Figure 10 contains two curves roughly averaging those of figure 9. A flame-stability diagram, such as figure 10, contains 2 curves - 1 for flashback and 1 for blowoff. These 2 curves define 3 regions of flame behavior on burners - a region where flames flash back (beneath the flashback curve), one where flames blow off (above the blowoff curve), and a stable flame region (between the flashback and the blowoff curves). The diagram is characteristic of the fuel gas and correlates the flashback and blowoff limits of the fuel for all burners, except in certain definable instances. The flame-stability diagram of any fuel can be determined experimentally in the laboratory with comparative ease, or it can be calculated somewhat less accurately by procedures given in chapter II.

C. Some Uses of Flame-Stability Diagrams

The coordinates of a flame-stability diagram - the critical boundary velocity gradient and fraction of stoichiometric - are relatively new concepts and may require explanation beyond the theoretical arguments presented above. As a first step, let us see how the units of the flame-stability diagram are related into units familiar to the gas industry.

The abscissa of a flame-stability diagram is the fraction of stoichiometric F and may be used to calculate the percent primary air, which is the ordinate of the gas-industry type of diagram for representing flame characteristics. The equation

---

9/ The flashback curve for the 1.550-cm. tube has been drawn in accordance with revision by Lewis and von Elbe (17).

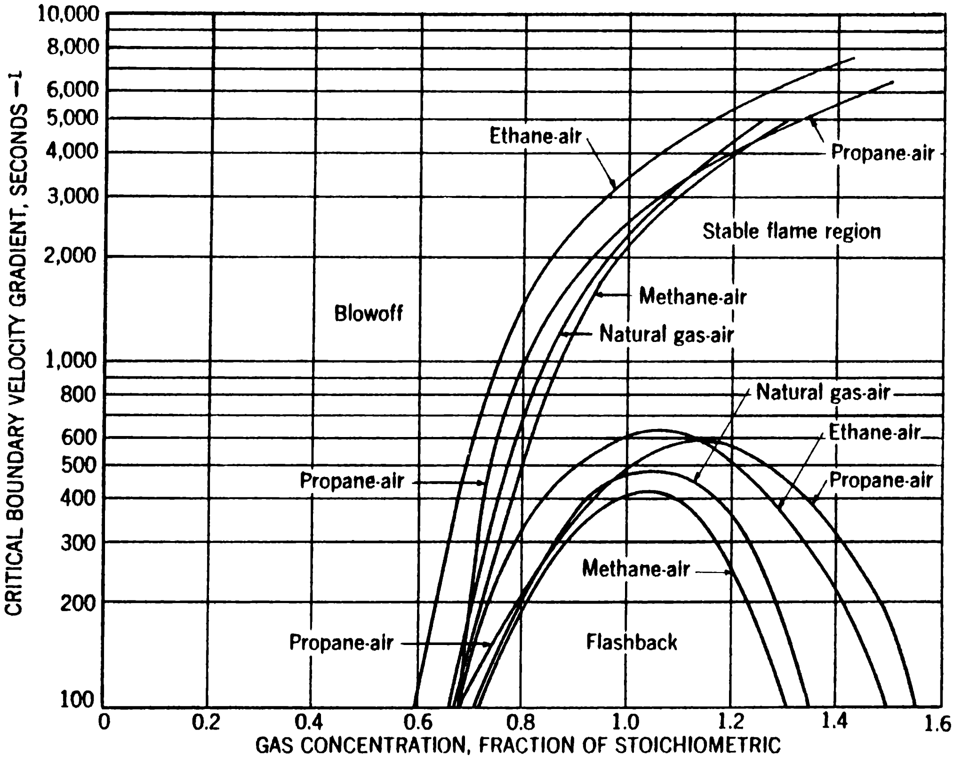

Figure 9. - Flame-stability diagrams for paraffin-air mixtures.

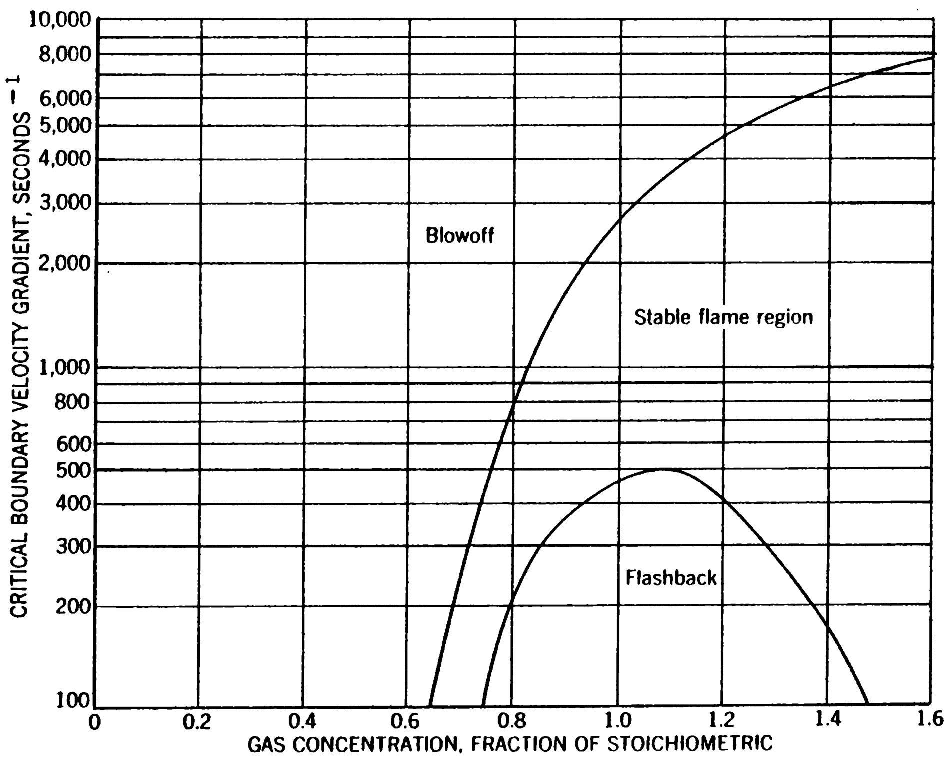

Figure 10. - Average flame-stability diagram for paraffin-air mixtures.

relating the fraction of stoichiometric and the percent primary air is

$$L = 100(1 - FS)/F(1 - S), \quad = \frac{100\left(\frac{1}{F} - S\right)}{(1 - S)} \tag{2}$$

where L = percent primary air = $\left[100\ (\text{air/gas})_{\text{actual}}/(\text{air/gas})_{\text{stoichiometric}}\right]$; F = gas concentration, fraction of stoichiometric; S = mole fraction of fuel in a stoichiometric mixture. In addition, P, the volume of air required for complete combustion of 1 volume of fuel, and FS are

$$FS = 100/(LP + 100) = \text{percent fuel}/100, \tag{2a}$$

$$P = (1 - S)/S. \tag{2b}$$

An alternate to equation 2 is

$$L = \frac{100(P + 1 - F)}{FP}\ . \tag{2c}$$

The ordinate of a flame-stability diagram is the critical boundary velocity gradient (g_F or g_B) and may be used to calculate the heat input, M, B.t.u./hr.in.^{2}, when the port diameter D_i is specified. If the port is cold, held upright, and long enough to establish steady laminar flow, then

$$M\ (\text{B.t.u./hr.in.}^2) = 0.26\ gH_oD_iFS, \tag{3}$$

where M = flow of fuel through port, B.t.u./hr.in.^{2}; g = boundary velocity gradient, seconds $^{-1}$; H_o = heating value of fuel, B.t.u./cu.ft.; D_i = diameter of port, inches; 0.26 = numerical constants. An alternate form of equation 3 is

$$M = \frac{0.26\ gH_oD_iF}{P + 1}\ . \tag{3a}$$

The advantages in using the flame-stability parameter critical boundary velocity gradient over the above heat-input factors are threefold:

(1) The critical boundary velocity gradient concept can be derived theoretically and used to explain the phenomena of flashback and blowoff, which cannot be done on the basis of heat-input units alone.

(2) The flame-stability gradients are characteristic of the fuel-air mixture and are largely independent of the port size and shape and probably of its inclination. However, for a given fuel the heat-input limits differ for each port size (see figure 6), shape, and inclination.

(3) Furthermore, the heat-input factor results in different exchangeability (interchangeability, supplementability, etc.) diagrams that depend upon the particular burner employed for the calculation. Other difficulties arise when predicting the exchangeability of fuel gases, which will not be discussed here.

The use of either F values (fraction of stoichiometric) in a flame-stability diagram or percent primary air results in a similar grouping of flame-stability curves.

(1) However, use of percent primary air in plotting flashback and blowoff data spreads out the region of lean flames (values between 100 and infinity) and

compresses the region of rich flames (values between 100 and 0) in which most burners operate. Use of F values leads to a more realistic relative emphasis on the lean ($F < 1$) and rich ($F > 1$) regions.

(2) Moreover, the percent primary air function complicates the equations for the entrainment of air in gas burners, which are essential in any method for predicting the exchangeability of fuels on air-entraining burners.

(3) In addition, use of percent primary air produces different limits for fuels consisting of a combustible (as propane) and fuels consisting of the same combustible mixed with air (as propane-air). This is not the case when the term fraction of stoichiometric is used as shown in the following example. Consider a mixture of fuel (propane) plus primary air, such that the percent primary air is 60. The percent propane in total air is 6.5 $\left[P = 24,\ 0.60(24) = 14.4,\ \% = \frac{1(100)}{1 + 14.4} = 6.5\right]$. Next take a mixture of fuel (1,120 B.t.u. propane-air, 43.3 percent C_3H_8, 56.7 percent air) plus 60 percent primary air. The percent propane in total air is 6.3 $\left[P = 9.8,\ 0.60(9.8) = 5.88,\ \% = \frac{0.433(100)}{1 + 5.88} = 6.3\right]$. Obviously, we are dealing with two mixtures of fuel and total air. We have limits for each. On the other hand, take the same two fuels at some identical value of F, and we find that the percent propane in total air is identical for both fuels. To illustrate, at $F = 1.4$ the percent propane in total air for the pure porpane fuel is $1.4\,(0.0402)(100) = 5.6$, and the percent propane in total air for the 1,120-B.t.u. propane-air fuel, 43.3 percent propane in fuel, is $1.4(0.0928)(100)(0.433) = 5.6$.

Apart from the question of units, a flame-stability diagram can be used in very much the same fashion as the well-known limit curves used by the gas industry (1, 23). For example, the performance of a particular burner can be shown on a flame-stability diagram. If the air shutter and gas rate are fixed, the burner can be represented by a single performance point, such as x in figure 11. If in another burner the gas rate is fixed and the air shutter is raised from partly open to wide open, as for instance in the Rochester test burner (RTB) (24), the performance points may form such a line as A, where point f corresponds to an RTB flashback number and point b to an RTB blowoff number (see fig. 11). For a third burner, with a fixed air shutter and a gas rate that is varied from off to wide open, the performance points of the burner may form a line such as B. More important still, the performance point x in figure 11 can represent many burners. This is a great advantage in dealing with vast numbers of burners with many port diameters and port loadings. Flame-stability diagrams can also be used to predict the exchangeability of fuels on gas distribution systems. (See refs. A, D, F, I, L and N of Special Bibliography, pp. 118-119.)

How can the flashback and blowoff limits of a specific burner port diameter be calculated from the flame-stability diagram of a given fuel in terms of B.t.u./hr.in.^{2} versus percent primary air? Let us consider the case of a single-port burner with steady laminar flow through the port. The port is burning in free air, it is held upright, it is circular in cross section (diameter, 0.25 inch), the flow and ports are at room temperature and pressure, and the fuel is methane.

Intercepts of F_F, g_F, and F_B, g_B are read from the two curves in figure 20 (see table 1, columns 1 and 3). Using equation 2 (p. 13), F, the gas concentration, fraction of stoichiometric, is converted to L, the percent primary air (see table 1, column 2). Thus for $F = 0.8$ and $S = 0.0946$, we have:

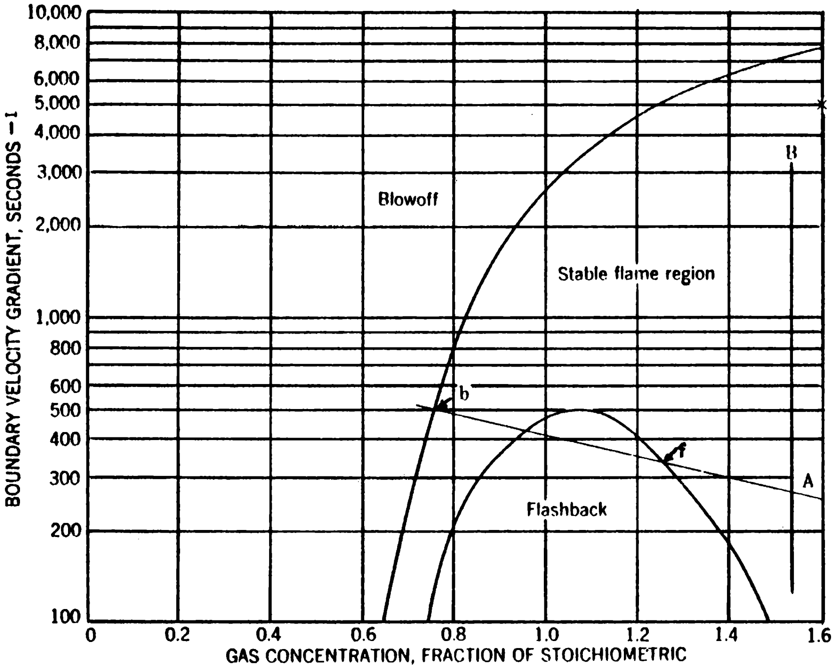

Figure 11. - Use of average flame-stability diagram for paraffin-air mixtures to show performance of burners.

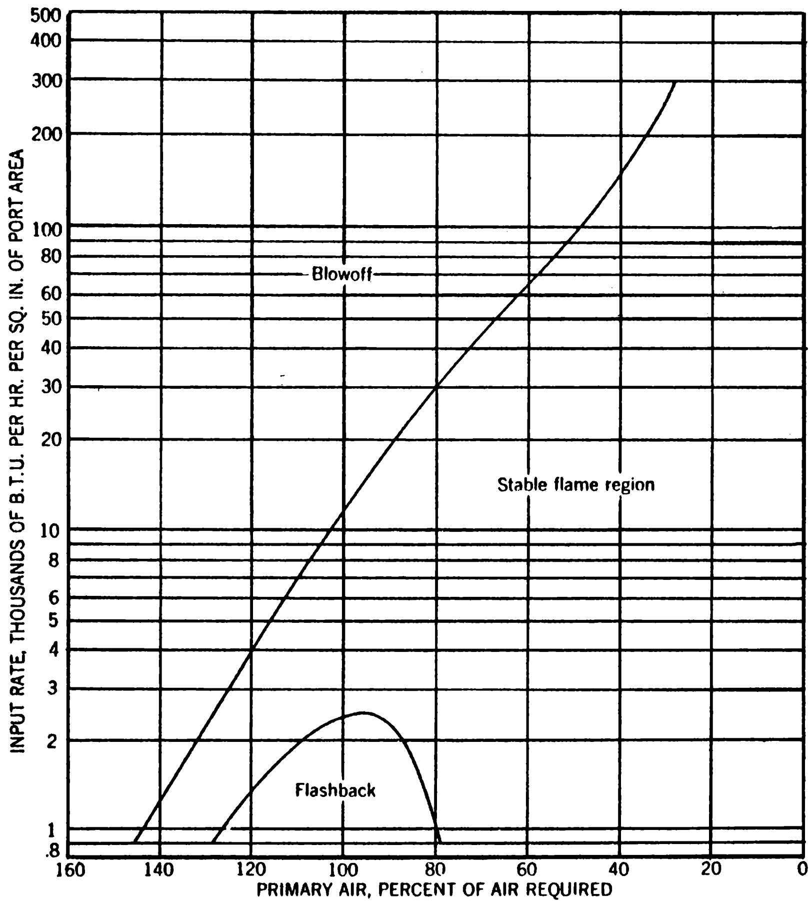

Figure 12. - Gas-industry type of flashback and blowoff limit curves for methane for 0.25-inch port with steady laminar flow.

TABLE 1. - Converting the flame-stability diagram of methane to limit curves for a 0.25-inch port burner with steady laminar flow

F.	L	g	M
		Flashback	
0.8	128	190	945
.9	112	330	1,848
1.0	100	390	2,425
1.1	90	340	2,325
1.2	82	180	1,345
		Blowoff	
0.8	128	510	2,540
1.0	100	1,950	12,140
1.2	82	3,750	28,000
1.6	59	6,800	67,700
2.0	45	9,500	118,000
2.4	36	12,500	186,500
2.8	29	16,200	282,000

$$L = 100\left(1 - 0.8(0.0946)\right)/0.8(1 - 0.0946) = 128.$$

Using equation 3 (p. 13), the critical boundary velocity gradients are converted into M, B.t.u./hr.in.^{2} (for the 0.25-inch-diameter port) (see table 1, column 4). These values hold only for a 1/4-inch port (D_i = 0.25); they apply to no other port size. To obtain values of M for another diameter, another value must be assigned to D_i. For the same condition as above:

$$M = 0.26(190)(1{,}013)(0.25)(0.8)(0.0946) = 945.$$

When the newly calculated intercepts (see table 1, columns 2 and 4) are plotted, the result is the usual gas-industry type of limit-curves diagram (figure 12). (The yellow-tip limit involves separate considerations discussed in chs. III and IV.)

It should be emphasized that figure 12 represents the condition for the particular burner described above. For other burner conditions, such as a hot port, a short drill port, a multiport burner, or a burner operating in an appliance with restricted secondary air, additional considerations are necessary.

D. Limitations of Flame-Stability Diagrams

Limits of applicability and reservations pertaining to the numerical values of gradients listed in this chapter must be recognized. In some instances we possess adequate knowledge to make necessary corrections; in others we have yet to learn the answers. However, these difficulties are not associated uniquely with the concept of critical boundary velocity gradients for flashback and blowoff; they arise also when burner performance is rated in terms of B.t.u./hr.in.^{2} or other units. In all these instances the following limitations must be considered:

(1) Temperature. Flashback and blowoff gradients are raised by increasing the initial temperature of the stream before it is ignited. The listed values are for room temperature (around 78° F.). The method for correlating these listed

values with temperature is known, but correction factors are known at present only for methane (natural gas) and propane. (See ch. VI on temperature dependence of fuel characteristics.)

(2) Pressure. Flame-stability gradients are directly proportional to the ambient pressure; however, near atmospheric pressure the flame-stability gradients change little with the usual small fluctuations in barometric or ambient pressure in the appliance. The listed values were obtained around 74 cm. of mercury.

(3) Chemical composition of secondary air. The listed values were obtained on monoports in free still air. The flashback gradients are not affected by partly vitiated secondary air that may occur in an appliance, but we know that the blowoff gradients are strongly affected, although adequate quantitative information is lacking. Figure 13 (19) gives an example of how partly vitiated secondary air lowers the blowoff gradient.

(4) Chemical composition of primary air. The listed measurements are for primary air containing 20.9 percent oxygen. They do not apply to primary air containing much less or more oxygen or where nitrogen is replaced by another inert gas. The magnitude of this effect for methane and for propane can be judged from figures 14-17 (15), where the oxygen percentage in the primary "air" is either 20.9 or 100 percent oxygen while the secondary air remains at 20.9 percent oxygen.

(5) Motion of secondary air. The basic aspects of this phase of burner performance has not been studied adequately, but it is expected that numerical values of critical boundary velocity gradients are unaffected by the motion of secondary air. However, the flow profile at the rim of the port can be altered by sufficient draft. Consequently, the boundary velocity gradient corresponding to the altered flow profile is not the same as for the stream flowing into free still air. This complication needs further study.

(6) Angle of port axis with the vertical. Measurements reported in this chapter were made with upright ports and upward flow. Information for nonvertical ports and inclined or downward flow is inadequate. It appears probable that the critical boundary velocity gradients are not changed by varying the orientation of the port but that the flow corresponding to a particular gradient is affected.

(7) Diameter of port. These critical flame-stability gradients are valid for all port diameters, with the following exceptions:

(a) Flashback is impossible when the port diameter is equal to or smaller than the quenching distance of the mixture, provided that the port depth is greater than about 1/16 inch. When the port diameter is only slightly greater than the quenching distance for the particular fuel-air mixture, the flashback gradient is decreased. It is lowered because the burning velocity of the mixture is appreciably decreased by ports of near quenching dimensions to a nonstandard value. Furthermore, the concept of critical boundary velocity gradients for flashback is increasingly inexact as the port diameter decreases to quenching distance. In such ports, owing to quenching by the wall, the flame cannot extend far enough from the axis to be thought of as existing near the boundary, and the stream-velocity profile across the quenched distance from the wall is not sufficiently linear. Linearity of the boundary velocity profile across the quenched distance is one of the requirements underlying the concept of critical boundary velocity gradients. This

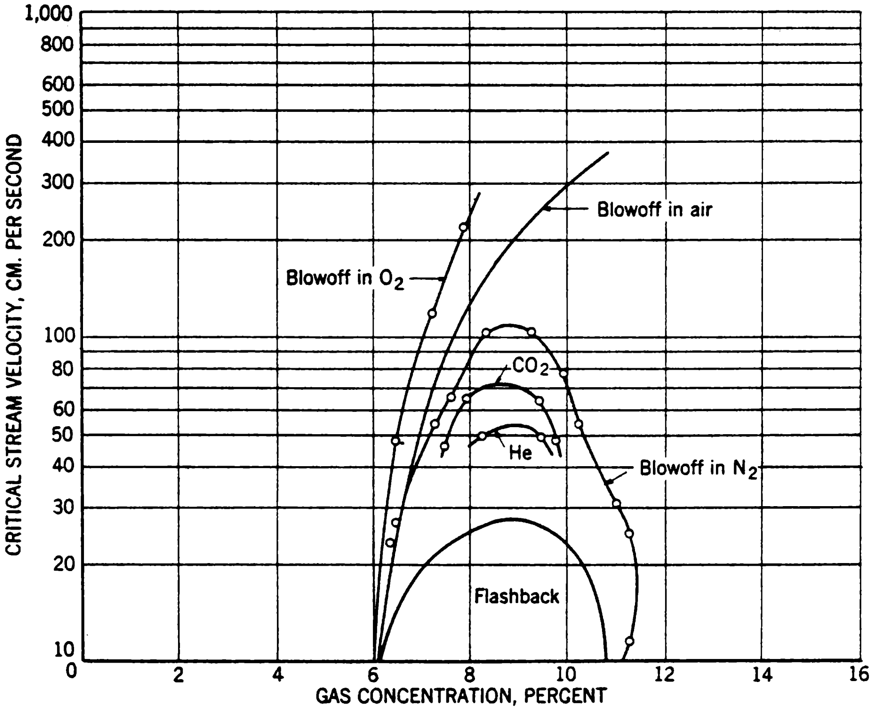

Figure 13. - Effect of nature of surrounding atmosphere on blowoff of natural gas-air flames; tube diameter, 0.577 cm. (Lewis and von Elbe).

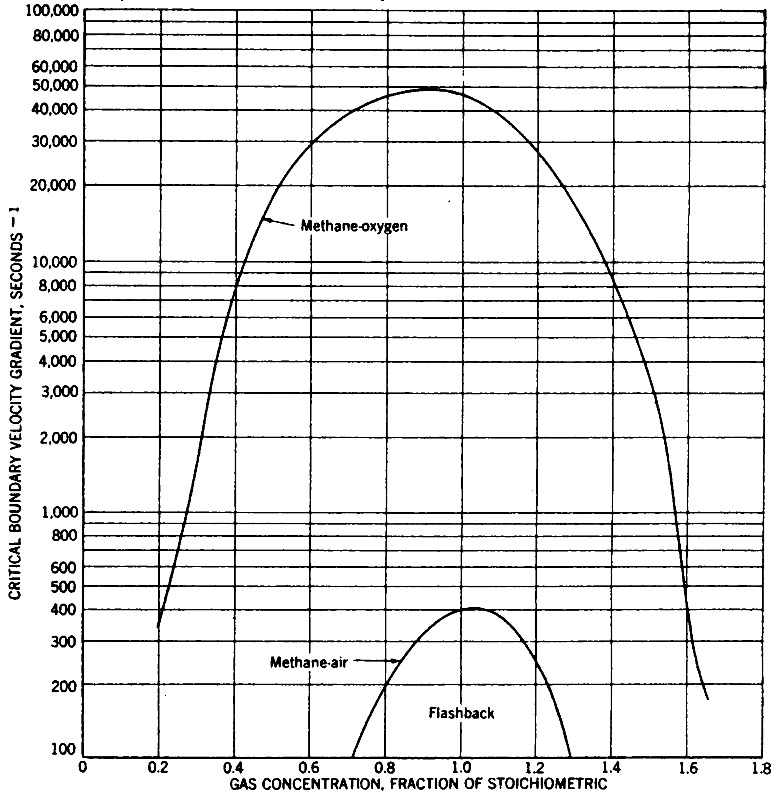

Figure 14. - Critical boundary velocity gradients for flashback of methane-air and methane-oxygen mixtures.

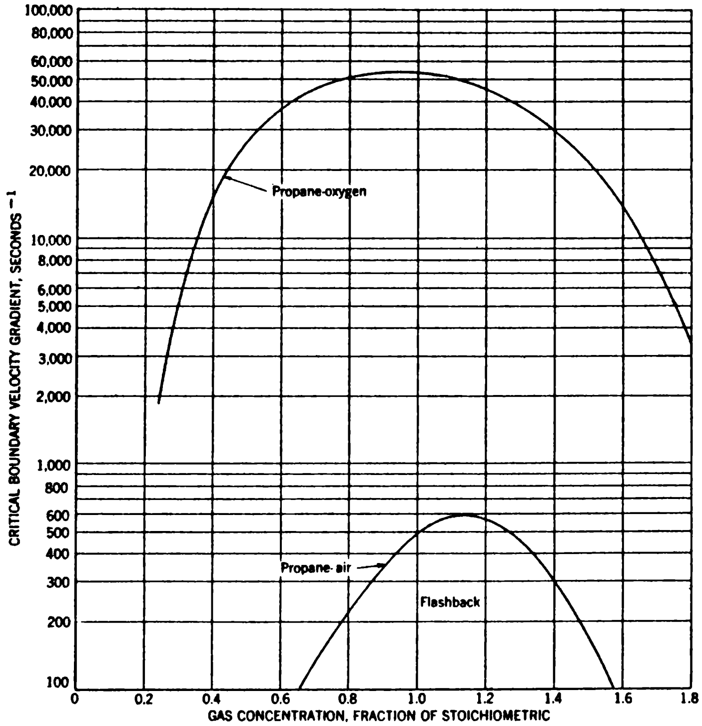

Figure 15. - Critical boundary velocity gradients for flashback of propane-air and propane-oxygen mixtures.

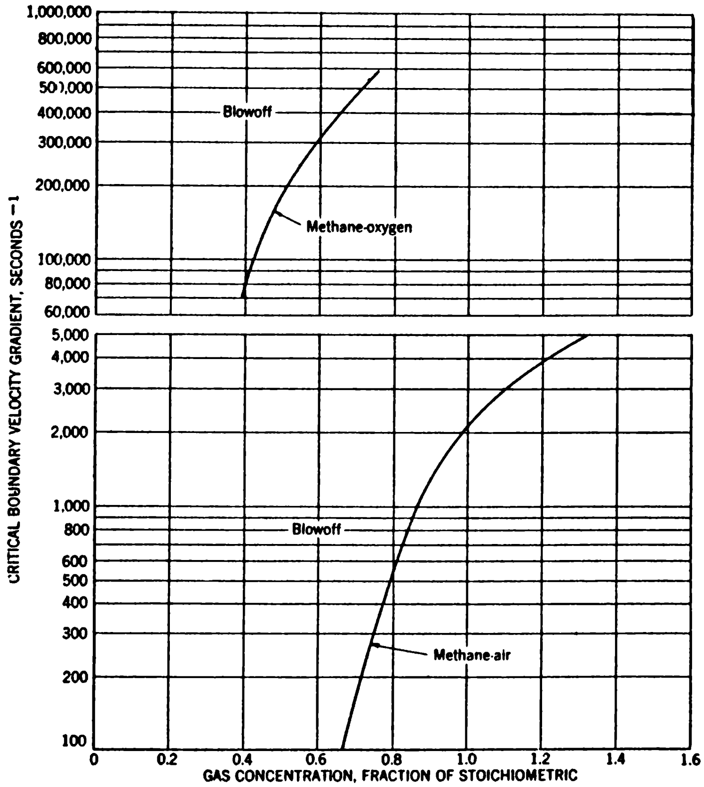

Figure 16. - Critical boundary velocity gradients for blowoff of methane-air and methane-oxygen mixtures.

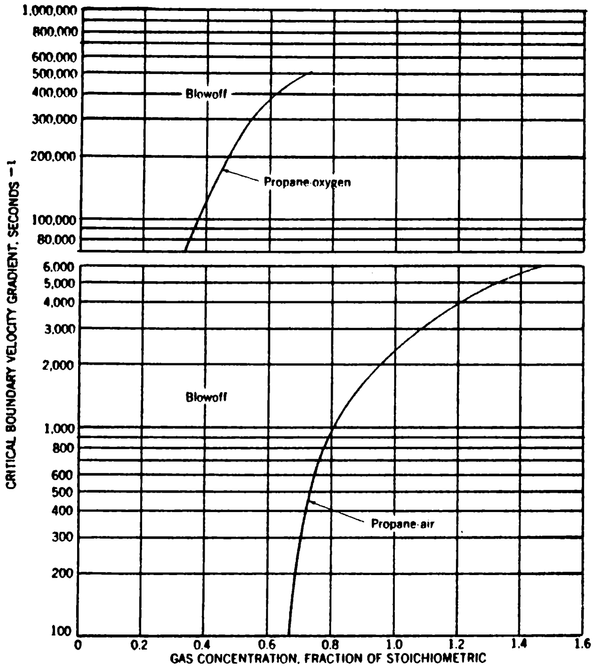

Figure 17. - Critical boundary velocity gradients for blowoff of propane-air and propane-oxygen mixtures.

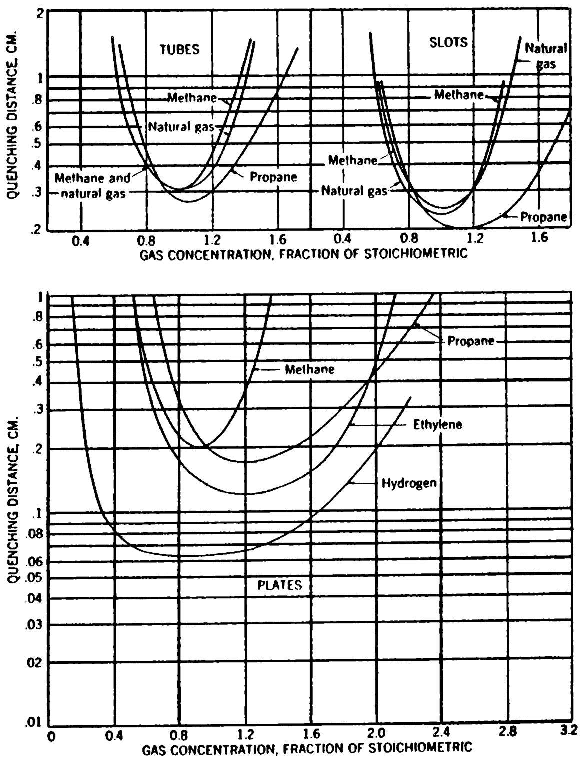

Figure 18. - Quenching distances of tubes, slots (von Elbe and Mentser), and plates (Blanc, Sikora, Guest, von Elbe and Lewis) for mixtures of several fuels with air.

limitation introduces a safety factor because the flashback gradients in this report represent upper limits for flashback on small ports, all factors other than diameter being excluded from consideration for the moment.[10] The magnitude of quenching distances for ports at room temperature may be judged from figure 18 (2, 14, 15, 28).

Another exception exists for rather large diameter ports where the backward thrust of the flame can cause chance asymmetry in the stream-velocity profile for flows somewhat exceeding the flashback limit. The result may be a tilted flame (28) that flashes back with an irregular flame front, thus increasing the flashback region beyond the standard limits. Usually this effect is small, particularly for slow-burning fuels such as natural gas and on smaller ports. However, tilted flames could profitably bear further investigation.

(b) Blowoff gradients are less affected by port diameters near quenching dimensions. Near blowoff the flame is stabilized above the port while near flashback the flame is virtually within the rim of the port. Thus less heat energy from the flame reaches the port at blowoff than at flashback, and the quenching effect of the port is less. For rich fuel-air flames in air the blowoff gradient is valid for all port diameters. Very rich flames (fraction of stoichiometric greater than about 3) are basically diffusion flames. Their blowoff limits are not treated in this report, as the blowoff characteristics of very rich flames are not described in the main by the concept of critical boundary velocity gradients (32). Lean flames blow off from ports of near quenching diameters at flows far below those corresponding to the critical boundary velocity gradients for blowoff, while very lean flames may even be extinguished (19).

(8) Multiport burners. No conclusive tests were conducted with such burners. However, it is apparent that, if the flow from all ports on a burner were exactly the same and all ports were spaced far enough apart so that each was in free, still air, the performance of the burner would be that of a monoport. However, when the ports are close, the atmosphere surrounding each port contains combustion products that change the flame-stability characteristics. The operating temperature of the burner may also be affected, thus changing the stability gradients still more.

10/ All flashback measurements in this report have been made with ports large enough to avoid partial quenching of the flame. Otherwise, gradients that are characteristic of the fuel and independent of the burner would not be obtained. On ports where partial or complete quenching can occur, flashback takes place at less than standard gradients or not at all. A port that is small for a slow-burning gas, such as natural gas, may be large for a rapidly burning gas, such as a coke-oven gas. It is interesting to note that a 0.294-cm. port (about a D.M.S. 32-hole), which is too small for natural gas, is not too small for a hydrogen-carbon monoxide fuel consisting of 74.5 percent carbon monoxide, 25.1 percent hydrogen, and 0.4 percent carbon dioxide (A-T/2a-No./18). (Note. - Material in the Appendix will be referred to in the text as in the following example: (A-T/2a-No./18). This means Appendix, table 2a, and fuel No. 18.) Flashback gradients obtained with this small port fall on the curve for the flashback data obtained with large ports.

If the total flow is divided unevenly among the ports, those ports receiving less than average flow flash back when their particular flow equals or falls below that corresponding to the critical boundary velocity gradient for flashback. The entire burner flashes back as soon as the flame from one of the ports strikes into the manifold. Thus flashback becomes possible, even when the average flow exceeds the flow corresponding to the critical gradient.

Similarly, those ports receiving more than average flow will blow off when the flow equals or exceeds that corresponding to the critical boundary velocity gradient for blowoff. The entire burner then shows lifting of flames or partial blowoff, which, for practical purposes, the industry rates as a blowoff condition. This partial blowoff is possible even though the average flow is less than that corresponding to the critical gradient.

(9) Flow profiles and port shape. In calculating boundary velocity gradients from data on volumetric or linear flows or the converse, it should be remembered that equations 1 and 3 are only for steady laminar flow through a long circular port. The critical boundary velocity gradients given in this report are correct for other types of flows and port shapes, but the equations relating the flow and the gradient differ (see ch. V).

CHAPTER II. - FLAME-STABILITY DATA OF FUELS; CALCULATION OF FLAME-STABILITY DIAGRAMS

Often, as, for example, when gas burners are being designed or the exchangeability of fuels on gas burners is predicted, information on the flashback, blowoff, and yellow-tip limits of the fuels is needed by the gas industry. In principle, it is always possible to measure these limits, and it would always be best to do so. However, the gases and laboratory facilities may not always be available. Furthermore, it is clear that it would be a great advantage to the gas industry to have these measurements made once and for all. This chapter purposes to present flame-stability gradients or means of calculating these for all possible combinations of combustible gases and inerts likely to occur in a gas-distribution system and all mixtures of such fuels with air extending from very lean to very rich mixtures. These data are limited to flames on upright ports in free air at room temperature and pressure. Yellow-tip data are presented in chapters III and IV.

A. Flame-Stability Diagrams of Natural Gases, Liquid-Petroleum Gases, and Single-Component Fuels

Let us first consider the simplest case - a single-component fuel. There are about a half-dozen of these fuels that interest gas suppliers. Their flame-stability diagrams[11] have been measured, as well as the flame-stability diagram for natural gas (A-T/1a,1b-No./1),[12] which, though not truly a single-component fuel, may conveniently be treated as such. The data for figure 19 were obtained with natural gas containing methane, 91.5 percent; ethane, 5.2 percent; propane, 1.3 percent; propylene, 0.2 percent; butane, 0.2 percent; butylene, 0.1 percent; carbon dioxide, 0.9 percent; and nitrogen, 0.6 percent. As the chemical compositions of natural gases do not differ greatly and because the flame-stability diagrams of the

---

11/ A flame-stability diagram need not show experimental points, as the curves suffice to characterize the fuel. Experimental points are usually given in this report to show experimental error and conditions.

12/ See footnote 10.

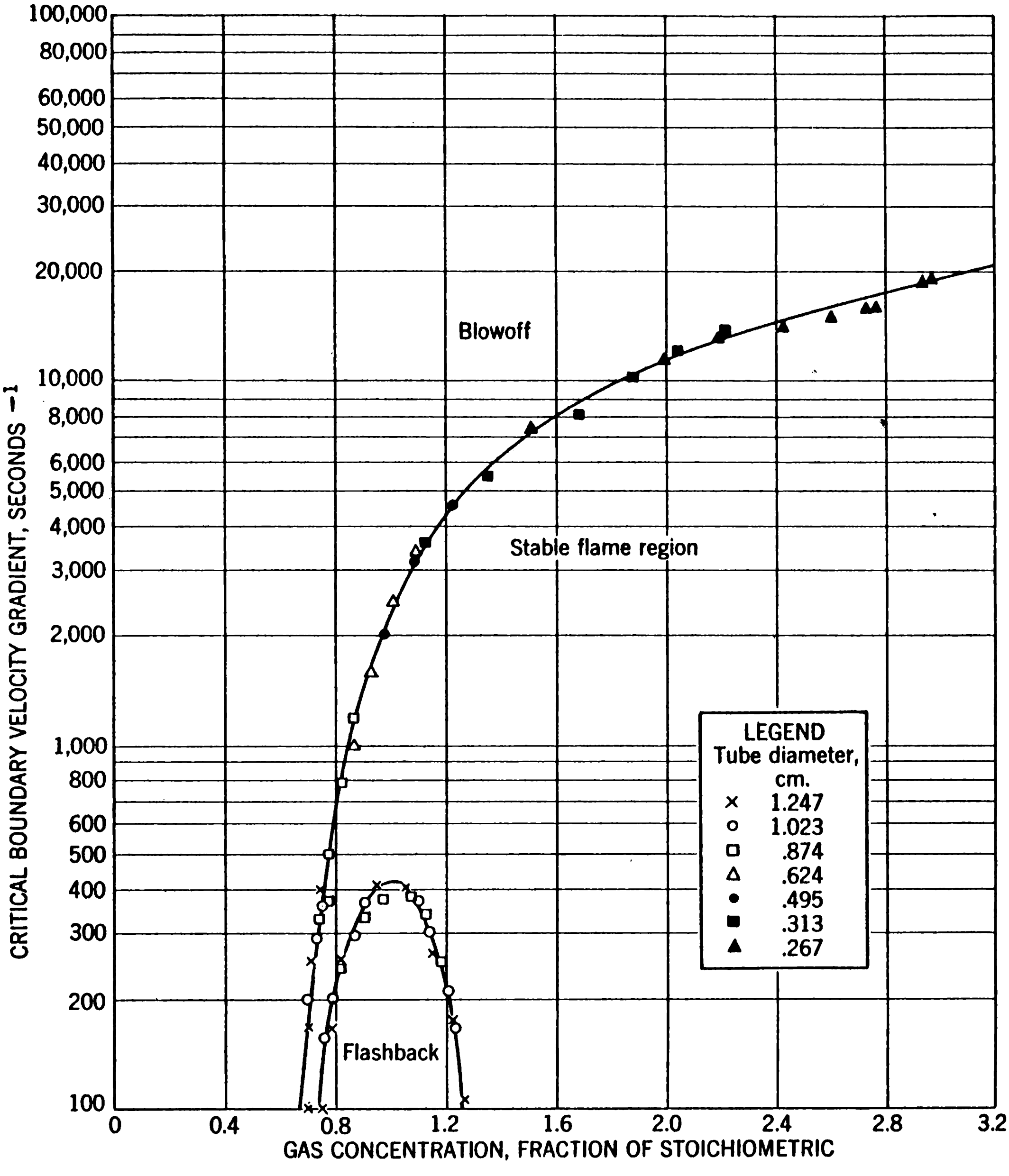

Figure 19. - Flame-stability diagram for fuel No. 1 (91.5% CH_4, 5.2% C_2H_6, 1.3% C_3H_8, 0.2% C_3H_6, 0.2% C_4H_{10}, 0.1% C_4H_8, 0.9% CO_2, 0.6% N_2).

components making up natural gas are very similar (see figure 9, p. 12), figure 19 may be used for all natural gases. Even natural gases containing low inerts can be represented by figure 19, as the data tabulated in (A-T/2a,2b-No./40) show that about 10 percent nitrogen does not seriously change the flame-stability limits of methane.

The diagram for 100 percent methane (A-T/1a,1b-No./2) is shown in figure 20.

Figure 21, for propane (A-T/1a,1b-No./3), differs little from figure 19 or 20. Liquid petroleum-air fuels, such as propane-air, also are represented by figure 21, because it does not matter to the flame whether combustible and air are mixed in 1 or 2 steps. To use figure 21 for a liquid-petroleum fuel, we need only remember that S, the mole fraction of fuel in a stoichiometric mixture, varies with the composition of the fuel, for example, S = 0.0402 for pure propane, and S = 0.0928 for an 1,120-B.t.u. propane-air fuel (43.3 percent propane - 56.7 percent air). This distinction is needed when converting F into percent fuel or percent primary air. Although the flashback and blowoff gradients were not measured for butane, other authors (32) have found that the flame-stability gradients of butane nearly coincide with those of propane.

The next diagram, figure 22, is for ethylene (A-T/1a,1b-No./4).

Figure 23 is for propylene (A-T/1a,1b-No./5).

Figure 24 is for the aromatic fuel benzene (A-T/1a,1b-No./6).

Figure 25 is for hydrogen (A-T/1a,1b-No./7).

Figure 26 is for a mixture of 88.9 percent carbon monoxide, 9.7 percent methane, 1.3 percent hydrogen, and 0.1 percent carbon dioxide (A-T/1a,1b-No./8). The flame-stability characteristics of absolutely pure carbon monoxide are drastically changed by the presence of small quantities of water or other hydrogen-bearing materials, such as hydrocarbons. The fuel used here is more typical of carbon monoxide in mixtures than would be the diagram for the absolutely pure material.

These experimental flame-stability diagrams are believed to meet the needs of the gas industry as regards flashback and blowoff limits for single-component fuels.

B. Flame-Stability Diagrams of Two-Component Fuels

The simplest method of representing binary mixtures of fuels is to assume that the flame-stability limits correspond to weighted averages of the critical gradients of the single components making up the mixture. This is the case for combinations of alkanes and alkenes, such as methane, ethane, propane, butane, and ethylene. For example, figure 27 is the flame-stability diagram of a mixture consisting of 79.4 percent methane and 20.6 percent ethylene (A-T/2a,2b,4-No./41). The points shown were determined experimentally; the curves were calculated by taking a weighted average of the gradients of the single components of the mixture, in the same way as we calculate the heating value or the specific gravity of a mixture. Thus,

$$g_{a+b+c+\ldots} = n_a g_a + n_b g_b + n_c g_c + \cdots, \qquad (4)$$

where g = the flashback or blowoff gradient of the component, and n = the mole fraction of each component in a multicomponent mixture. Values of g_a, g_b, etc., can

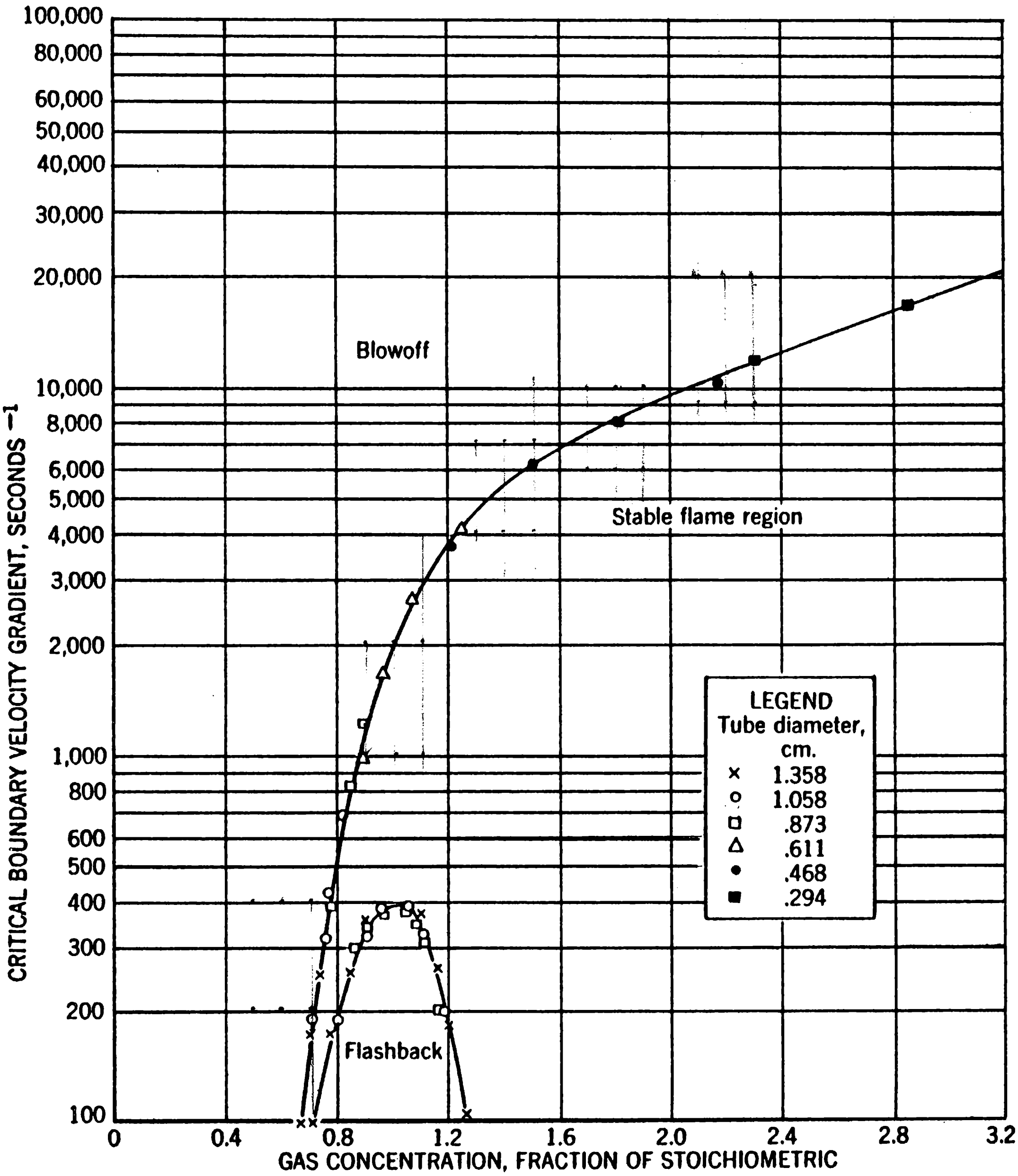

Figure 20. - Flame-stability diagram for fuel No. 2 (100% CH_4).

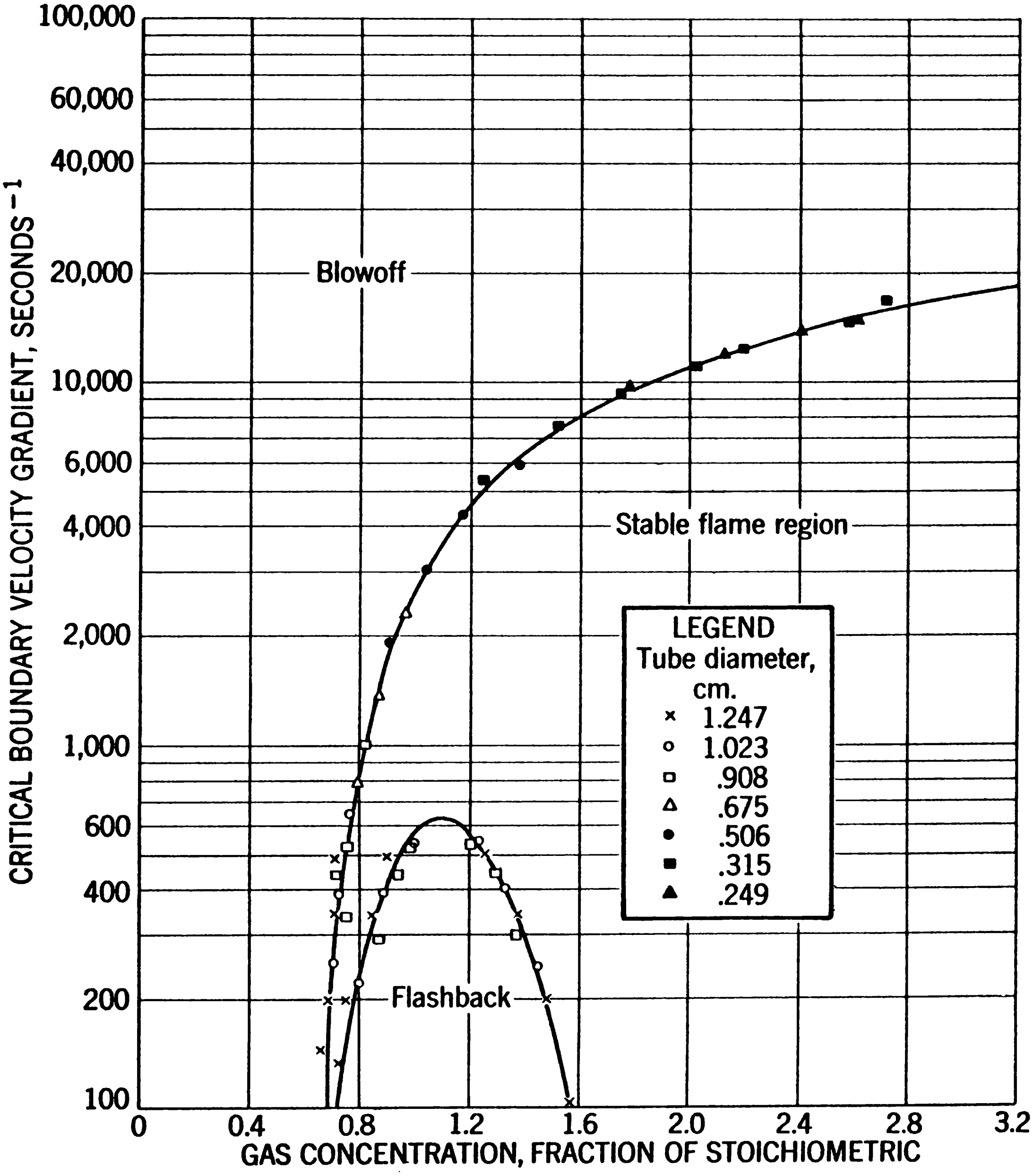

Figure 21. - Flame-stability diagram for fuel No. 3 (98.6% C_3H_8, 1.4% C_3H_6).

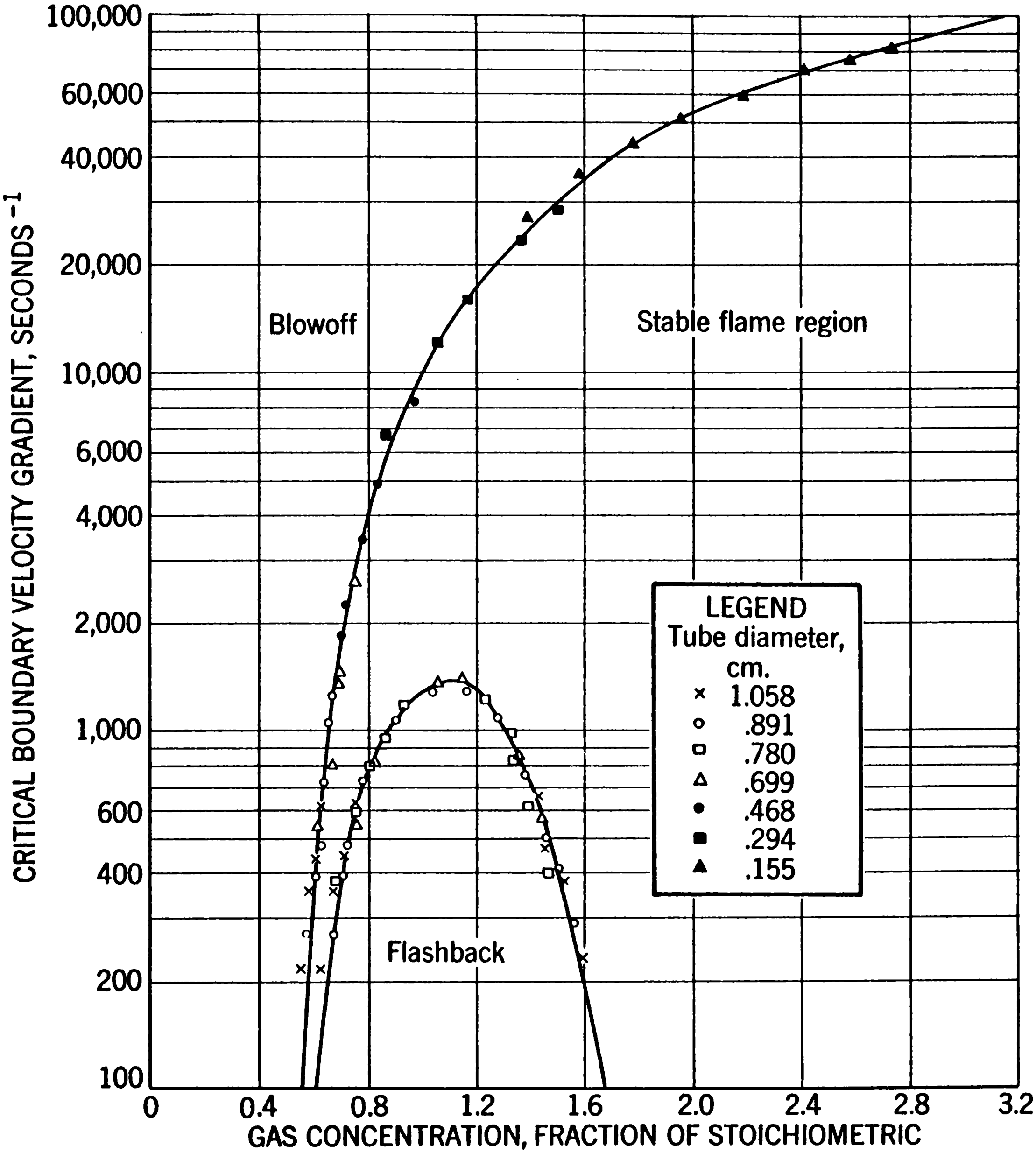

Figure 22. - Flame-stability diagram for fuel No. 4 (99.7% C_2H_4, 0.2% C_4H_8, 0.1% C_3H_6).

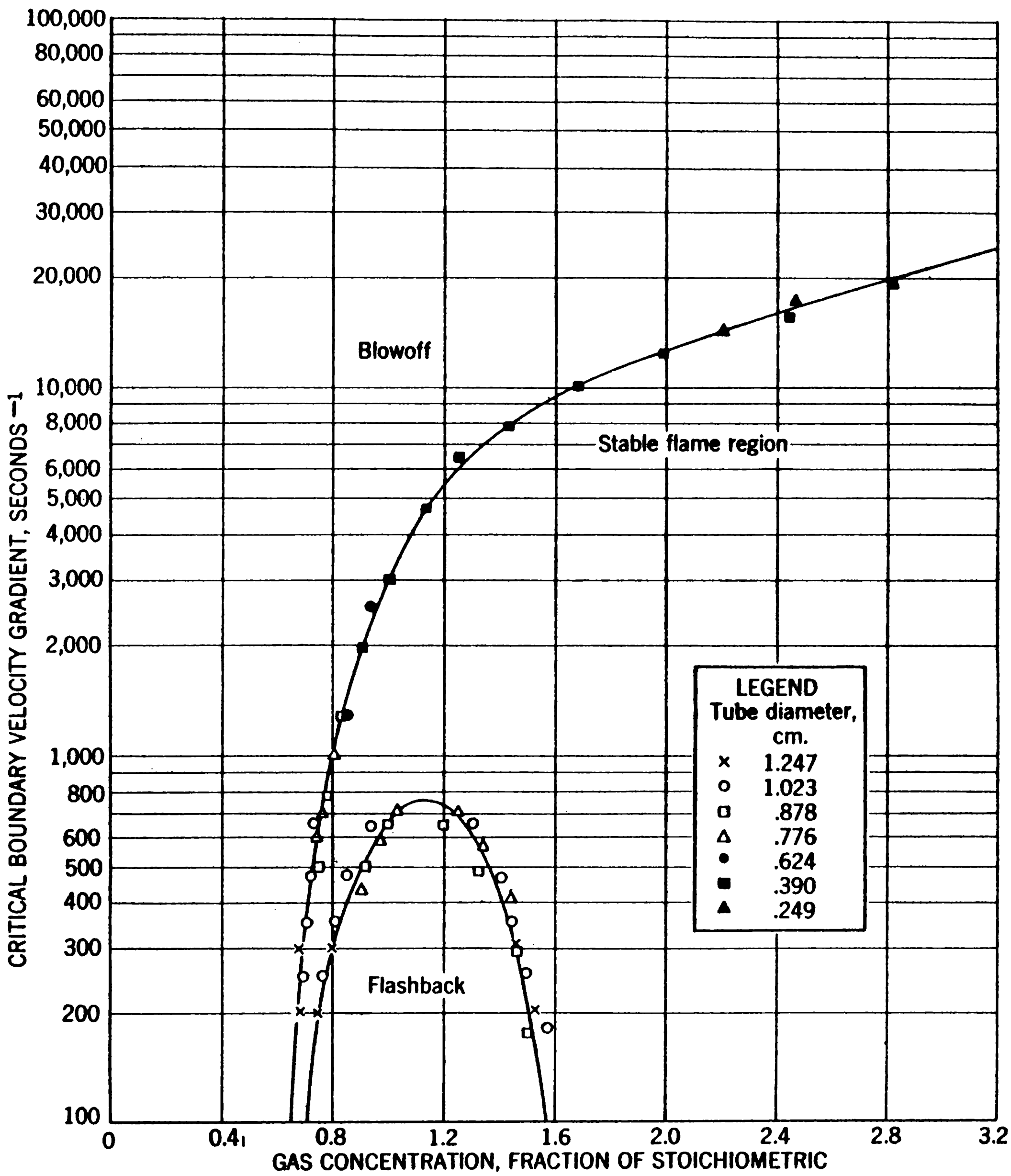

Figure 23. - Flame-stability diagram for fuel No. 5 (99.2% C_3H_6, 0.4% C_2H_6, 0.4% C_3H_8).

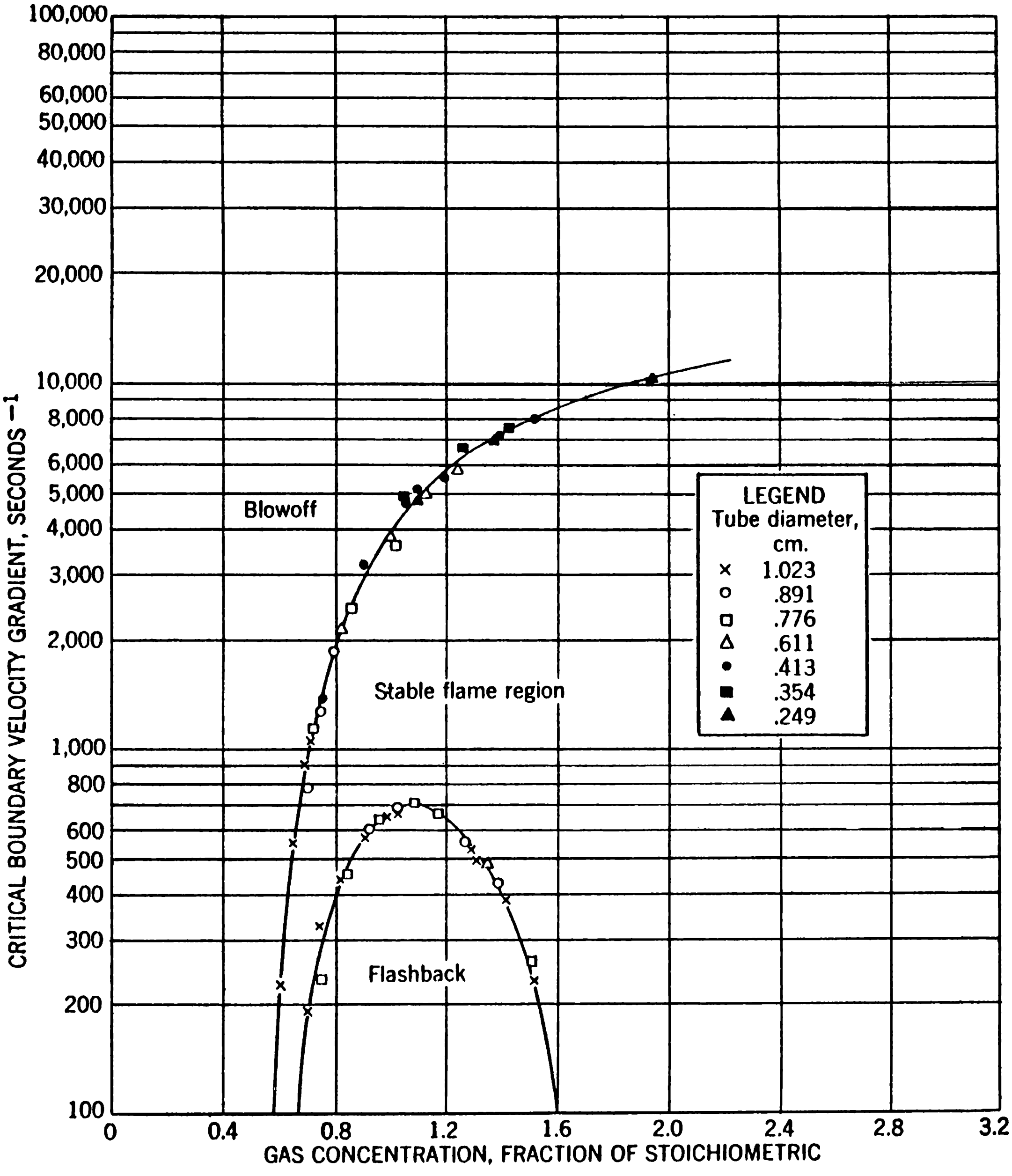

Figure 24. - Flame-stability diagram for fuel No. 6 (100% C_6H_6).

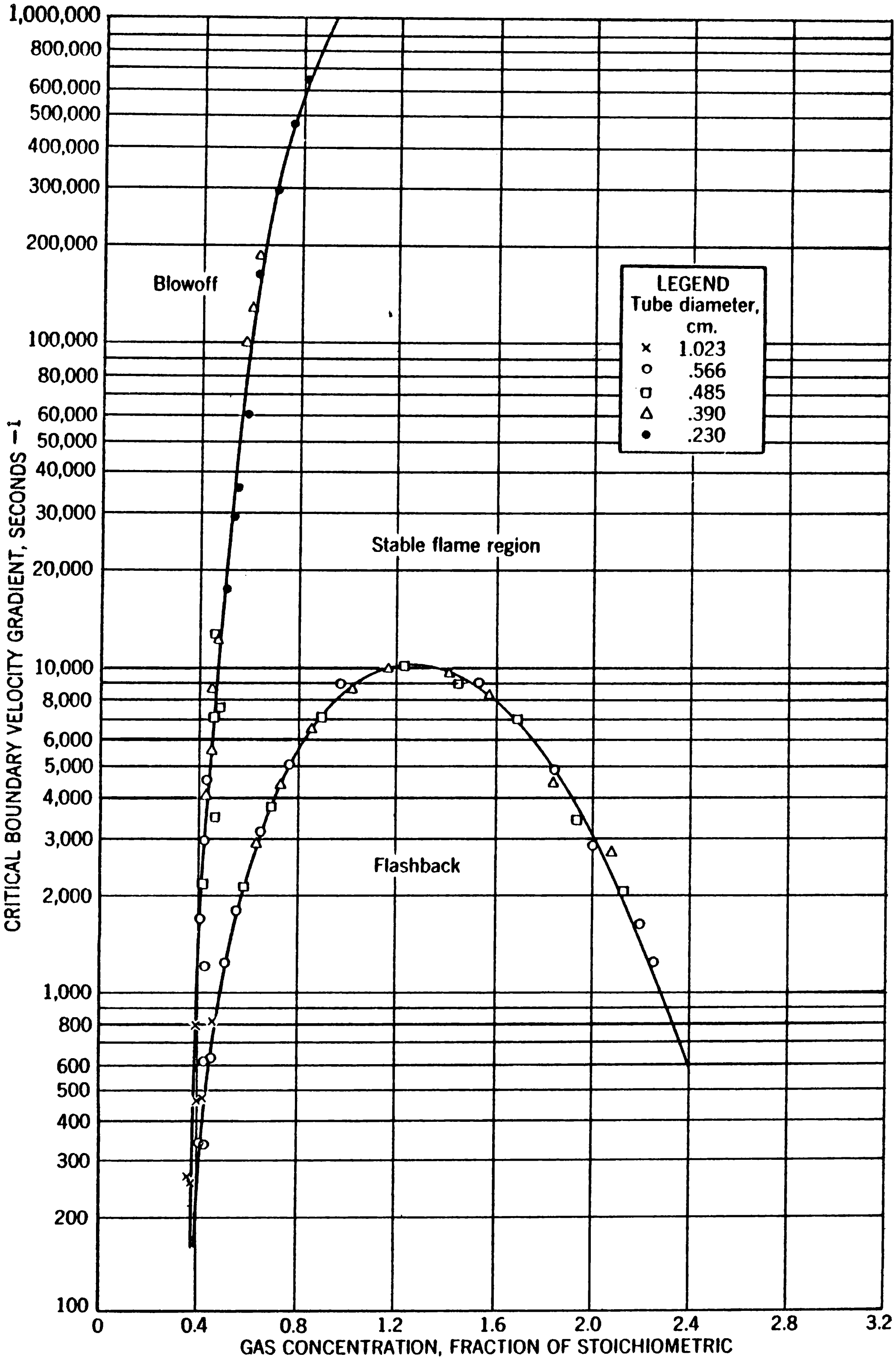

Figure 25. - Flame-stability diagram for fuel No. 7 (99.7% H_2, 0.3% O_2).

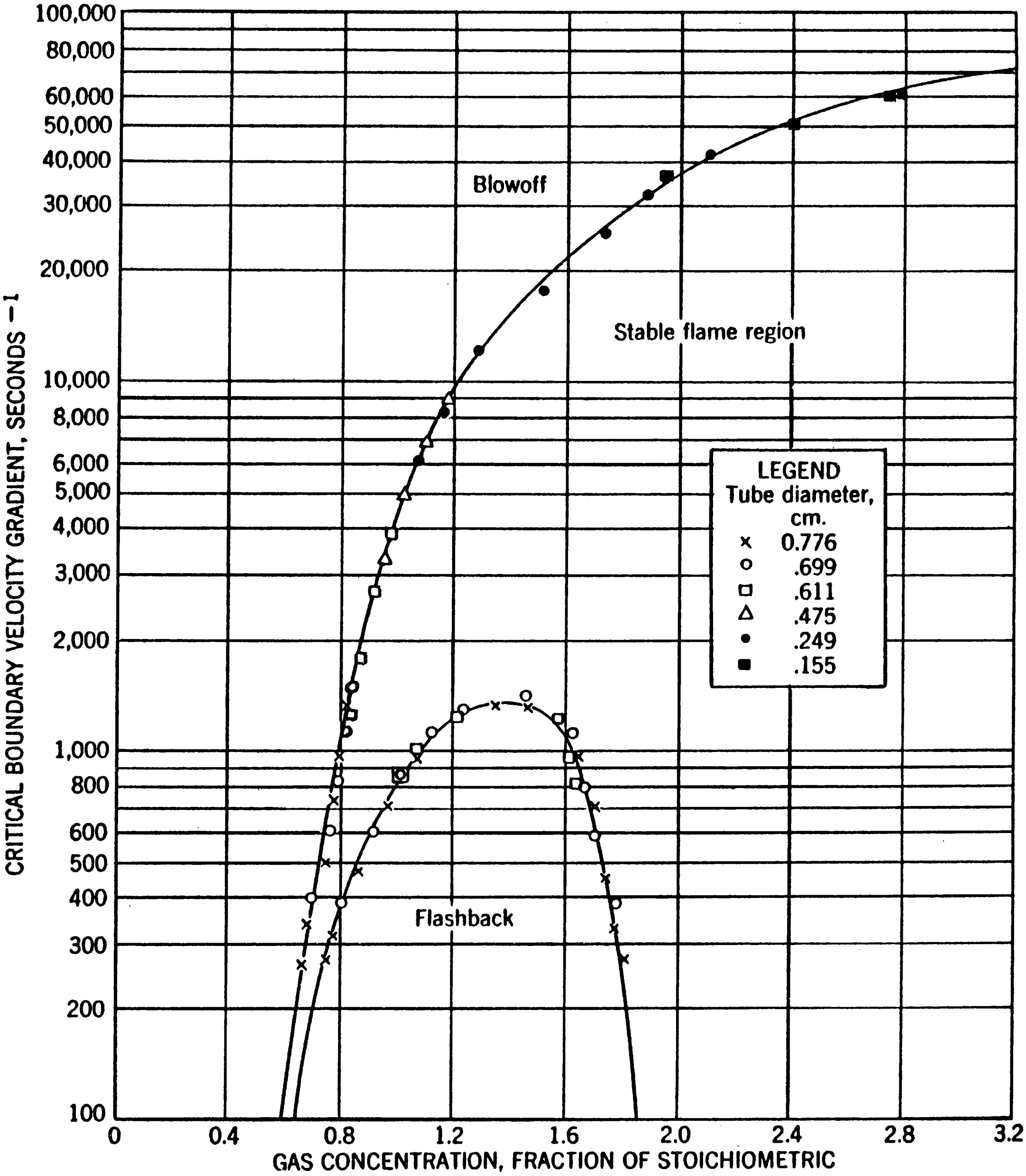

Figure 26. - Flame-stability diagram for fuel No. 8 (88.9% CO, 9.7% CH_4, 1.3% H_2, 0.1% CO_2).

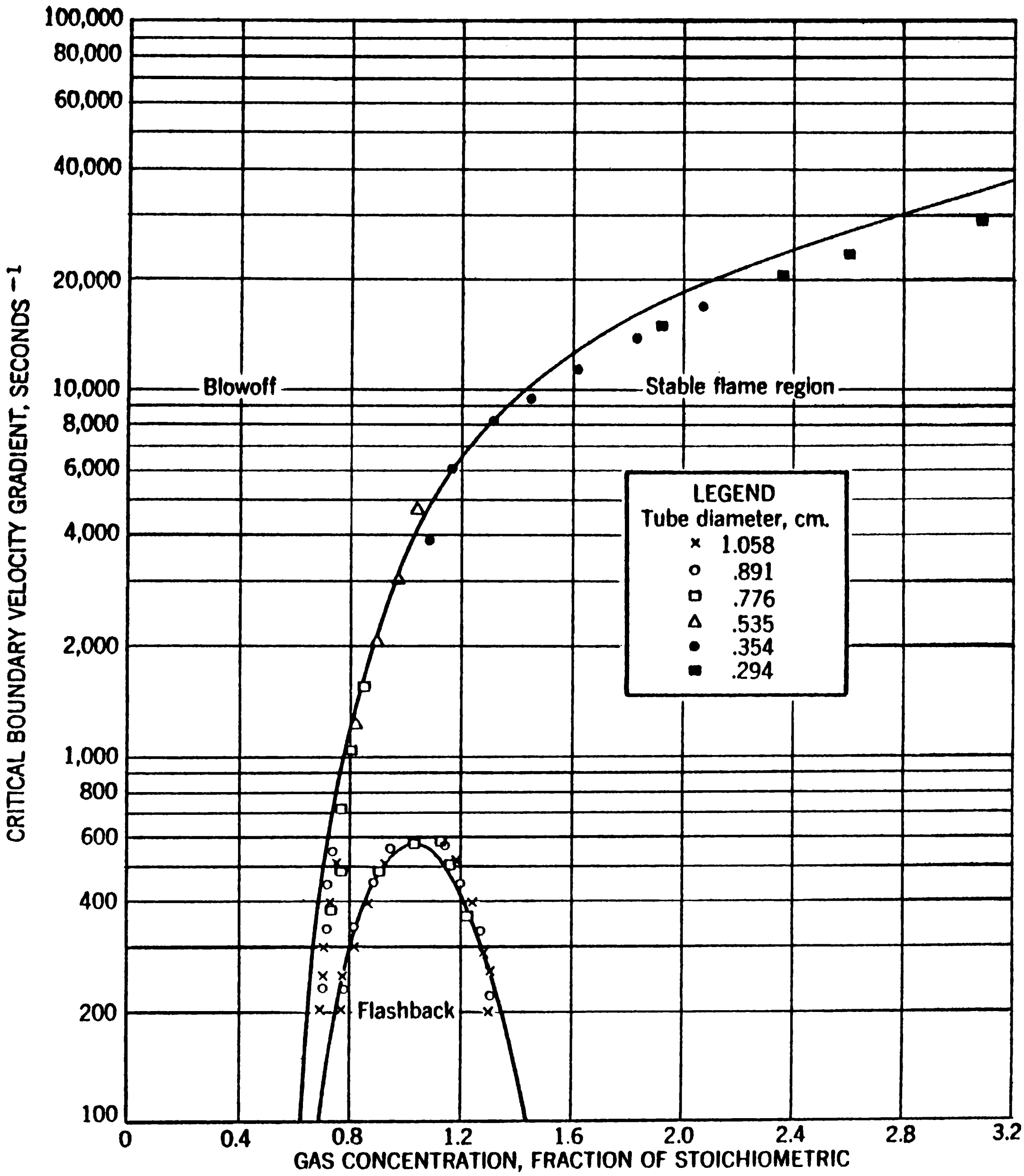

Figure 27. - Flame-stability diagram for fuel No. 41 (79.4% CH_4, 20.6% C_2H_4); comparison of calculated curves and experimental points.

be read from the pertinent flame-stability diagram in section A of this chapter. The agreement between the experimental points and the calculated curve is excellent for this fuel. A second mixture, containing 78.6 percent ethylene and 21.4 percent methane, shows equally good agreement with curves predicted by means of equation 4 (A-T/2a,2b,4-No./42).

However, not all binary mixtures of combustibles lend themselves to this simple procedure. In all these exceptions the binary mixture contains hydrogen or carbon monoxide. In such instances recourse is taken to the following graphical method.

Flame-stability diagrams are measured for a number of mixtures of two single gases, covering the concentration range of 0 to 100 percent for each gas. The resulting data obtained are used to construct composite flame-stability diagrams for corresponding binary mixtures, such as figure 28, which summarizes the flashback gradients for all mixtures of methane and hydrogen. Such graphs show a family of curves along each of which the fuel-air composition, F, expressed as gas concentration, fraction of stoichiometric, is constant. Each curve of constant fuel-air composition is a plot of critical boundary velocity gradients for flashback versus ratios of methane to hydrogen. From 0 to 50 percent hydrogen, the ratio plotted as the abscissa is hydrogen/methane; and from 50 to 100 percent hydrogen, it is methane/hydrogen. This avoids a value of infinity. Figure 28 can be used to draw the flashback curve of a particular methane-hydrogen fuel by taking the ordinates on each F curve corresponding to the desired hydrogen-methane ratio and plotting these ordinates (critical boundary velocity gradients for flashback) against the F values. Similarly, figure 29 summarizes the blowoff gradients for all methane-hydrogen mixtures and makes it possible to plot the blowoff curve for any mixture (A-T/2a,2b-No./9,10,11,12,13,14,15). The graphical method is applicable to any binary system of gases. It makes for ready interpolation between measured data and eliminates the experimental measurement of flame-stability characteristics for every possible combination of two single fuels.

Similarly, figures 30 and 31 are for the binary system of carbon monoxide-hydrogen (A-T/2a,2b-No./16,17,18,19,20,21,22,23).

Figures 32 and 33 are for the binary system of methane-carbon monoxide (A-T/2a,2b-No./8,24,25,26,27).

Figures 34 and 35 are for binary mixtures of propane-hydrogen (A-T/2a,2b-No./28,29,30,31).

Figures 36 and 37 are for binary mixtures of ethylene-hydrogen (A-T/2a,2b-No./32,33,34,35,36).

Figures 38 and 39 are for binary mixtures of nitrogen-hydrogen (A-T/2a,2b-No./37,38,39).

To illustrate the use of these diagrams, let us calculate flashback and blowoff curves from composite flame-stability diagrams for an 83.3-percent carbon monoxide and 16.7-percent hydrogen fuel (see figures 30 and 31).

Intercepts for flashback (table 2, columns F_F and g_F) are obtained from figure 30, the composite diagram for flashback of carbon monoxide-hydrogen fuels. Similarly, intercepts for blowoff (table 2, columns F_B and g_B) are obtained from figure 31, the composite diagram for blowoff of carbon monoxide-hydrogen fuels. A plot of these intercepts is presented in figure 40, which is the flame-stability diagram for our particular carbon monoxide-hydrogen fuel.

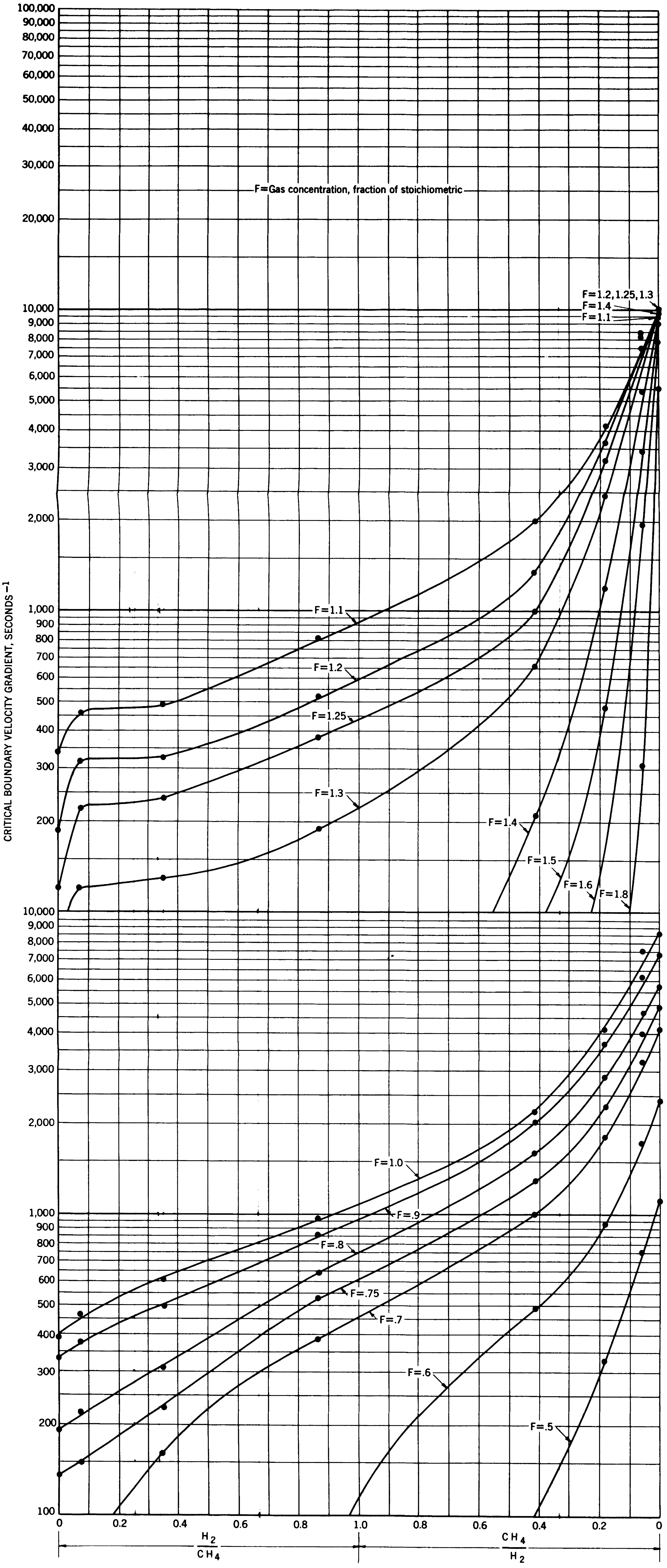

Figure 28. - Critical boundary velocity gradients for flashback of methane-hydrogen fuels; composite diagram.

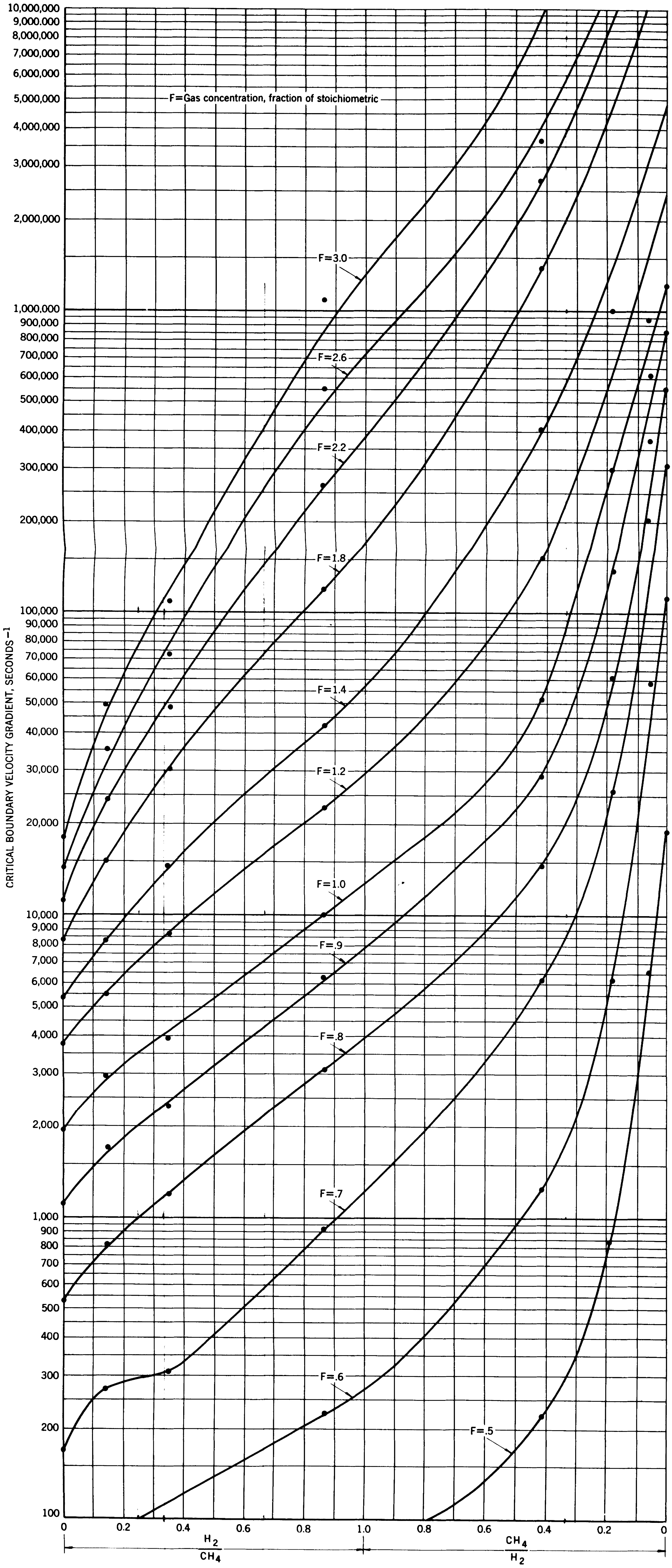

Figure 29. - Critical boundary velocity gradients for blowoff of methane-hydrogen fuels; composite diagram.

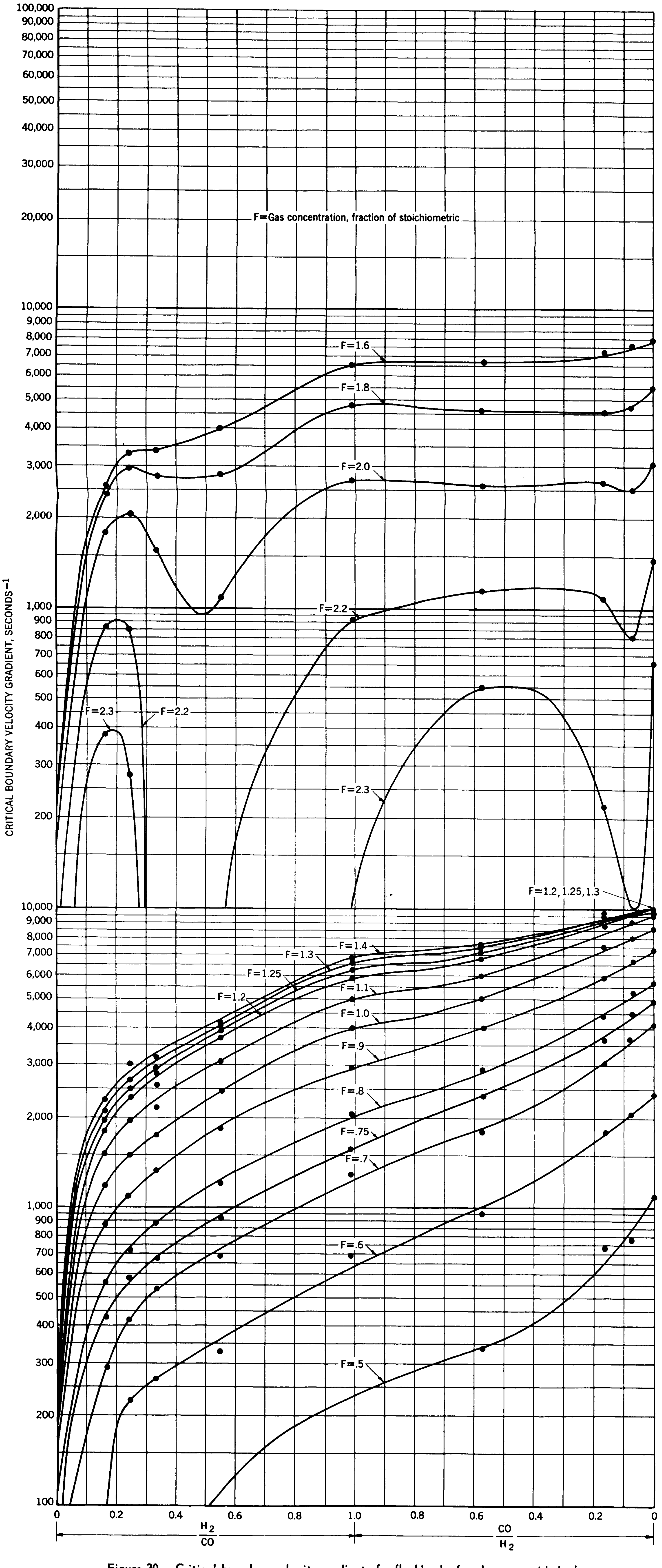

Figure 30. - Critical boundary velocity gradients for flashback of carbon monoxide-hydrogen fuels; composite diagram.

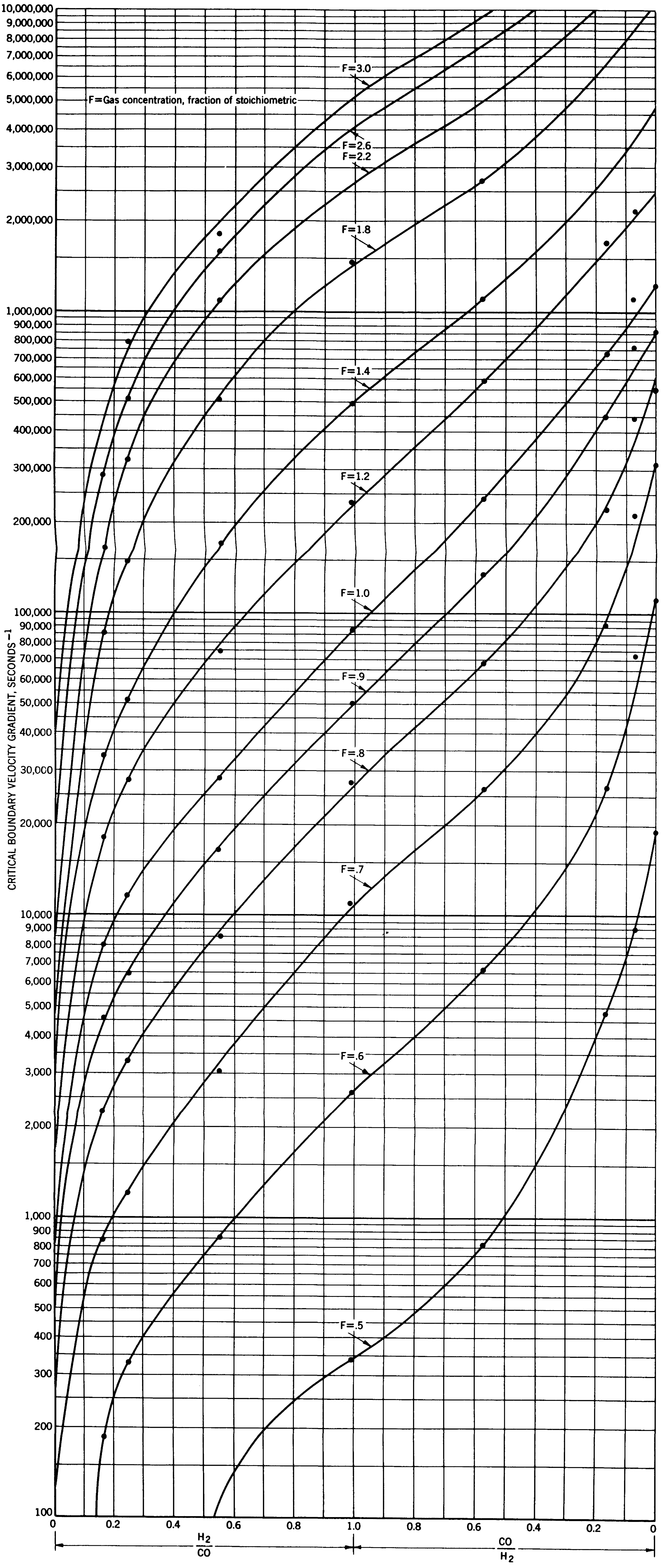

Figure 31. - Critical boundary velocity gradients for blowoff of carbon monoxide-hydrogen fuels; composite diagram.

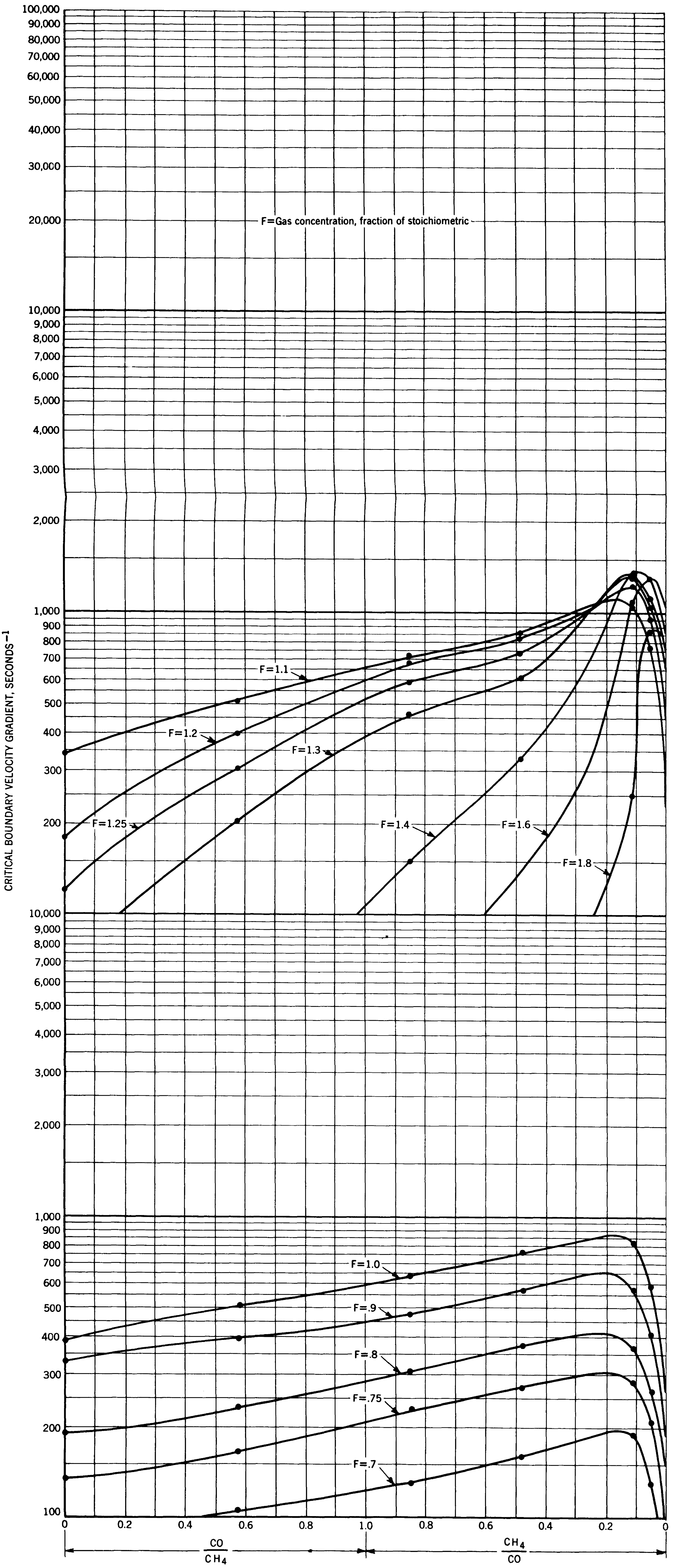

Figure 32. - Critical boundary velocity gradients for flashback of methane-carbon monoxide fuels; composite diagram.

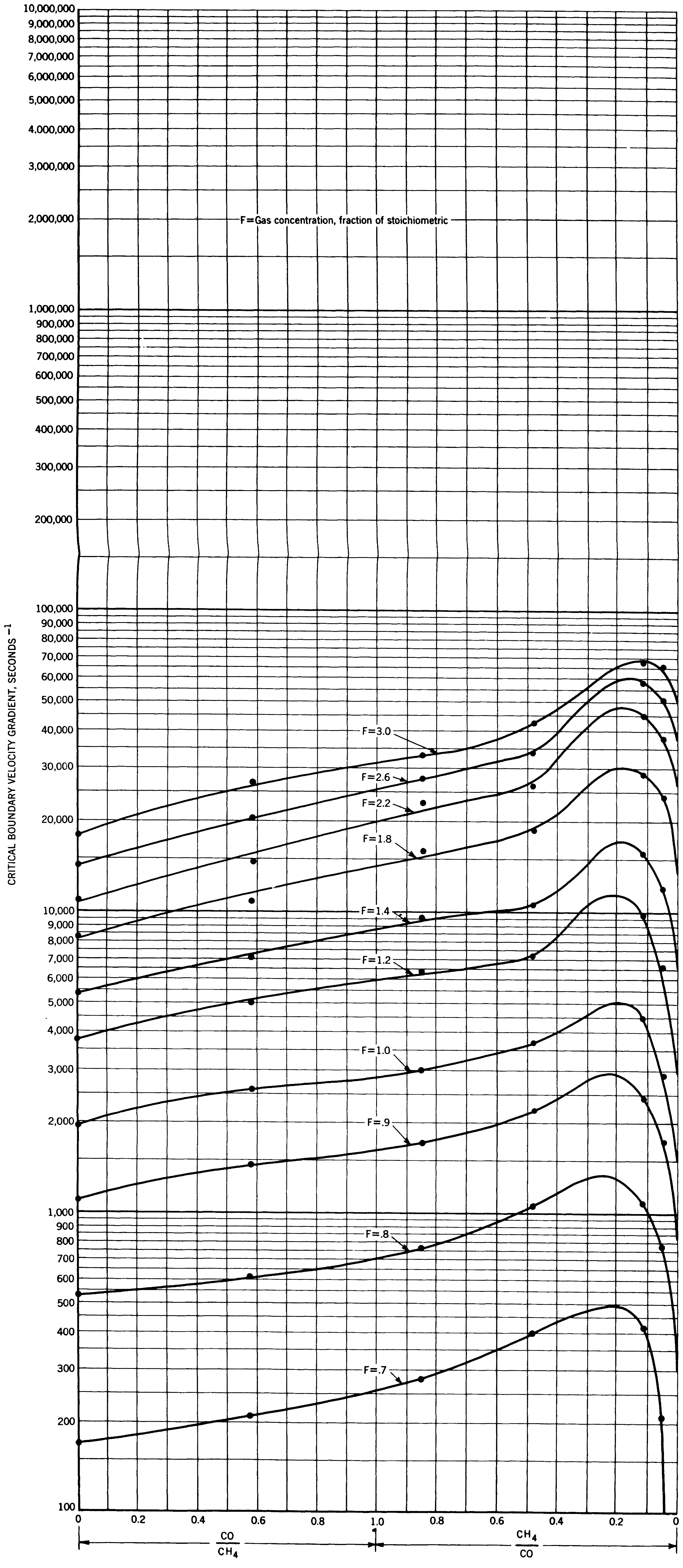

Figure 33. - Critical boundary velocity gradients for blowoff of methane-carbon monoxide fuels; composite diagram.

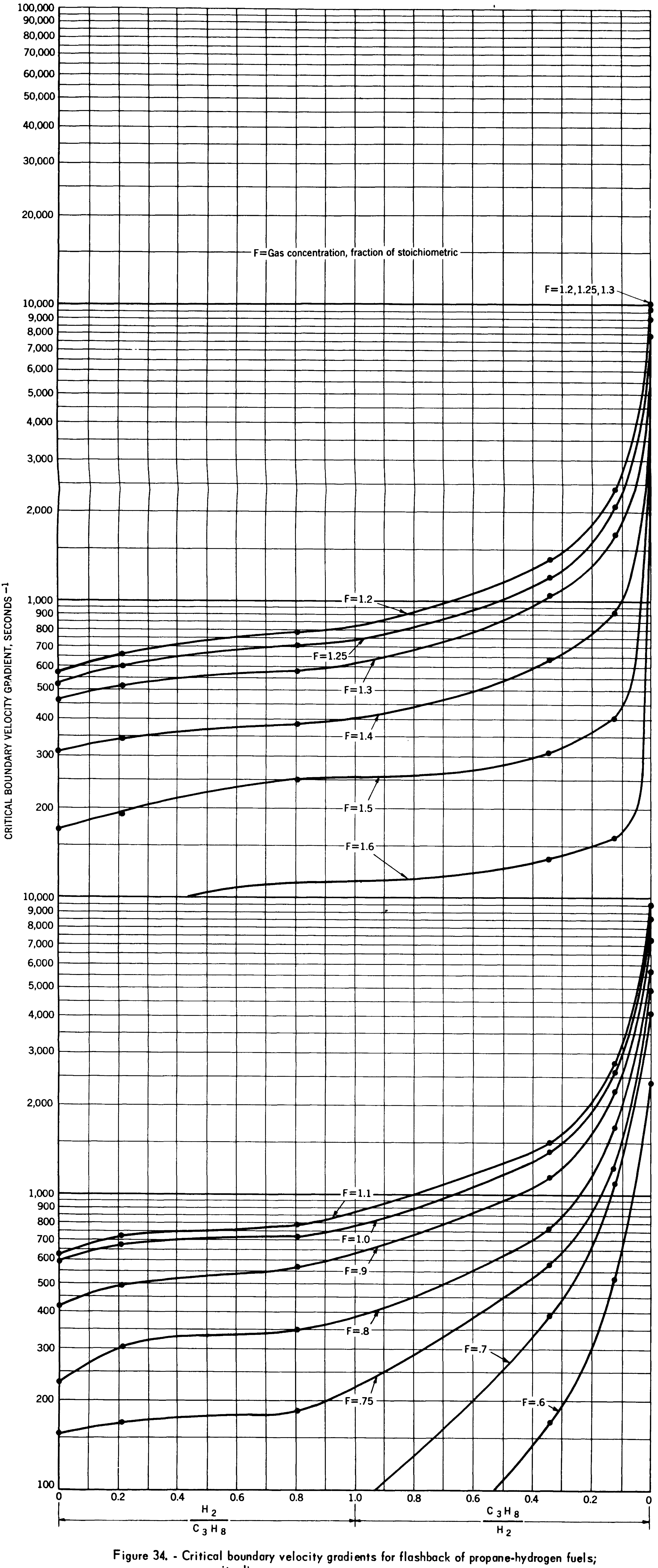

Figure 34. - Critical boundary velocity gradients for flashback of propane-hydrogen fuels; composite diagram.

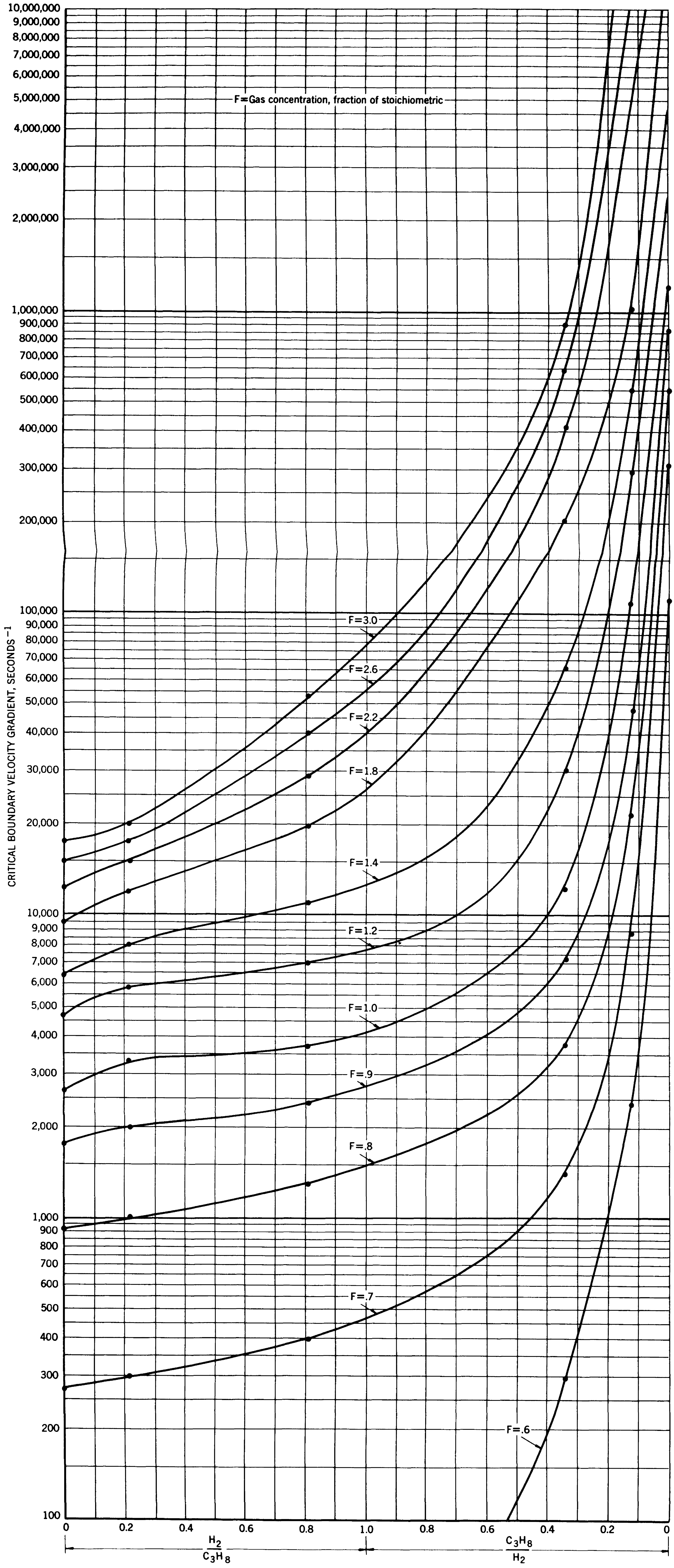

Figure 35. - Critical boundary velocity gradients for blowoff of propane-hydrogen fuels; composite diagram.

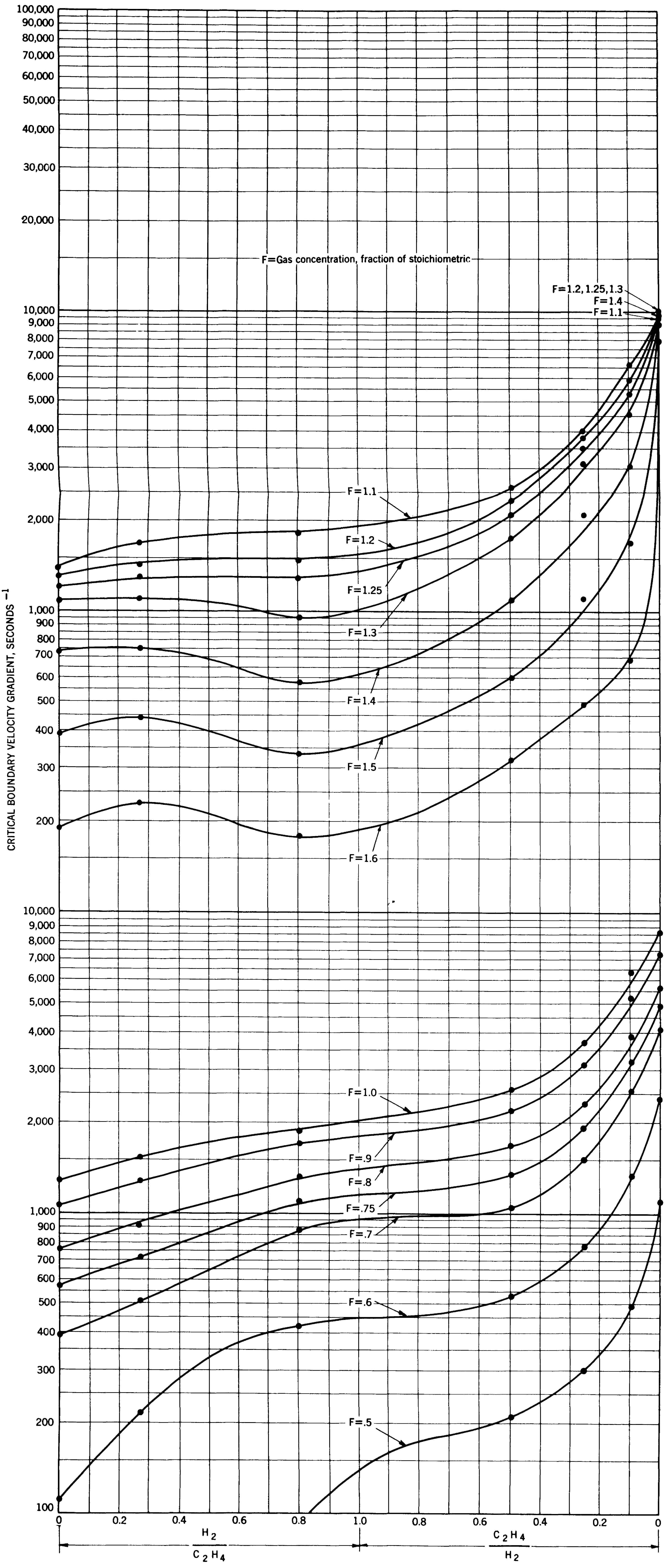

Figure 36. - Critical boundary velocity gradients for flashback of ethylene-hydrogen fuels; composite diagram.

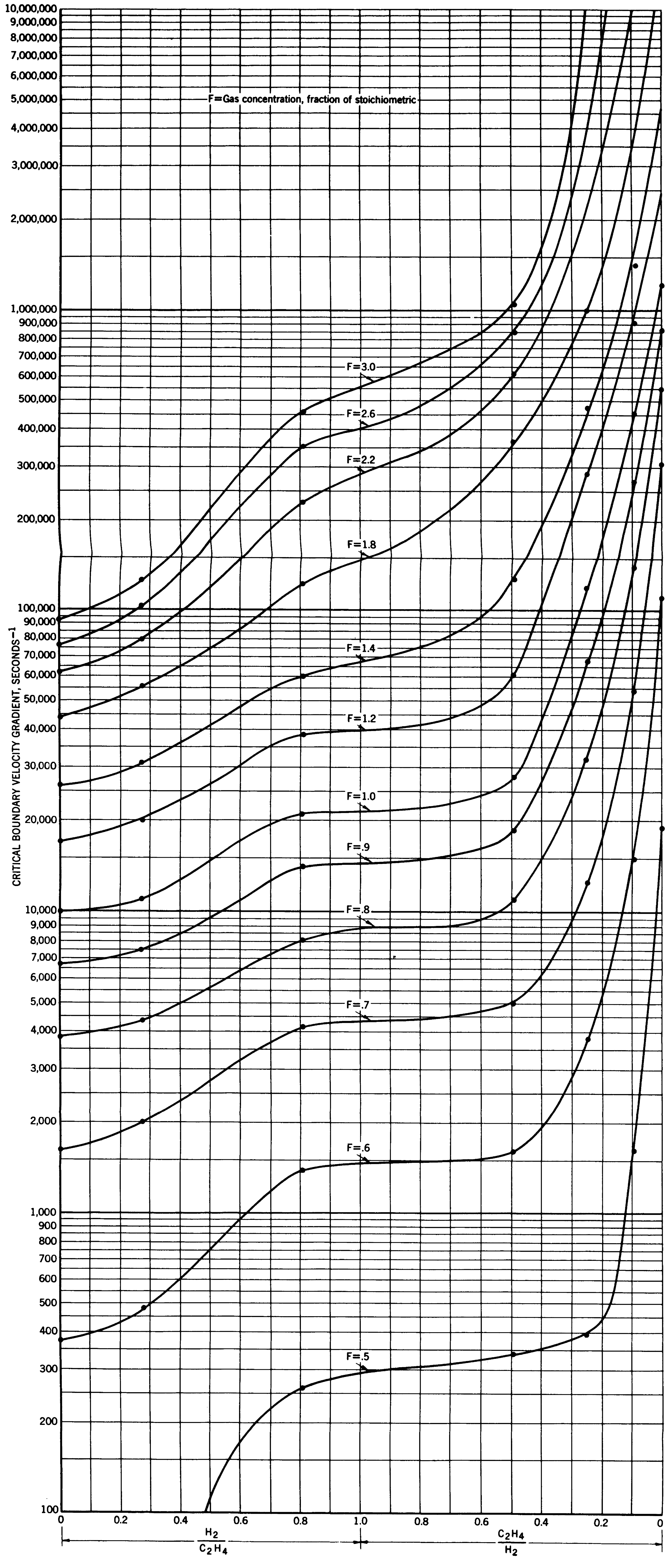

Figure 37. - Critical boundary velocity gradients for blowoff of ethylene-hydrogen fuels; composite diagram.

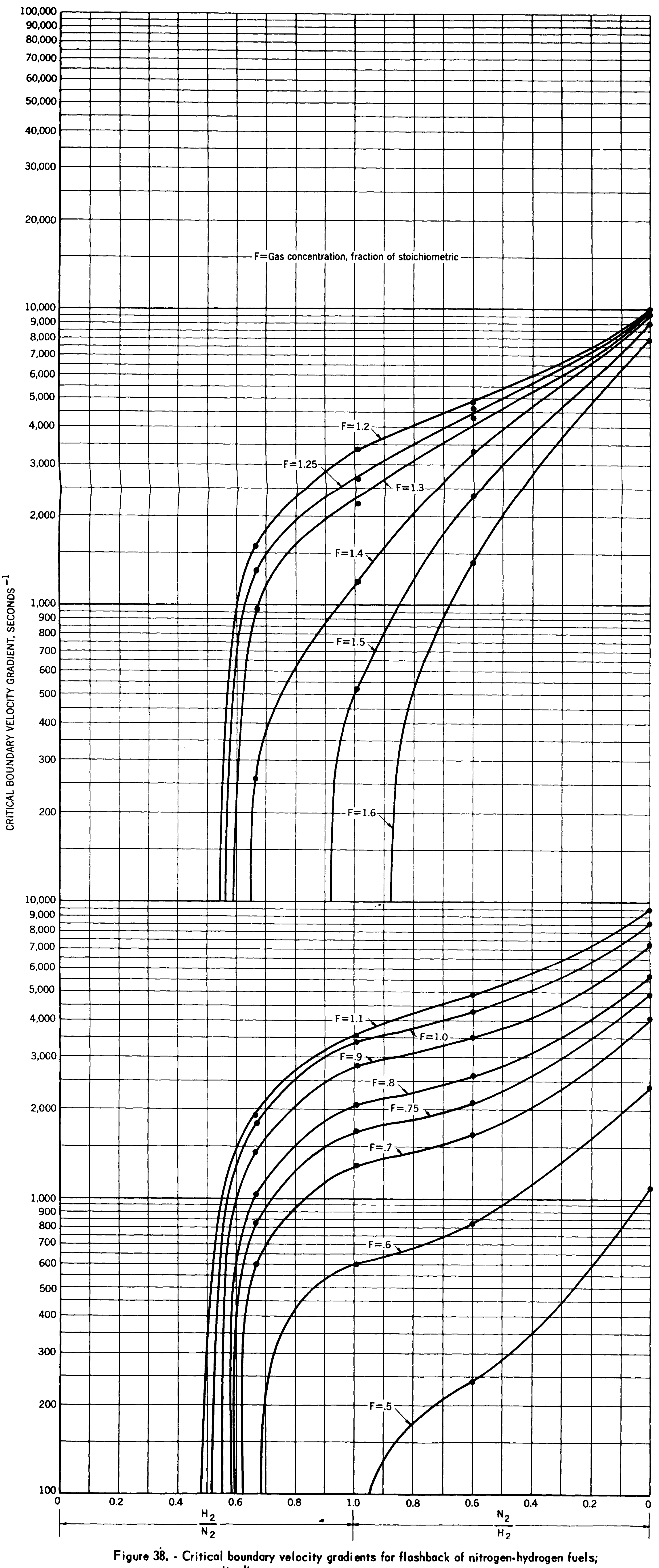

Figure 38. - Critical boundary velocity gradients for flashback of nitrogen-hydrogen fuels; composite diagram.

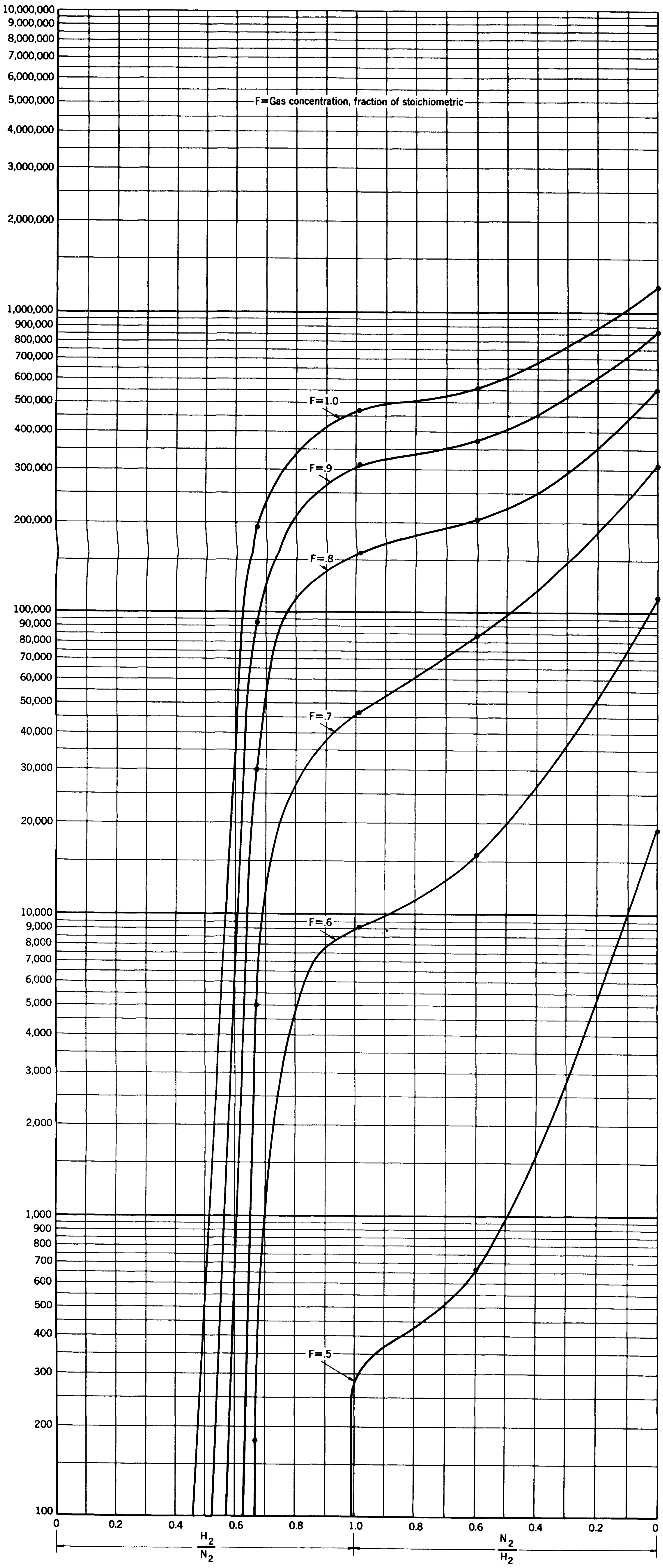

Figure 39. - Critical boundary velocity gradients for blowoff of nitrogen-hydrogen fuels; composite diagram.

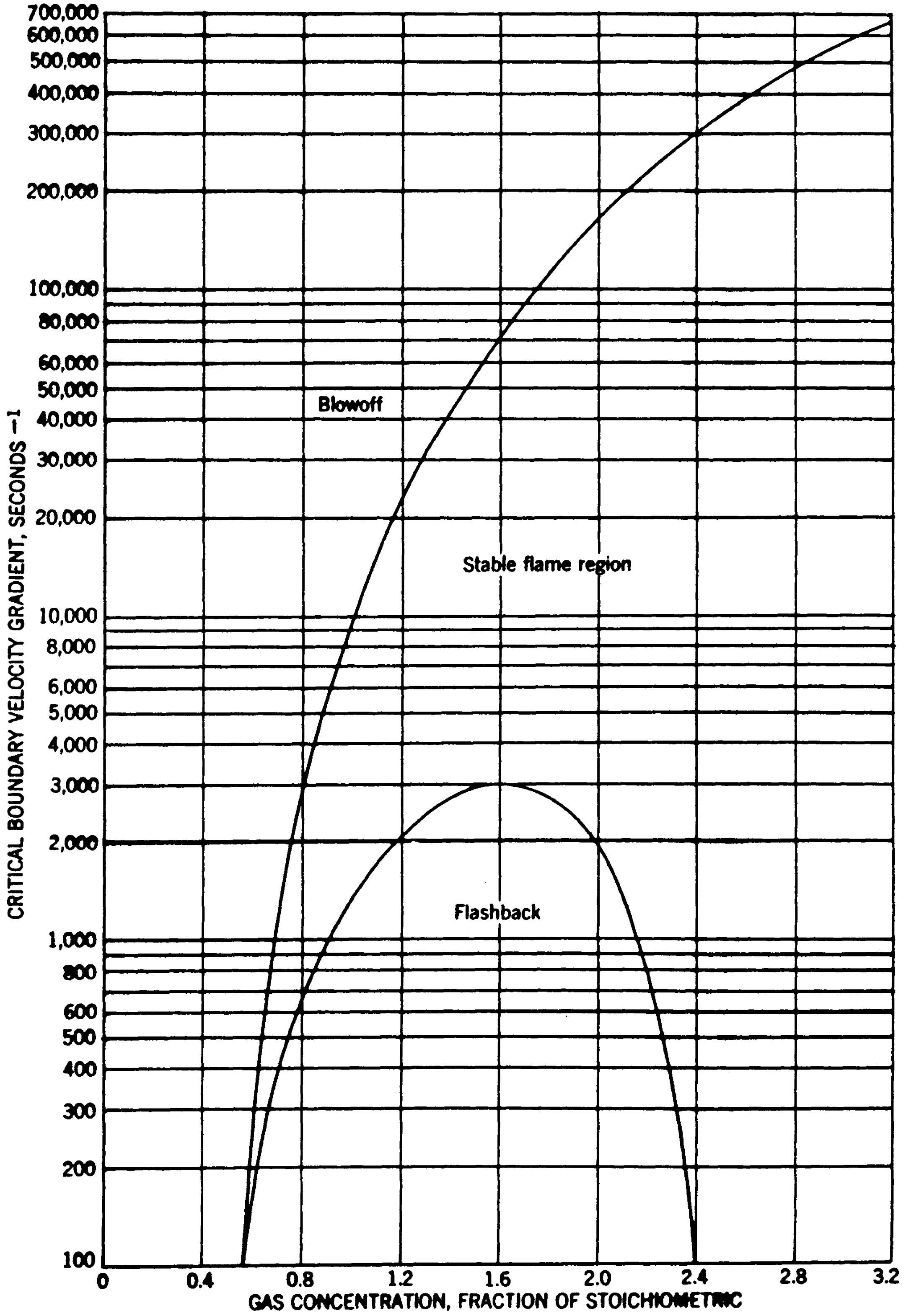

Figure 40. - Flame-stability diagram for 83.3% CO, 16.7% H_2.

TABLE 2. - Flashback and blowoff gradients for a two-component fuel, taken from composite flame-stability diagrams

Composition, percent: 83.3 CO, 16.7 H_2
H_2/CO = 16.7/83.3 = 0.20

F_F or F_B	g_F (figure 30)	g_B (figure 31)
0.6	175	250
.7	345	1,000
.75	490	
.8	635	2,700
.9	965	5,300
1.0	1,310	9,500
1.1	1,700	
1.2	2,030	22,000
1.25	2,200	
1.3	2,400	
1.4	2,550	41,000
1.6	3,000	
1.8	2,750	111,000
2.0	1,970	
2.2	810	225,000
2.3	390	
2.6		380,000
3.0		560,000

C. Flame-Stability Diagrams of Multicomponent Fuels

The task of organizing flame-stability data for multicomponent fuels is more complex. As it would be impractical to make measurements with every possible combination of some dozen constituents that may occur in fuels distributed by utilities, a method of calculation was developed based on the flame-stability gradients of single- and two-component fuels. This method assumes that, although addition of the weighted averages of the flashback and blowoff gradients for two single-component fuels does not always yield the gradients of the corresponding binary mixture, the gradients of binary fuels and some single fuels probably can be combined satisfactorily to give the gradients of multicomponent fuels. In effect, it was decided to treat binary complexes as new, hybridlike, single-component fuels, wherein all the original nonlinearity of the single components would be absorbed in the measured behavior of the binary complex.

Let us consider a three-component mixture of methane, hydrogen, and carbon monoxide. Which are the hybrids? Is it methane-hydrogen, methane-carbon monoxide, carbon monoxide-hydrogen, or all three? The question must be answered empirically. The only restrictions on the method are that the hybrid or hybrids chosen must be reasonable and consistently applicable to an extensive group of fuels that are related by their chemical analyses. These specifications have been tested for 25 multicomponent fuels which may be grouped as follows:

(1) The coke-oven gases, consisting essentially of methane, hydrogen, and carbon monoxide, with or without inerts.

(2) The oil gases, consisting essentially of ethylene, hydrogen, and methane with or without inerts, ethylene concentration varying between 10 to 50 percent.

(3) High-ethylene fuels containing hydrogen, where the ethylene content exceeds 50 percent and hydrogen is present in fair amounts.

1. Coke-Oven Gases

These fuels consist essentially of hydrogen, methane, and carbon monoxide, although other components may be present in small amounts. A gas of this type is fuel No. 43 (A-T/3a,3b,4-No./43), which simulates a real coke-oven gas. It contains 58.4 percent H_2, 26.3 percent CH_4, 10.6 percent CO, 4.6 percent N_2, and 0.1 percent CO_2. The method of calculating critical boundary velocity gradients for flashback and blowoff for this type of fuel is illustrated in tables 3a and 3b of this chapter, which are also part of table 4 of the Appendix.

The flashback and blowoff gradients of any multicomponent fuel are calculated by equation 4:

$$g_{a+b+c+\dots} = n_a g_a + n_b g_b + n_c g_c + \dots, \qquad (4)$$

where g = the flashback or blowoff gradient of the hybrid component and n = the mole fraction of each component in a multicomponent mixture. It can be seen from table 3a that, to calculate the critical boundary velocity gradients for flashback of a coke-oven-type fuel, one considers the fuel as made up of the hybrids (methane + carbon monoxide) and (methane + hydrogen). As methane appears in both hybrids it must be proportioned between the carbon monoxide and the hydrogen. This is done on the basis of the relative amounts of carbon monoxide and hydrogen in the fuel:

$$\frac{10.6\%\ CO}{10.6\%\ CO + 58.4\%\ H_2}(26.3\%\ CH_4) = 4.04\%\ (CH_4\ \text{going with}\ CO);$$

$$CH_4/CO = 4.04/10.6 = 0.381.$$

$$\frac{58.4\%\ H_2}{10.6\%\ CO + 58.4\%\ H_2}(26.3\%\ CH_4) = 22.26\%\ (CH_4\ \text{going with}\ H_2);$$

$$CH_4/H_2 = 22.26/58.4 = 0.381.$$

Adding the indicated percentages of methane to the carbon monoxide and to the hydrogen, respectively, we obtain the percentage of each hybrid in the total fuel:

$4.04\%\ CH_4 + 10.6\%\ CO = 14.64\%$ (methane + carbon monoxide);

$22.26\%\ CH_4 + 58.4\%\ H_2 = 80.66\%$ (methane + hydrogen).

Columns F_F and A of table 3a give the flashback coordinates of a hybrid (methane + carbon monoxide) where the ratio of methane to carbon monoxide is 0.381. These coordinates are obtained from figure 32. The appropriate values of g_F are multiplied by the percent of this hybrid in the fuel (14.64%), and the answer is recorded in column B. This is the contribution of the (methane + carbon monoxide) hybrid to the flashback gradient of the total fuel. The contribution of the (methane + hydrogen) hybrid is obtained in the same way (see columns F_F, C, and D). Columns B and D are added to give column (B + D), which lists the critical boundary velocity gradient for flashback of the total fuel in accord with equation 4. Columns F_F and (B + D) list the coordinates for the calculated flashback curve of fuel No. 43.

TABLE 3a. - Calculation of flashback curve for fuel No. 43 by linear mixture rule

Mixture composition, percent: 58.4 H_2, 26.3 CH_4, 10.6 CO, 4.6 N_2, 0.1 CO_2
Stoichiometric percentage: 19.4

Complexes for flashback: (CH_4 + CO)(CH_4 + H_2)(N_2 and CO_2).
Calc. of complexes:
(10.6/10.6 + 58.4) x 26.3 = 4.04 (CH_4 going with CO); CH_4/CO = 4.04/10.6 = 0.381;
(58.4/10.6 + 58.4) x 26.3 = 22.26 (CH_4 going with H_2); CH_4/H_2 = 22.26/58.4 = 0.381.
Total percentage of CH_4/CO = 4.04 + 10.6 = 14.64.
Total percentage of CH_4/H_2 = 22.26 + 58.4 = 80.66.

F_F	A (figure 32) g_F for CH_4/CO = 0.381	B A x 0.1464	C (figure 28) g_F for CH_4/H_2 = 0.381	D C x 0.8066	B+D g_F for total fuel
0.5	1/	1/	117	94	94
.6			520	420	420
.7	170	25	1,070	864	889
.75	285	42	1,370	1,105	1,147
.8	390	57	1,700	1,370	1,427
.9	605	89	2,160	1,743	1,832
1.0	795	116	2,400	1,935	2,051
1.1	950	139	2,150	1,735	1,874
1.2	910	133	1,530	1,235	1,368
1.25	845	124	1,140	920	1,044
1.3	735	108	765	617	725
1.4	440	64	250	202	266
1.6	190	28	100	81	109

TABLE 3b. - Calculation of blowoff curve for fuel No. 43 by linear mixture rule

Complexes for blowoff: (CH_4 + H_2)(H_2/CO = 0.20)(N_2 and CO_2).
Calc. of complexes:
H_2/CO = 0.20, 0.20 x 10.6 = 2.12 (H_2 going with CO); H_2/CO = 2.12/10.6 = 0.20;
58.4 - 2.12 = 56.28 (H_2 going with CH_4); CH_4/H_2 = 26.3/56.28 = 0.467.
Total percentage of H_2/CO = 2.12 + 10.6 = 12.72.
Total percentage of CH_4/H_2 = 26.3 + 56.28 = 82.58.

F_B	A (figure 31) g_B for H_2/CO = 0.20	B A x 0.1272	C (figure 29) g_B for CH_4/H_2 = 0.467	D C x 0.8258	B+D g_B for total fuel
0.5	1/	1/	185	153	153
.6	250	32	1,050	866	898
.7	1,000	127	5,000	4,130	4,257
.8	2,700	343	12,500	10,320	10,660
.9	5,300	674	25,000	20,630	21,300
1.0	9,500	1,208	41,500	34,250	35,460
1.2	22,000	2,800	125,000	103,200	106,000
1.4	41,000	5,220	325,000	268,000	273,200
1.8	111,000	14,120	1,100,000	908,000	922,100
2.2	225,000	28,600	2,150,000	1,775,000	1,804,000
2.6	380,000	48,300	3,260,000	2,690,000	2,738,000
3.0	560,000	71,200	7,150,000	5,900,000	5,971,000

1/ Values of g low enough to be insignificant may be neglected in these calculations.

In the case of blowoff, the hybrids are the binary systems (methane + hydrogen) and (carbon monoxide + hydrogen), the ratio of hydrogen to carbon monoxide in the hybrid being kept at 0.2.[13/] The remainder of the hydrogen is proportioned with the methane to make up the (methane + hydrogen) complex. This is done as follows: H_2/CO = 0.20; 0.20 x 10.6% CO = 2.12% (H_2 going with CO); H_2/CO = 2.12/10.6 = 0.20. 58.4% H_2 - 2.12% H_2 = 56.28% (H_2 going with CH_4); CH_4/H_2 = 26.3/56.28 = 0.467. By adding the proportioned percentages of hydrogen to the carbon monoxide and the methane, we obtain the percentage of each hybrid in the total fuel:

2.12% H_2 + 10.6% CO = 12.72% (hydrogen + carbon monoxide);

26.3% CH_4 + 56.28% H_2 = 82.58% (methane + hydrogen).

Thus for the two hybrids for blowoff of fuel No. 43, we have a hydrogen/carbon monoxide ratio of 0.2 and a methane/hydrogen ratio of 0.467. Columns F_B and A of table 3b list the blowoff coordinates of the hybrid (hydrogen + carbon monoxide) for H_2/CO = 0.2. These coordinates can be obtained from figure 31 or 40. These values of g_B are multiplied by the percentage of this hybrid in the fuel (12.72%), and the answer is recorded in column B. This is the contribution of the (hydrogen + carbon monoxide) hybrid to the blowoff gradient of the total fuel. The contribution of the (methane + hydrogen) hybrid is obtained in the same way (see columns F_B, C and D. Addition of columns B and D gives column (B + D), which lists the critical boundary velocity gradients for blowoff of the total fuel in accord with equation 4. Columns F_B and (B + D) of table 3b list the coordinates for the calculated blowoff curve of fuel No. 43.

Thus the first and last columns of tables 3a and 3b give the coordinates for the calculated flashback and blowoff curves of fuel No. 43. These curves are plotted in figure 41, which also gives experimental points for flashback and blowoff of the same fuel. The agreement between experiment and prediction can be judged by the proximity of the experimental points to the calculated curves. Agreement of this order has been obtained with 10 other coke-oven gases (A-T/3a,3b,4-No./44,45,46,47,48,51,52,53,61,65). It can be seen from the chemical composition of these 11 fuels that most possibilities have been bracketed. An example of the linear mixture rule applied to an eight-component fuel (fuel No. 65) is shown in figure 42.

2. Oil Gases

The type of fuel considered here is obtained by the current practice of gasifying oils pyrolytically. It consists of ethylene (less than about 50 percent), hydrogen, methane, and sometimes inerts. An example of this type is fuel No. 55 (A-T/3a,3b,4-No./55), which will be used to illustrate the method of calculating flashback and blowoff gradients of oil gases. In calculating flashback gradients, fuels of this kind are treated as (ethylene + hydrogen) hybrid and (methane); in calculating blowoff gradients they are treated as (methane + hydrogen) and (ethylene)(see tables 4a and 4b). The values in the first and last columns of

---

13/ The limitation that the hydrogen/carbon monoxide ratio is to be maintained at about 0.2 is based on the shape of the curves in figures 30 and 31, which show a considerable change of slope near this ratio of hydrogen/carbon monoxide. This is taken to indicate that the reactivity of carbon monoxide is strongly accelerated by the addition of hydrogen up to this point. When more hydrogen is added, there appears to be an averaging effect between pure hydrogen and the species (H_2/CO, about 0.2). (Figure 40 is the flame-stability diagram for the fuel H_2/CO = 0.2.)

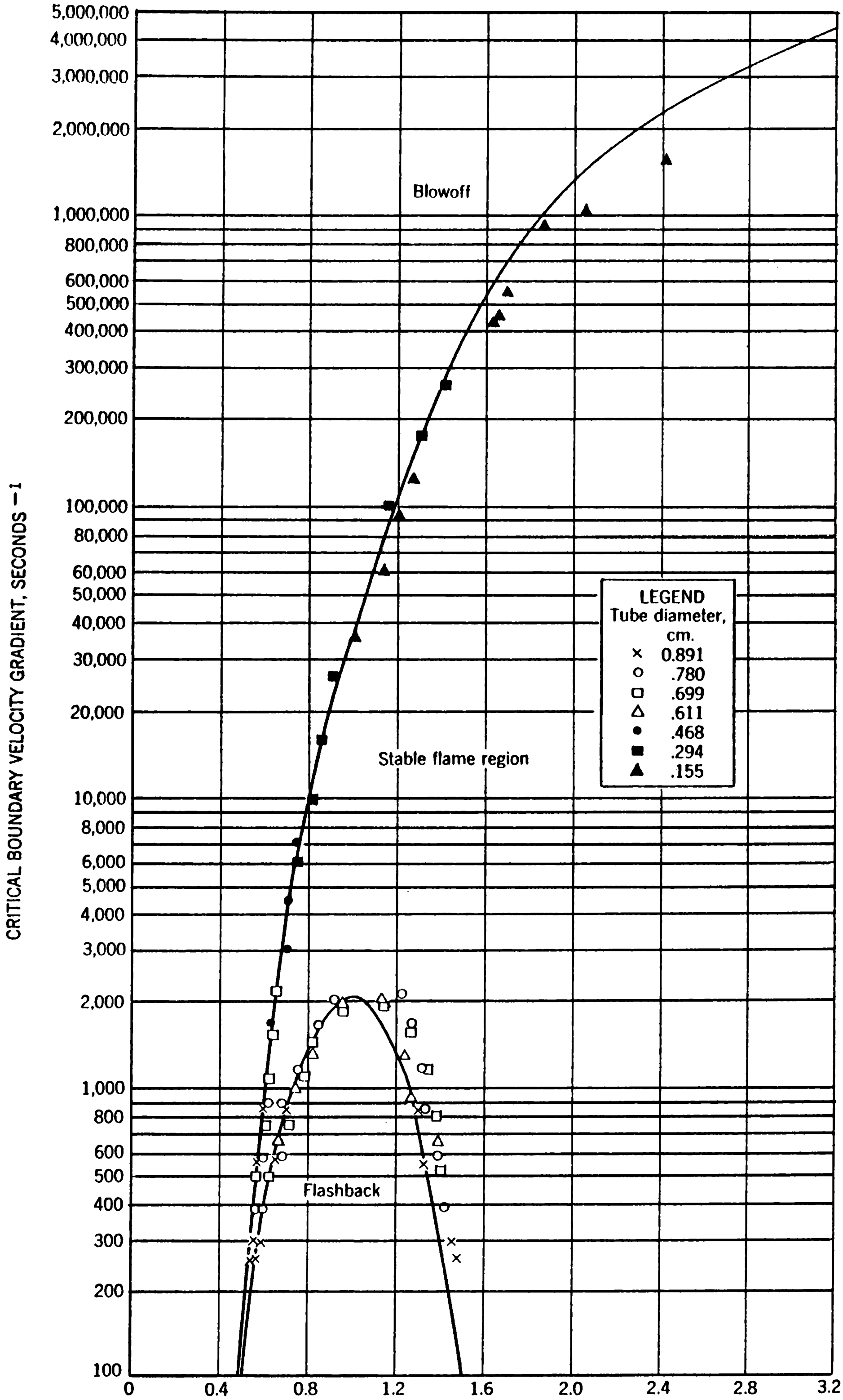

Figure 41. - Flame-stability diagram for fuel No. 43 (58.4% H_2, 26.3% CH_4, 10.6% CO, 4.6% N_2, 0.1% CO_2); comparison of calculated curves and experimental points.

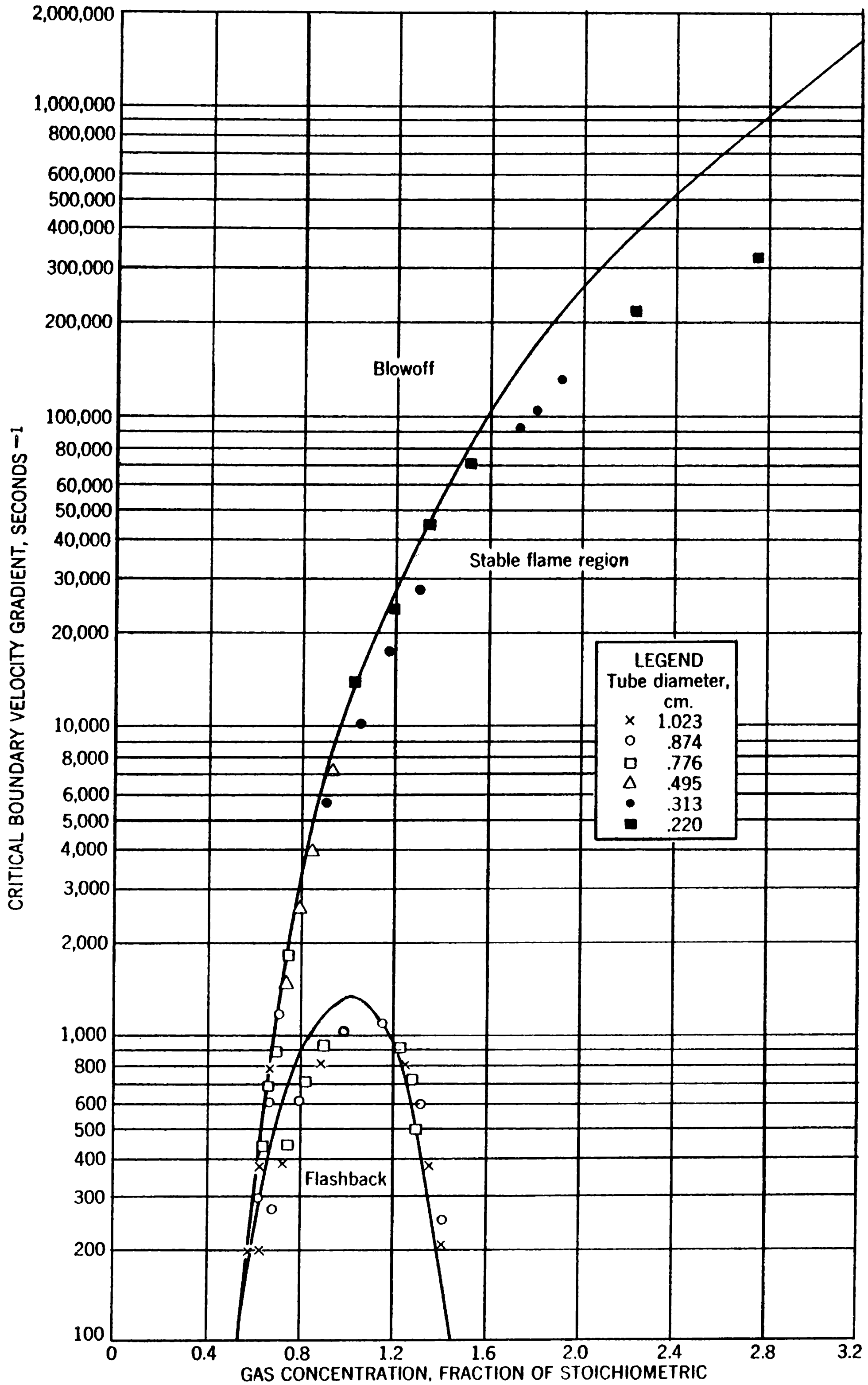

Figure 42. - Flame-stability diagram for fuel No. 65 (36.4% H_2, 22.6% CO, 13.3% CH_4, 7.2% C_2H_6, 5.8% C_2H_4, 1.9% C_3H_8, 0.1% C_3H_6, 9.8% N_2, 2.9% CO_2); comparison of calculated curves and experimental points.

tables 4a and 4b, respectively, are used as coordinates for the flame-stability diagram presented in figure 43. The adequacy of these calculations in predicting the flashback and blowoff curves of this fuel can be judged as before by comparing the calculated curves with the experimental points shown. Similar calculations were made for four other multicomponent oil-gas fuels (A-T/3a,3b,4-No./56,57,66,67). The agreement appears adequate for practical use. As a second illustration, experimental points and calculated curves are compared for a six-component fuel (fuel No. 67) in figure 44.

TABLE 4a. - Calculation of flashback curve for fuel No. 55 by linear mixture rule

Mixture composition, percent: 37.4 CH_4, 33.4 C_2H_4, 15.2 H_2, 14.0 N_2
Stoichiometric percentage: 10.3

Complexes for flashback: $(C_2H_4 + H_2)(CH_4)(N_2)$.
Calc. of complexes:
H_2/C_2H_4 = 15.2/33.4 = 0.455; use 100% CH_4 flame-stability diagram.
Total percentage of H_2/C_2H_4 = 15.2 + 33.4 = 48.6; total percentage of CH_4 = 37.4.

F_F	A (figure 36) g_F for H_2/C_2H_4 = 0.455	B A x 0.486	C (figure 20) g_F for 100% CH_4	D C x 0.374	B+D g_F for total fuel
0.6	305	148	1/	1/	148
.7	615	299			299
.75	830	403	135	51	454
.8	1,060	515	190	71	586
.9	1,430	695	330	124	819
1.0	1,680	816	390	146	962
1.1	1,770	860	340	127	987
1.2	1,480	719	180	67	786
1.25	1,300	632	120	45	677
1.3	1,090	530			530
1.4	715	348			348
1.5	413	201			201
1.6	220	107			107

TABLE 4b. - Calculation of blowoff curve for fuel No. 55 by linear mixture rule

Complexes for blowoff: $(CH_4 + H_2)(C_2H_4)(N_2)$.
Calc. of complexes:
H_2/CH_4 = 15.2/37.4 = 0.406; use 100% C_2H_4 flame-stability diagram.
Total percentage of H_2CH_4 = 15.2 + 37.4 = 52.6; total percentage of C_2H_4 = 33.4.

F_B	A (figure 29) g_B for H_2/CH_4 = 0.406	B A x 0.526	C (figure 22) g_B for 100% C_2H_4	D C x 0.334	B+D g_B for total fuel
0.6	120	63	370	124	187
.7	330	174	1,600	534	708
.8	1,330	700	3,850	1,285	1,985
.9	2,650	1,395	6,700	2,240	3,635
1.0	4,500	2,370	10,000	3,340	5,710
1.2	9,650	5,080	17,000	5,680	10,760
1.4	15,900	8,360	26,000	8,680	17,040
1.8	35,500	18,700	44,000	14,700	33,400
2.2	61,000	32,100	61,500	20,550	52,650
2.6	95,000	50,000	76,000	25,400	75,400
3.0	143,000	75,200	92,000	30,700	105,900

1/ Values of g low enough to be insignificant may be neglected in these calculations.

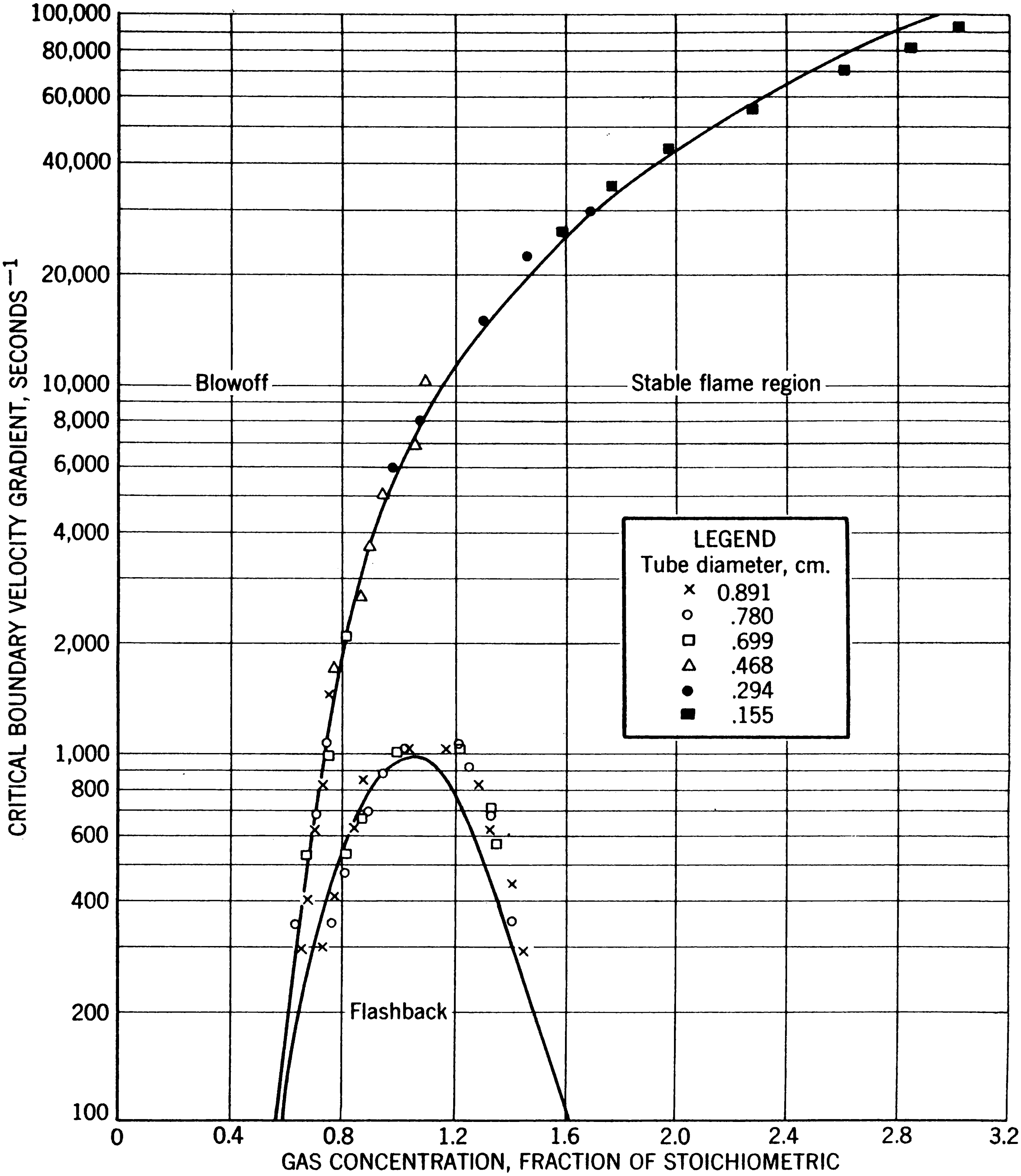

Figure 43. - Flame-stability diagram for fuel No. 55 (37.4% CH_4, 33.4% C_2H_4, 15.2% H_2, 14.0% N_2); comparison of calculated curves and experimental points.

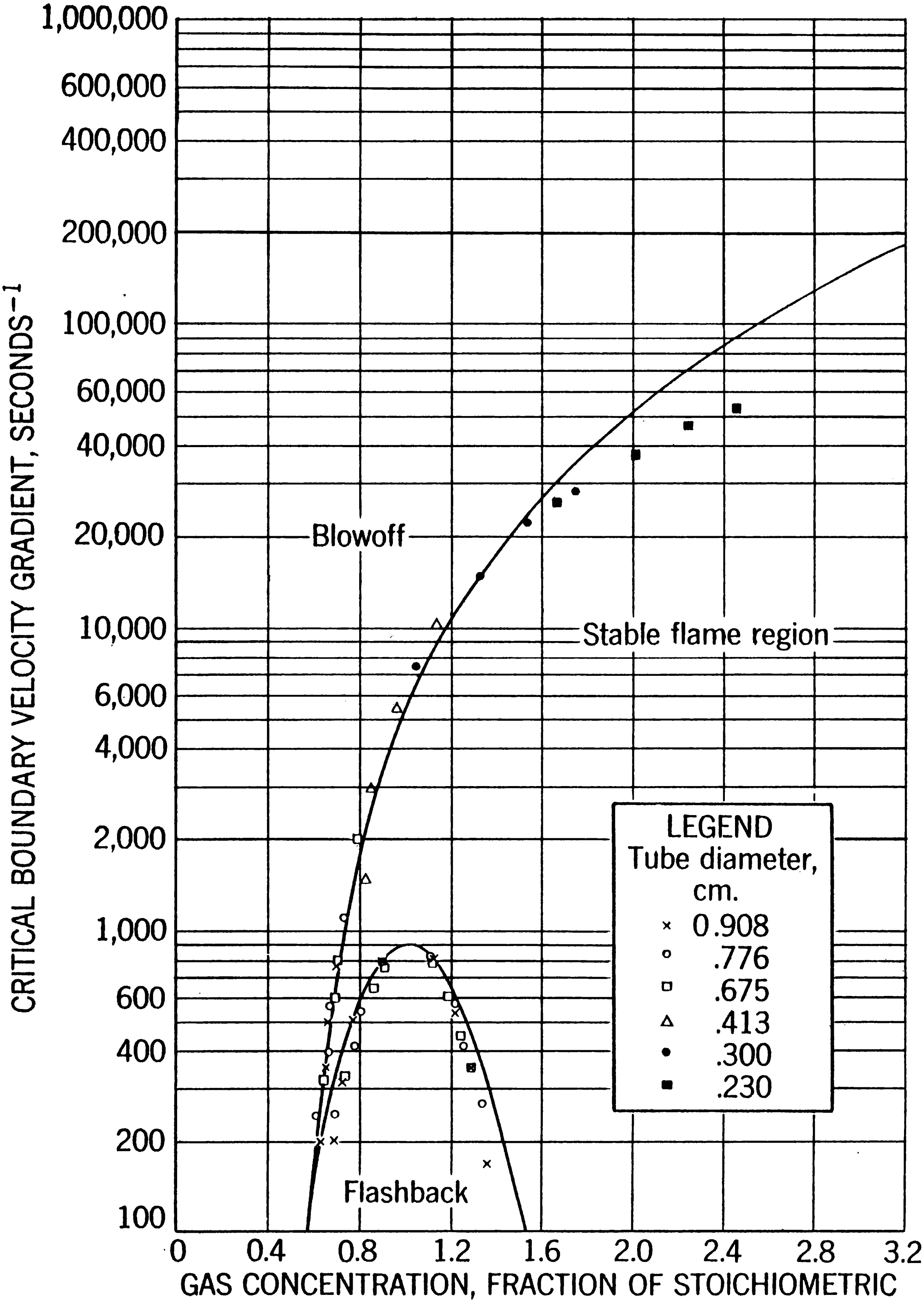

Figure 44. - Flame-stability diagram for fuel No. 67 (37.5% CH_4, 20.4% C_2H_4, 17.5% H_2, 3.9% CO, 13.3% N_2, 7.4% CO_2); comparison of calculated curves and experimental points.

3. High-Ethylene Fuels Containing Hydrogen (More Than About 50 Percent Ethylene)

Although not widely used at present, these fuels are considered here because a slightly different method of calculation is required to obtain their blowoff curves. Calculations are based on the assumption that the fuel consists of the hybrid (ethylene + hydrogen) and (methane) for both flashback and blowoff. Fuel No. 63 is an example of this class of fuels. Experimental data and calculations of flashback and blowoff gradients for this fuel are in tables (A-T/3a,3b,4-No./63). The resultant flashback and blowoff curves are plotted in figure 45, where experimental points again are given for comparison. The method has been checked with two other fuels (A-T/3a,3b,4-No./62,64).

4. Fuels Containing Nitrogen and Carbon Dioxide

Tests have shown that, except in binary mixtures with hydrogen and tertiary mixtures with hydrogen and carbon monoxide, nitrogen acts as an inert diluent. In other words, zero values are assigned to the gradients of the inerts in equation 4. Let us, for example, compare the experimental points and the calculated curves in figure 46 for a mixture of 62.5 percent methane, 22.2 percent hydrogen, and 15.3 percent nitrogen (A-T/3a,3b,4-No./58). The curves are calculated from equation 4 with satisfactory agreement, in view of the approximations involved. Similar agreement was found for 12 other fuels (A-T/3a,3b,4-No./40,43,45,47,52,55,56,57,63,65,66, 67).

Anomalous results were obtained when calculating flashback gradients of producer-gas-type fuels consisting of carbon monoxide, hydrogen and nitrogen only. The disagreement can be illustrated by comparing the experimental data and calculated curves for flashback of these fuels (A-T/3a,3b,4-No./59,60).[14/]

Carbon dioxide behaves like nitrogen up to concentrations of about 15 percent (A-T/3a,3b,4-No./53,61,65,66,67). At higher concentrations of carbon dioxide the greater heat capacity of the material as compared to nitrogen becomes evident, and the flame-stability gradients are lowered more than by equal quantities of nitrogen. The disagreement for concentrations of carbon dioxide above 15 percent can be seen by comparing the experimental data and calculated curves of these fuels (A-T/3a,3b,4-No./49,50,54).[15/]

14/ Experimental flashback gradients for fuels consisting only of carbon monoxide, hydrogen, and nitrogen were considerably lower than predicted on the assumption that the fuel consists of the complex (hydrogen + carbon monoxide) and (nitrogen), or the complex (hydrogen + nitrogen) and (carbon monoxide). Experimental blowoff gradients were adequately matched by values calculated on the basis of the first of these two alternatives. This exception does not impose a severe operating limitation in the use of these data, as gases consisting of only carbon monoxide, hydrogen, and nitrogen, which are of the producer and blue-gas type, are generally mixed with other fuels before going into the gasline. All tests to date have shown that in more complex mixtures, nitrogen behaves as a simple diluent.

15/ The observation that carbon dioxide when present in excess of about 15 percent depresses flame-stability gradients more strongly than the same percentages of nitrogen may be attributed to the greater heat capacity of carbon dioxide. No attempt has been made to cover the range of fuels containing more than about 15 percent carbon dioxide because such mixtures are rarely supplied to consumers of piped gas. When present in small percentages, carbon dioxide may be treated as equivalent to nitrogen.

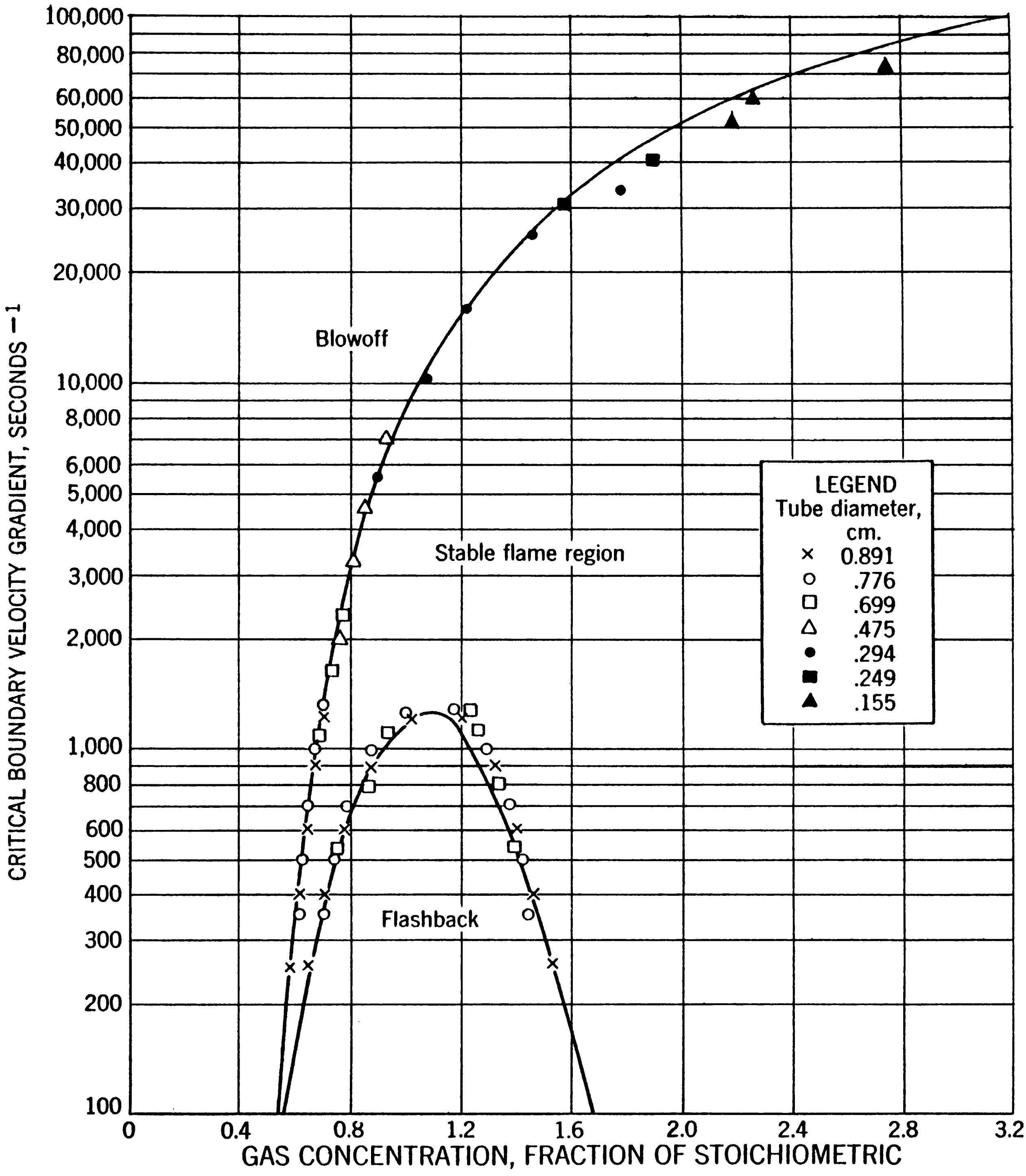

Figure 45. - Flame-stability diagram for fuel No. 63 (56.5% C_2H_4, 15.8% H_2, 13.8% CH_4, 0.1% C_3H_6, 13.8% N_2); comparison of calculated curves and experimental points.

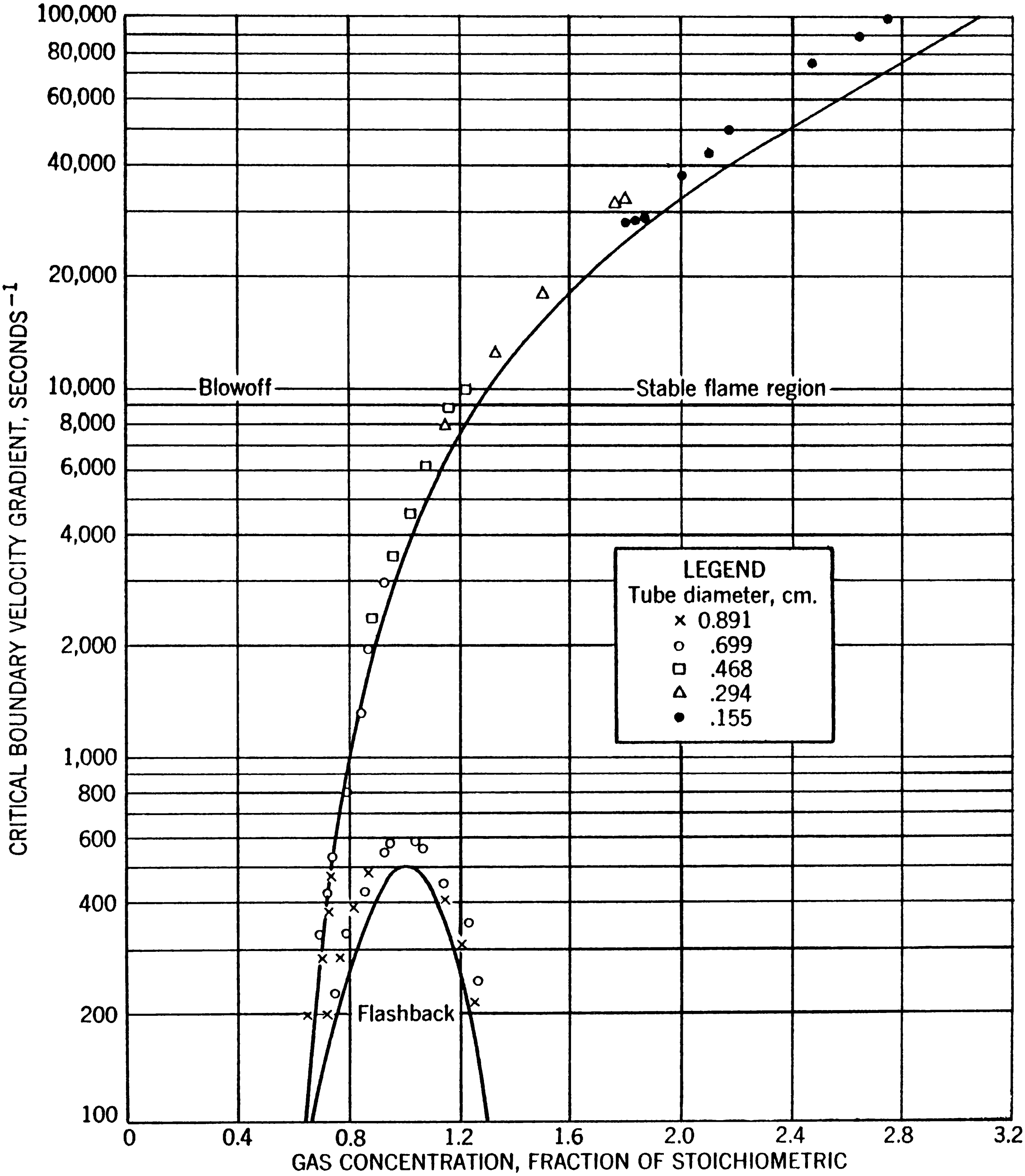

Figure 46. - Flame-stability diagram for fuel No. 58 (62.5% CH_4, 22.2% H_2, 15.3% N_2); comparison of calculated curves and experimental points.

The following listing may be useful to the reader in pointing up fuels of current special interest.

(1) Natural Gases. - This group consists of methane with or without small amounts of other saturated hydrocarbons, nitrogen, and carbon dioxide. The flame-stability diagram for natural gas (figure 19, p. 23), represents these gases adequately for practical purposes. Figure 20 (p. 25) for pure methane is nearly identical with figure 19.

(2) Liquid-Petroleum and Liquid Petroleum-Air Gases. - This category includes propane, butane, propylene, and the butylenes, also mixtures of these gases with air. Figure 21 (p. 26) for propane represents these fuels adequately; figure 23 (p. 28) for propylene is not different enough from the flame-stability diagram for propane to warrant distinction.

(3) Coke-Oven Gases. - Fuels that contain high percentages of hydrogen and carbon monoxide and lesser amounts of saturated hydrocarbons, particularly methane, as well as small amounts of unsaturated hydrocarbons, inert gases, and oxygen, are included in this group. The method of calculating flame-stability diagrams for these fuels is given in tables 3a and 3b of this chapter and requires the use of composite flame-stability diagrams for blowoff and flashback of three types of binary mixtures. Required composite diagrams are given for methane-hydrogen mixtures in figures 28 and 29 (pp. 34 and 35), for carbon monoxide-hydrogen mixtures in figures 30 and 31 (pp. 36 and 37), and for methane-carbon monoxide mixtures in figures 32 and 33 (pp. 38 and 39).

(4) Oil Gases. - Gases that are high in ethylene (up to about 50 percent) and methane, with lesser amounts of hydrogen and inerts and possibly small amounts of carbon monoxide or oxygen, fall into this class of fuels. The method of calculating flame-stability diagrams for such gases is explained in tables 4a and 4b of this chapter. These calculations make use of the composite flame-stability diagrams for flashback and blowoff of ethylene-hydrogen fuels (figures 36 and 37, pp. 42 and 43) and the flame-stability diagram for methane (figure 20, p. 25).

These four types of fuels cover most of the fuels that are currently of industrial interest. The procedures for obtaining flashback and blowoff curves for these fuels are based on direct measurement, interpolation between direct measurements, or tested calculations based on certain reasonable premises. Such calculations have been made successfully on 28 fuels with 2 to 8 constituents.

CHAPTER III. - YELLOW TIPPING AND CONSTANT YELLOW-TIP LIMITS

The phenomenon of yellow tipping differs completely from that of flashback and of blowoff and requires separate explanation.

Yellow tipping is not as serious a limitation in gas-burner operation as are flashback and blowoff. A burner that is in flashback or blowoff does not heat satisfactorily, but a burner operating with yellow flames can be used for heating. Many such burners are used, especially where radiant heat is desired. Yellow-tipped flames are undesirable for certain purposes because they deposit carbonaceous material, which fouls surfaces above the burner and decreases heating efficiency. Moreover, under some circumstances yellow-tipped flames may also give off irritating aldehydes, or carbon monoxide in concentrations exceeding safe limits. Therefore it may often be important to avoid yellow flames in designing burners or exchanging gases on existing burners and to understand the fundamental nature of the yellow-tipping phenomenon.

The yellow-tip limits of most yellow-tipping fuels have been measured and correlated as follows: Each fuel has a minimum characteristic fuel-air ratio for which yellow appears in the flame. The corresponding fuel-gas concentration, fraction of stoichiometric, is called the constant yellow-tip limit, F_c. When secondary air diffuses into the entire flame, the fuel-air ratio in the flame is leaner than in the burner, and the apparent yellow-tip limit for the burner and fuel becomes richer. The corresponding fuel-gas concentration, fraction of stoichiometric, is called the nonconstant yellow-tip limit, F_y.

Theory

In formulating a theory for yellow tipping of flames in free air, the following experimental facts must be considered:

1. The leanest limit for each fuel (in terms of fuel-air composition of the stream in the port) is independent of flow, burner diameter, and oxygen content of the secondary air (4).

2. For a given flow, the limit is richest for narrow flames (small diameters) and becomes independent of diameter for wide flames (large diameters).

3. For a given diameter, the limit is richest for small flames (low flows) and becomes independent of flow for tall flames (high flows).

4. At the limit, yellow does not appear below or as part of the primary combustion zone. For many hydrocarbon mixtures, particularly liquid-petroleum gases, the top of the primary cone is open. When a yellow ethylene flame is inverted,[16] the blue-green primary combustion surface is clearly visible under the yellow in the burned gas. The same result is obtained by inverting a yellow toluene-air flame and a yellow acetylene-air flame.

These observations lead to the conclusions that, for all flames at the yellow-tip limit:

(1) There is a characteristic fuel-air composition for each yellow-tipping fuel at which the flame shows yellow. This value can be determined experimentally by finding the limit that is independent of increasing flow and increasing diameter.

(2) Diffusion of secondary air into the flame can produce apparent limits that are richer than the characteristic limit. This happens only if secondary air can diffuse into the yellow zone of the flame in the time the gas takes to flow from the port to the yellow zone.

(3) Yellow tipping is not a primary-combustion-zone phenomenon.

These conclusions can be extended as follows to give a general method of correlating yellow-tip limits: Let us consider an idealized yellow-tip-limit flame (figure 47). The yellow zone is a spot at the axis at some height above the port. The flame is tall enough so that only radial diffusion of secondary air is

---

16/ These inverted flames are ones where the apex of the primary cone is the part of the flame nearest the plane of the port. Many rich flames can be inverted by holding a wire at the axis of the port and passing a slow coaxial stream of nitrogen around the port. This makes it possible to observe the primary cone without looking through the secondary mantle.

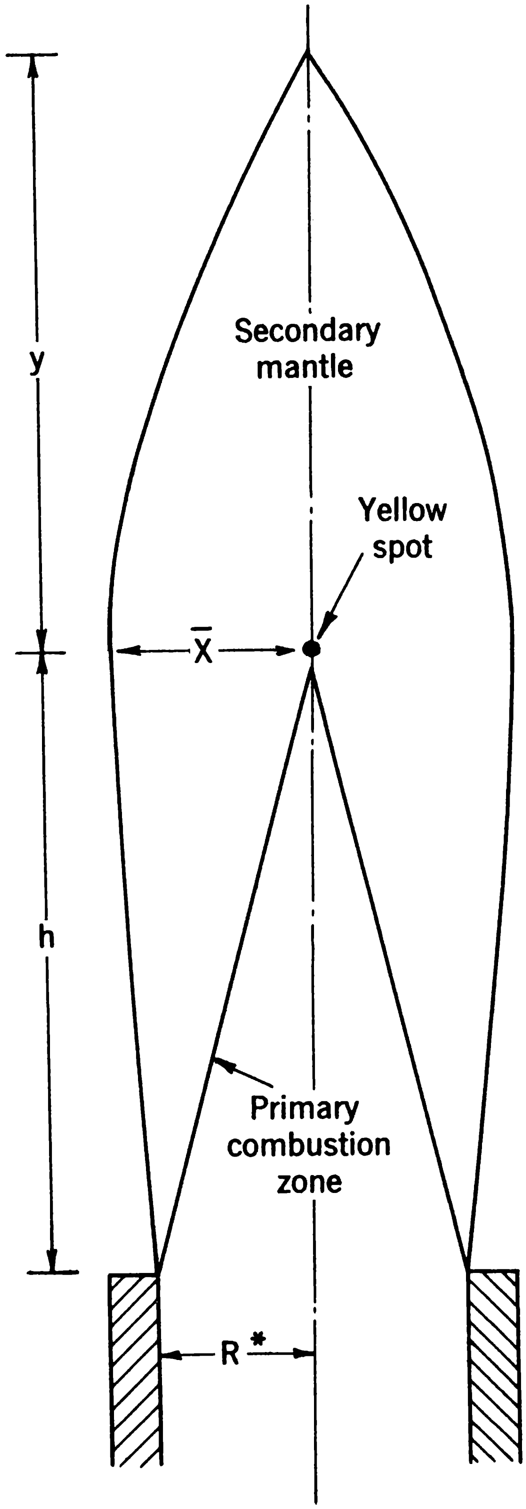

Figure 47. - A schematic yellow-tip limit flame for the critical port radius, R*.

significant and the diameter (2R*) is such that secondary air just fails to reach the axis at the plane of the yellow spot in the time the gas takes to flow from the port to that plane. For such a flame $F_y = F_c$, and the yellow-tip fraction F_c/F_y = 1.0.

The average displacement $\bar{X}$ of a diffusing molecule is given by the equation

$$\bar{X}^2 = 2\ D't, \qquad (5)$$

where D' is the diffusion coefficient and t is the time available for diffusion. In figure 47 the distance $\bar{X}$ is the width of the flame at the plane of the yellow spot. For large ports, this about equals the radius, and so for figure 47, $\bar{X} \simeq R^*$. The time, t, is the quotient of the height h of the yellow spot in the flame and U_a the axial velocity. Accordingly,

$$(R^*)^2 = 2\ D' \frac{h}{U_a}, \qquad (6)$$

U_a being related to the product of the radius and the boundary velocity gradient g. (For parabolic flow, $U_a = gR^*/2$.) We then may write that

$$(R^*)^3 = kD'h/g, \qquad (7)$$

where k is a proportionality constant.

Equation 7 shows the parameters that affect the yellow-tip limit, F_y, displacing it so that $F_c/F_y < 1$. By definition, $F_c/F_y > 1$ is impossible. These parameters affect F_y as follows:

(a) If $R > R^*$, $F_c/F_y = 1$, because secondary air can only penetrate as far as R*. As R increases beyond R*, the yellow zone enlarges from a point to a streak of appreciable width and height.

If $R < R^*$, $F_c/F_y < 1$, because secondary air can reach the axis. More fuel has to be added to the burner stream to compensate for this excess secondary air if yellow is to be obtained.

(b) k is some function essentially relating the velocity at the axis to the boundary velocity gradient. It reflects changes in velocity profiles brought about by changing port shape, depth, etc. As values of k for two types of ports need not differ appreciably,17/ F_c/F_y may or may not vary with port geometry and type of flow. Predictions are possible when the flow profiles are known.

(c) D' should be approximately the same for all fuels or for large groups of fuels. The hot gases through which secondary air diffuses to the axis are composed largely of nitrogen, water, carbon dioxide, carbon monoxide, and some hydrogen. The temperatures of these hot gases do not differ enough for various fuels to affect the diffusion coefficient appreciably. Accordingly, the diffusion coefficient produces little if any change in F_c/F_y.

17/ See chs. V and VI for discussions of influences of port length, depth, and temperature on yellow tipping.

(d) h depends on the flow and on the average burning velocity of the primary combustion cone of the yellow-tipping flame. The flow is easily evaluated. The differences in average burning velocities of various yellow-tipping fuels will be treated in chapter IV.

The gross variations in the average burning velocity of yellow-tipped flames are illustrated by figure 48, which shows yellow-tipped flames of natural gas, propane, propylene, ethylene, and benzene. The natural gas flame is a long, soft, ill-defined, bushy flame, very similar in shape to diffusion flames. It has an extremely slow burning rate. Yellow-tip-limit flames of fuels such as propane and propylene have low burning rates, with soft primary cones that are often open-topped. Fuels containing large quantities of ethylene, such as rapidly burning oil gases, have yellow-tip-limit flames with fairly sharp, fully formed primary cones, showing that these flames have appreciable burning rates. Flames of pure aromatic fuels, such as benzene, also have sharply defined primary cones at the yellow-tip limit. The same is true of acetylene, which has a very high burning rate, as evidenced by short, sharp, full primary cones at the yellow-tip limit.

(e) If g (or U_a) is low enough, the flame height above the yellow zone may be of the order of R*. It should be noted that this height is y of figure 47, not h of equation 7. In this case, secondary air reaches the yellow zone as readily from the top of the flame as from the side and as the amount of secondary air at the yellow is increased, $F_c/F_y < 1$.

This analysis of the influence of the parameters in equation 7 on F_c/F_y shows that, to systematize the yellow tipping of fuels, we need relationships of F_c/F_y to R and g for the various fuel compositions. The organization of the four parameters will be discussed in chapter IV.

Further Consideration of the Constant Yellow-Tip Limit

The basic quantity in characterizing yellow-tip limits is F_c, the constant yellow-tip limit. Only 11 single-component fuels can produce yellow and probably appear in significant quantities at burners connected to gas-distribution lines. These fuels are listed in table 5, with corresponding values of F_c determined experimentally.

TABLE 5. - Constant yellow-tip limits for single-component fuels

Fuel	F_c, exp.	Fuel	F_c, exp.
Methane	1.80	Isobutylene	1.40
Ethane	1.87	Acetylene	2.10
Propane	1.61	Benzene	1.18
n-Butane	1.57	Toluene	1.34
Ethylene	1.88	Natural gas	1.78
Propylene	1.44		

Tests have shown that the F_c of a mixture of these fuels can be calculated by taking a weighted average of the experimentally determined constant yellow-tip limits of the single-component fuels (table 5). Oxygen, inerts, hydrogen, and

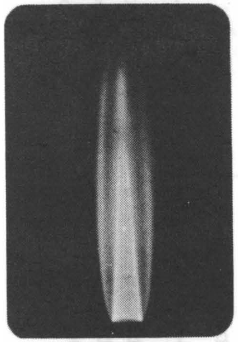

ETHYLENE
ROUND PORT

NATURAL GAS FLAME
ROUND PORT

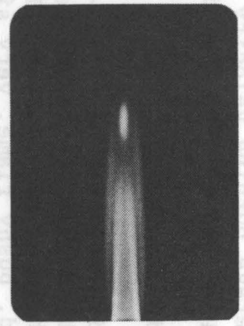

PROPANE
ROUND PORT

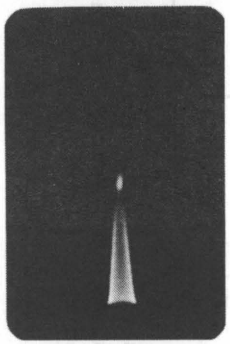

PROPYLENE
ROUND PORT

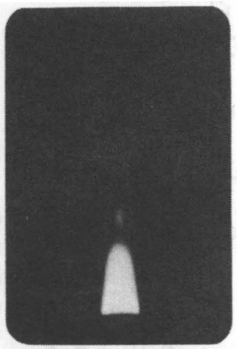

PROPYLENE
FRONT VIEW
SLOT PORT

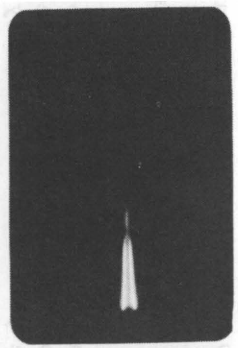

PROPYLENE
SIDE VIEW
SLOT PORT

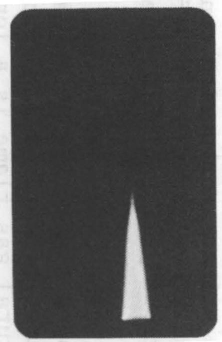

BENZENE
ROUND PORT

Figure 48. - Yellow-tipped aerated flames.

carbon monoxide were given zero weight. The averaging is done by the following linear rule.[18]

$$(F_c)_{calc.} = \frac{1}{\Sigma n}\left[n_a(F_c)_a + n_b(F_c)_b + n_c(F_c)_c \;\ldots\right], \tag{8}$$

where n_a, n_b, n_c, etc., are the mole fractions of each of the yellow-tipping components, and $\Sigma n = n_a + n_b + n_c \ldots$. The validity of equation 8 is shown by the data in table 6, which lists experimental and calculated values of F_c for a wide variety of mixtures.

TABLE 6. - Comparison of experimental and calculated values of F_c for two-component and multicomponent fuels

Fuel composition	F_c, exp.	F_c, calc.
Two-component fuels		
Fuel No. 79: (76.0% C_2H_4, 24.0% H_2)	1.90	1.88
Fuel No. 83: (72.5% C_2H_4, 27.5% CH_4)	1.85	1.86
Fuel No. 76: (53.1% C_2H_4, 46.9% C_3H_8)	1.72	1.75
Fuel No. 77: (74.4% C_2H_4, 25.6% C_3H_8)	1.68	1.81
Fuel No. 78: (90.0% C_2H_4, 10.0% C_3H_8)	1.78	1.85
Fuel No. 29: (55.4% C_3H_8, 44.6% H_2)	1.76	1.61
Fuel No. 28: (81.6% C_3H_8, 17.4% H_2, 1.0% C_3H_6)	1.61	1.61
Multicomponent fuels		
Fuel No. 72: (70.1% C_3H_8, 15.7% H_2, 13.7% CO, 0.5% C_3H_6)	1.60	1.61
Fuel No. 55: (37.4% CH_4, 33.4% C_2H_4, 15.2% H_2, 14.0% N_2)	1.90	1.84
Fuel No. 82: (33.5% CH_4, 30.1% C_2H_4, 13.4% H_2, 12.8% N_2, 10.2% CO_2)	1.88	1.84
Fuel No. 56: (29.1% CH_4, 26.2% C_2H_4, 22.1% C_3H_8, 11.8% H_2, 0.2% C_3H_6, 10.6% N_2)	1.76	1.77
Fuel No. 57: (32.1% CH_4, 28.4% C_2H_4, 12.5% H_2, 27.0% N_2)	1.90	1.84
Fuel No. 66: (42.6% CH_4, 18.1% C_2H_4, 17.0% H_2, 9.1% CO, 2.2% C_2H_6, 1.9% C_3H_8, 0.2% C_3H_6, 0.2% C_4H_{10}, 0.1% C_4H_8, 5.2% CO_2, 3.4% N_2)	1.80	1.82
Fuel No. 69: (75.2% CH_4, 22.2% C_3H_8, 2.6% C_2H_6)	1.76	1.76
Fuel No. 71: (62.1% CH_4, 35.5% C_3H_8, 2.4% C_2H_6)	1.71	1.73
Fuel No. 70: (74.2% CH_4, 13.4% C_3H_6, 9.6% C_3H_8, 2.5% C_2H_6, 0.3% CO_2)	1.66	1.74
Fuel No. 80: (72.5% CH_4, 15.9% C_2H_4, 7.7% H_2, 2.6% C_2H_6, 0.4% C_3H_8, 0.2% C_3H_6, 0.2% C_4H_{10}, 0.5% CO_2)	1.76	1.81
Fuel No. 81: (67.6% CH_4, 26.8% C_2H_4, 2.3% C_2H_6, 2.2% H_2, 0.4% C_3H_8, 0.2% C_3H_6, 0.1% C_4H_{10}, 0.4% CO_2)	1.79	1.82
Fuel No. 86: (84.2% CH_4, 7.6% C_2H_2, 5.3% C_2H_6, 1.6% C_3H_8, 0.6% C_4H_{10}, 0.3% C_3H_6, 0.4% CO_2)	1.77	1.82
Fuel No. 87: (91.6% CH_4, 4.0% C_7H_8, 3.2% C_2H_6, 0.7% C_3H_8, 0.2% C_3H_6, 0.3% CO_2)	1.74	1.78

18/ This rule is not expected to apply when the concentration of non-yellow-tipping components is very large.

CHAPTER IV. - CALCULATION OF NONCONSTANT YELLOW-TIP LIMITS OF FUEL GASES

In the preceding chapter, yellow-tip limits of fuels on ports of diameters $\geq R^*$ were considered. For such ports F_y is equal to F_c, except at low flows. Let us now consider yellow tipping on smaller ports, using a graphical method that also will include the low flames on large ports. For these flames, the yellow-tip fraction $F_c/F_y < 1.0$.

Figures 49, 50, and 51 (A-T/5-No./2,68,3) contain yellow-tip limits (F_y) for methane, natural gas, and propane, respectively, over a wide range of ports and flows.[19] The yellow-tip curves in these three graphs are plots of F_y versus g_y. For each diameter, yellow-tipped flames occur to the right of the respective curve. This type of yellow-tip-limit plot has two disadvantages. Interpolation between diameters is difficult; and there appears to be no way of extrapolating data obtained for one fuel to a new and untested fuel.

Let us now systematize the yellow-tip limits of fuels, excluding those that are very largely made up of hydrogen, carbon monoxide, and inerts. As fuels containing much more than 50 percent non-yellow-tipping constituents have not been tested, it is not known how far beyond 50 percent the data to be presented are applicable. However, this is not a serious practical limitation.

It will be recalled that four parameters must be considered in dealing with nonconstant yellow-tip limits. One is the chemical composition of the fuel. The second is the fuel-air composition in the burner port. This is F_y, which will be converted into the yellow-tip fraction, F_c/F_y, which weighs all fuels with respect to their fundamental yellow-tipping tendencies. The third parameter is the port diameter. The fourth is the flow expressed as the critical boundary velocity gradient g_y. These four variables are organized for wide ranges of fuel composition

---

19/ In figures 49-51 the stable blue-flame region marks the area where flashback, blowoff, and yellow tipping are absent. Yellow-tipped flames are possible but not necessarily present for values of F greater than F_c. Port diameter and flow must be taken into consideration in predicting yellow tipping when F is greater than F_c. Flame-characteristics diagrams such as these combine the flashback, blowoff, and yellow-tipping characteristics of the fuel gas in one plot of critical boundary velocity gradient versus fuel-air composition expressed as fraction of stoichiometric. The constant yellow-tip limit F_c, included in the diagram as a vertical line, is the measure of the yellow-tipping properties inherent in the fuel gas. The other yellow-tip curves involve a particular port diameter. Therefore these nonconstant yellow-tip limits are a combination of the inherent yellow-tipping qualities of the fuel and the interaction between this quantity and the port diameter, the latter being a burner-design factor. Other burner-design factors, namely port shape and port temperature, will be treated in chs. V and VI, respectively.

The yellow-tip-limit curves for methane and natural gas on large tubes bend back on themselves over a short range of flows (see figures 49 and 50). These may be characteristic of a breakdown within the flame into a transition region before turbulence. Once turbulence is established in the flame, the characteristic constant yellow-tip limit is again restored. The anomaly occurs over only a small range and has been observed exclusively with methane and natural gas. It can be ignored for practical purposes.

The yellow-tip curves for propane include points on small tube diameters at very low flows. The exact limits are somewhat in doubt but lie between the doublets shown.

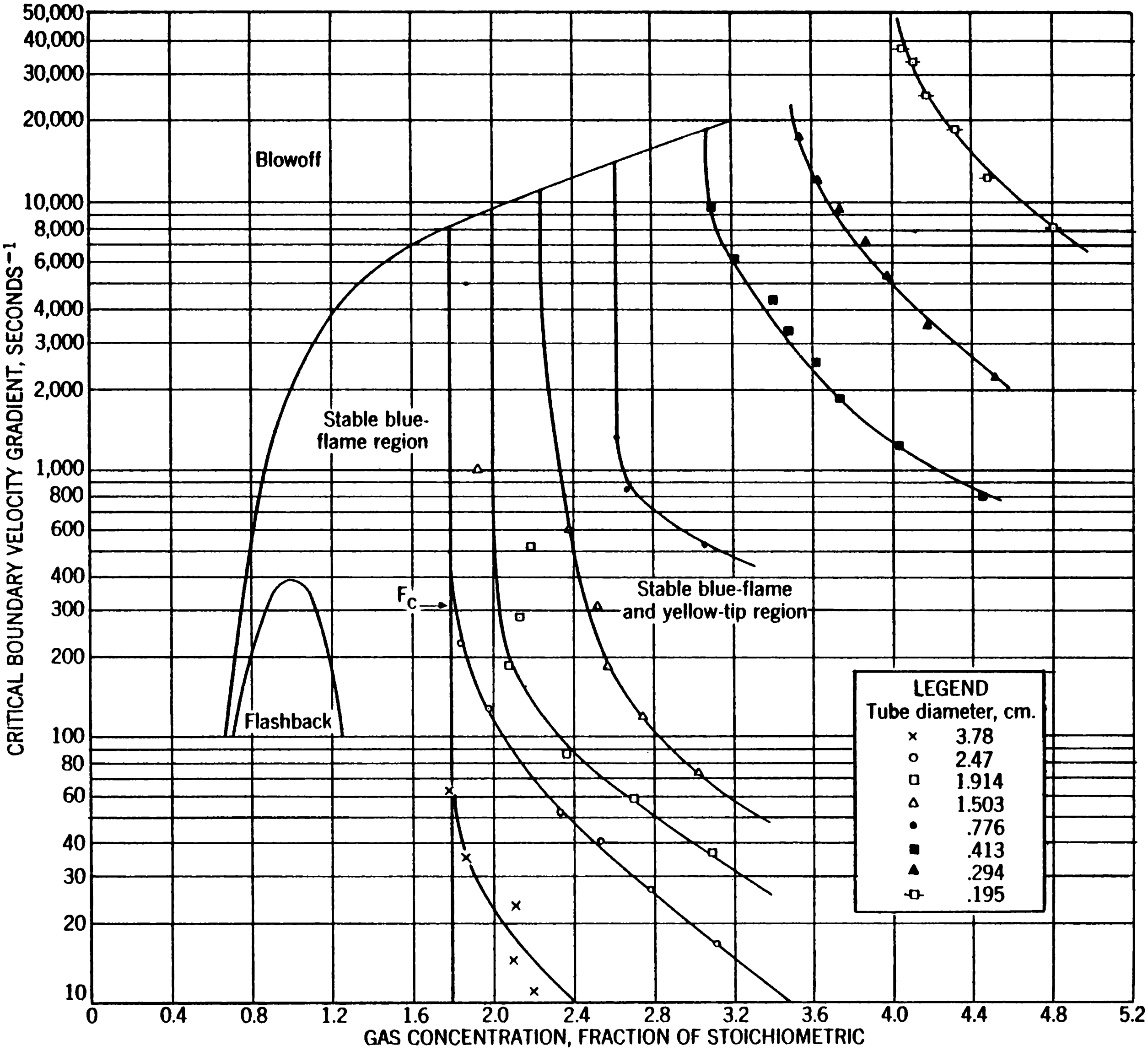

Figure 49. - Flame-characteristics diagram for fuel No. 2 (100% CH_4).

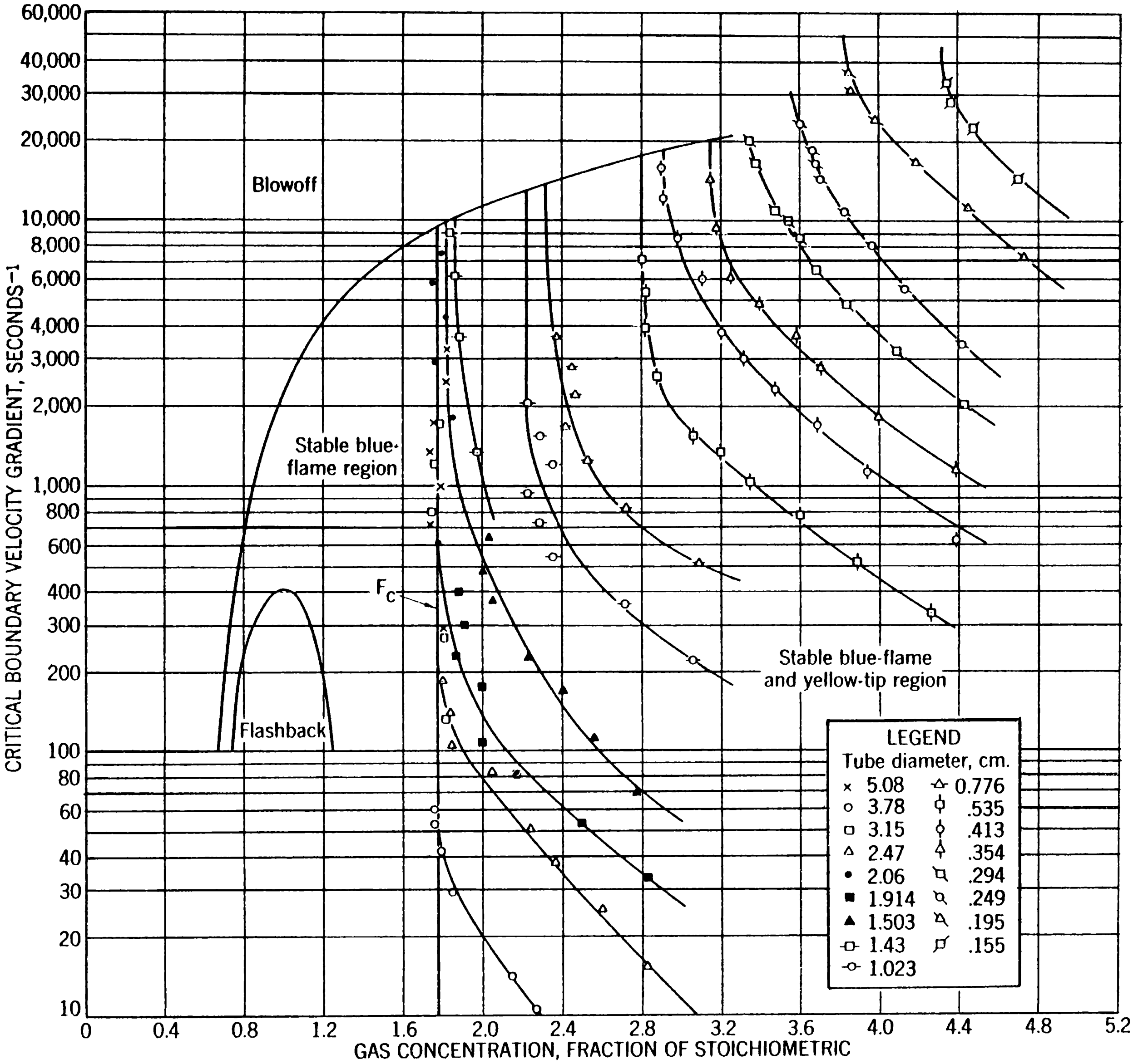

Figure 50. - Flame-characteristics diagram for fuel No. 68 (89.5% CH_4, 6.7% C_2H_6, 2.7% C_3H_8, 0.4% C_3H_6, 0.4% C_4H_{10}, 0.3% CO_2).

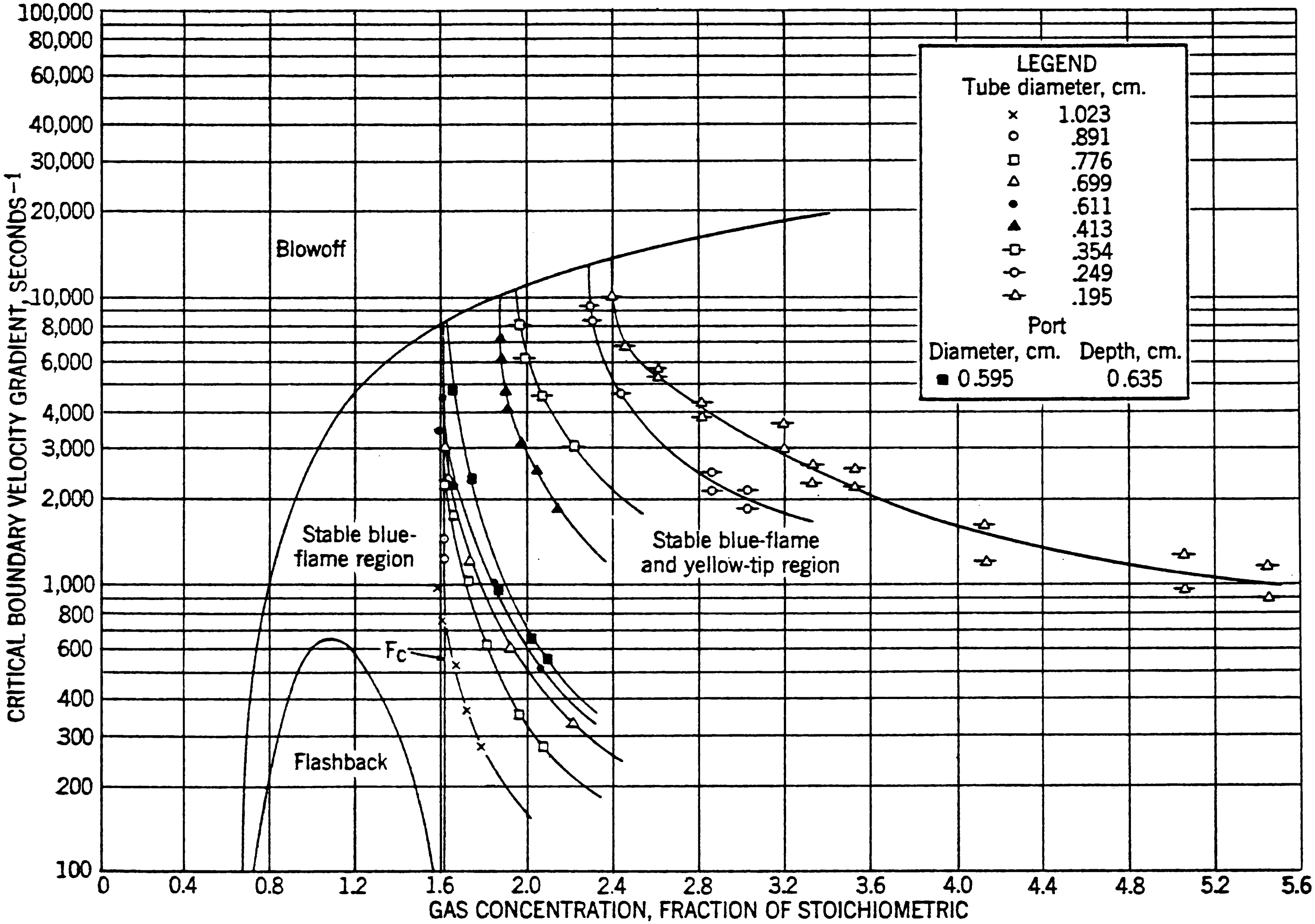

Figure 51. - Flame-characteristics diagram for fuel No. 3 (98.6% C_3H_8, 1.4% C_3H_6).

by diagrams, such as figures 52-56. These diagrams represent fuel mixtures of methane (natural gas) and the propane group[20] and mixtures of the propane group with ethylene (A-T/5-No./2,68,69,70,71,29,28,72,73,3,5,74,75,76,77,78,79,4). Figures 57-59 (A-T/6-No./2,80,81,57,55,82,83,79,4) represent fuels made up of methane and ethylene, including oil gases. In addition to the yellow-tipping fuels listed, quantities of hydrogen, carbon monoxide, nitrogen, and carbon dioxide may occur in these mixtures, provided that these non-yellow-tipping constituents are not the predominant fraction of the fuel. The above diagrams were constructed as follows:

(1) Starting with a fuel, such as natural gas (figure 50), values of F_y are selected so that F_c/F_y = 1.0, 0.95, 0.90, etc. (see table 7, column 1). Corresponding values of F_y are obtained (column 2) by dividing F_c by F_c/F_y. For each diameter (column 3) and F_y (column 2), corresponding values of g_y (column 4) are obtained from figure 50. Plotting the values in column 3 as the abscissa and the values in column 4 as the ordinate, we obtain curves of constant F_c/F_y for natural gas (figure 60). This operation is repeated to prepare similar curves of constant F_c/F_y for each fuel to be used in constructing yellow-tip-fraction composites (figures 52-59).

(2) Values of tube diameter for each value of F_c/F_y and for arbitrarily chosen critical boundary velocity gradients are obtained from these constant F_c/F_y curves. These diameters become the ordinates of a new set of graphs, the abscissa being the fuel composition expressed as ratios of the fuel constituents. Each graph of a given set is characterized by a constant value of the critical boundary velocity gradient (g_y = 300, 800, 3,000, 10,000, 20,000 and above) and includes a family of curves. Each curve is the locus of points of constant F_c/F_y for the selected flow and over the pertinent range of tube diameters and fuel compositions.

Thus this graphical method covers the four variables affecting nonconstant yellow-tip limits (fuel composition, fuel-air composition, diameter, and flow), to give composite yellow-tip-fraction diagrams.

The application of these composite yellow-tip-fraction diagrams can be illustrated by calculations of yellow-tip limits for a fuel composed of a mixture of natural and liquid petroleum gases, as follows: 62.1 percent CH_4, 35.5 percent C_3H_8, and 2.4 percent C_2H_6(A-T/5-No./71).

(1) The chemical composition of the fuel places it in the methane-propane group - ethylene class of yellow-tipping fuels, and figures 52-56 are to be consulted. The fuel is located on the composite diagram by its ratio of CH_4/C_3H_8 group or C_3H_8group/CH_4 (the fuel-composition-ratio coordinate has been arranged to be between 0 and 1). In this case it is C_3H_8 group/CH_4 = 37.9/62.1 = 0.61.

20/ The midpoint of figures 52-56 is an average of ethane, propane, butane, propylene, and isobutylene. These five fuels make up the "propane group" and show about the same yellow-tip fractions.

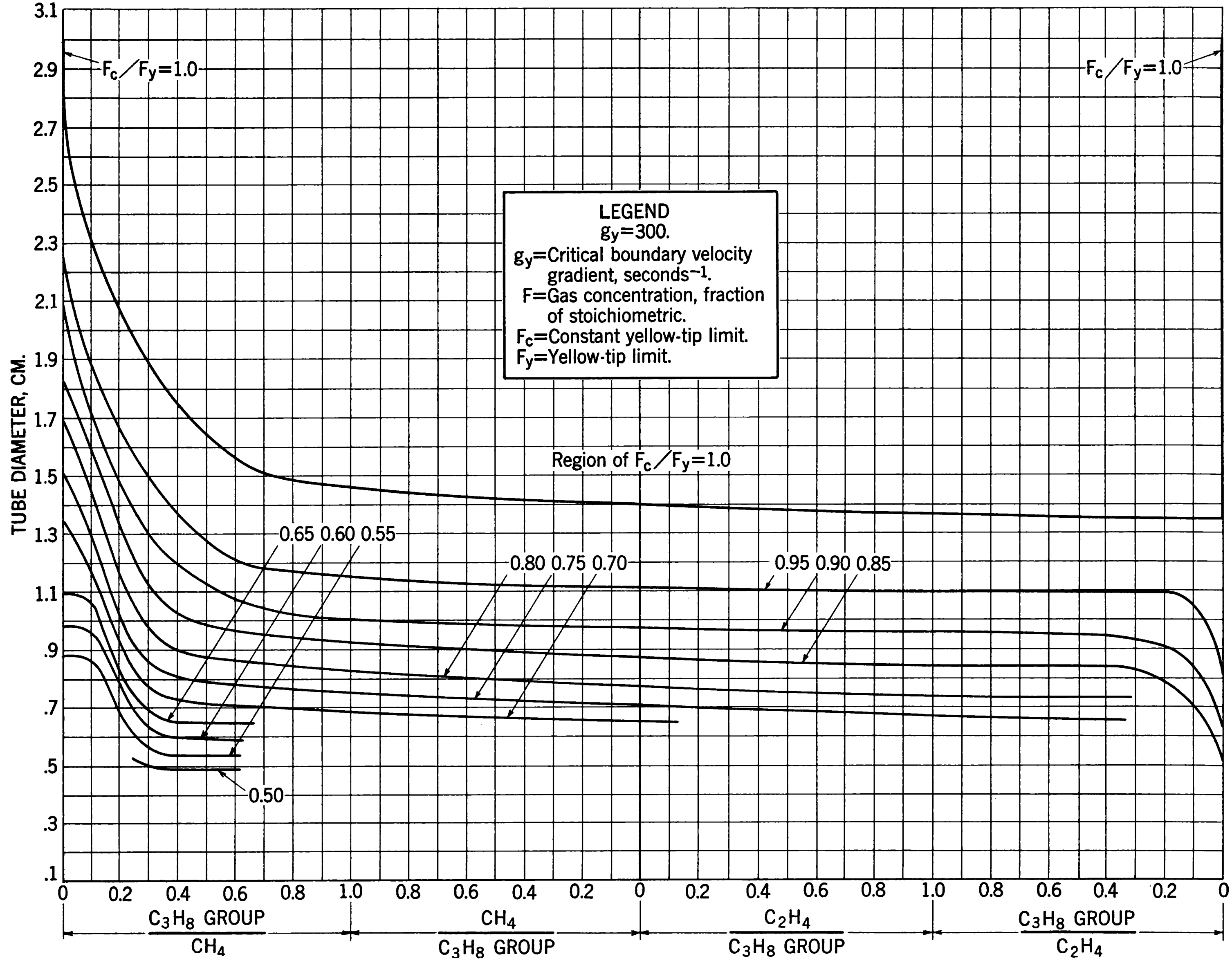

Figure 52. • Yellow-tip fractions for methane-propane group-ethylene fuels for $g_y = 300$; propane group is the average of ethane, propane, propylene, n-butane, and isobutylene; composite diagram.

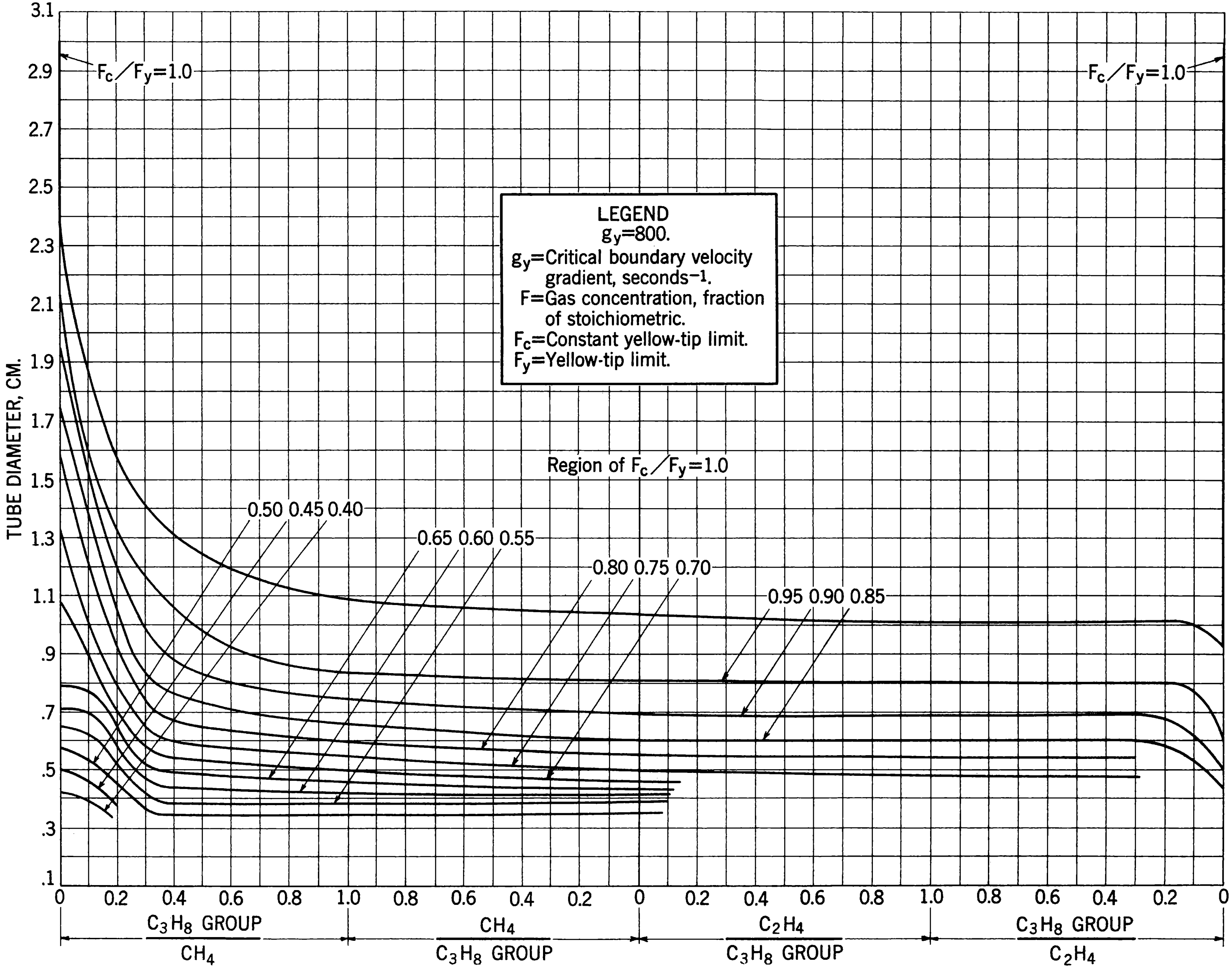

Figure 53. - Yellow-tip fractions for methane-propane group-ethylene fuels for g_y = 800; propane group is the average of ethane, propane, propylene, n-butane, and isobutylene; composite diagram.

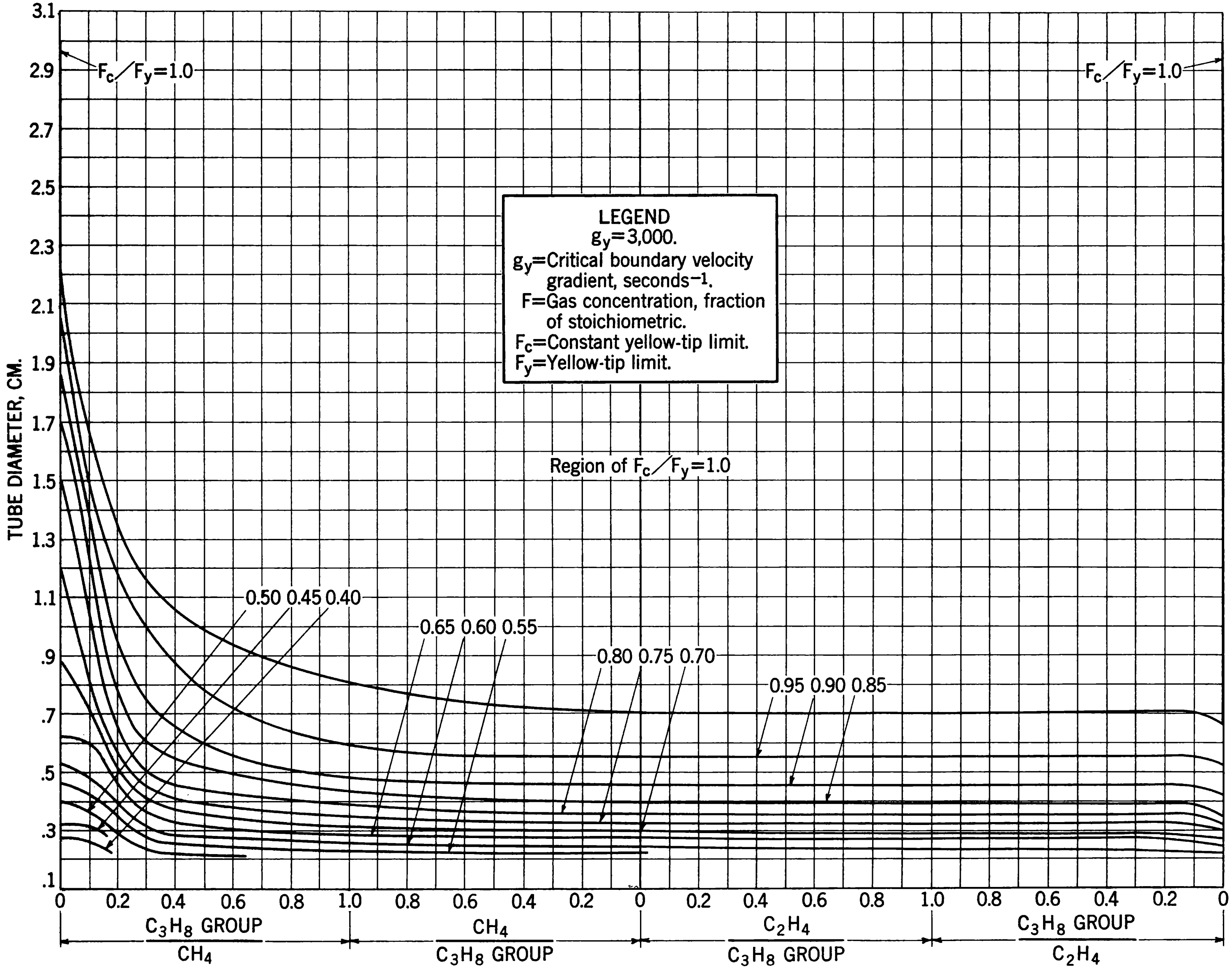

Figure 54. - Yellow-tip fractions for methane-propane group-ethylene fuels for g_y = 3,000; propane group is the average of ethane, propane, propylene, n-butane, and isobutylene; composite diagram.

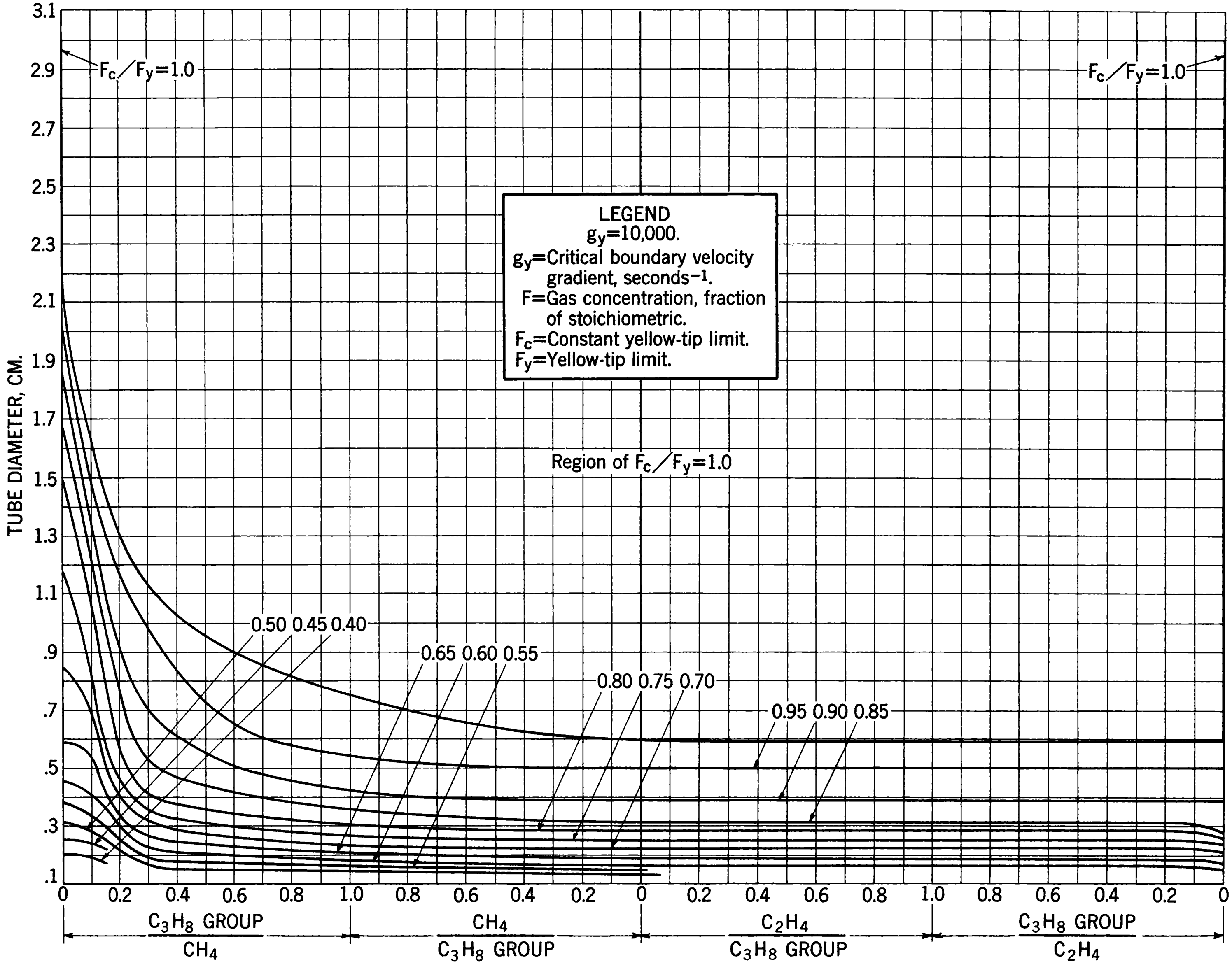

Figure 55. - Yellow-tip fractions for methane-propane group-ethylene fuels for g_y = 10,000; propane group is the average of ethane, propane, propylene, n-butane, and isobutylene; composite diagram.

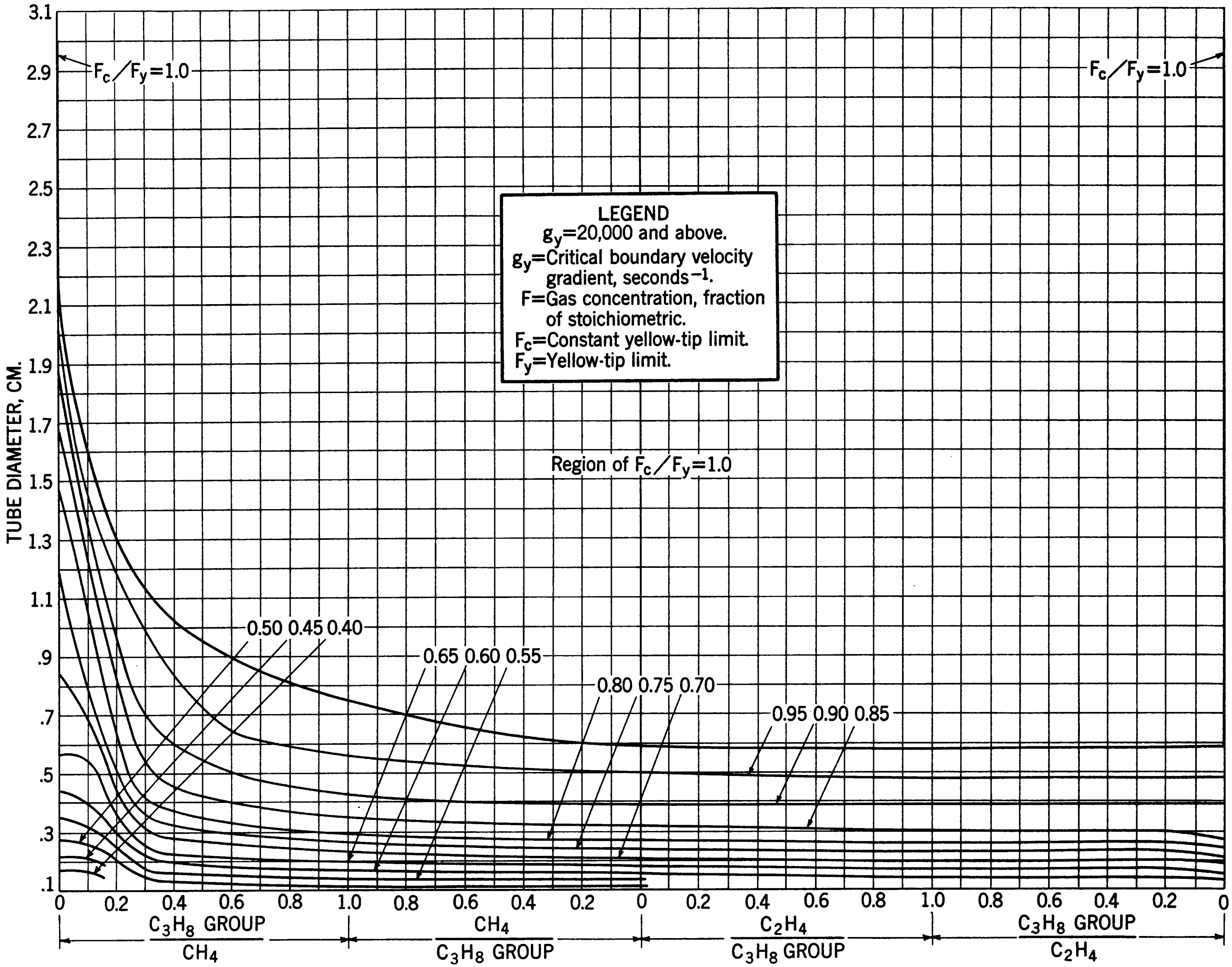

Figure 56. - Yellow-tip fractions for methane-propane group-ethylene fuels for g_y = 20,000 and above; propane group is the average of ethane, propane, propylene, n-butane, and isobutylene; composite diagram.

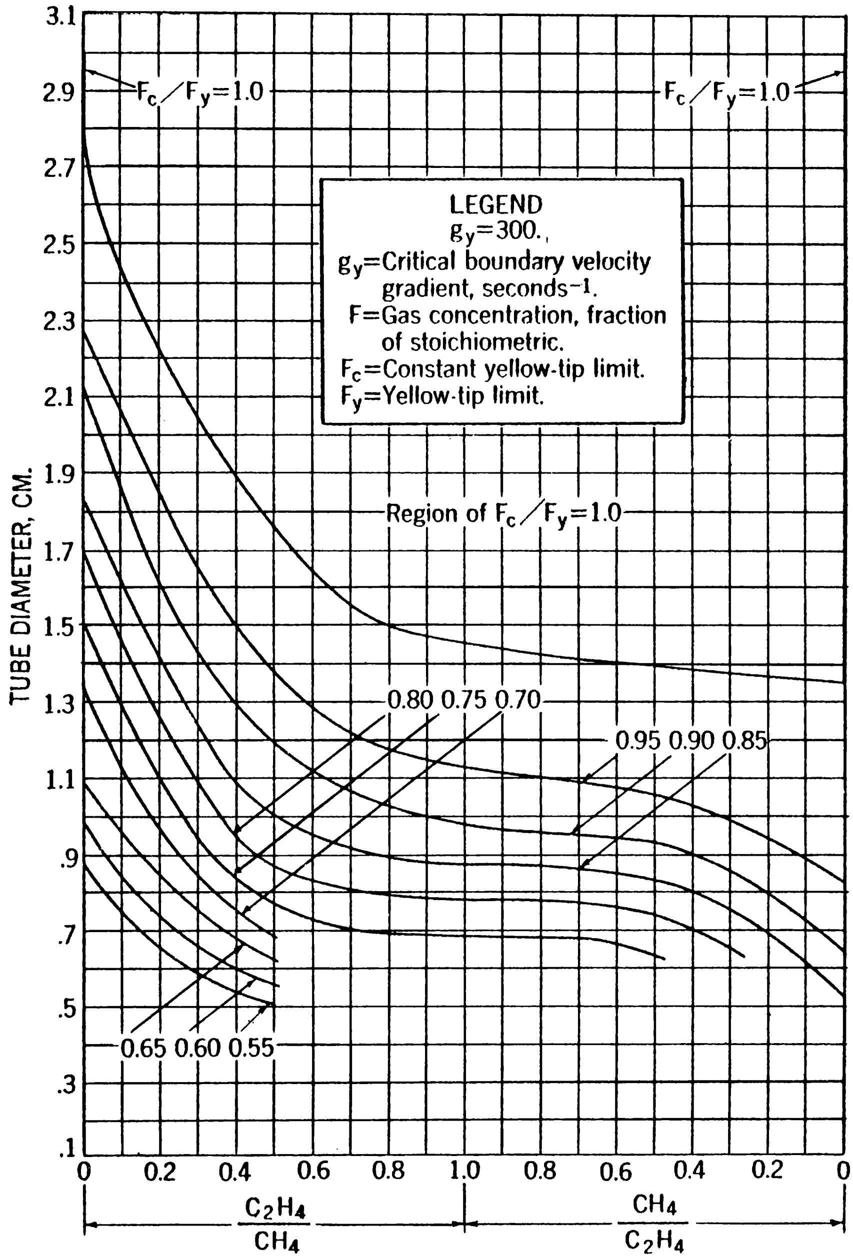

Figure 57. - Yellow-tip fractions for methane-ethylene fuels for $g_y = 300$; composite diagram.

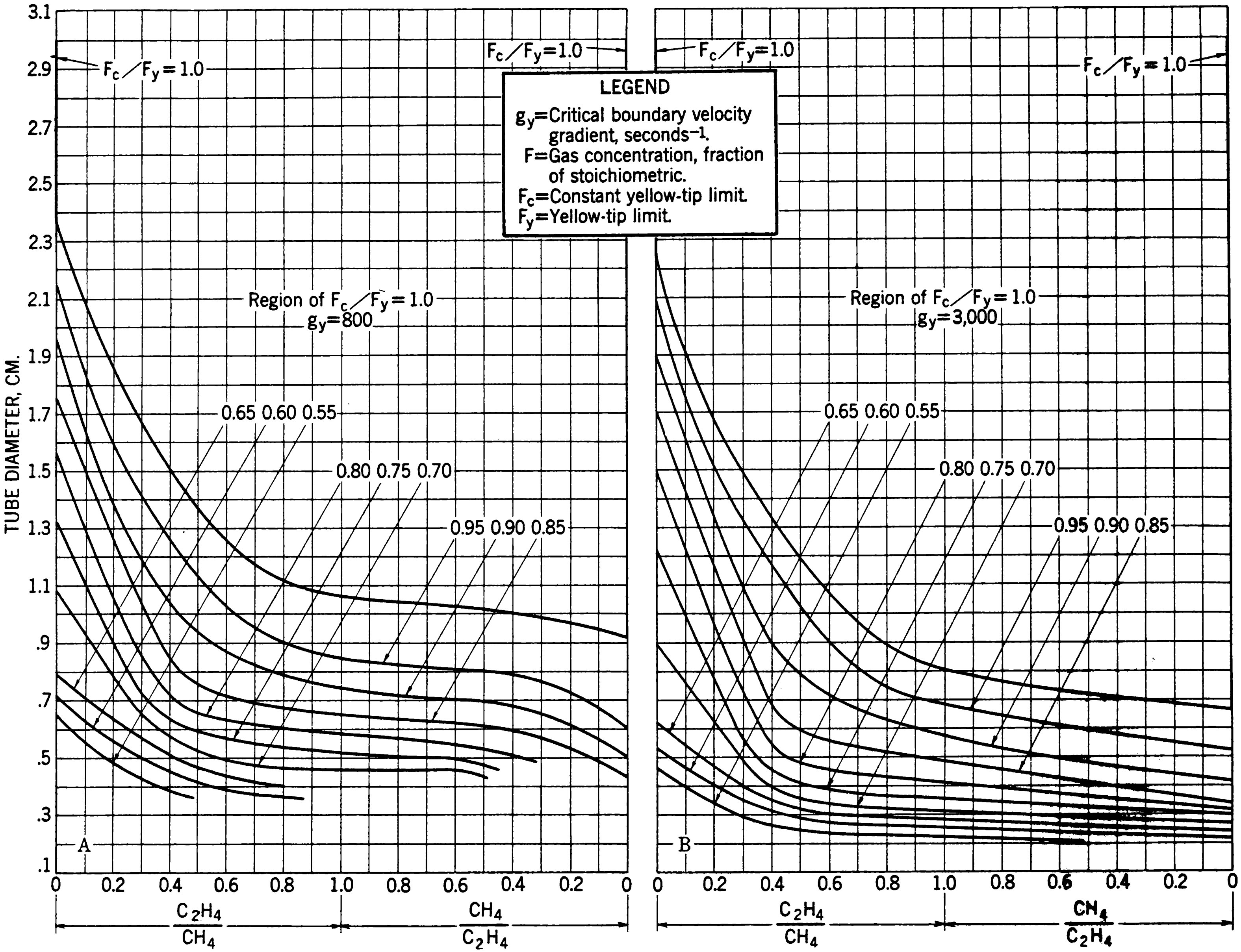

Figure 58. - Yellow-tip fractions for methane-ethylene fuels for g_y = 800 and 3,000; composite diagram.

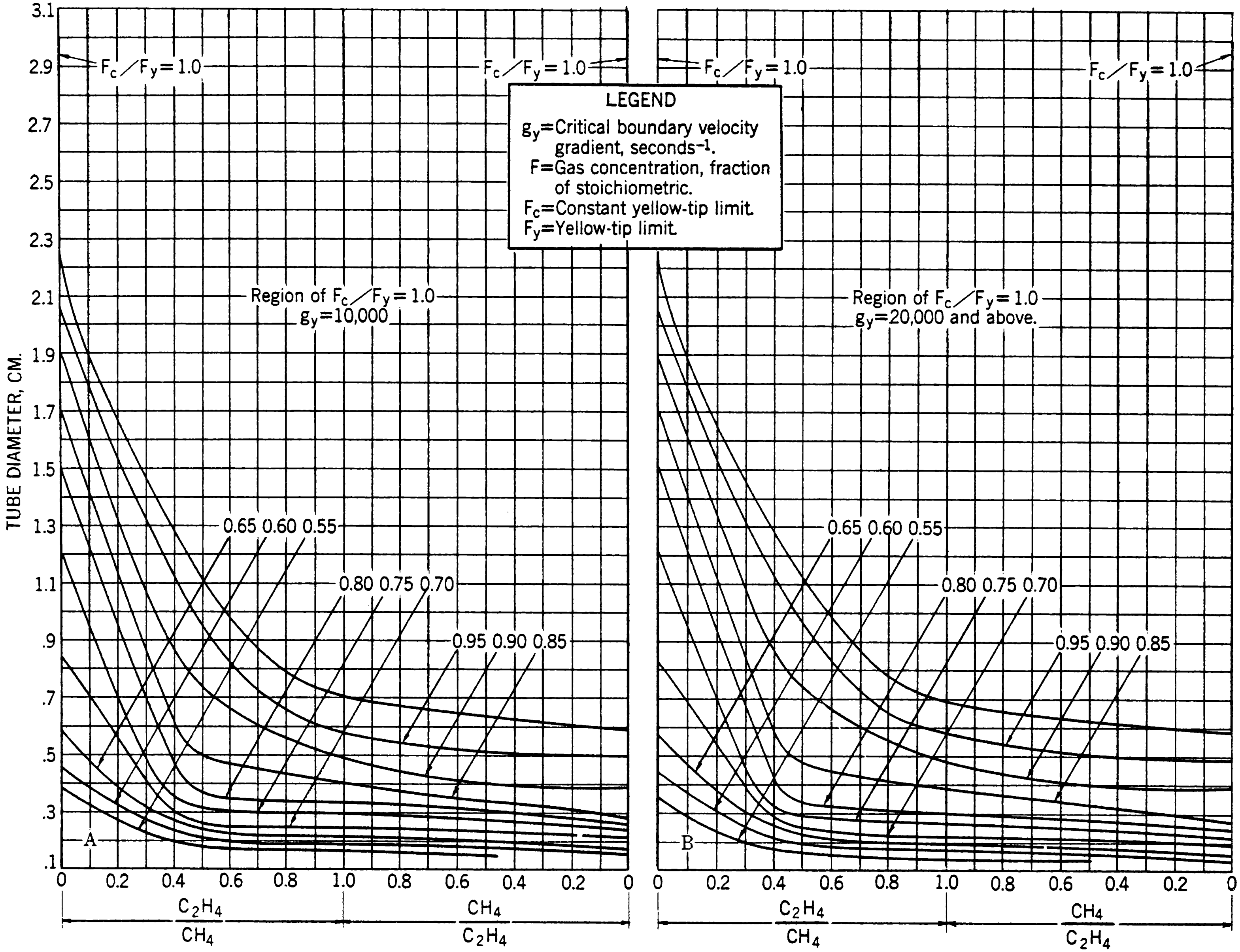

Figure 59. - Yellow-tip fractions for methane-ethylene fuels for g_y = 10,000, 20,000 and above; composite diagram.

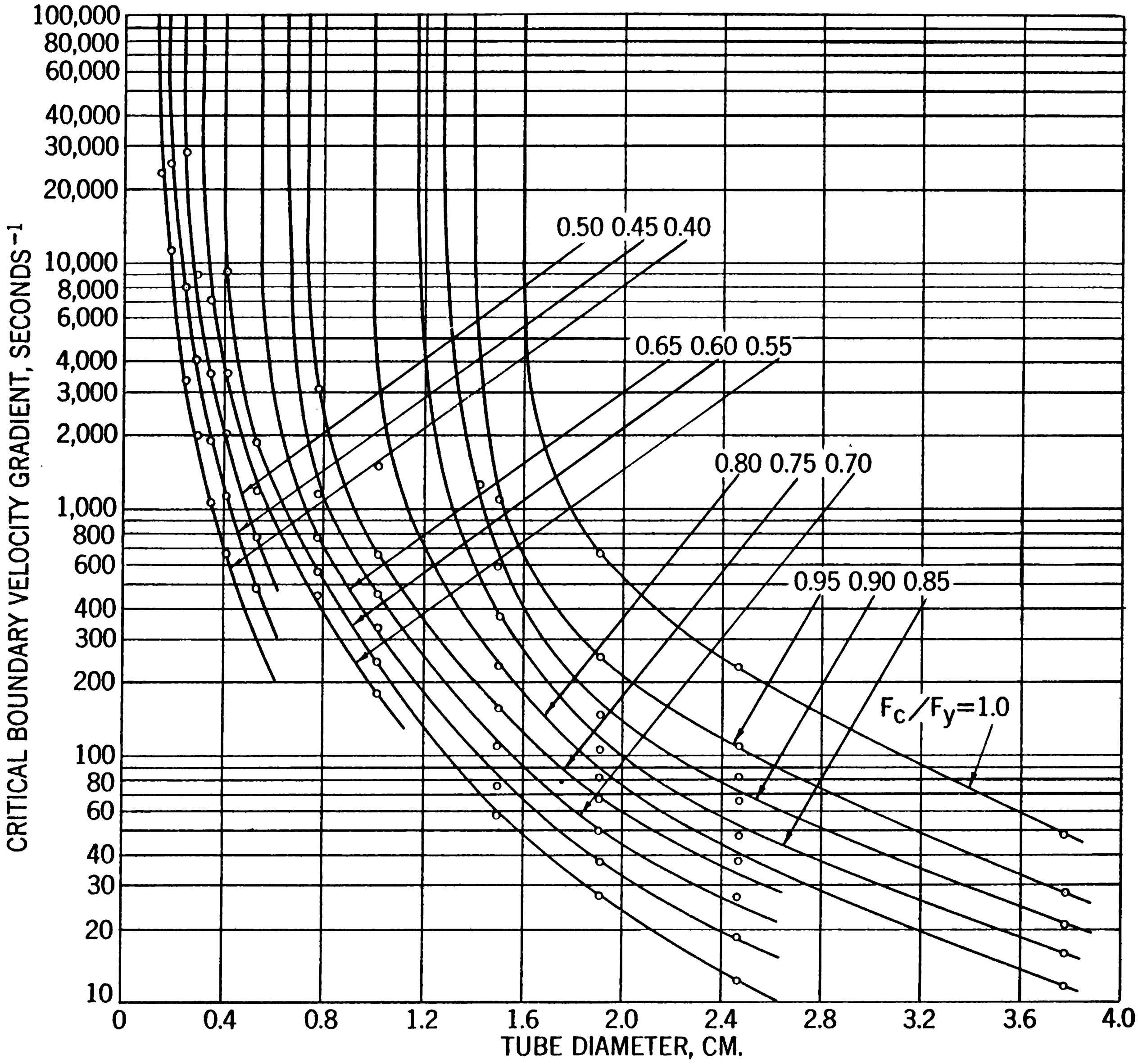

Figure 60. - Curves of constant yellow-tip fractions for fuel No. 68 (89.5% CH_4, 6.7% C_2H_6, 2.7% C_3H_8, 0.4% C_3H_6, 0.4% C_4H_{10}, 0.3% CO_2).

TABLE 7. - Curves of constant yellow-tip fractions for fuel No. 68

$F_c = 1.78$							
(1) F_c/F_y	(2) F_y	(3) Tube diam., cm.	(4) g_y	(1) F_c/F_y	(2) F_y	(3) Tube diam., cm.	(4) g_y
1.0	1.78	3.78	48	0.65	2.74	2.47	19
		2.47	230			1.914	38
		1.914	660			1.503	76
						1.023	335
.95	1.87	3.78	28			.776	770
		2.47	110				
		1.914	255	.60	2.97	2.47	12
		1.503	1,100			1.914	28
		1.43	4,100			1.503	58
						1.023	245
.90	1.98	3.78	21			.776	570
		2.47	82			.535	1,880
		1.914	148			.413	9,300
		1.503	590				
		1.43	1,280	.55	3.24	1.023	180
						.776	455
.85	2.09	3.78	16			.535	1,200
		2.47	66			.413	3,600
		1.914	108			.354	7,100
		1.503	390				
		1.43	550	.50	3.56	.535	780
						.413	2,030
.80	2.23	3.78	12			.354	3,550
		2.47	48			.294	9,000
		1.914	82			.249	28,000
		1.503	235				
		1.023	1,500 and up	.45	3.96	.535	480
						.413	1,150
						.354	1,900
.75	2.37	2.47	38			.294	4,050
		1.914	66			.249	8,000
		1.503	158			.195	25,300
		1.023	670				
		.776	3,100	.40	4.45	.413	670
						.354	1,080
.70	2.54	2.47	27			.294	2,000
		1.914	50			.249	3,350
		1.503	110			.195	11,300
		1.023	460			.155	23,000
		.776	1,160				

(2) Next, let us select several tube diameters for which we have experimental data for comparison with predicted limits: 0.776-, 0.413-, and 0.249-cm. tubes. From figure 52, we find that, for an abscissa of 0.61 and an ordinate of 0.776, F_c/F_y is about 0.75. This reading is noted in column 1 of table 8. The flow for this point is given in the legend of figure 52 and is found in column 2 of table 8. For the same abscissa and ordinate, other $F_c/_y$ values are obtained from figures 53-56, with the flows shown in the legends. The same procedure is used to obtain the data in columns 1 and 2 of table 8 for 0.413- and 0.249-cm. tubes.

TABLE 8. - Sample calculations of yellow-tip curves for fuel No. 71

F_c = 1.71			
Tube diameter, cm.	(1) F_c/F_y	(2) g_y	(3) F_y
0.776	0.75	300	2.28
	.89	800	1.92
	.97	3,000	1.76
	.98	10,000	1.75
	.98	20,000	1.75
	.98	40,000	1.75
.413	.58	800	2.95
	.79	3,000	2.17
	.85	10,000	2.01
	.86	20,000	1.99
	.86	40,000	1.99
.249	.56	3,000	3.05
	.69	10,000	2.48
	.69	20,000	2.48
	.69	40,000	2.48

(3) The constant yellow-tip limit, F_c, is calculated from table 5 and equation 8. For the fuel considered here it is $1/1.0\,[(0.621 \times 1.8) + (0.355 \times 1.61) + (0.024 \times 1.87)] = 1.73$. The experimental value of F_c, 1.71, was used in constructing table 8 and figure 61. Its calculated value, 1.73, could have been used equally well.

(4) Dividing F_c by F_c/F_y (column 1), we obtain values of F_y (column 3).

(5) Plotting g_y (column 2) versus F_y (column 3) for each tube diameter, we obtain the curves in figure 61. Comparison of these calculated curves with the experimental points shows a satisfactory order of agreement.

As a second illustration, let us take a fuel consisting of 32.1 percent CH_4, 28.4 percent C_2H_4, 12.5 percent H_2, and 27.0 percent N_2 (A-T/6-No./57).

(1) As its yellow-tipping constituents are mainly methane and ethylene, the composite yellow-tip fraction diagrams to be consulted are those for

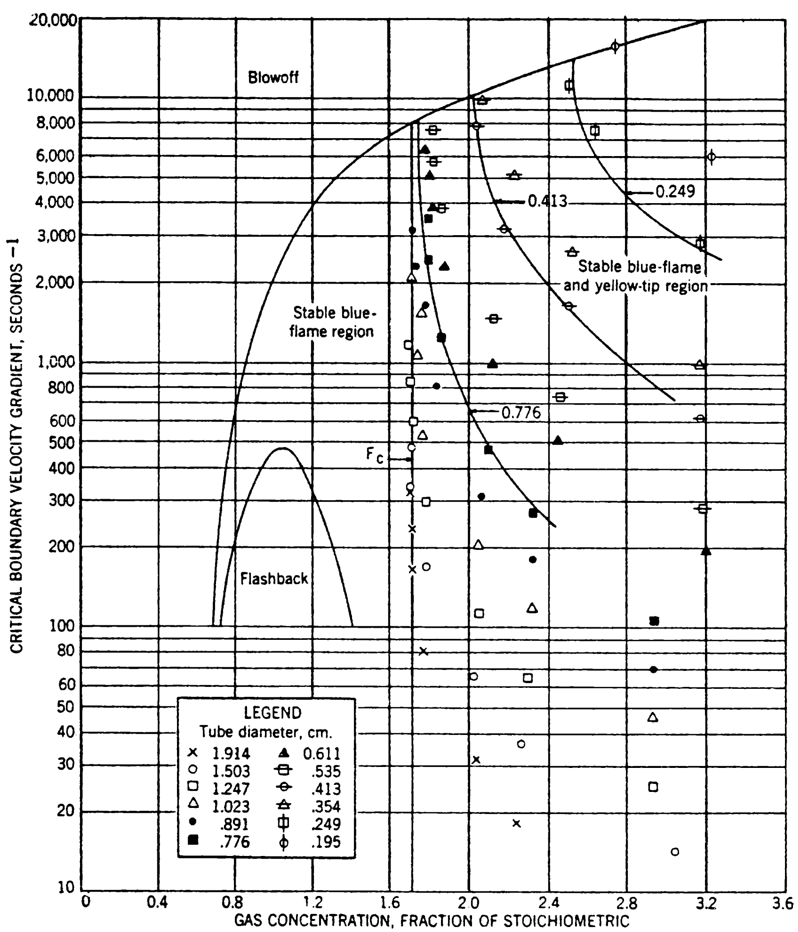

Figure 61. - Flame-characteristics diagram for fuel No. 71 (62.1% CH_4, 35.5% C_3H_8, 2.4% C_2H_6); comparison of experimental points and calculated curves.

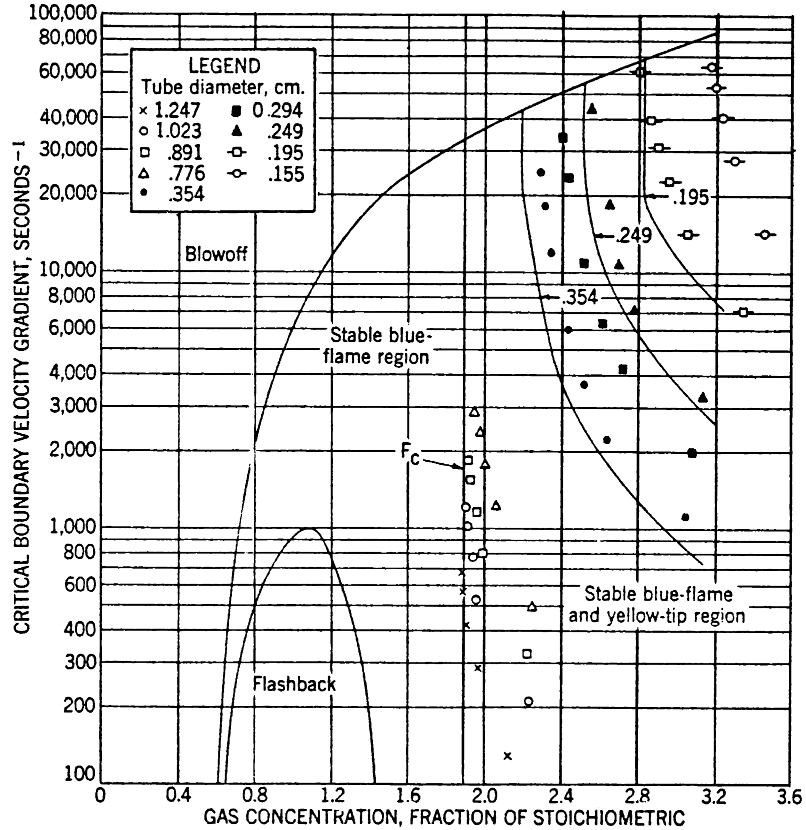

Figure 62. - Flame-characteristics diagram for fuel No. 57 (32.1% CH_4, 28.4% C_2H_4, 12.5% H_2, 27.0% N_2); comparison of experimental points and calculated curves.

methane-ethylene fuels, namely, figures 57-59. The fuel is located on the composite diagram by its ratio of CH_4/C_2H_4 or C_2H_4/CH_4. In this case it is C_2H_4/CH_4 = 28.4/32.1 = 0.885.

(2) Next let us select several tube diameters for which we have experimental data for comparison with predicted limits: 0.354-, 0.249-, and 0.195-cm. tubes. From figure 57 we find that, for an abscissa of 0.885 and an ordinate of 0.354, F_c/F_y is about 0.60. This reading is noted in column 1 of table 9. The flow for this point is given in the legend of figure 57 and is found in column 2 of table 9. For the same abscissa and ordinate, other F_c/F_y values are obtained from figures 58 and 59, with the flows shown in the legends. This same procedure is used to get columns 1 and 2 of table 9 for the 0.249- and 0.195-cm. tubes.

TABLE 9. - Sample calculations of yellow-tip curves for fuel No. 57

F_c = 1.84			
Tube diameter, cm.	(1) F_c/F_y	(2) g_y	(3) F_y
0.354	0.60	800	3.07
	.75	3,000	2.45
	.81	10,000	2.27
	.83	20,000	2.2
	.83	40,000	2.2
.249	.59	3,000	3.12
	.70	10,000	2.63
	.73	20,000	2.52
	.73	40,000	2.52
.195	.60	10,000	3.07
	.65	20,000	2.83
	.65	40,000	2.83

(3) The constant yellow-tip limit, F_c, is calculated from table 5 and equation 8. For the fuel considered here, it is $1/0.605\left[(0.321 \times 1.8) + (0.284 \times 1.88)\right] = 1.84$. This value was used in constructing table 9 and figure 62. However, the experimental value of F_c, 1.90, could have been used with almost perfect agreement between experimental points and calculated curves.

(4) Dividing F_c by F_c/F_y (column 1), we obtain values of F_y (column 3).

(5) Plotting g_y (column 2) versus F_y (column 3) for each tube diameter, we obtain the curves in figure 62. These calculated curves may be compared with the experimental points in the figure to note the order of agreement.

Another application of this procedure is the conversion of yellow-tip limits into the units percent primary air and B.t.u./hr.in.^{2} (see ch. I, pp. 11 and 13). As an example, let us take Cleveland natural gas (91.6 percent CH_4, 4.3 percent C_2H_6, 1.0 percent C_3H_8, 0.4 percent C_4H_{10}, 1.9 percent N_2, and 0.8 percent CO_2), with a stoichiometric percent of 9.39. The diagrams representative of this fuel are figures 52-56. For comparison, the tubes selected have the same diameters as burners 8 and 9 in AGA Research Report 1192,21/ namely, 0.2705 and 0.2308 cm., respectively.

(a) The fuel and each of these two diameters are located, respectively, on the abscissa at a ratio of C_3H_8 group/CH_4 = 0.0622 and the ordinates of 0.2705 and 0.2308 cm. in figures 52-56. Each of these graphs yields a value of F_c/F_y versus g_y for each of the two diameters, and these are tabulated in columns 2 and 3 of table 10.

(b) F_c for natural gas is 1.78 (table 5). Dividing F_c = 1.78 by the F_c/F_y values (table 10, column 2), we obtain values of F_y (column 4). The yellow-tip limit curves for the two diameters are obtained by plotting F_y (column 4) against g_y (column 3). The resulting curves are found in figure 63, A. For each diameter, yellow-tipped flames will occur on the right of the corresponding curve.

TABLE 10. - Sample calculations of yellow-tip curves in units of L and M

(1) Port diameter, cm.	(2) F_c/F_y	(3) g_y	(4) F_y	(5) L	(6) M
0.2705	0.40	3,000	4.45	14.4	35,600
	.47	10,000	3.79	18.8	101,000
	.50	20,000	3.56	20.7	190,000
	.50	40,000	3.56	20.7	380,000
.2308	.43	10,000	4.14	16.3	94,000
	.46	20,000	3.87	18.2	176,000
	.46	40,000	3.87	18.2	352,000

(c) Using equations 2 and 3 (ch. I, p. 13), and knowing that h = 1,025 B.t.u./cu.ft. (29) and that S is equal to 0.0939 (from P = 9.65) (29), F_y is converted into L, percent primary air (column 5), and g_y into M, B.t.u./hr.in.^{2} (column 6).

For the first line in table 10,

$$L = \frac{100\left(1 - 4.45(0.0939)\right)}{4.45(1 - 0.0939)} = 14.4,$$

$$M = 0.26(3{,}000)(1{,}025)(0.1065)(4.45)(0.0939) = 35{,}600.$$

L is plotted against M in figure 63, B. The resulting curves are the yellow-tip limit curves predicted by the Bureau of Mines method. These are the curves in figure 63, B, based on points marked ⊙ and • and are for the ports in free air. Figure 63, B, also gives yellow-tip-limit curves for two contemporary burners with

21/ The data in AGA Research Report 1192 were obtained with multiport burners, many of which had inclined ports operating hot. Our calculations are for upright ports in free air (such as a monoport) at room temperature and pressure.

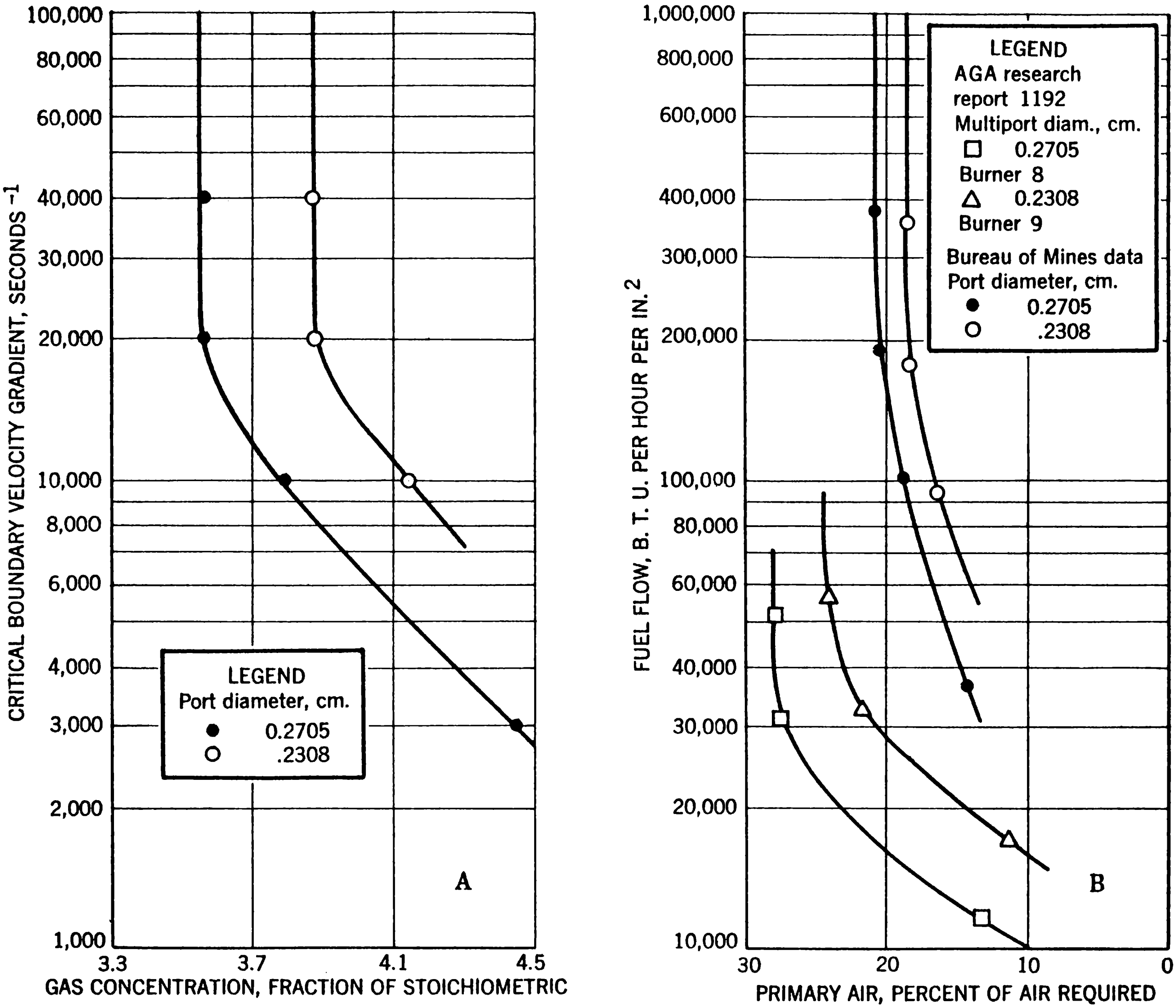

Figure 63. - A, Yellow-tip limit curves for burners in free air, natural gas; B, comparison of predicted yellow-tip limits for burners in free air and observed limits on multiports; natural gas.

multiports of the same diameter spaced one-fourth inch apart (data taken from AGA Research Report 1192 (29)). The yellow-tip limits on the multiport burners are leaner than predicted, because each port is partly surrounded by products of combustion from adjacent ports. Thus it will be seen that more factors are involved in predicting the yellow tipping of contemporary burners than for flames in free air on cold ports.

Figures 64, 65, and 66 (A-T/7-No./6,84,85) give additional data of laboratory interest for benzene, toluene, and acetylene. Figure 67 (A-T/7-No./86) is for a mixture of natural gas and acetylene, while figure 68 (A-T/7-No./87) is for a mixture of natural gas and toluene. These mixtures are not likely to appear as such in gas-distribution systems and accordingly have not been given the same treatment as the natural gases, liquid-petroleum fuels, and oil gases. They are included for their general interest and, in the case of figures 67 and 68, to show that small quantities of aromatics and acetylene, when mixed with natural gas increase yellow tipping of the mixture more than equal quantities of the ethylene or the propane group. The constant yellow-tip limits can be predicted from equation 8.

Fuels may, of course, consist of mixtures containing methane, the propane group, and ethylene. In such instances the procedure for calculating values of F_c/F_y outlined above is varied to divide the methane between the ethylene and propane groups in a manner similar to that employed in chapter II for calculating flashback and blowoff gradients (p. 48). The methane is proportioned in the ratio of percent C_3H_8 group/percent C_3H_8 group + C_2H_4 and percent C_2H_4/percent C_3H_8 group + C_2H_4. Values of F_c/F_y obtained from the CH_4-C_3H_8 group composites (figures 52-56) and from the CH_4-C_2H_4 composite (figures 57-59) are substituted in equation 9.

$$(F_c/F_y)_{calc.} = \frac{1}{n}\left[a(F_c/F_y)_{CH_4\text{-}C_3H_8 \text{ group}} + b(F_c/F_y)_{CH_4\text{-}C_2H_4} + \cdots \right], \quad (9)$$

where $n = \Sigma\, a,b,\ldots$, and $a = \Sigma\,(C_3H_8 \text{ group}) + (CH_4$ proportioned to the C_3H_8 group) and $b = \Sigma\,(C_2H_4) + (CH_4$ proportioned to $C_2H_4)$. This procedure has been tested with two fuels (A-T/7-No./66,56). Good agreement between experiment and prediction was obtained with fuel No. 56, consisting of 29.1 percent CH_4, 26.2 percent C_2H_4, 22.1 percent C_3H_8, 11.8 percent H_2, 0.2 percent C_3H_6, and 10.6 percent N_2, but not with fuel No. 66, consisting of 42.6 percent CH_4, 18.1 percent C_2H_4, 17.0 percent H_2, 9.1 percent CO, 2.2 percent C_2H_6, 1.9 percent C_3H_8, 0.2 percent C_3H_6, 0.2 percent C_4H_{10}, 0.1 percent C_4H_8, 5.2 percent CO_2, and 3.4 percent N_2. Results with the latter fuel showed good agreement for the constant yellow-tip limit but only passable agreement for nonconstant limits, the predicted yellow-tip limits being leaner than the experimental. The combination of high non-yellow-tipping constituents (34.7 percent) plus methane (42.6 percent) may be responsible for this discrepancy.

It may be desired to evaluate fuels in the order of their tendency to yellow-tip. This cannot be done by comparing F_c values of the fuels with the expectation that the tendency to yellow tip increases with decreasing F_c. The R* value also must be considered. For extremely slow burning fuels, such as methane, R* is larger than 2 cm. It decreases progressively as other constituents are added to methane, until it reaches a value of about 6 mm. for all other fuels except acetylene. The value for acetylene is about 3 mm. Values of R* can be obtained for most fuels by locating the ratio of the fuel on diagrams 56 and 59B and noting the diameter for which F_c/F_y is unity.

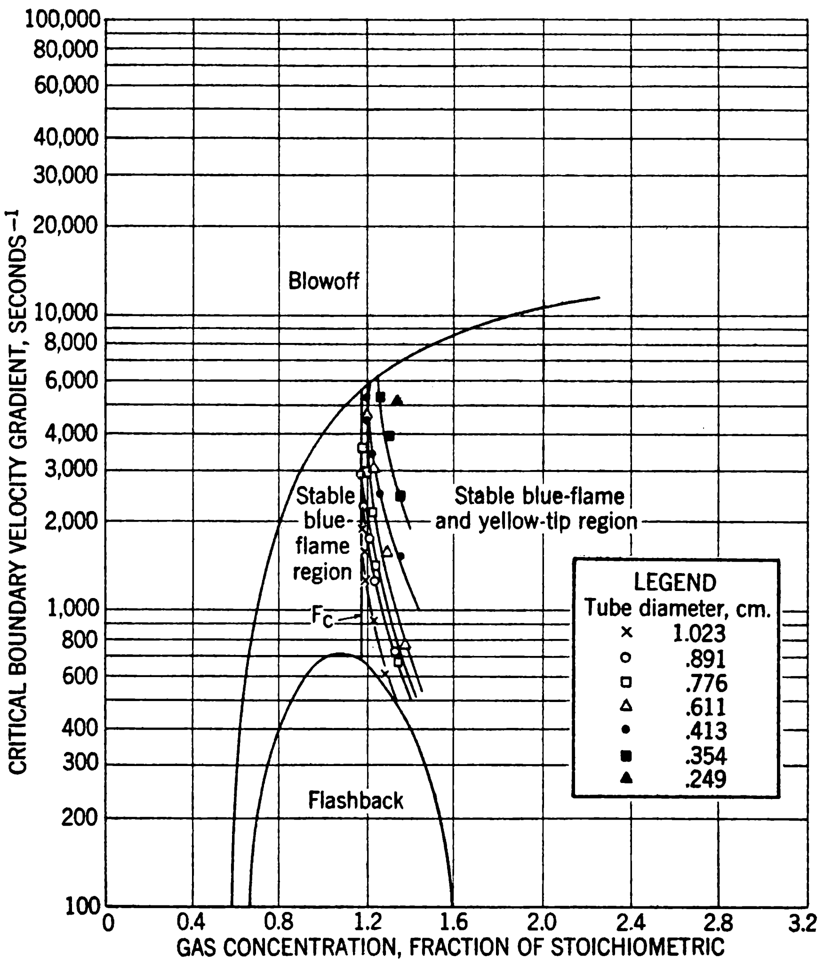

Figure 64. - Flame-characteristics diagram for fuel No. 6 ($100\% C_6H_6$).

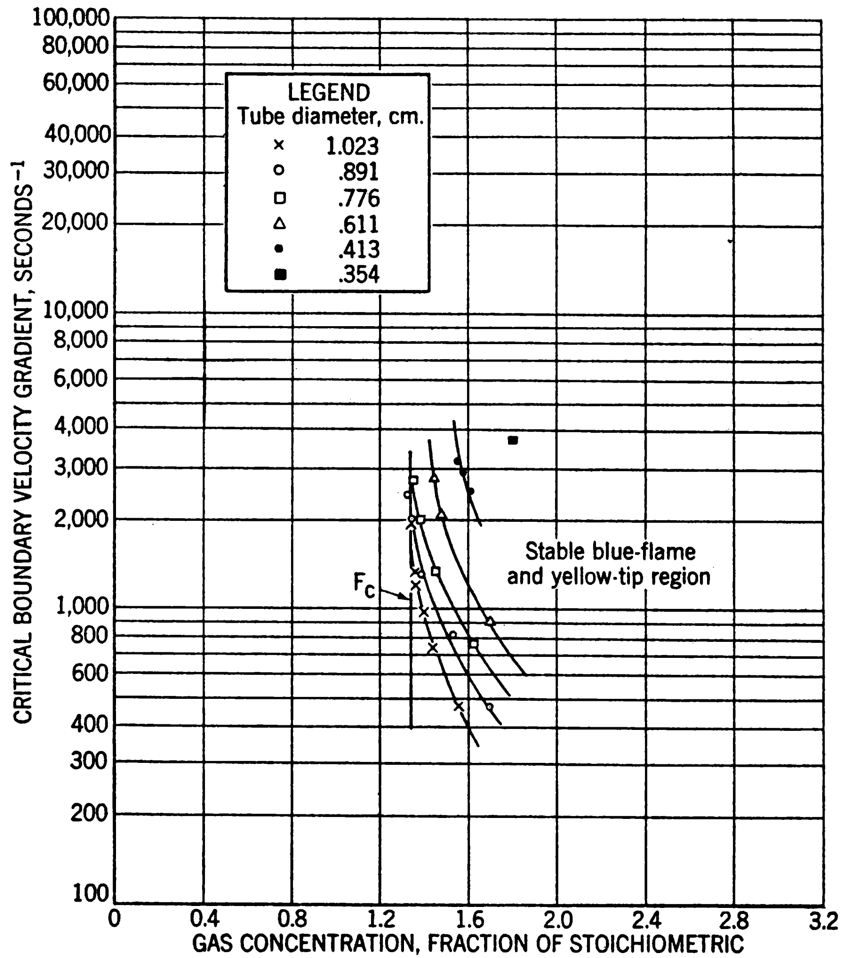

Figure 65. - Yellow-tip limits for fuel No. 84 ($100\% C_7H_8$).

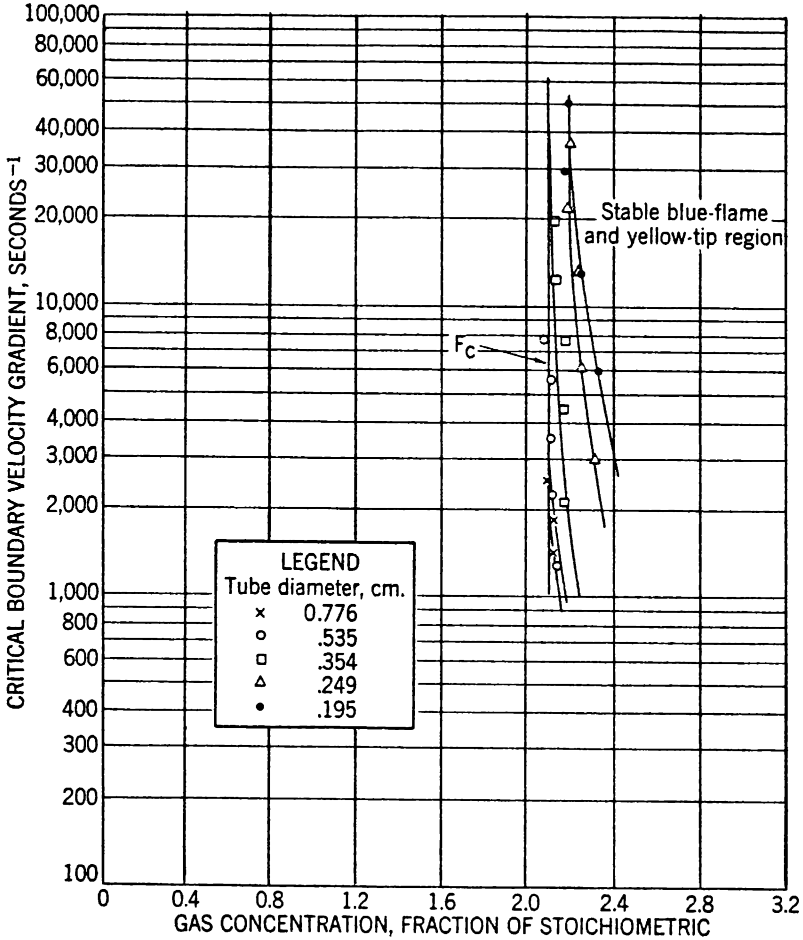

Figure 66. - Yellow-tip limits for fuel No. 85 (97.3% C_2H_2, 2.7% CH_3COCH_3).

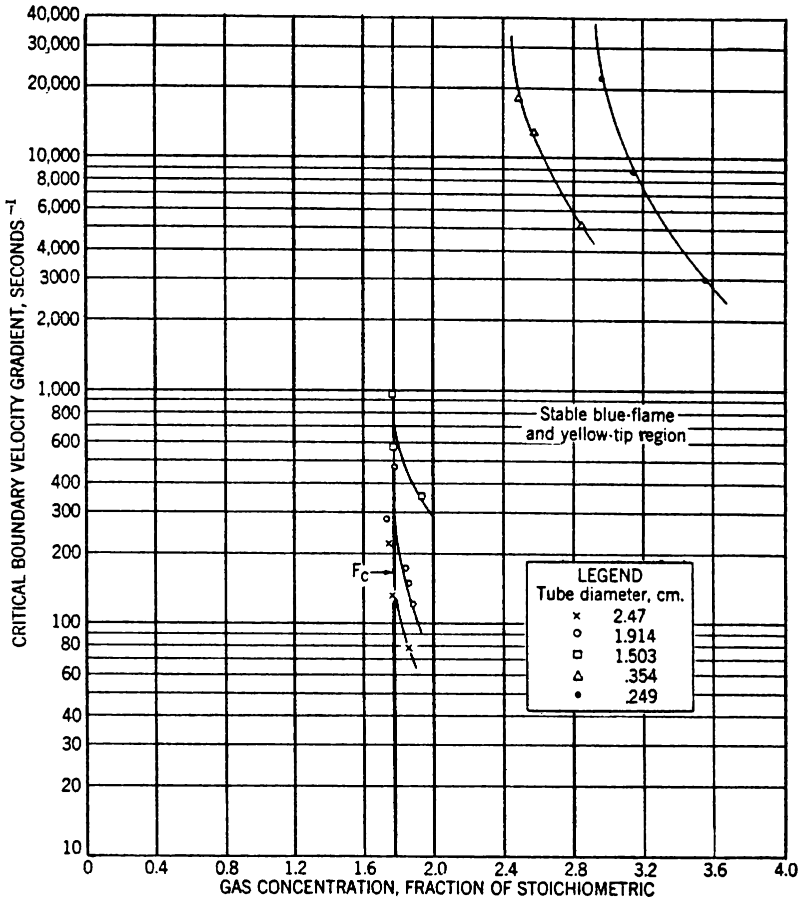

Figure 67. - Yellow-tip limits for fuel No. 86 (84.2% CH_4, 7.6% C_2H_2, 5.3% C_2H_6, 1.6% C_3H_6, 0.6% C_4H_{10}, 0.3% C_3H_6, 0.4% CO_2).

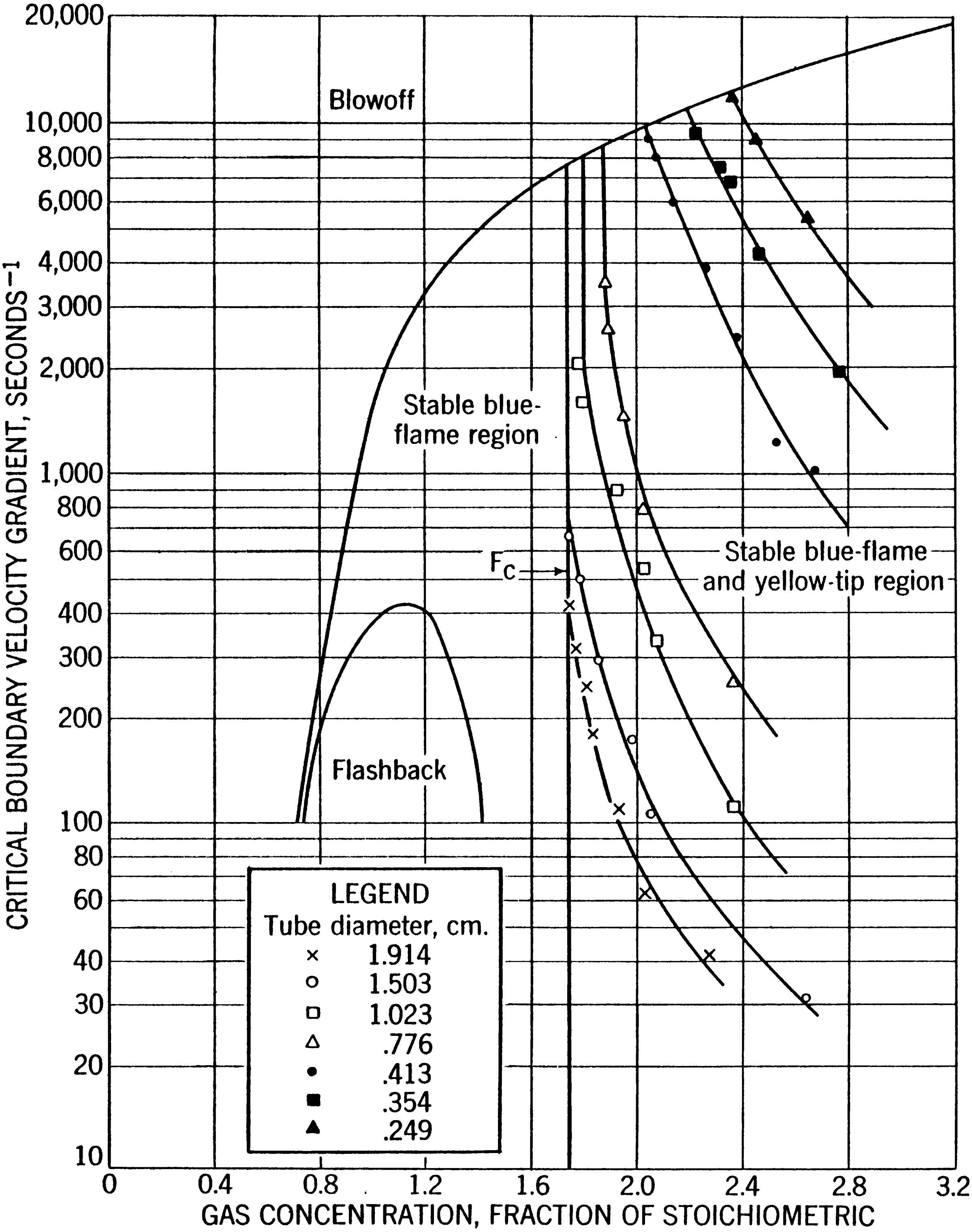

Figure 68. - Flame-characteristics diagram for fuel No. 87 (91.6% CH_4, 4.0% C_7H_8, 3.2% C_2H_6, 0.7% C_3H_8, 0.2% C_3H_6, 0.3% CO_2).

As an example, let us compare the yellow-tipping tendencies of acetylene and methane. The constant yellow-tip limit of acetylene is 2.10; that of methane is 1.80. Judging by this alone, we might conclude that methane is more prone to form yellow-tipped flames than acetylene; however, the reverse is true. For acetylene, F_c is observed on all tubes larger than about 3 mm. diameter, whereas for methane (figure 49, p. 67), F_c is observed on tubes larger than about 22 mm. On a 3-mm. tube the yellow-tip limits of methane flames are about double the F_c value. The difference between methane and acetylene is due to the nature of the flames each forms. Yellow-tipped methane flames are very soft, long, slow-burning diffusion flames. The yellow appears a long distance downstream of the port, and correspondingly the time t of equation 5 is large. When t is large, the distance $\bar{X}$ (also R*) over which secondary air diffuses radially is great. Such is the case for methane and natural gas. The yellow-tipped flame of acetylene burns rapidly, with a sharp, very short, inner cone, and yellow appears a very short distance downstream of the port. Correspondingly, t is much smaller for acetylene than for methane, and the critical diameter is very much smaller. Thus yellow-tipping tendencies of fuels can be compared by comparing values of F_c, if the values of R* are virtually the same for the fuels. If the R* values are very different, the comparison is not precise, and flow and port diameter must be taken into consideration.

CHAPTER V. - FLASHBACK, BLOWOFF, AND YELLOW TIPPING ON BURNERS WITH SHORT PORTS (DRILL PORTS) OR NONCIRCULAR CHANNELS (SQUARE, RECTANGULAR, AND TRIANGULAR CHANNELS)

A. Flashback and Blowoff

It has been well established that, for each fuel, the flashback and blowoff characteristics of burners with circular flame ports with steady laminar flow can be described by 1 curve of critical boundary velocity gradients versus gas-air mixture composition for flashback and 1 corresponding curve for blowoff. For steady laminar (Poiseuille) flow the boundary velocity gradient is given by the equation

$$g = 4V/\pi R^3, \tag{1}$$

where V is the volumetric flow through a port of radius R. As most gas appliances do not have circular ports with Poiseuille flow, it is of theoretical and practical significance to demonstrate that the concept of critical boundary velocity gradients is generally applicable to burner ports of all types.

Let us first consider the distinctions between the variety of flow profiles possible in burner ports. The simplest case is that of steady laminar flow through a long tube. There are two ways of calculating a gradient for this type of flow. The surer method is to differentiate the equation for Poiseuille flow and solve the result for the slope near the wall of the port. The equation for a tube is

$$U = 2V/\pi R^2 \left(1 - \frac{r^2}{R^2}\right). \tag{10}$$

Differentiating for the limit $r \to R$ gives the boundary velocity gradient

$$g = \lim_{r \to R} (-dU/dr) = 4V/\pi R^3. \tag{11}$$

In equation 10, U is the velocity at the distance r from the axis in a tube of radius R with a total volumetric flow V. The advantage of this formulation for the gradient g is that it requires no experimental measurements of the boundary velocity profile.

In principle, g may be determined by the extremely difficult feat of measuring the change in U as a function of r in the vicinity of the wall with some instrument such as a Pitot tube. The slope near the wall of the plot of U against r would be the desired gradient.

In both nonsteady and steady laminar flow, more general considerations can be applied to the evaluation of the gradient. Any stream, whether overall turbulent or laminar,[22/] has a laminar boundary layer, and its boundary velocity gradient is related to the pressure drop, $\Delta p/\ell$ (ℓ being the channel length), through the channel by equation 12:

$$\eta \, g \, 2\pi R = (\Delta p/\ell)\, \pi R^2 = \lambda \rho V^2/4\pi R^3, \tag{12}$$

22/ The gross difference between laminar and turbulent flow lies in the nature of radial motion for most of the stream. In laminar flow, except for molecular diffusion, there is no exchange of "particles" between stream tubes in a radial direction. In turbulent flow, there is such an exchange of "particles." Usually the change from laminar to turbulent flow occurs at a Reynolds number of about 2,000. However, laminar flow is possible at much higher Reynolds numbers, and turbulent flow is possible at very low Reynolds numbers. In the former instance great care is needed to free the stream of any precipitating disturbances, such as slightly rough walls or obstructions in the stream. In the latter instance some disturbance can be introduced into a slowly moving stream, such as a fast fuel jet into relatively slow moving air, and turbulence will persist for quite a distance downstream until viscous forces smooth out the flow. Moreover, there are various types of laminar flow: (a) If the tube is long enough (about 60 diameters or more) there is steady laminar flow of Poiseuille type. It is laminar because there is no radial interchange of matter from one stream tube to the other, apart from molecular diffusion; it is steady because there is no further change in the velocity profile with downstream travel. In tubes the velocity profile corresponding to this type of flow is a parabola. In nonsteady laminar flow the flow profile tends to become a parabola as the stream moves along the tube. (b) If the channel is noncylindrical, for example, square, rectangular, or triangular channels, but is long enough, the flow remains steady laminar but not Poiseuille because of the asymmetry of the channel. (c) Using a nozzle port of the Mach-Hebra type, we have a nonsteady laminar flow with a square profile where the velocity drops precipitously to zero at the boundary of the stream. Over almost the entire cross section of the stream, the local velocity equals the average stream velocity. (d) Nonsteady laminar flow is possible in short ports of the drill-port type if the flow enters the ports from a large chamber with nearly zero stream velocity. When the approach flow is rapid, a mixture of nonsteady laminar and turbulent flow is possible, with turbulence near the axis of the port and laminar flow over a relatively large stream width near the wall of the port. The boundary velocity gradient of each of the above types of flow can be correlated with the average velocity by means of the coefficient of friction, λ, which in turn can be determined experimentally as a function of the Reynolds number and channel geometry.

where η is the viscosity, poise; ρ is the density, gm./sec.; and λ is the coefficient of friction, relating the boundary velocity to the average velocity. Equation 12 relates the viscous force at the wall which retards the flow to the pressure that induces flow. Introducing the Reynolds number $Re = 2V\rho / \pi R \eta$ reduces equation 12 to

$$g = \lambda V \, Re/16\pi R^3. \tag{13}$$

The task of converting values of V into g now hinges on the dependence of λ on Re, which in turn depends on V and R.

Application of Equation 13 to Poiseuille Flow

For Poiseuille flow in long tubes (parabolic flow), Hagen (22) found that

$$\lambda = 64/Re. \tag{13a}$$

The combination of equations 13 and 13a yields equation 1, showing agreement between equations 1 and 13.

Application of Equation 13 to Turbulent Flow

Similarly, Blasius (22) observed that for turbulent flow of Reynolds numbers from about 3,000 to 100,000, in tubes with hydraulically smooth walls,

$$\lambda = 0.316/Re^{1/4}. \tag{13b}$$

Wohl and others (32) and Bollinger and Williams (3) used equations 13 and 13b to calculate critical boundary velocity gradients for blowoff from observed volumetric flows at blowoff under turbulent flow conditions. These gradients agreed with those obtained with steady laminar flow, showing that the concept of critical boundary velocity gradients is valid for the blowoff of turbulent flames. However, Wohl (31), Edse (7), and this laboratory observed flashback of turbulent flames at flows very much in excess of those corresponding to the flashback gradient measured in steady laminar flow. Further study of the nature of flashback of turbulent flames is obviously in order.

Application of Equation 13 to Sharp-Edged Short Ports (Drill Ports)

Wilson (30) used equation 13 to study blowoff of ethylene-air flames from sharp-edged, short, cylindrical ports, approximating the kind commonly employed in gas appliances. The dependence of λ on Re was determined from measurements of the pressure drop through the porthole. Wilson's results show excellent agreement between the critical boundary velocity gradient curve for blowoff of ethylene obtained with cylindrical burners and the blowoff points obtained with equation 13 for sharp-edged short ports.

λ can be determined by another method. Measurements were made in this laboratory of the critical flows for flashback and blowoff on a number of sharp-edged short ports (0.635- and 0.318-cm. depth) using carbon monoxide-hydrogen as the fuel. In all, 74 points were obtained. Values of the critical flame-stability gradients obtained with tubes, figure 69 (A-T/2a,2b-No./17), were substituted in equation 13,

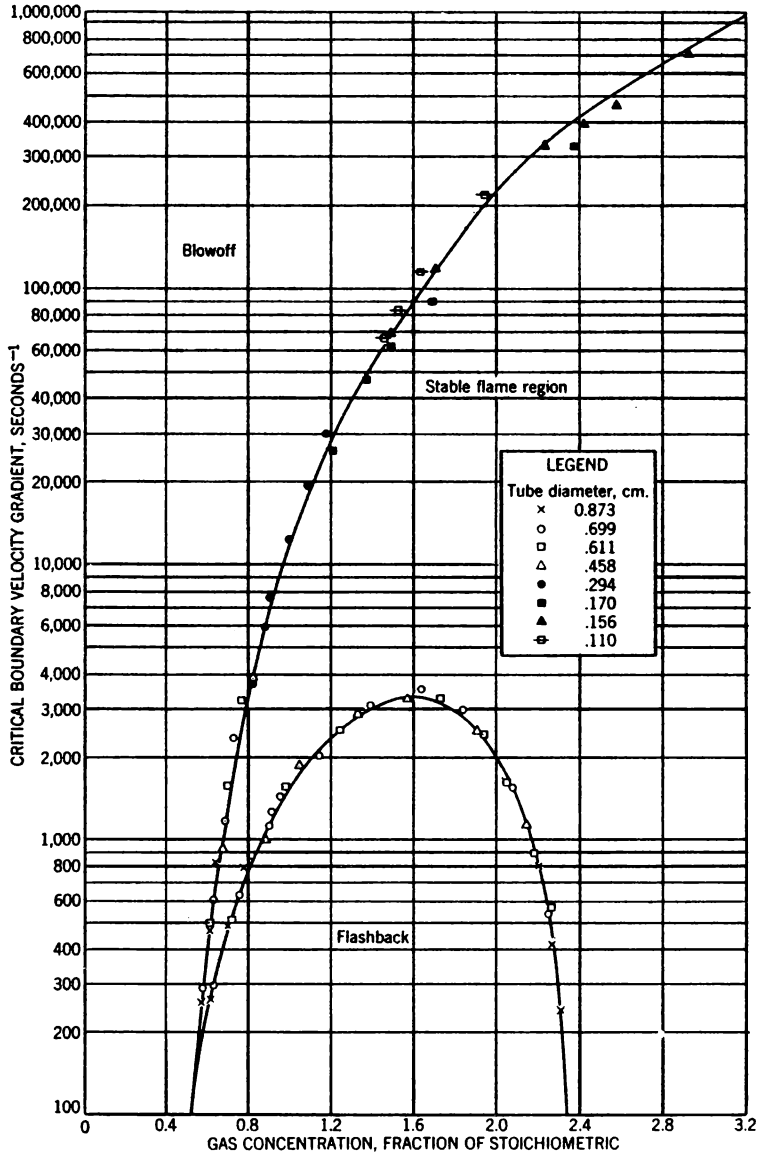

Figure 69. - Flame-stability diagram for fuel No. 17 (79.3% CO, 19.7% H_2, 0.6% N_2, 0.3% CO_2, 0.1% O_2).

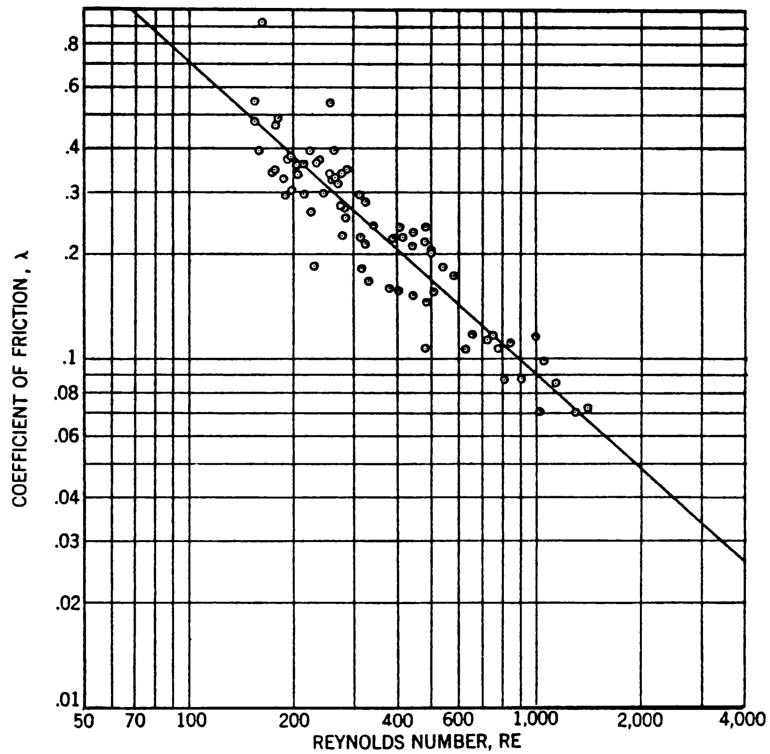

Figure 70. - Coefficients of friction for sharp-edged short ports (data obtained with a CO-H_2 fuel with port depths of 0.635 and 0.318 cm.).

and the equation was solved for λ (A-T/8a-No./17).[23/] The points scattered about a straight line as shown in figure 70. The best line was obtained by the method of least squares. It is represented by the equation

$$\lambda = 41.4/Re^{0.89} \qquad (CO - H_2). \qquad (13c)^{24/}$$

The reverse procedure may be employed to calculate g_F and g_B for the same fuel (A-T/8b-No./17) from observed critical volumetric flows, using equations 13 and 13c. The points obtained in this manner are compared in figure 71 with the flame-stability diagram of the fuel for laminar flow with tubes. The agreement is of course attributable to the fact that the same data were used to obtain equation 13c. It is cited to show that flame-stability data provide a novel means of measuring coefficients of friction. Wilson (30) measured coefficients of friction by an independent method, and his experiments prove even more clearly that flame-stability gradients of cylindrical, sharp-edged short ports with nonsteady laminar flow are identical with those of long cylindrical tubes with steady laminar flow.

Further evidence may be obtained by using equation 13c to calculate flame-stability gradients of another fuel, such as methane. For reasons that are not clear, the agreement is only fair. Values of the critical boundary velocity gradients for methane obtained with tubes, figures 20 (A-T/1a,1b-No./2) (p. 25) and 72 (A-T/9-No./2), and critical flows for sharp-edged short ports were substituted in equation 13 and solved for λ (A-T/8a-No./2). In all, 112 points were obtained. These tests were conducted at 300°, 348°, and 423° K. No dependence of λ on temperature was observed. The best line representing these data is given by the equation

$$\lambda = 20.4/Re^{0.80} \qquad (CH_4). \qquad (13d)$$

Although this is contrary to the expectation that coefficients of friction should not be a function of the chemical identity of the fuel, the difference between equations 13c and 13d is not enough to affect the argument of this chapter. It may stem from a second-order effect due to the different back pressures of flames of methane and of carbon monoxide-hydrogen mixtures.

Applications of Equation 13 to Noncircular Channels With Steady Laminar Flow

The effect of the shape of a flame-port cross section for a well-defined flow profile may be investigated on long channels of uniform square, rectangular, or triangular cross section. Such channels produce steady laminar flow at the port, but not the symmetrical flow of tubes. The symmetry of a long cylinder makes the flow velocity and burning velocity uniform at all points equidistant from the wall. Thus the probability of flashback or blowoff is the same for all points on the tube boundary. This is not the case for noncircular channels. Here the velocity and velocity gradients are higher near the midpoint of the sides than at the corners, where

---

23/ These calculations were made using values of g_F and g_B for tubes obtained from figure 69 for the fuel containing 79.3 percent carbon monoxide, 19.7 percent hydrogen, 0.6 percent nitrogen, 0.3 percent carbon dioxide, and 0.1 percent oxygen; values of V_F and V_B for ports were obtained with a fuel containing 79.7 percent carbon monoxide, 20.1 percent hydrogen, and 0.2 percent carbon dioxide. Both fuels had virtually the same composition and were found experimentally to show identical flashback limits on a 0.611-cm. tube. They are treated as one fuel in this discussion.

24/ Equations 13c, e, g, and h differ slightly from 3c-3f of reference (12) because of added data, rearrangements, and a few corrections.

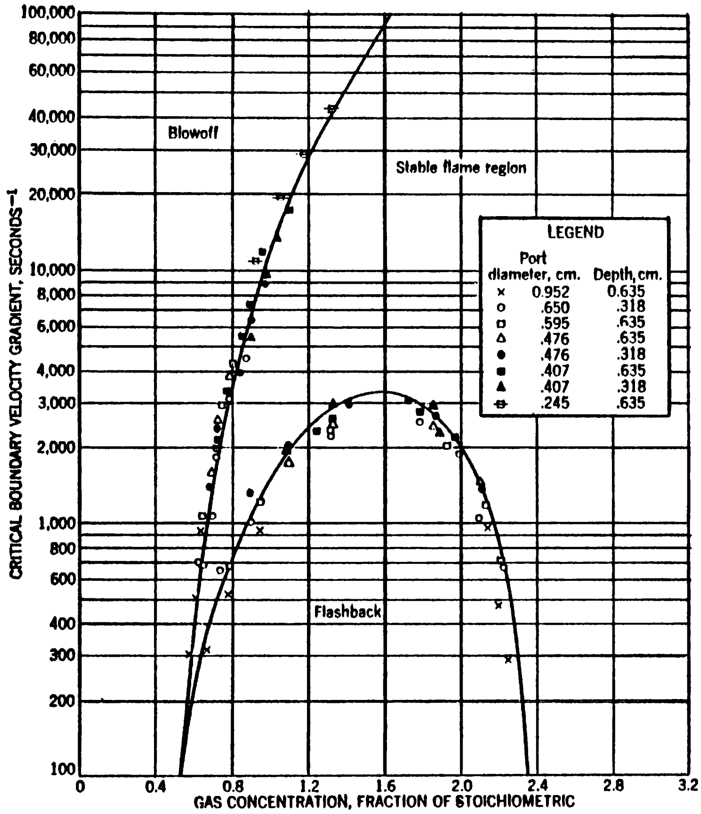

Figure 71. - Flame-stability diagram for fuel No. 17 (79.7% CO, 20.1% H_2, 0.2% CO_2); comparison of points for sharp-edged short ports and curves for long cylindrical tubes.

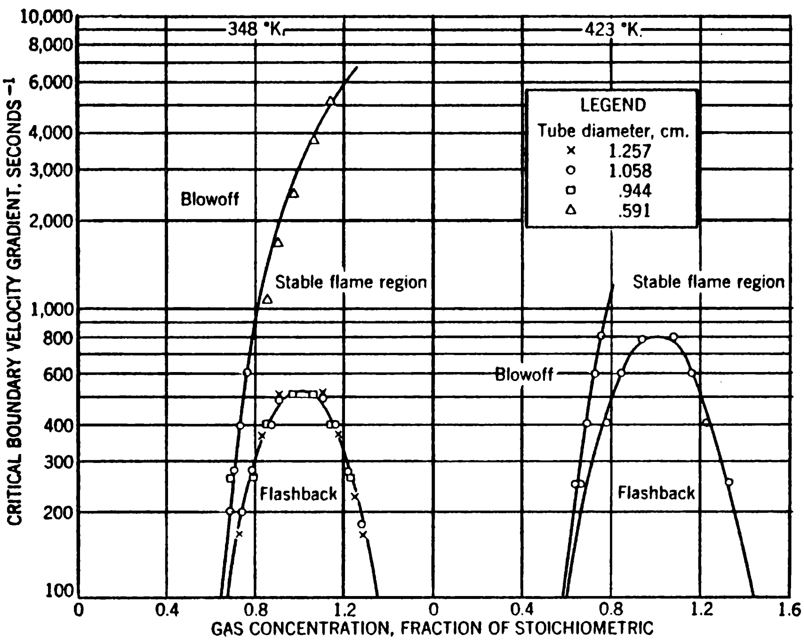

Figure 72. - Flame-stability diagram for fuel No. 2 (100% CH_4) at 348° and 423° K. for long cylindrical tubes.

increased quenching forces the flame deeper into the stream. Accordingly, in channels of noncircular cross section there is a specific location where the flame is stabilized. It was reasoned that, if the critical region for flame stabilization were near the midpoint of a side of an angular channel, flame-stability data for squares, rectangles, and triangles would agree among themselves. However, no such correlation was found, and the critical flame-stability gradients calculated in this way were much greater than those for tubes. When the critical region was assumed to be in the corners, the gradients were much lower than for tubes.

The apparent lack of agreement between flame-stability gradients for cylindrical tubes and noncircular channels may be explained as follows: Flame pressures are of the order of average velocity pressures at flashback and blowoff flows for these flames. For example, the flame pressure of a stoichiometric methane-air flame is about 0.01 cm. water, which is roughly equivalent to a flow of 130 cm./sec. This is approximately the velocity pressure at the axis for parabolic flow for flashback of a stoichiometric methane flame in a 1.3-cm. I.D. tube and blowoff from a 0.26-cm. I.D. tube. Examination of flames on noncircular channels, such as the methane flames near flashback in figure 73,a and b, clearly show that the primary cone does not cover the entire port, being nonexistent near the corners. The flame outlines in figure 73,a and b, are circular rather than angular. The dark lines are attributed to the fact that methane diffuses through the primary combustion zone more rapidly than oxygen (20), a phenomenon without bearing on this discussion. Cusps are visible near the corners of figure 73,c and d. (The burner in figure 73,c, is oriented so that one corner is in the center of the photograph.) These cusps suggest that the flame is going to flash back, starting at the corners. As the port is not completely covered by flame, part of the flow is opposed by the flame pressure, and part is not. The flame distorts the original velocity distribution, causing an increase at the corners and a decrease elsewhere. No such change in flow profile is suffered by a stream leaving a cylindrical tube, because the flame covers the channel uniformly.

It is extremely difficult to measure the flow profile in the unburned gas experimentally because the velocity pressures are low, the ports are small, and the flame may be affected by the measuring device. Notwithstanding these difficulties, measurements were made to determine whether, in an angular channel, the velocity profile of the unburned gas is changed by a flame. The following results prove the point at issue. A hypodermic needle serving as a Pitot tube was mounted on a mechanical stage and connected to a null-point slope gage mounted on a micrometer screw. The slope gage was filled with water and a trace of wetting agent. The liquid level was observed through the crosshairs of a telescope. Readings were reproducible to 0.003 cm. of water. A slightly rich methane-air stream was used in these experiments (F = 1.06, V = 269 cc./sec., channel dimensions = 1.068 x 1.075 cm.). Figure 74,A, shows that the apparatus is accurate enough for measuring total pressure profiles of the above stream. The traverse was made 1 mm. beneath the plane of the port, moving from the axis to the corner. The points were obtained experimentally in the absence of flame; the curve was calculated from steady laminar flow considerations (25). When a similar traverse was made in the presence of flame, the pressure increments given in figure 74,B, were observed. In addition, the pressure increase 1 mm. beneath the tip of the flame was within the reading error of 0.003 cm. If the flame had no effect on the original flow, one would note everywhere the flame exists a uniform increase of total pressure equal to the flame pressure (0.01 cm. in this instance). Instead near the corners the increase is even greater than the flame pressure. This demonstrates that due to the absence of flame pressure in the corners and the presence of such pressure elsewhere over the port, there is greater flow at the corners with a flame than without a flame. Therefore, the critical boundary velocity gradients for a noncircular channel cannot be calculated from the flow

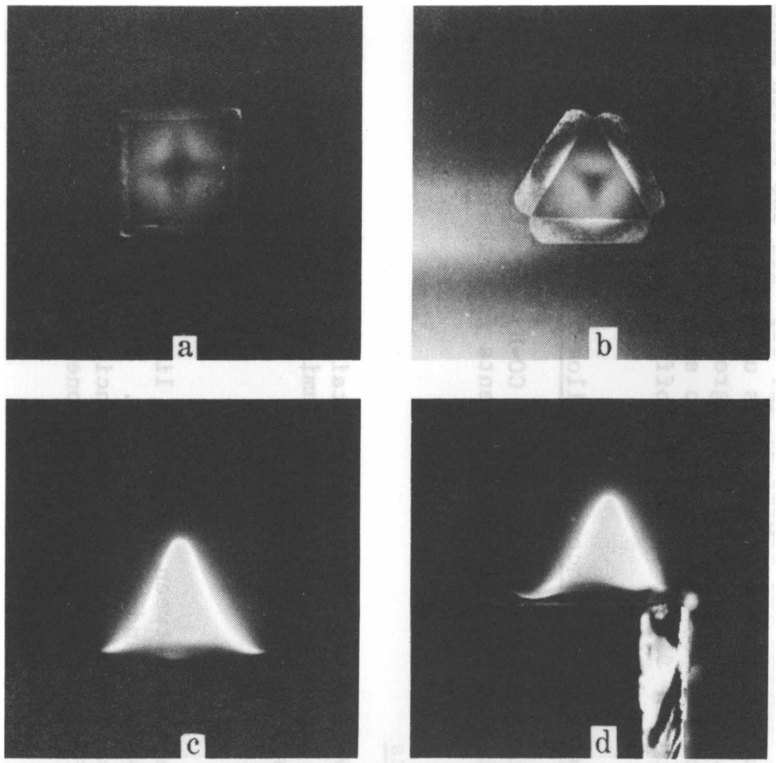

	View	Burner	Gas concentration
a	Top	1-cm. square	F = 0.88
b	do.	1.25-cm. equilateral triangle	.99
c	Front	1-cm. square	1.13
d	do.	1.25-× 1.25-× 1.75-cm. triangle	1.07

Figure 73. - Top and front views of methane flames near flashback on noncircular channels.

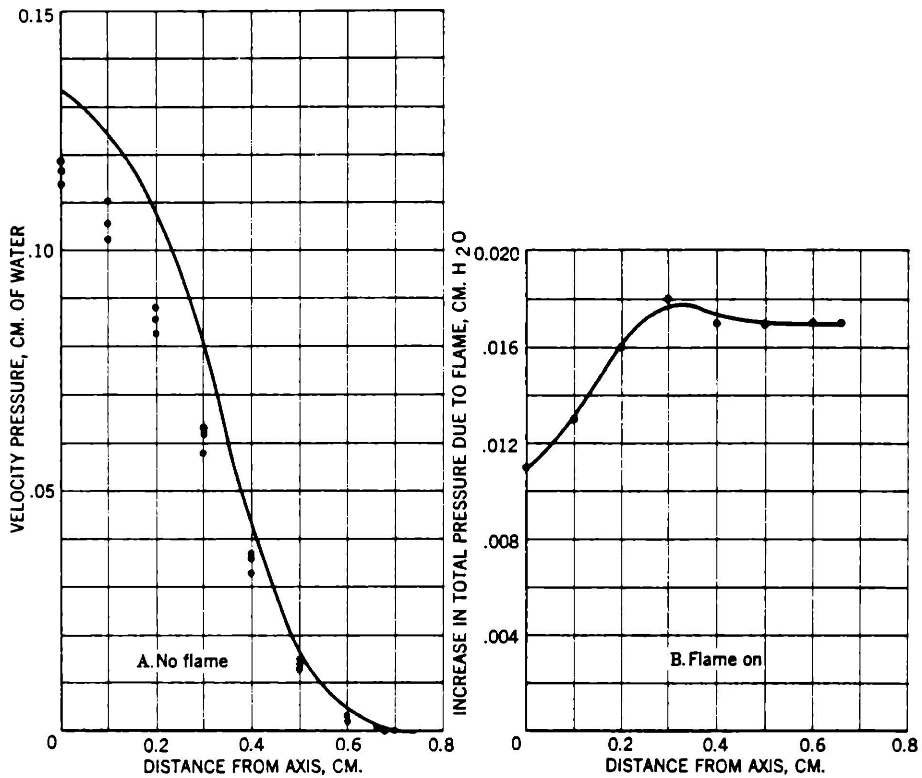

Figure 74. - A, Comparison of experimental and calculated velocity pressures; square channel, 1.068 x 1.075 cm.; B, effect of flame on flow profile in square channel, 1.068 x 1.075 cm.; theoretical flame pressure, 0.010 cm.

profile without flame. However, use may be made of the interdependence shown in equation 13 of the boundary velocity gradient and the pressure drop. (R becomes the equivalent hydraulic radius.) The constants in the equation, $\lambda = a/Re^b$, may be obtained from flame-stability data by the technique described above to determine equation 13c. The values of the constants a and b depend on the type of channel and reflect the magnitude of the change from steady laminar flow. Equations 13e and 13f (A-T/10a-No./2,17) were found for squares, 13g (A-T/11a-No./2) for rectangles, and 13h (A-T/12a-No./2) for triangles.

$$\lambda = 156.4/Re^{1.22} \quad (CO\text{-}H_2), \qquad (13e)$$

$$\lambda = 61.4/Re^{1.09} \quad (CH_4), \qquad (13f)$$

$$\lambda = 125.8/Re^{1.24} \quad (CH_4), \qquad (13g)$$

$$\lambda = 90.6/Re^{1.25} \quad (CH_4). \qquad (13h)$$

The lines of λ versus Re are shown in figure 75 for equations 13a-13h. It is most unlikely that the correlations of equations 13c-13h are fortuitous. Furthermore, there are the experimental data of Hagen (22) (equation 13a), Blasius (22) (equation 13b), and Wilson (30) to be considered. In these instances the dependence of λ on Re was determined independent of any consideration of flame stability. Use of the values of λ determined in this way to calculate critical boundary velocity gradients for flashback and blowoff of sharp-edged short ports on square, rectangular, and triangular channels produces excellent agreement with gradients calculated by equation 1 for long tubes.

The correlation is illustrated by the comparison in figure 71 and like comparisons that can be made, using (A-T/10b-No./2,17) for square channels, (A-T/11b-No./2) for rectangular channels, and (A-T/12b-No./2) for triangular channels in conjunction with figure 20 (p. 25 for methane and figure 69 (p. 93) for the carbon monoxide-hydrogen fuel. These show that when equation 13 is used with the appropriate forms of the relation $\lambda = a/Re^b$, there is satisfactory agreement between flame-stability data for tubes and noncircular channels. They also show that the concept of critical boundary velocity gradients for flashback and blowoff is widely applicable to burner ports of different shapes and depths.

B. Constant and Nonconstant Yellow-Tip Limits

Coefficients of friction obtained with CH_4 or $CO\text{-}H_2$ (equations 13c-13h) were used to calculate critical boundary velocity gradients from the volumetric flows at the yellow-tip limit.

1. Sharp-Edged Short Ports

Virtually identical yellow-tip limits were obtained on sharp-edged short ports of 1/4-inch length and on long tubes with steady laminar flow (see figure 51, p. 69 and (A-T/5-No./29,3,5,74,4)).

2. Noncircular Channels

Some comparisons were made between yellow-tip limits on rectanguiar, square, and triangular channels (A-T/5-No./4 and A-T/7-No./56). Virtually identical constant yellow-tip limits were observed on circular and noncircular channels. The constant yellow-tip limits of the fuels were obtained when one side of the noncircular channel

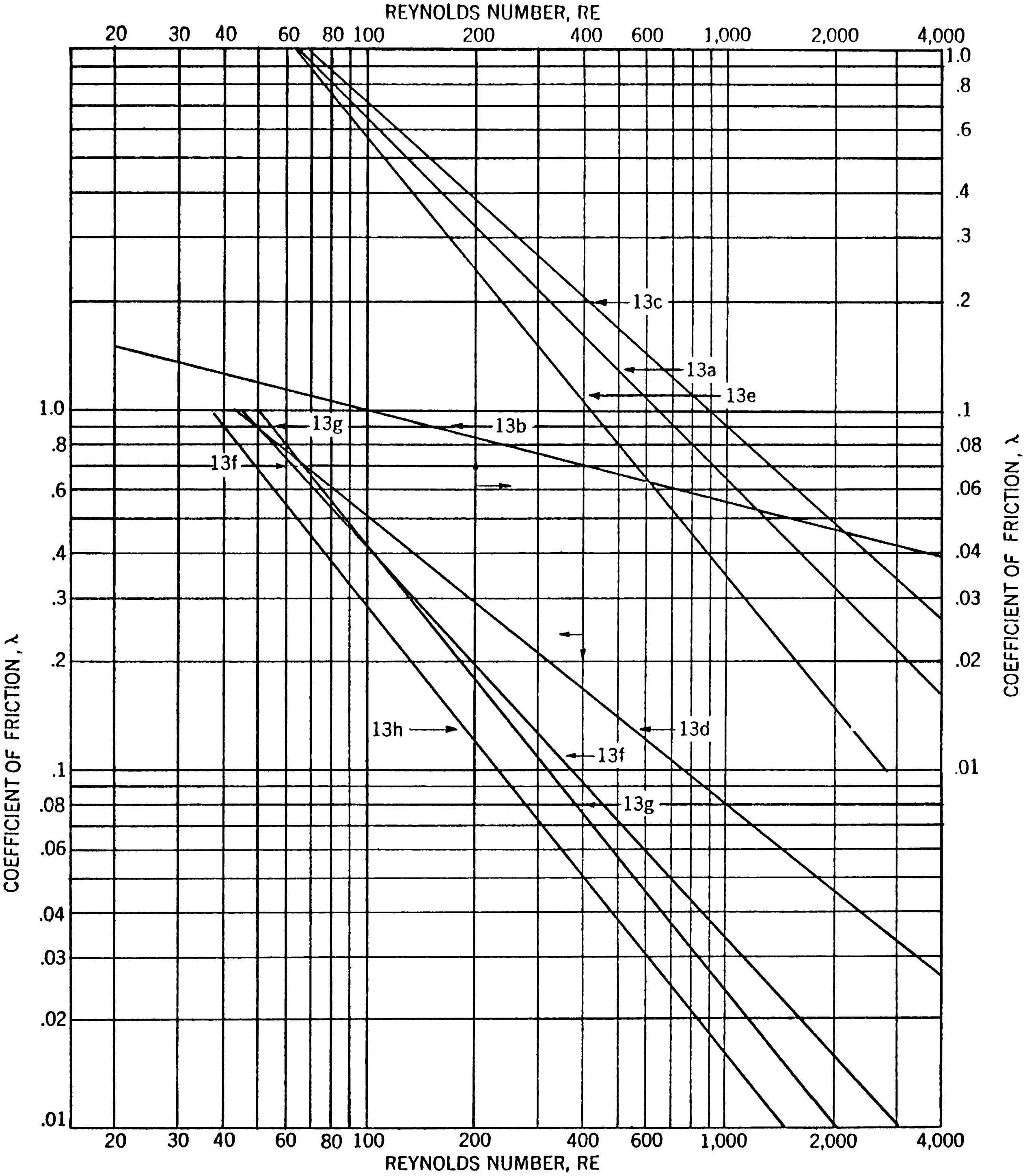

Figure 75. - λ coefficients for several flow profiles (equations 13 a-h).

was longer than R* (see ch. III, figure 47, p. 61). When, in addition, the short side was much smaller than R*, there was some evidence that the port behaved as a tube diameter 2 to 3 times the short side. This is attributable to the reduced availability of secondary air for this type of noncircular channel as compared to the circular port. For the latter, the yellow spot in a flame receives diffusing secondary air equally along radial paths from all points on the secondary mantle; for the former, secondary air can only reach the yellow spot from a small section along the center of the long sides of the channel.

3. Multiport Burners

No tests were conducted with multiport burners. However, it is apparent that, if the flow from each port on a burner were exactly the same and all ports were spaced far enough apart so that each was in free still air, the performance of the burner would be that of a monoport. On the other hand, if ports are close enough, the flames will more or less coalesce, and this system of ports will tend to behave as a single large port, probably showing the constant yellow-tip limit of the fuel.

It may be seen from this chapter that, in problems of overall gas-appliance performance, fuel factors can be largely dissociated from burner and appliance factors. Flashback and blowoff gradients and constant yellow-tip limits are characteristic of the fuel gas. The coefficient of friction, λ, reflects elements of burner design, such as port shape, depth, and flow profile. The effect of temperature - an appliance or ambient environmental factor - will be considered in chapter VI.

CHAPTER VI. - TEMPERATURE DEPENDENCE OF FLAME-STABILITY AND YELLOW-TIP LIMITS

To establish a standard state for flame-characteristics data, considerations in chapters I-V have been limited to burners where the ports and the flowing gases are at room temperature (approximately 78° F.). However, burners in practical use generally operate with their ports and the gases flowing through the ports at elevated temperatures. This chapter purposes to relate the data of the preceding five chapters to burners with hot ports. The range of temperature is limited to conditions excluding chemical reaction in the unburned gas upstream of the flame, so that we may know the composition of the unburned gas feeding the flame.[25] The burner employed in this study is diagramed in figure 76. The unburned-gas temperature (°K.) was regulated to within ± 1 percent of desired values. To prevent appreciable fluctuations in the flow profile, port-wall temperatures were held to ± 3 percent or better of the unburned-gas temperature.[26] For sharp-edged, short circular ports, as on the burner in figure 76, the boundary velocity gradient is given by

$$g = \lambda V \, Re/16 \pi R^3. \quad (13)$$

The coefficient of friction, λ, has been determined empirically as explained in chapter V and is

$$\lambda = 20.4/Re^{0.80} \quad (CH_4). \quad (13d)$$

25/ Judging from the experience of this laboratory and the study at NACA of the effect of preflame reaction on burning velocity of propane-air mixtures (6), it is unlikely that an appreciable preflame reaction occurs up to temperatures in the unburned gas of roughly 500° C., provided that the heating time at this temperature is less than about 5 seconds.

26/ In contemporary appliances port-wall temperatures of burners are probably higher than the unburned-gas temperature because of limitations of heat transfer from hot walls to flowing gases. This factor makes the room-temperature data of chapters I-V more universal than might be concluded from considerations of burner-wall temperatures alone.

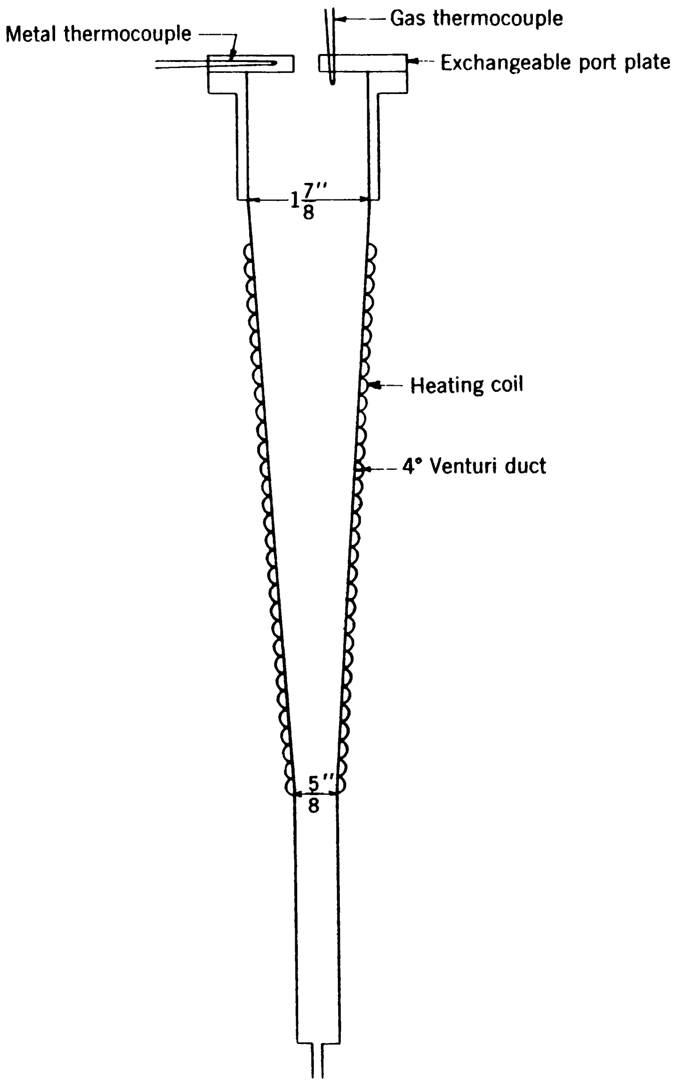

Figure 76. - Venturi burner with exchangeable, sharp-edged, short hot ports.

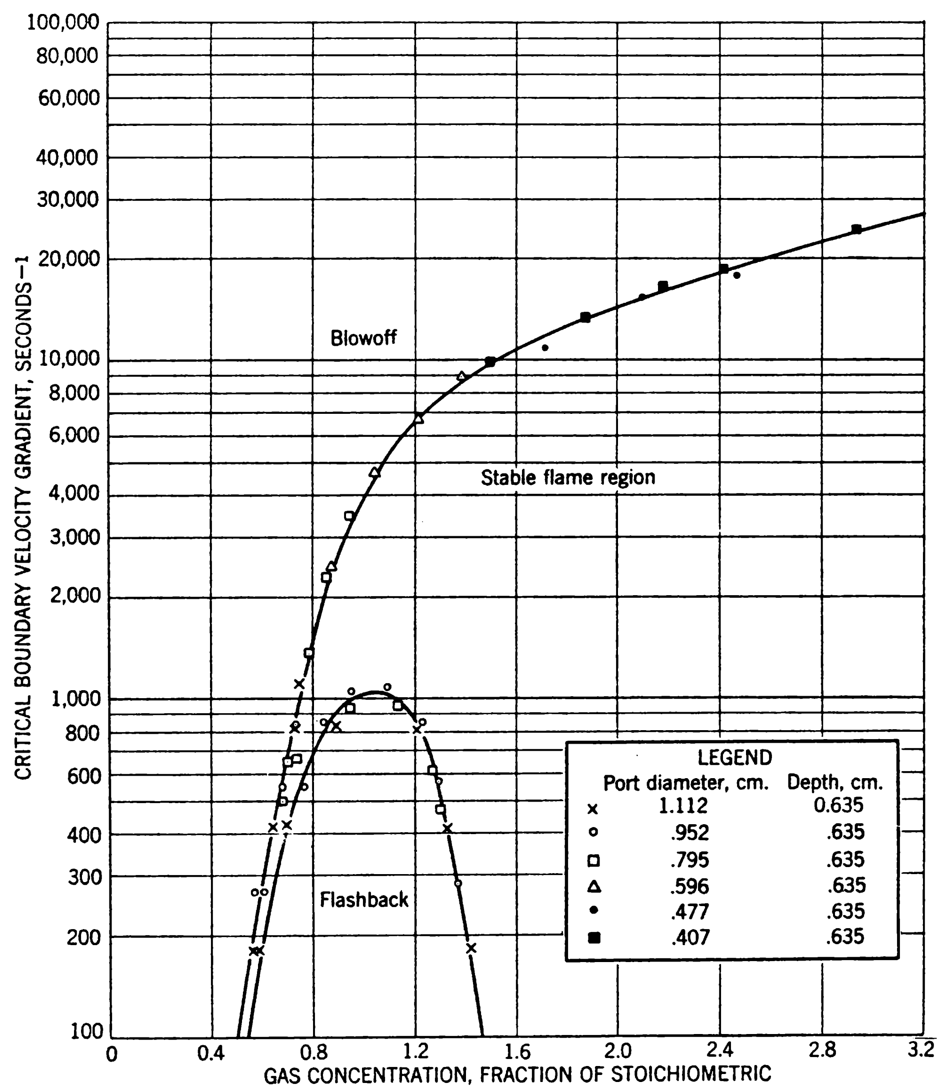

Figure 77. - Flame-stability diagram for fuel No. 2 (100% CH_4) at 473° K. for sharp-edged short ports.

The experiments were performed with methane, noting the flows and mixture composition at which flashback and blowoff occurred and using equations 13 and 13d to calculate the corresponding critical boundary velocity gradients for flashback and blowoff. Flashback and blowoff gradients for methane at 473° K. unburned-gas temperature are given in figure 77 (A-T/13-No./2) and show that the concept of critical gradients for flashback and blowoff is applicable at elevated temperatures. Figure 77 may be compared with the flashback and blowoff gradients for methane at room temperature (see figure 20, ch. II, p. 25); the increment due to the increase in the unburned-gas temperature is appreciable. All flashback data obtained with methane at a number of unburned-gas temperatures are summarized in figure 78 (A-T/13-No./2), and all blowoff data are summarized in figure 79[27/] (A-T/13-No./2). In addition, data on the temperature dependence of blowoff gradients of propane-air mixtures (5) are found in the literature. These were obtained on long cylindrical burners with steady laminar flow at the port and are summarized in figure 80.

All of the above data may be correlated by means of the following theoretical considerations:

Flashback

The flashback gradient g_F is equal to the burning velocity S_u divided by d_F, the quenching distance at flashback (10, 18):

$$g_F = \frac{S_u}{d_F} . \tag{14}$$

The burning velocity is the rate at which the flame tends to propagate into the unburned gas in a direction perpendicular to its surface. The quenching distance referred to in equation 14 is the depth of penetration of the chilling effect of the wall on the flame. At the flashback limit this particular quenching distance is the space between the wall and the edge of the flame. The temperature dependence of these two parameters is related to the temperature dependence of the flashback gradient as follows:

$$\frac{(g_F)_1}{(g_F)_2} = \frac{(S_u)_1}{(S_u)_2} \frac{(d_F)_2}{(d_F)_1} , \tag{14a}$$

where subscripts 1 and 2 indicate two different initial temperatures.

One of the several available equations for burning velocity is that proposed by Mallard and Le Chatelier. It is an approximate dimensional analysis of the balance of the heat released by the flame against that required to raise the gases to the temperature of burning. It is preferred here because it is simple in form and is generally applicable to all usual flames and because it makes no assumptions about the kinetics that control the combustion. Mallard and Le Chatelier's equation may be written as

$$S_u = \frac{\mu}{\rho_u c_p \delta} \frac{T_b - T_\iota}{T_\iota - T_u} , \tag{15}$$

27/ No control was exercised over the temperature of the ambient secondary air, as tests showed that this temperature had no significant effect on the measurements.

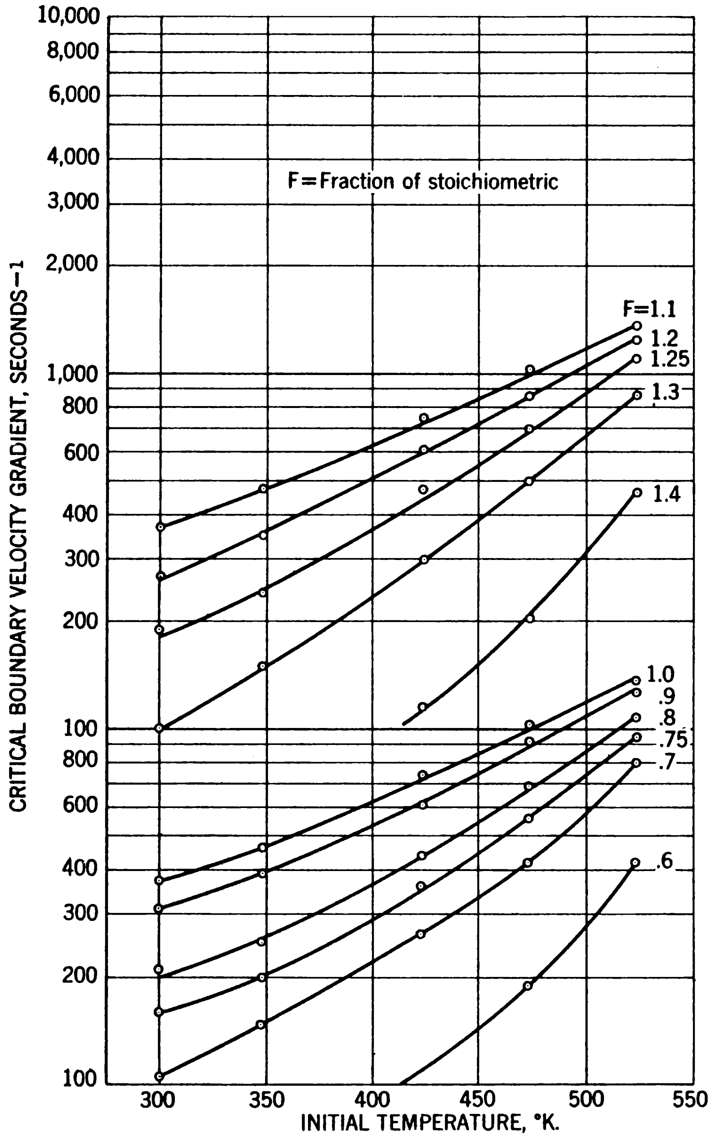

Figure 78. - Critical boundary velocity gradients for flashback of methane-air flames at various initial temperatures.

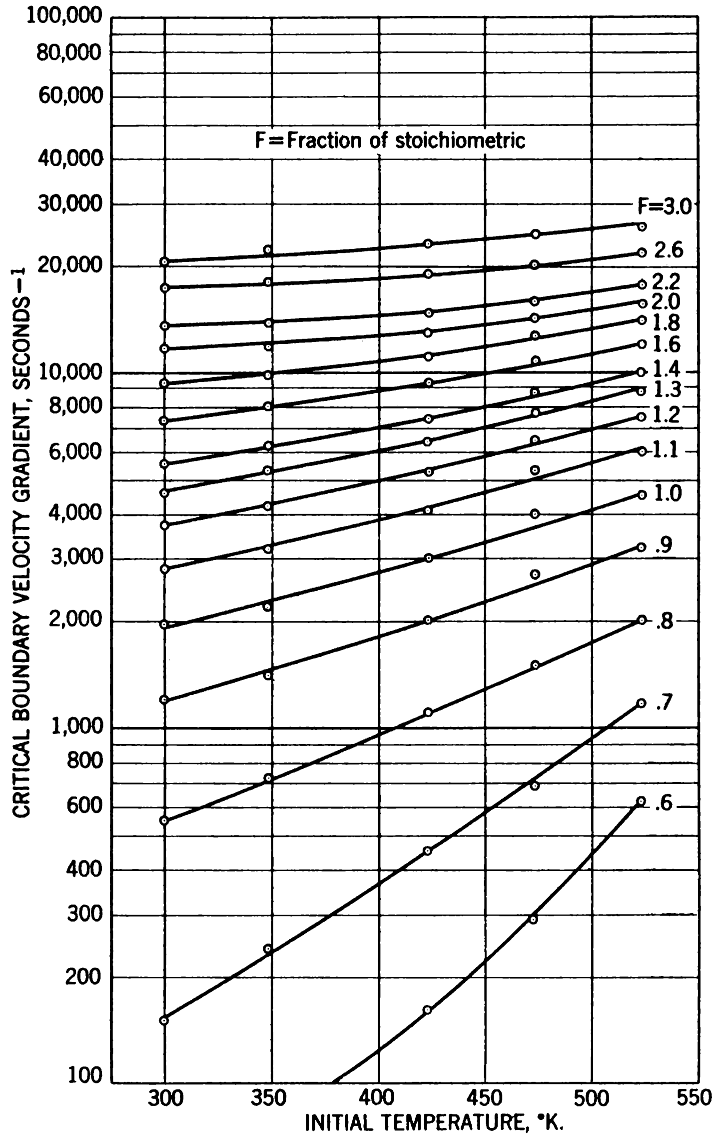

Figure 79. - Critical boundary velocity gradients for blowoff of methane-air flames at various initial temperatures.

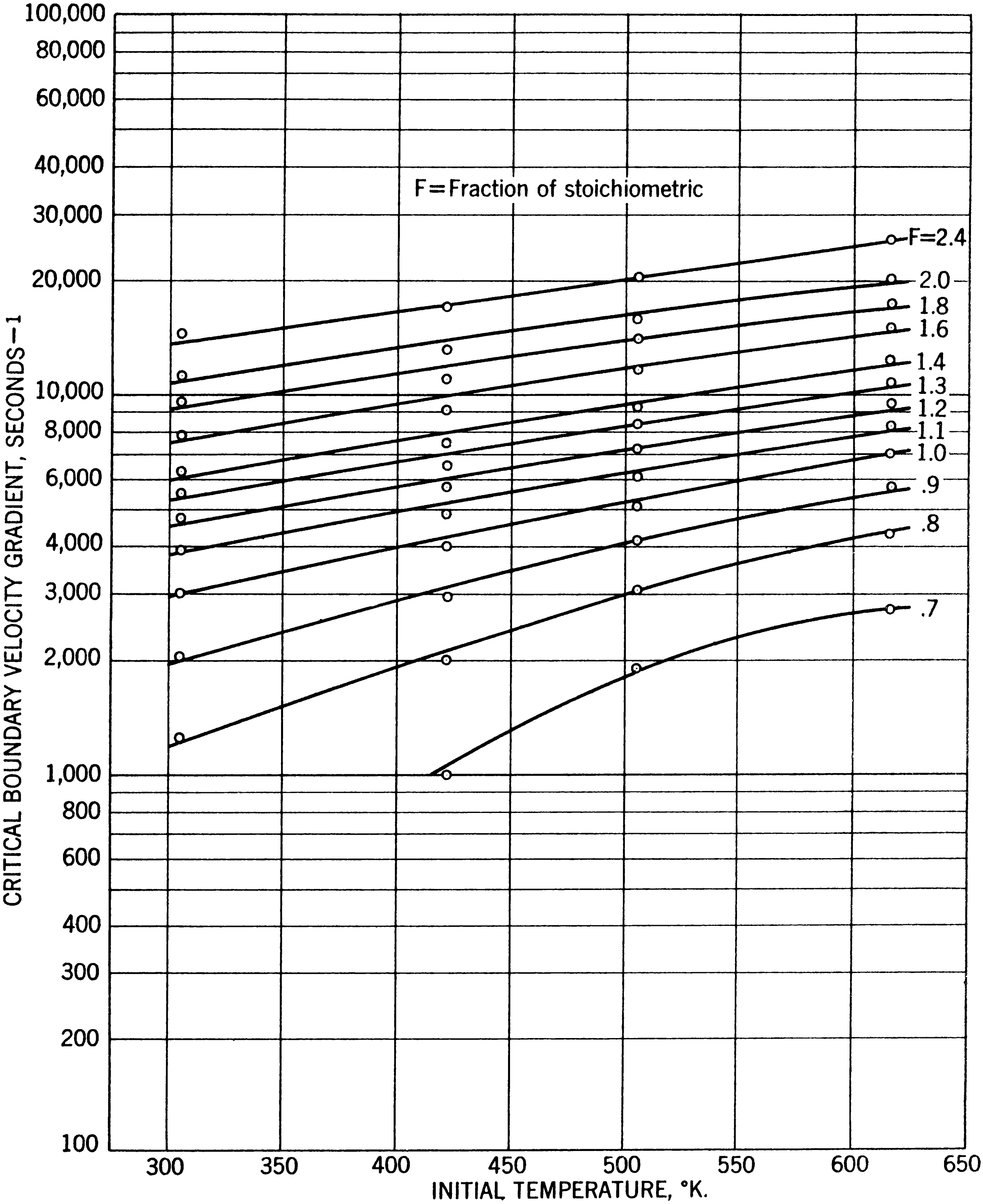

Figure 80. - Critical boundary velocity gradients for blowoff of propane-air flames at various initial temperatures (Dugger).

where μ is the coefficient of thermal conductivity, ρ_u is the density, c_p is the specific heat capacity at constant pressure, δ is the thickness of the combustion wave, T_b is the thermodynamic flame temperature, and T_u is the initial temperature. T_ℓ is the minimum temperature possible in the primary combustion zone of a stationary flame of the mixture and would correspond to the temperature of the fringe of the flame near the port wall. Assuming also that the fraction $\mu/c_p\delta$ is independent of initial temperature,[28] equations 15a and 15b follow from equation 15.

$$\frac{\left(\frac{\delta \rho_u c_p}{\mu}\right)_1}{(\rho_u)_1 \left(\frac{\delta c_p}{\mu}\right)_2} = \frac{(S_u)_2}{(S_u)_1} \frac{(T_u)_1}{(T_u)_2} \frac{(T_b - T_\ell)_1}{(T_b - T_\ell)_2} \frac{(T_\ell - T_u)_2}{(T_\ell - T_u)_1} \doteq 1. \tag{15a}$$

$$\frac{(S_u)_1}{(S_u)_2} \doteq \frac{(T_u)_1}{(T_u)_2} \frac{(T_b - T_\ell)_1}{(T_b - T_\ell)_2} \frac{(T_\ell - T_u)_2}{(T_\ell - T_u)_1} . \tag{15b}$$

Assuming that the temperature gradient across the zone of flame quenching is linear and the same for all initial temperatures,[28]

$$\frac{T_\ell - T_u}{d_F} \doteq \text{const.} , \tag{16}$$

and

$$\frac{(T_\ell - T_u)_1}{(T_\ell - T_u)_2} \doteq \frac{(d_F)_1}{(d_F)_2} . \tag{16a}$$

Combining equations 14a, 15b, and 16a, we have

$$\frac{(g_F)_1}{(g_F)_2} \doteq \frac{(T_u)_1}{(T_u)_2} \frac{(T_b - T_\ell)_1}{(T_b - T_\ell)_2} \frac{(T_\ell - T_u)_2^2}{(T_\ell - T_u)_1^2} . \tag{17}$$

<u>Blowoff</u>

The blowoff gradient is equal to the burning velocity divided by the quenching distance at blowoff. In this instance, quenching takes place largely through dilution of the boundary layer by secondary air diffusing into it (<u>10</u>, <u>18</u>). Accordingly,

$$g_B = \frac{S_u}{d_B} , \tag{18}$$

where d_B is the quenching distance at blowoff, that is the width of the boundary layer wherein a noncombustible fuel-air mixture exists. The temperature dependence

[28] These assumptions have been shown to be acceptable in ref. 11.

of these two parameters can be related to the temperature dependence of the blowoff gradient by equation 18a:

$$\frac{(g_B)_1}{(g_B)_2} = \frac{(S_u)_1}{(S_u)_2} \frac{(d_B)_2}{(d_B)_1} , \tag{18a}$$

where subscripts 1 and 2 indicate two different initial temperatures.

Equation 15b applies to blowoff as well as to flashback, accounting for the dependence of S_u on T_u.

With regard to the depth of dilution of d_B, let us assume that the equation for molecular diffusion applies. This equation states that

$$d_B^2 = 2\ D't, \tag{19}$$

where D' is the diffusion coefficient of air and t is the time taken by molecules at the boundary of the primary stream to travel from the port to the base of the flame. The time t is the quotient of the distance between the base of the flame and the port and the local flow velocity at the point of flame stabilization. Both of them increase as the critical boundary velocity gradient for blowoff increases with initial temperature. Accordingly, t may be virtually independent of T_u; this is difficult to confirm experimentally, but assuming it to be so,

$$\frac{(d_B)_1}{(d_B)_2} \doteq \frac{(D')_1^{1/2}}{(D')_2^{1/2}} \doteq \frac{(T_u)_1^{3/4}}{(T_u)_2^{3/4}} , \tag{19a}$$

the diffusion coefficient being roughly proportional to the 3/2-power of the temperature, from kinetic theory. Equations 15b and 19a may now be substituted into equation 18a to given equation 20.[29/]

$$\frac{(g_B)_1}{(g_B)_2} \doteq \frac{(T_u)_1^{1/4}}{(T_u)_2^{1/4}} \frac{(T_b - T_\ell)_1}{(T_b - T_\ell)_2} \frac{(T_\ell - T_u)_2}{(T_\ell - T_u)_1} \tag{20}$$

Equations 17 and 20 relate flame-stability gradients, g_F and g_B, to the initial temperature T_u through two other temperatures, T_b, the thermodynamic flame temperature, and T_ℓ, the minimum primary combustion zone temperature. Values T_b (for each T_u) used in this report were taken from reference (26) and are presented in figures 81 and 82. Values of T_ℓ cannot as yet be gotten independently but have been

29/ Equation 20 is limited in that values of T_b are meaningless for mixtures richer than the rich limit of flammability; however, the usefulness of equation 20 may be extended to very rich mixtures, although the inaccuracy grows as the primary air concentration of the burner stream decreases. The experimental data of figure 79 show that, for very rich mixtures, the blowoff gradients change little with initial temperature. Accordingly, the effect of T_u on the blowoff gradients of a given very rich mixture is the same as on other similar mixtures. As the calculation can be made for the rich flammability limit, values of T_b (and T_ℓ) of that mixture can be used for even richer mixtures.

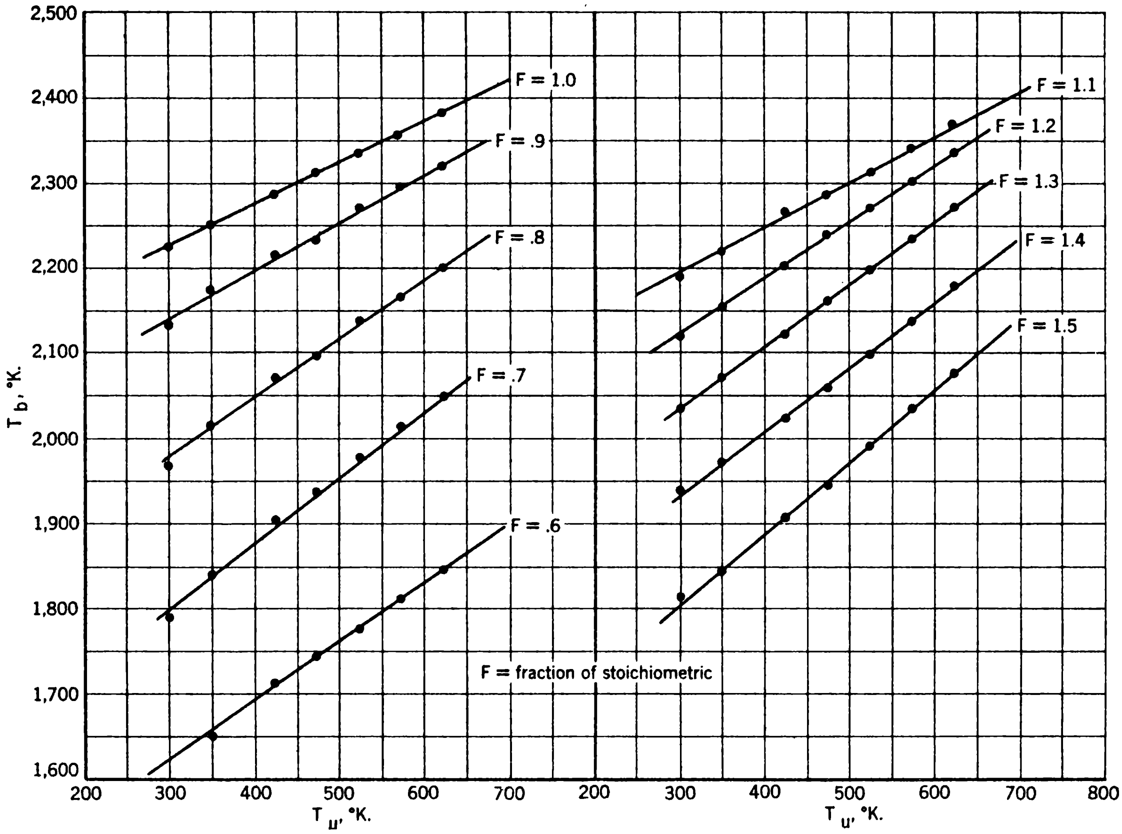

Figure 81. - Flame temperatures for methane-air (Smith, Edwards, and Brinkley).

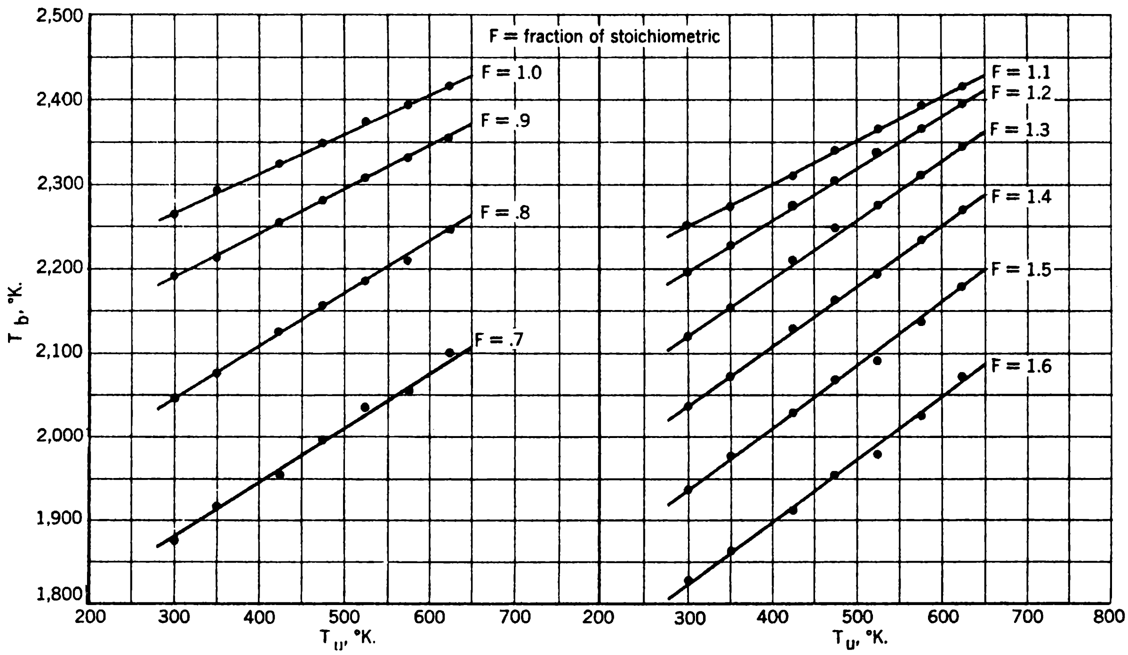

Figure 82. - Flame temperatures for propane-air (Smith, Edwards, and Brinkley).

obtained by substituting values of $(g_F)_1/(g_F)_2$ in equation 17 and $(g_B)_1/(g_B)_2$ in equation 20, and solving for T_l.

Values of T_l calculated by means of these two equations may be used to test the validity of the above theory. For each mixture of fuel and air, T_l should be independent of T_u. The lowest temperature at which flame is possible in a fuel-air mixture should not depend upon the temperature history of the nonreacting unburned stream and should not be strongly influenced by the nature of the quenching process at the boundary of the flame. Therefore, for each mixture, equations 17 and 20 should give the same T_l for all initial temperatures, and no difference should exist between flashback and blowoff. Accordingly, the acceptability of these two equations may be tested by substituting experimental values of g_F at various temperatures (see figure 78) in equation 17 and experimental values of g_B in equation 20 (see figure 79) and solving for T_l. If the theory is adequate, T_l must be reasonably constant for each mixture and within the limits of flammability and be about the same for flashback and for blowoff. This test is met successfully, particularly by $(T_l)_a$, as shown in table 11.[30] Equations 17 and 20 and values of T_l from table 11 may be used to calculate flashback and blowoff curves for methane as a function of T_u, starting with the room-temperature flame-stability diagram of methane. Predicted curves and experimental points are compared in figures 84 and 85. The agreement is satisfactory, which it would not be if the average values of T_l were not correct for all values of T_u, as required by the above theory.

The same procedure can be followed for propane-air fuels, using the data obtained by Dugger (5). Values of T_l for propane-air are given in table 12. Experimental and calculated curves are compared in figure 86. The agreement is good.

30/ Equation 17 is cubic and 20 is quadratic, resulting in three roots of T_l ($(T_l)_{a,b,c}$). The lowest root $(T_l)_c$ is obviously without physical meaning, being roughly equal to T_u, and is not obtained from equation 20. The middle root $(T_l)_b$ is generally lower than the minimum temperatures reported in such flames of hydrocarbon-air mixtures (1,300°-1,700° K.) (8, 9). The highest root $(T_l)_a$ is the most constant for all mixtures, as shown in tables 11 and 12, and is the preferred root. All three roots may be artifacts of the theory. However, physical meaning can be postulated for (T_l) and $(T_l)_b$. Figure 83 shows the probable temperature profile when passing from the unburned gas to the burned gas. $(T_l)_b$ is at the inflection point in the temperature curve where chemical reaction sets in, generating heat. Below it the unburned gas is heated by conduction and diffusion from the flame and the unburned gas. At $(T_l)_a$ chemical reaction has become so fast that a flame forms. On the burned gas side of the flame the thermodynamic flame temperature should exist. Where not otherwise specified, T_l is $(T_l)_a$ in this report.

The imaginary values in tables 11 and 12 are felt to be chance products of experimental difficulties and mathematics and not contradictory to the thesis of this chapter. Most of the imaginary values occur when the temperature interval is small or near the limits of flammability. The T_l values in tables 11 and 12 differ slightly from those in tables 1 and 2 of reference 11 owing to reasons given in footnote 24 and reaveraging of curves.

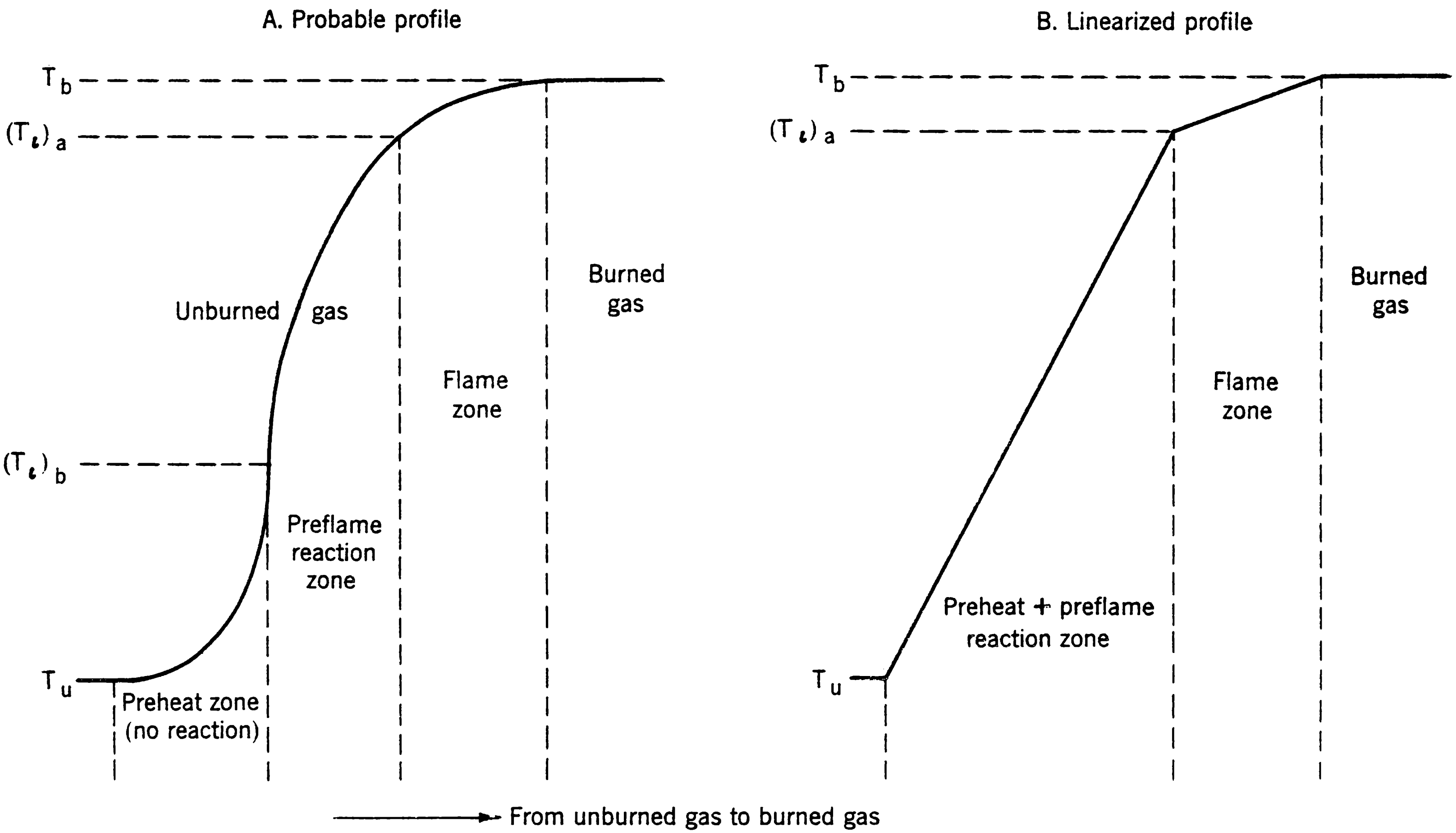

Figure 83. - Schematic temperature profiles for a flame.

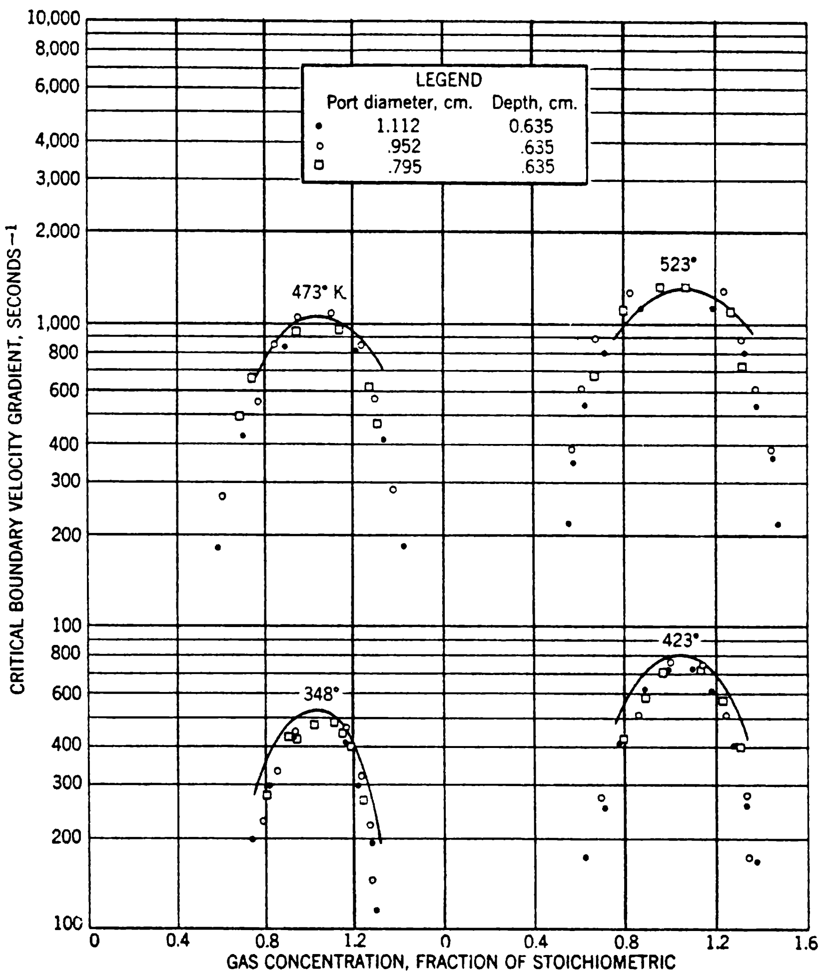

Figure 84. - Comparison of experimental points and calculated curves for flashback of methane-air flames at various initial temperatures.

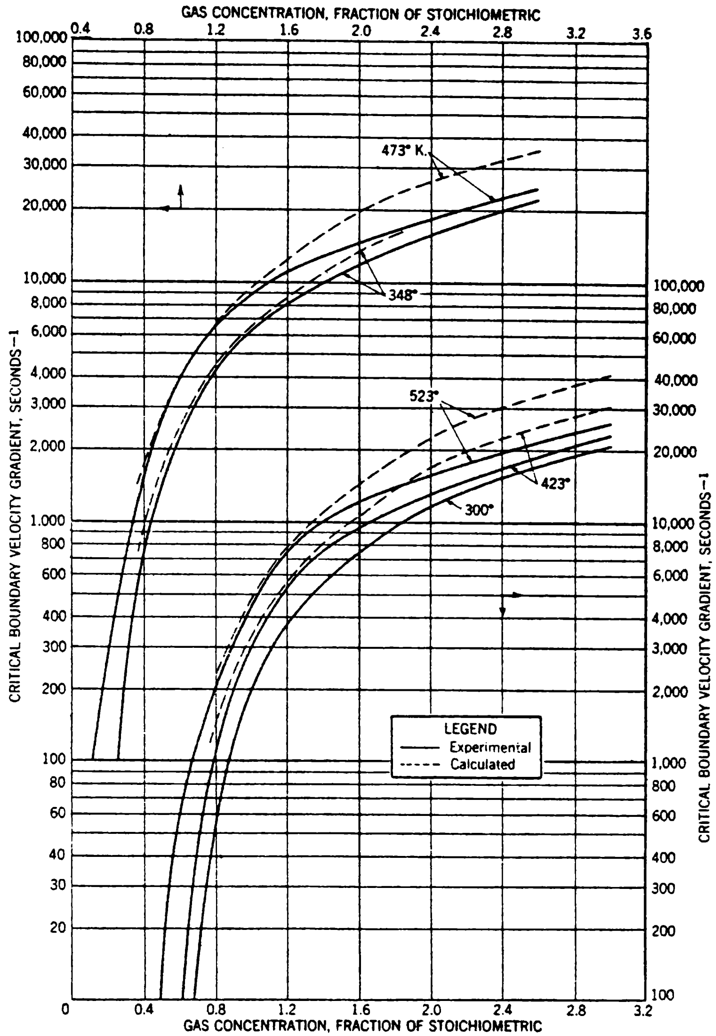

Figure 85. - Comparison of experimental and calculated curves for blowoff of methane-air flames at various initial temperatures.

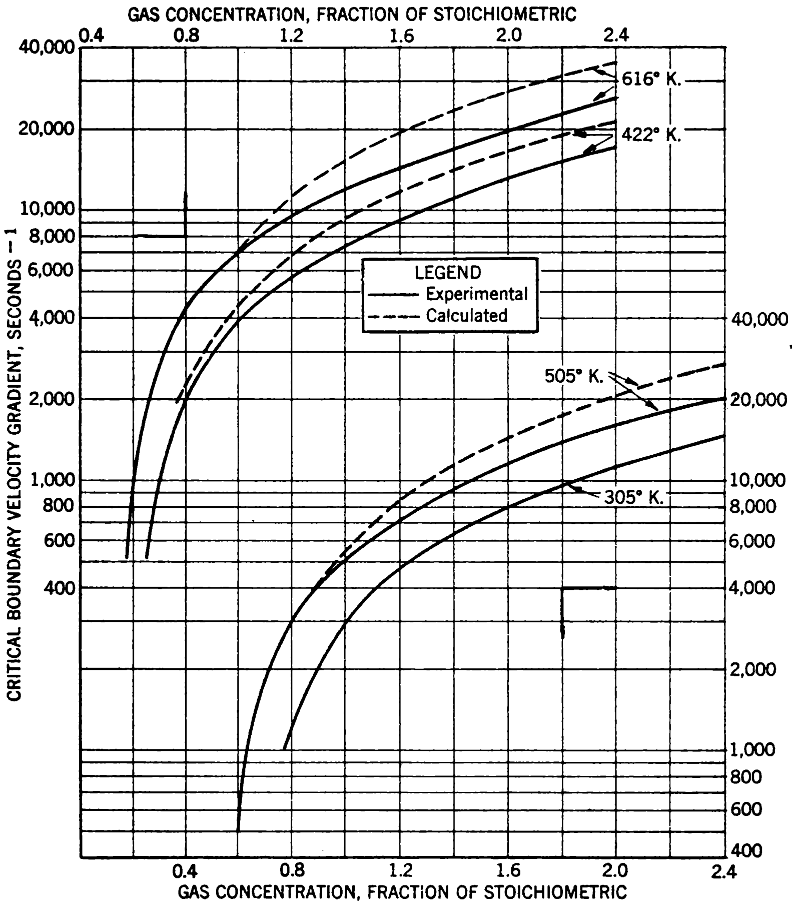

Figure 86. - Comparison of experimental (Dugger) and calculated curves for blowoff of propane-air flames at various initial temperatures.

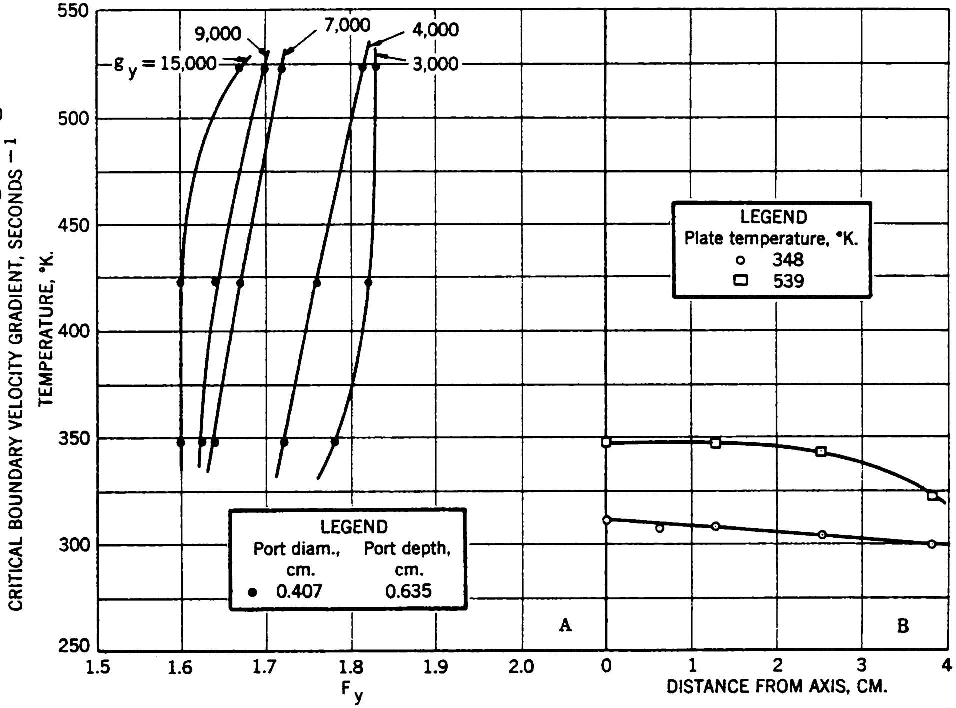

Figure 87. - A, Influence of initial temperature on yellow tipping of propylene; B, ambient air temperatures above a 7.95-cm. O. D. plate, 0.346-cm. I. D. drill port; no flame.

TABLE 11. - Calculation of ignition temperatures versus initial temperatures for methane-air flames

$(T_u)_1/(T_u)_2$, °K.	F = 0.6			F = 0.7			F = 0.8			F = 0.9			F = 1.0		
	$(T_\ell)_a$	$(T_\ell)_b$	$(T_\ell)_c$	$(T_\ell)_a$	$(T_\ell)_b$	$(T_\ell)_c$	$(T_\ell)_a$	$(T_\ell)_b$	$(T_\ell)_c$	$(T_\ell)_a$	$(T_\ell)_b$	$(T_\ell)_c$	$(T_\ell)_a$	$(T_\ell)_b$	$(T_\ell)_c$
Values of T_ℓ from flashback measurements, °K.															
300/348				Imaginary		325	Imaginary		324	Imaginary		324	Imaginary		324
300/423				1,575	863	370	1,452	1,304	367	1,667	1,340	366	1,952	1,202	366
300/473				1,643	827	404	1,758	954	401	1,927	1,028	399	2,020	1,108	397
300/523				1,706	767	447	1,817	903	438	1,959	1,019	433	2,049	1,099	430
348/423				1,700	778	392	1,817	943	388	1,955	1,029	388	2,098	948	388
348/473				1,731	784	421	1,890	840	420	2,042	912	418	2,107	965	418
348/523				1,776	740	461	1,910	835	455	2,050	940	451	2,117	998	450
423/473	1,647	699	451	1,791	779	450	1,956	769	450	2,127	822	450	2,127	985	449
423/523	1,675	667	486	1,832	726	483	1,961	798	481	2,105	904	479	2,134	1,030	478
473/523	1,703	651	502	1,866	700	501	1,967	825	500	2,072	1,000	499	2,147	1,075	499
Average	1,675	672	480	1,736	774	425	1,836	908	422	1,989	999	421	2,083	1,046	420
Deviation .... percent	1.7	2.6	4.0	4.1	4.7	10.1	6.1	11.7	10.0	5.0	9.3	9.9	2.5	6.4	9.8
$(T_b)_{300°} - (T_\ell)_{av.}$				57			131			143			143		
Values of T_ℓ from blowoff measurements, °K.															
300/348				1,689	445		1,736	571		1,661	887		Imaginary		
300/423				1,722	503		1,828	594		1,927	705		2,022	788	
300/473				1,741	537		1,858	614		2,006	670		2,095	715	
300/523				1,756	568		1,869	646		2,003	721		2,079	789	
348/423				1,765	530		1,898	608		2,037	653		2,110	700	
348/473				1,783	557		1,917	623		2,076	646		2,144	674	
348/523				1,802	581		1,919	659		2,065	710		2,125	758	
423/473	1,675	545		1,826	584		1,947	643		2,132	647		2,184	658	
423/523	1,691	563		1,845	599		1,944	680		2,098	739		2,141	791	
473/523	1,709	574		1,872	602		1,942	712		1,994	907		1,908	1,209	
Average	1,692	561		1,780	551		1,886	635		2,000	729		2,090	787	
Deviation .... percent	0.7	1.8		2.6	6.8		2.7	5.2		4.2	9.6		2.8	12.1	
$(T_b)_{300°} - (T_\ell)_{av.}$				13			81			132			136		

$(T_u)_1/(T_u)_2$, °K.	F = 1.1			F = 1.2			F = 1.3			F = 1.4		
	$(T_\ell)_a$	$(T_\ell)_b$	$(T_\ell)_c$	$(T_\ell)_a$	$(T_\ell)_b$	$(T_\ell)_c$	$(T_\ell)_a$	$(T_\ell)_b$	$(T_\ell)_c$	$(T_\ell)_a$	$(T_\ell)_b$	$(T_\ell)_c$
Values of T_ℓ from flashback measurements, °K.												
300/348	Imaginary		325	Imaginary		325	Imaginary		325			
300/423	1,876	1,167	367	1,896	976	368	1,928	723	372			
300/473	1,965	1,086	398	1,934	961	400	1,958	714	410			
300/523	1,996	1,086	431	1,974	939	436	1,979	724	452			
348/423	1,972	1,057	388	1,990	852	389	1,959	715	390			
348/473	2,037	1,020	417	2,005	885	419	1,986	710	424			
348/523	2,052	1,040	449	2,029	891	453	2,009	723	462			
423/473	2,125	980	449	2,031	933	449	2,031	706	450	1,942	678	451
423/523	2,114	1,030	478	2,064	914	479	2,057	726	483	1,982	653	487
473/523	2,100	1,084	499	2,097	900	500	2,093	743	500	2,025	641	503
Average	2,026	1,061	420	2,002	917	422	2,000	720	427	1,983	657	480
Deviation .... percent	3.3	3.7	9.8	2.4	3.4	9.9	2.1	1.1	10.0	1.4	2.1	4.1
$(T_b)_{300°} - (T_\ell)_{av.}$	164			120			37					
Values of T_ℓ from blowoff measurements, °K.												
300/348												
300/423	1,883	865		1,709	965		1,345	1,238		Imaginary		
300/473	2,004	770		1,828	866		1,603	995		Do.		
300/523	1,990	839		1,831	913		1,617	1,038		Do.		
348/423	1,946	836		1,811	894		Imaginary					
348/473	2,064	739		1,901	825		1,627	1,001		1,369	1,177	
348/523	2,042	822		1,888	888		1,638	1,051		Imaginary		
423/473	2,170	685		1,998	774		1,821	840		1,649	908	
423/523	2,106	816		1,945	885		1,786	956		1,570	1,060	
473/523	1,904	1,140		1,841	1,058		1,716	1,134		Imaginary		
Average	2,012	835		1,861	896		1,644	1,032		1,529	1,048	
Deviation .... percent	3.7	9.1		3.4	6.1		5.9	8.1		7.0	8.9	
$(T_b)_{300°} - (T_\ell)_{av.}$	178			261			393			409		

TABLE 12. - Calculation of ignition temperatures versus initial temperatures for propane-air flames

$(T_u)_1/(T_u)_2$, °K.	F = 0.7		F = 0.8		F = 0.9		F = 1.0	
	$(T_\ell)_a$	$(T_\ell)_b$	$(T_\ell)_a$	$(T_\ell)_b$	$(T_\ell)_a$	$(T_\ell)_b$	$(T_\ell)_a$	$(T_\ell)_b$
	Values of T_ℓ from blowoff measurements, °K.							
305/422			1,815	750	1,914	872	1,759	1,216
305/505			1,902	715	1,993	823	1,953	1,034
305/616			1,896	826	2,010	908	2,026	1,035
422/505	1,891	614	1,991	704	2,099	774	2,127	895
422/616	1,860	770	1,950	863	2,079	914	2,125	993
505/616	1,699	1,041	1,866	1,043	2,037	1,042	2,135	1,052
Average	1,817	808	1,903	817	2,022	889	2,021	1,038
Deviation ..... percent	4.3	19.2	2.3	11.5	2.5	7.4	5.4	6.2
$(T_b)_{300°} - (T_\ell)_{av.}$	68		142		168		249	

$(T_u)_1/(T_u)_2$, °K.	F = 1.1		F = 1.2		F = 1.3		F = 1.4	
	$(T_\ell)_a$	$(T_\ell)_b$	$(T_\ell)_a$	$(T_\ell)_b$	$(T_\ell)_a$	$(T_\ell)_b$	$(T_\ell)_a$	$(T_\ell)_b$
	Values of T_ℓ from blowoff measurements, °K.							
305/422	Imaginary		Imaginary					
305/505	do.		do.					
305/616	1,861	1,191	do.					
422/505	2,028	978	1,965	957	1,881	941	1,661	1,074
422/616	2,056	1,029	1,881	1,152	1,805	1,142	1,613	1,245
505/616	2,075	1,071	1,756	1,356	1,627	1,423	Imaginary	
Average	2,005	1,067	1,867	1,155	1,771	1,169	1,637	1,160
Deviation ..... percent	3.6	6.0	4.0	11.6	5.4	14.5	1.5	7.4
$(T_b)_{300°} - (T_\ell)_{av.}$	240		328		356		403	

Although the experiments discussed in this chapter have been limited to propane-air and methane-air fuels, the theory applies to all fuels. Room-temperature flame-stability diagrams are available for all fuels, as in chapter II of this report. Flame temperatures can be calculated thermodynamically as functions of T_u. Values of T_ℓ are lacking for most fuels but may be determined experimentally, as has been done for methane and propane. Until such determinations are made, it may suffice to make educated guesses of values of T_ℓ by assuming it to be less than T_b (when T_u = 300° K.) by the order of difference shown in the last lines of tables 11 and 12.

Yellow Tipping

With propylene as the test fuel the effect of preheat was found to be very small. The experimental equipment is identical with that used in the study of the effect of preheat on flashback and blowoff limits (figure 76). Propylene was chosen because it is a fairly typical yellow-tipping gas. The temperature range covered was from room temperature to 523° K. The experimental results need to be examined to show the effect of preheat with respect to the constant yellow-tip limit, F_c (for large ports and large flows, see ch. III) and of the yellow-tip fraction, F_c/F_y (on small ports or small flows, see ch. IV). F_y is the nonconstant yellow-tip limit on small ports and depends on flow and port diameter as well as on the fuel; F_c is the constant yellow-tip limit and is characteristic of the fuel alone.

The constant yellow-tip limit for propylene was observed to be invariant with preheat within experimental error, the data between 300° and 523° K. varying from 1.44 to 1.47. The yellow-tip limit for a given port diameter and flow (critical boundary velocity gradient) was found to vary slightly with the initial temperature. Figure 87,A, for propylene illustrates the change in the yellow-tip limit with preheat. This figure is derived from data in (A-T/14-No./5). The change in F_y is small and is attributed to a combination of experimental uncertainty and the observation that the secondary air around the flame was heated by the burner. Measured temperatures of ambient air above the port, with the burner at 348° and 539° K., are given in figure 87,B. The secondary air temperature at the height of the yellow in the test flame was about 40°-50° above room temperature when the port was at roughly 523° K. With the port at 348° K., the ambient air was about 10° above room temperature. Thus in most experiments dealing with yellow tipping on hot ports, secondary air surrounding the flame was virtually at room temperature in the plane of the yellow zone. Had the secondary air been kept at exactly room temperature for all experiments, it is likely that the yellow-tip fraction (F_c/F_y) would be independent of the initial temperature. This conclusion is corroborated by the experiments of Street and Thomas (27) for propane, propylene, benzene, and kerosine. They observed that increasing the temperature up to 773° K. slightly reduced the critical air-fuel ratio for suppressing yellow in flames. Clark (4) noted an appreciable lowering of air-fuel ratios for yellowing of preheated benzene flames but did not evaluate the ambient air temperature. Except for the latter, these observations support the judgment that, for practical purposes, the yellow-tip limits are independent of the initial temperature of the burner stream, provided that temperatures are low enough and flows rapid enough to preclude chemical reaction within the burner.

CLOSING COMMENTS

The purpose of this investigation has been to provide theoretical foundation and data for the flashback, blowoff, and yellow-tipping characteristics of fuel gases, as distinct from factors inherent in the burner or appliance design. This has been accomplished through the critical boundary velocity gradients for flashback and blowoff (chs. I and II), the constant and nonconstant yellow-tip limits (chs. III and IV), the effect of port depth and shape on flashback, blowoff, and yellow tipping (ch. V), and the effect of preheat on flashback, blowoff, and yellow tipping (ch. VI). From a practical point of view, the resulting picture is incomplete because information still is needed on air entrainment; on the effects of adjacent ports on one another; on the effect of port direction; on the effect of flow and chemical content of secondary "air," etc. Once such studies have been completed, it should be possible to coordinate this report with new information on burner and appliance-design characteristics. Very limited experience to date indicates that the data in this report are rough approximations of the behavior of contemporary burners.

This study has given considerable attention to the problem of exchangeability of fuel gases under peak load or complete exchange situations. The nature of flashback on turndown has also been examined briefly.

These two studies have been reported in references A, B, D, F, I, L and N on pages 118 and 119.

Although detailed burner and appliance-design data at the drafting-desk level are not given, the present report includes fundamental concepts and principles that should be widely applicable in training engineers for the gas industry and in developing a science of gas-burner and appliance design. The application of fundamental knowledge often is advanced most advantageously by men in industry rather than by men in research who supply such knowledge. It is with this in mind that the engineer is invited to experiment with the concepts and test the data presented in this report.

DEFINITIONS AND NOMENCLATURE

Definitions

1. Flashback is the passing of flame into a port counter-current to a steady stream of combustible mixture flowing through the port.

2. Blowoff is the nonpropagation of flame above a port in a steady stream of combustible mixture issuing from the port.

3. A stable flame is a stationary flame propagating on a port in a flowing mixture; it may be blue or yellow.

4. A yellow-tipped flame is one in which yellow is perceptible anywhere in the flame on the port.

5. The fraction of stoichiometric, F, is the volumetric gas percentage divided by the percentage of gas in a stoichiometric mixture of fuel with air. For a stoichiometric mixture (equivalent quantities of fuel and oxygen), F is equal to unity; for lean mixtures, F is less than unity; and for rich mixtures, F is greater than unity;

$$F = \frac{\text{Volumetric flow of fuel}}{\text{Volumetric flow of fuel + flow of air}} \times \begin{array}{l}\text{1 + volumes of air required to}\\ \text{burn stoichiometrically a unit}\\ \text{volume of fuel.}\end{array}$$

5a. The nonconstant yellow-tip limit, F_y, is the fuel-air composition in the burner manifold for which yellow is just perceptible anywhere in the flame on the port. This limit depends on the fuel, the flow rate, the port characteristics, and the properties of the atmosphere around the flame.

5b. The constant yellow-tip limit, F_c, is the characteristic and leanest fuel-air composition which, if ignited in the absence of a secondary atmosphere, produces yellow. For a given temperature and pressure of the unburned mixture, this limit depends only on the fuel and is characteristic of the fuel.

5c. The yellow-tip fraction is F_c/F_y. It can have values only from zero to unity, and values below 0.4 rarely appear.

6. The boundary velocity gradient, g, seconds^{-1}, is the rate of change of stream velocity at the edge of the stream mixture at the exit plane of the burner port. For steady laminar flow through a round port, $g = 4V/\pi R^3$, where V is the volumetric rate of flow, cc./sec.; and R is the radius of port, cm. (V and R must be in related units).

6a. The critical boundary velocity gradient for flashback, g_F in seconds^{-1}, is the boundary velocity gradient at which flashback just occurs for a given fuel-air mixture. This quantity is a characteristic property of the fuel-air mixture.

6b. The critical boundary velocity gradient for blowoff, g_B in seconds^{-1}, is the boundary velocity gradient at which blowoff just occurs for a given fuel-air mixture. This quantity is a characteristic property of the fuel-air mixture.

7. A flame-stability diagram is a coplot of fundamental flashback and blowoff curves of the fuel, bounding the regions of flashback, blowoff, and stable flames of the fuel.

8. A flame-characteristics diagram is a flame-stability diagram plus fundamental yellow-tip-limit data.

9. A composite flame-stability diagram for flashback is a summary diagram of all characteristic flashback curves of a family of two-component fuels.

9a. A composite flame-stability diagram for blowoff is a summary diagram of all characteristic blowoff curves of a family of two-component fuels.

9b. A composite yellow-tip diagram is a summary diagram of yellow-tip limits of a group of yellow-tipping fuels related by their burning velocities at the yellow-tip limit.

10. The standard burning velocity, S_u, in centimeters per second, is the rate at which an adiabatic plane combustion wave moves relative to the oncoming fuel-oxidant mixture in a direction perpendicular to the flame surface, the unburned stream being at room temperature and atmospheric pressure. Nonstandard burning velocities depend on the standard burning velocity and such matters as curvature of flame, proximity to liquid or solid surfaces, ambient pressure and temperature, etc.

11. The quenching distance, in centimeters, is the minimum spacing of walls of a channel, through which a given flame can propagate in quiescent mixture. There are several quenching distances for each flame, depending upon the geometry of the channel (tubes, slots, triangles, etc.).

11a. The quenching distance at flashback, d_F, in centimeters, is the depth of penetration of the chilling effect of the wall on the flame whose base is in the same plane as the wall. This particular quenching distance is the space between the wall and the edge of the flame near it as the flame flashes back. It differs from the dead space, which is the space between the top of a port and the base of a stable flame above it, in that the dead space varies with the flow rate through the port, whereas the quenching distance at flashback is a fundamental property of the mixture and does not vary with flow rate.

11b. The quenching distance at blowoff, d_B, in centimeters, reflects quenching of the flame, largely through dilution of the boundary layer by secondary air diffusing into it and partly, to a lesser degree, through loss of heat to the top face of the port. It is the radial width of the annular boundary layer of the stream as it leaves the port, wherein a noncombustible fuel-air mixture exists.

12. The coefficient of friction, λ, relates the boundary velocity of a stream to the average velocity. It can be expressed as a function of the Reynolds number.

13. Mole fraction equals volumetric percent/100.

The following parameters are fundamental properties of the flame of a fuel-air mixture flowing through a port in free air, the port and the mixture being at a given pressure and temperature: S_u, the burning velocity; d_F, the quenching distance at flashback; d_B, the quenching distance at blowoff; g_F, the critical boundary velocity gradient at flashback; g_B, the critical boundary velocity gradient at blowoff; and F_c, the constant yellow-tip limit. They are highly useful because they make it possible to describe the combustion characteristics of each fuel-oxidant mixture, independent of burner-design parameters and environmental parameters.

Nomenclature

c_p = specific heat capacity at constant pressure, cal./(gram)(°C.).

d_B = quenching distance at blowoff, cm.

d_F = quenching distance at flashback, cm.

D_i = diameter of port, inches.

D' = diffusion coefficient, sq.cm./sec.

F = fuel-gas concentration, fraction of stoichiometric.

F_B = fuel-gas concentration for blowoff, fraction of stoichiometric.

F_c = fuel-gas concentration for the constant yellow-tip limit, fraction of stoichiometric.

F_F = fuel-gas concentration for flashback, fraction of stoichiometric.

F_y = fuel-gas concentration for the nonconstant yellow-tip limit, fraction of stoichiometric.

F_c/F_y = yellow-tip fraction.

g = boundary velocity gradient, $seconds^{-1}$.

g_B = critical boundary velocity gradient for blowoff, $seconds^{-1}$.

g_F = critical boundary velocity gradient for flashback, $seconds^{-1}$.

g_y = critical boundary velocity gradient for yellow tipping, $seconds^{-1}$.

h = height, cm.

H_o = heating value of fuel, B.t.u./cu.ft.

k = proportionality constant.

L = percent primary air $[100\ (air/gas)_{actual}/(air/gas)_{stoichiometric}]$.

M = flow of fuel through port, $B.t.u./hr.in.^2$

n = mole fraction of each component in a multicomponent mixture.

P = $(air/gas)_{stoichiometric}$.

R = radius of port, cm.

R^* = minimum radius of port for constant yellow-tip limit, cm.

r = radial distance from axis of port.

Re = Reynolds number.

S = mole fraction of fuel in a stoichiometric mixture.

S_u = burning velocity, cm./sec.

T_b = burned-gas temperature, °K.
T_u = temperature of unburned gas, °K.
T_l = minimum temperature in primary combustion zone, °K.
t = time, sec.
U = flow velocity, cm./sec.
U_a = flow velocity at axis of port, cm./sec.
V = volumetric rate of flow, $cm.^3$/sec.
$\bar{X}$ = displacement of molecule by diffusion.
δ = flame thickness, cm.
η = viscosity, poise.
λ = coefficient of friction.
μ = coefficient of thermal conductivity, cal./(sec.)(cm.)(°C.).
ρ = density, $grams/cm.^3$
ρ_u = density of unburned gas, $grams/cm.^3$
$\Delta p/\ell$ = pressure gradient in port along direction of flow.

SPECIAL BIBLIOGRAPHY OF BUREAU OF MINES PUBLICATIONS ON FUNDAMENTAL COMBUSTION CHARACTERISTICS OF FUEL GASES

A. GRUMER, J. Combustion Characteristics of Fuel Gases. Proc. Am. Gas Assoc., 1952, pp. 852-6.

B. _____ . Nature of Gas-Burner Flashback on Turndown. Ind. Eng. Chem., vol. 45, 1953, pp. 1775-1776.

C. _____ . New Theories of Gas Burner Performance - Calculating the Old From the New. Special Report to Am. Gas Assoc., May 20, 1953, 16 pp.; pub. in Gas, vol. 30, March 1954, pp. 47-51.

D. _____ . Predicting Burner Performance With Interchanged Fuel Gases. Ind. Eng. Chem., vol. 41, 1949, pp. 2756-2761.

E. _____ . A Study of Combustion Characteristics of Fuel Gases. Am. Gas Assoc., Project PDC-3-GU, Interim Rept. 1, October 1951.

F. GRUMER, J., and HARRIS, M. E. Flame-Stability Limits of Methane, Hydrogen, and Carbon Monoxide Mixtures. Ind. Eng. Chem., vol. 44, 1952, pp. 1547-1553.

G. _____ . Temperature Dependence of Stability Limits of Burner Flames. Ind. Eng. Chem., vol. 46, 1954, pp. 2424-2430.

H. GRUMER, J., HARRIS, M. E., and ROWE, V. R. Study of the Yellow-Tipping Characteristics of Fuel Gases. Am. Gas Assoc., Project PDC-3-GU, Interim Rept. 2, April 1954.

I. GRUMER, J., HARRIS, M. E., and ROWE, V. R. Yellow-Tipping of Bunsen-Burner Flames and Related Exchangeability of Fuels In Gas Utility Systems. Pub. in Ind. Eng. Chem. (in press).

J. GRUMER, J., HARRIS, M. E., and SCHULTZ, H. Flame-Stability Limits of Ethylene, Propane, Methane, Hydrogen, and Nitrogen Mixtures. Ind. Eng. Chem., vol. 47, 1955, pp. 1760-1767.

K. _____. Flame Stabilization on Burners With Short Ports or Noncircular Ports. 4th Symposium (International) on Combustion, Williams & Wilkins Co., Baltimore, Md., 1953, pp. 695-701.

L. _____. Predicting Interchangeability of Fuel Gases; Interchangeability of Oil Gases or Propane-Air Fuels With Natural Gases. Ind. Eng. Chem., vol. 44, 1952, pp. 1554-1559.

M. HARRIS, M. E., GRUMER, J., VON ELBE, G., and LEWIS, B. Burning Velocities, Quenching and Stability Data on Nonturbulent Flames of Methane and Propane With Oxygen and Nitrogen. Application of the Theory of Ignition, Quenching, and Stabilization to Flames of Propane and Air. 3d Symposium on Combustion, Flame and Explosion Phenomena, Williams & Wilkins Co., Baltimore, Md., 1949, pp. 80-89.

N. LEWIS, B., and GRUMER, J. Application of Fundamental Concepts to the Problem of Mixing and Changeover in the Gas Industry. Gas Age, May 11, 1950, pp. 25-28, 72-80.

O. LEWIS, B., and VON ELBE, G. Ignition and Flame Stabilization in Gases. Trans. Am. Soc. Mech. Eng., May 1948, pp. 307-316.

P. _____ . Stability and Structure of Burner Flames. Jour. Chem. Phys., vol. 11, 1943, pp. 75-97.

Q. VON ELBE, G., and GRUMER, J. Air Entrainment in Gas Burners. Ind. Eng. Chem., vol. 40, 1948, pp. 1123-1129.

R. VON ELBE, G., and MENTSER, M. Further Studies on the Structure and Stability of Burner Flames. Jour. Chem. Phys., vol. 13, 1945, pp. 89-100.

Table 1a. - Critical boundary velocity gradients for flashback of single-component fuels

F_F	g_F	F_F	g_F	F_F	g_F	F_F	g_F
Fuel No. 1 composition, percent: (Natural gas) 91.5 CH_4, 5.2 C_2H_6, 1.3 C_3H_8, 0.2 C_3H_6, 0.2 C_4H_{10}, 0.1 C_4H_8, 0.9 CO_2, 0.6 N_2							
Stoichiometric percentage: 9.04 (Points for figure 19)							
Tube diam. 1.247 cm.		Tube diam. 1.023 cm.		Tube diam. 0.874 cm.			
0.745	100	0.756	157	0.806	246		
1.26	106	1.23	165	1.18	252		
.780	167	.795	201	.898	336		
1.22	175	1.21	210	1.12	343		
.815	258	.862	298	.968	377		
1.15	266	1.14	306	1.07	381		
.943	403	.908	368				
1.05	406	1.09	375				
Fuel No. 2 composition, percent: 100 CH_4							
Stoichiometric percentage: 9.46 (Points for figure 20)							
Tube diam. 1.358 cm.		Tube diam. 1.058 cm.		Tube diam. 0.873 cm.			
0.712	100	0.800	193	1.17	204		
1.26	106	1.18	202	.861	301		
.776	178	.912	323	1.11	309		
1.20	186	1.10	329	.909	341		
.846	257	.963	382	1.08	347		
1.16	265	1.05	385	.964	373		
.904	362			1.04	376		
1.10	370						
Fuel No. 3 composition, percent: 98.6 C_3H_8, 1.4 C_3H_6							
Stoichiometric percentage: 4.02 (Points for figure 21)							
Tube diam. 1.247 cm.		Tube diam. 1.023 cm.		Tube diam. 0.908 cm.			
0.730	134	0.800	222	0.863	292		
1.57	102	1.45	246	1.37	300		
.756	200	.882	394	.941	440		
1.48	200	1.33	401	1.30	447		
.847	347	.997	540	.986	534		
1.38	346	1.23	546	1.21	540		
.900	498						
1.25	505						
Fuel No. 4 composition, percent: 99.7 C_2H_4, 0.2 C_4H_8, 0.1 C_3H_6							
Stoichiometric percentage: 6.51 (Points for figure 22)							
Tube diam. 1.058 cm.		Tube diam. 0.891 cm.		Tube diam. 0.780 cm.		Tube diam. 0.699 cm.	
0.621	218	0.665	272	0.680	383	0.760	548
1.59	233	1.56	290	1.46	404	1.44	574
.674	359	.705	393	.746	596	.822	825
1.52	381	1.50	415	1.39	624	1.35	856
.710	449	.731	483	.806	803	1.06	1,387
1.45	473	1.46	508	1.34	834	1.15	1,395
.753	628	.780	728	.863	952		
1.43	660	1.38	756	1.33	984		
		.912	1,070	.930	1,187		
		1.28	1,097	1.23	1,212		
		1.04	1,282				
		1.17	1,295				
Fuel No. 5 composition, percent: 99.2 C_3H_6, 0.4 C_3H_8, 0.4 C_2H_6							
Stoichiometric percentage: 4.45 (Points for figure 23)							
Tube diam. 1.247 cm.		Tube diam. 1.023 cm.		Tube diam. 0.878 cm.		Tube diam. 0.776 cm.	
0.750	201	1.57	181	1.50	176	0.900	438
1.53	202	.760	250	1.46	296	1.44	417
.800	302	1.50	256	.920	506	.970	590
1.46	305	.810	351	1.32	488	1.34	568
		1.44	351	1.00	654	1.03	704
		.850	472	1.20	657	1.25	711
		1.41	461				
		.940	652				
		1.30	657				
Fuel No. 6 composition, percent: 100 C_6H_6							
Stoichiometric percentage: 2.71 (Points for figure 24)							
Tube diam. 1.023 cm.		Tube diam. 0.891 cm.		Tube diam. 0.776 cm.		Tube diam. 0.611 cm.	
0.704	193	1.39	1/ 428	0.750	232	1.35	487
1.52	234	.919	600	1.51	1/ 263		
.742	329	1.02	681	.852	455		
1.41	1/ 381	1.27	556	.960	642		
.828	439			1.17	664		
.912	579			1.08	716		
.983	654						
1.31	1/ 495						
1.02	674						
1.29	1/ 534						

1/ Yellow flame.

TABLE 1a. - Critical boundary velocity gradients for flashback of single-component fuels (Con.)

F_F	g_F	F_F	g_F	F_F	g_F	F_F	g_F
Fuel No. 7 composition, percent: 99.7 H_2, 0.3 O_2; Stoichiometric percentage: 29.7 (Points for figure 25)							
Tube diam. 1.023 cm.		Tube diam. 0.566 cm.		Tube diam. 0.485 cm.		Tube diam. 0.390 cm.	
0.375	256	0.427	335	0.578	2,120	0.636	2,900
.415	463	.452	622	2.12	2,060	2.07	2,735
.461	813	.517	1,244	.683	3,740	.724	4,400
		2.25	1,235	1.93	3,420	1.83	4,450
		2.19	1,610	.892	7,000	.852	6,490
		.556	1,775	1.68	6,980	1.01	8,540
		.650	3,160	1.44	8,860	1.57	8,380
		2.00	2,840	1.22	10,030	1.16	10,040
		.762	5,090			1.41	9,640
		1.84	4,860				
		.978	8,860				
		1.53	9,080				
Fuel No. 8 composition, percent: 88.9 CO, 9.7 CH_4, 1.3 H_2, 0.1 CO_2; Stoichiometric percentage: 24.5 (Points for figure 26)							
Tube diam. 0.776 cm.		Tube diam. 0.699 cm.		Tube diam. 0.611 cm.			
0.744	270	0.800	385	1.00	861		
1.81	274	1.77	388	1.63	821		
.772	316	.914	604	1.07	1,000		
1.77	331	1.70	590	1.61	962		
.865	471	1.01	861	1.21	1,265		
1.74	456	1.66	794	1.56	1,220		
.972	718	1.12	1,115				
1.70	712	1.62	1,105				
1.07	962	1.23	1,295				
1.64	968	1.45	1,400				
1.35	1,330						
1.46	1,315						

TABLE 1b. - Critical boundary velocity gradients for blowoff of single-component fuels

F_B	g_B	F_B	g_B	F_B	g_B	F_B	g_B	F_B	g_B	F_B	g_B	F_B	g_B
Fuel No. 1 composition, percent: (Natural gas) 91.5 CH_4, 5.2 C_2H_6, 1.3 C_3H_8, 0.2 C_3H_6, 0.2 C_4H_{10}, 0.1 C_4H_8, 0.9 CO_2, 0.6 N_2; Stoichiometric percentage: 9.04 (Points for figure 19)													
Tube diam. 1.247 cm.		Tube diam. 1.023 cm.		Tube diam. 0.874 cm.		Tube diam. 0.624 cm.		Tube diam. 0.495 cm.		Tube diam. 0.313 cm.		Tube diam. 0.267 cm.	
0.693	100	0.707	200	0.737	331	0.876	1,005	0.976	2,032	1.12	3,640	1.51	7,460
.700	166	.728	294	.761	370	.928	1,590	1.08	3,210	1.35	5,500	2.00	11,520
.712	255	.753	363	.775	508	1.01	2,490	1.22	4,550	1.68	8,180	2.20	13,500
.740	396			.820	782	1.09	3,400			1.88	10,350	2.43	14,030
				.864	1,194					2.04	12,050	2.61	15,060
										2.21	13,830	2.73	15,950
												2.77	16,200
												2.94	18,800
												2.97	19,160
Fuel No. 2 composition, percent: 100 CH_4; Stoichiometric percentage: 9.46 (Points for figure 20)													
Tube diam. 1.358 cm.		Tube diam. 1.058 cm.		Tube diam. 0.873 cm.		Tube diam. 0.611 cm.		Tube diam. 0.468 cm.		Tube diam. 0.294 cm.			
0.672	100	0.717	192	0.780	389	0.896	976	1.21	3,700	1.81	8,120		
.706	176	.759	318	.854	837	.966	1,675	1.50	6,220	2.30	11,940		
.737	254	.778	425	.896	1,246	1.07	2,695	2.17	10,340	2.85	16,770		
		.820	697			1.25	4,180						
Fuel No. 3 composition, percent: 98.6 C_3H_8, 1.4 C_3H_6; Stoichiometric percentage: 4.02 (Points for figure 21)													
Tube diam. 1.247 cm.		Tube diam. 1.023 cm.		Tube diam. 0.908 cm.		Tube diam. 0.675 cm.		Tube diam. 0.506 cm.		Tube diam. 0.315 cm.		Tube diam. 0.249 cm.	
0.665	147	0.706	251	0.746	338	0.790	788	0.906	1,900	1.24	5,340	1.77	9,450
.680	200	.730	391	.718	440	.860	1,384	1.04	3,030	1.51	7,560	2.12	11,870
.714	348	.760	648	.757	530	.964	2,310	1.17	4,250	1.74	9,280	2.40	13,650
.714	494			.813	1,000			1.38	5,840	2.02	10,950	2.61	14,800
										2.19	12,200		
										2.57	14,450		
										2.71	16,500		

Table 1b. - Critical boundary velocity gradients for blowoff of single-component fuels (Con.)

F_B	g_B	F_B	g_B	F_B	g_B	F_B	g_B	F_B	g_B	F_B	g_B	F_B	g_B
Fuel No. 4 composition, percent: 99.7 C_2H_4, 0.2 C_4H_8, 0.1 C_3H_6; Stoichiometric percentage: 6.51 (Points for figure 22)													
Tube diam. 1.058 cm.		Tube diam. 0.891 cm.		Tube diam. 0.699 cm.		Tube diam. 0.468 cm.		Tube diam. 0.294 cm.		Tube diam. 0.155 cm.			
0.557	217	0.572	270	0.615	542	0.698	1,824	0.867	6,600	1.39	26,800		
.588	357	.608	390	.664	816	.720	2,255	1.06	12,170	1.58	35,220		
.605	443	.626	479	.688	1,352	.788	3,420	1.17	15,970	1.78	44,000		
.622	623	.642	720	.690	1,457	.841	4,870	1.37	23,420	1.96	52,000		
		.655	1,050	.756	2,584	.978	8,340	1.50	28,270	2.19	59,850		
		.672	1,250					3.57	1/ 95,600	2.41	69,600		
								4.31	1/121,200	2.58	74,500		
										2.73	81,800		
Fuel No. 5 composition, percent: 99.2 C_3H_6, 0.4 C_3H_8, 0.4 C_2H_6; Stoichiometric percentage: 4.45 (Points for figure 23)													
Tube diam. 1.247 cm.		Tube diam. 1.023 cm.		Tube diam. 0.878 cm.		Tube diam. 0.776 cm.		Tube diam. 0.624 cm.		Tube diam. 0.390 cm.		Tube diam. 0.249 cm.	
0.680	203	0.700	250	0.750	502	0.740	600	0.840	1,297	0.913	1,990	2.20	14,190
.680	302	.710	351	.780	788	.760	706	.930	2,521	1.00	2,988	2.46	17,340
		.720	471	.830	1,292	.800	1,006			1.13	4,708	2.82	19,240
		.730	655							1.25	6,519		
										1.43	7,952		
										1.68	9,981		
										1.99	12,390		
										2.44	15,560		
Fuel No. 6 composition, percent: 100 C_6H_6; Stoichiometric percentage: 2.71 (Points for figure 24)													
Tube diam. 1.023 cm.		Tube diam. 0.891 cm.		Tube diam. 0.776 cm.		Tube diam. 0.611 cm.		Tube diam. 0.413 cm.		Tube diam. 0.354 cm.		Tube diam. 0.249 cm.	
0.604	225	0.701	774	0.722	1,136	0.826	2,110	0.748	1,363	1.05	4,850	1.10	4,810
.645	556	.752	1,266	.857	2,435	1.00	3,775	.898	3,170	1.26	2/6,610	1.37	2/ 7,040
.683	905	.798	1,830	1.01	3,653	1.12	4,990	1.05	4,605	1.42	2/7,410	1.95	2/10,280
.718	1,050					1.24	5,780	1.09	5,080				
.711	1,058							1.19	5,430				
								1.39	7,100				
								1.52	2/ 7,860				
Fuel No. 7 composition, percent: 99.7 H_2, 0.3 O_2; Stoichiometric percentage: 29.7 (Points for figure 25)													
Tube diam. 1.023 cm.		Tube diam. 0.566 cm.		Tube diam. 0.485 cm.		Tube diam. 0.390 cm.		Tube diam. 0.230 cm.					
0.363	265	0.422	337	0.418	2,175	0.429	4,060	0.496	17,100				
.399	460	.436	618	.459	3,450	.441	5,600	.530	28,700				
.390	785	.424	1,200	.443	7,060	.451	8,600	.553	45,500				
		.411	1,690	.475	7,520	.468	12,080	.584	60,000				
		.430	2,920	.453	12,740	.580	1/ 99,400	.631	1/159,000				
		.432	4,530			.603	1/127,800	.702	1/291,000				
						.634	1/182,700	.766	1/472,000				
								.817	1/633,000				
Fuel No. 8 composition, percent: 88.9 CO, 9.7 CH_4, 1.3 H_2, 0.1 CO_2; Stoichiometric percentage: 24.5 (Points for figure 26)													
Tube diam. 0.776 cm.		Tube diam. 0.699 cm.		Tube diam. 0.611 cm.		Tube diam. 0.475 cm.		Tube diam. 0.249 cm.		Tube diam. 0.155 cm.			
0.660	263	0.694	395	0.833	1,270	0.950	3,260	1.07	6,020	1.94	36,700		
.682	340	.761	616	.869	1,765	1.02	4,890	1.16	8,210	2.40	50,100		
.741	496	.794	826	.918	2,700	1.09	6,840	1.28	12,050	2.78	61,200		
.774	738	.816	1,130	.972	3,830	1.17	8,890	1.51	17,700	2.74	61,800		
.790	974	.839	1,495					1.73	25,500				
.816	1,335							1.88	32,200				
								2.10	41,400				

1/ Turbulent flow.
2/ Yellow flame.

TABLE 2a. - Critical boundary velocity gradients for flashback of two-component fuels; methane-hydrogen mixtures

F_F	g_F	F_F	g_F	F_F	g_F	F_F	g_F	F_F	g_F
Fuel No. 9 composition, percent: 93.0 CH_4, 7.0 H_2; Stoichiometric percentage: 9.95 (Data for figure 28)									
Tube diam. 1.023 cm.		Tube diam. 0.891 cm.							
0.714	142	1.29	173						
1.30	140	.785	238						
1.28	197	1.24	241						
.786	202	.890	343						
.836	279	1.19	355						
1.24	291	.956	428						
.917	400	1.14	437						
1.17	405								
Fuel No. 10 composition, percent: 74.0 CH_4, 26.0 H_2; Stoichiometric percentage: 11.5 (Data for figure 28)									
Tube diam. 1.058 cm.		Tube diam. 0.873 cm.		Tube diam. 0.611 cm.					
1.27	211	1.28	215	0.926	520				
.736	197	.721	200	1.05	529				
1.17	392	1.16	405						
.823	375	.850	389						
1.06	578	1.08	550						
.924	568	.949	540						
Fuel No. 11 composition, percent: 53.6 CH_4, 46.4 H_2; Stoichiometric percentage: 13.8 (Data for figure 28)									
Tube diam. 1.058 cm.		Tube diam. 0.873 cm.		Tube diam. 0.611 cm.					
0.644	206	0.649	230	0.926	876				
1.29	228	1.27	254	1.05	892				
.718	414	.746	477						
1.21	448	1.20	512						
.814	668	.836	736						
1.14	704	1.13	772						
.960	930	.986	990						
1.05	944	.995	991.						
Fuel No. 12 composition, percent: 70.7 H_2, 29.3 CH_4; Stoichiometric percentage: 18.2 (Data for figure 28)									
Tube diam. 0.873 cm.		Tube diam. 0.699 cm.		Tube diam. 0.611 cm.		Tube diam. 0.458 cm.			
0.524	238	0.561	364	0.604	464	0.692	1,030		
1.38	287	1.35	433	1.32	540	1.23	1,160		
.620	584	.648	691	.682	870	.828	1,640		
1.31	680	1.28	794	1.26	990	1.12	1,750		
.693	1,015	.730	1,202	.769	1,330	.925	1,995		
1.22	1,140	1.22	1,330	1.20	1,465	1.06	2,055		
		.976	2,150	.854	1,767				
		1.07	2,195	1.15	1,888				
				.959	2,215				
				1.07	2,270				
Fuel No. 13 composition, percent: 84.6 H_2, 15.4 CH_4; Stoichiometric percentage: 22.2 (Data for figure 28)									
Tube diam. 0.873 cm.		Tube diam. 0.611 cm.		Tube diam. 0.458 cm.		Tube diam. 0.354 cm.			
0.471	240	0.528	527	0.646	1,250	0.788	2,830		
1.54	327	1.45	688	1.37	1,540	1.27	3,240		
.508	425	.672	1,499	.728	2,030	.880	3,710		
1.48	561	1.37	1,830	1.29	2,380	1.19	4,060		
.558	747	.785	2,610	1.01	3,880				
1.43	958	1.28	3,010	1.11	4,000				
		.989	4,240						
		1.15	4,440						
Fuel No. 14 composition, percent: 94.4 H_2, 5.6 CH_4; Stoichiometric percentage: 26.4 (Data for figure 28)									
Tube diam. 1.023 cm.		Tube diam. 0.878 cm.		Tube diam. 0.600 cm.		Tube diam. 0.485 cm.		Tube diam. 0.390 cm.	
0.418	284	0.439	400	0.576	1,360	0.603	1,633	0.688	2,780
1.83	275	1.79	394	1.65	1,360	1.59	1,950	1.54	3,010
.476	553	.520	870	.677	2,500	.790	4,250	.944	6,140
1.73	538	1.67	876	1.55	2,460	1.49	3,960	1.36	6,220
		.584	1,850	.833	5,110	1.03	7,100	1.02	6,970
		1.62	1,834	1.43	5,080	1.35	6,680	1.32	6,940
				.940	6,980				
				1.29	7,950				

TABLE 2a. - Critical boundary velocity gradients for flashback of two-component fuels (Con.); carbon monoxide-hydrogen mixtures

F_F	g_F	F_F	g_F	F_F	g_F	F_F	g_F	F_F	g_F
Fuel No. 16 composition, percent: 85.6 CO, 14.0 H_2, 0.4 CO_2									
Stoichiometric percentage: 29.6 (Data for figure 30)									
Tube diam. 0.891 cm.		Tube diam. 0.699 cm.		Tube diam. 0.611 cm.		Tube diam. 0.468 cm.			
0.689	264	0.784	517	0.854	706	1.06	1,370		
2.35	236	2.30	466	2.24	728	2.06	1,280		
.752	407	.902	870	.986	1,115	1.17	1,798		
2.29	367	2.19	899	2.16	1,085	1.98	1,664		
.834	658	1.14	1,580	1.32	2,063	1.57	2,535		
2.24	602	2.08	1,587	1.40	2,280	1.77	2,460		
1.02	1,287	1.36	2,224	1.85	2,448				
		1.69	2,660						
Fuel No. 17 composition, percent: 79.3 CO, 19.7 H_2, 0.6 N_2, 0.3 CO_2, 0.1 O_2									
Stoichiometric percentage: 29.7 (Data for figure 30)									
Tube diam. 0.873 cm.		Tube diam. 0.699 cm.		Tube diam. 0.611 cm.		Tube diam. 0.458 cm.			
0.632	261	0.640	295	0.722	509	0.882	996		
2.32	241	.761	631	2.27	561	2.15	1,140		
.707	488	2.26	548	.816	881	1.05	1,846		
2.27	418	.906	1,138	2.19	894	1.92	2,480		
.784	790	.919	1,270	.980	1,558	1.33	2,865		
2.21	810	.960	1,440	2.06	1,610	1.57	3,240		
		2.08	1,574	1.25	2,535				
		1.15	2,036	1.94	2,420				
		1.84	2,970	1.73	3,280				
		1.40	3,093						
		1.64	3,520						
Fuel No. 18 composition, percent: 74.5 CO, 25.1 H_2, 0.4 CO_2									
Stoichiometric percentage: 29.6 (Data for figure 30)									
Tube diam. 0.699 cm.		Tube diam. 0.611 cm.		Tube diam. 0.294 cm.					
0.598	243	0.584	243	1.94	2,250				
2.19	255	2.17	349	1.83	2,850				
.628	299	2.18	378	1.51	3,370				
2.17	354	.681	448						
.684	446	2.16	461						
2.16	538	2.15	564						
.765	633	.743	630						
2.13	692	2.14	693						
.767	803	.766	718						
2.11	878	.780	814						
2.09	956	.848	1,050						
2.08	1,150	.888	1,250						
.862	1,220	.895	1,265						
2.01	1,560	2.04	1,288						
.936	1,595	.942	1,475						
1.96	1,900	.983	1,625						
1.93	2,120	1.01	1,815						
1.10	2,185	1.95	1,890						
1.90	2,360	1.10	2,180						
1.21	2,570	1.87	2,340						
1.86	2,605	1.19	2,580						
1.23	2,780	1.24	2,745						
1.26	2,910	1.77	2,845						
1.79	2,910	1.69	3,150						
1.67	3,320	1.56	3,245						
1.64	3,350	1.50	3,245						
		1.45	3,255						
Fuel No. 19 composition, percent: 64.4 CO, 35.5 H_2, 0.1 CO_2									
Stoichiometric percentage: 29.5 (Data for figure 30)									
Tube diam. 0.891 cm.		Tube diam. 0.699 cm.		Tube diam. 0.611 cm.		Tube diam. 0.468 cm.		Tube diam. 0.354 cm.	
0.584	277	0.614	357	0.738	791	0.905	1,960	1.03	2,610
2.07	260	2.06	314	2.05	811	1.88	1,990	1.85	2,490
.604	412	.659	520	.840	1,344	1.23	3,580	1.05	2,950
2.05	400	2.05	460	1.97	1,284	1.74	3,270	1.75	3,290
.679	600	.702	684	1.11	2,960	1.52	4,150	1.18	3,860
2.06	590	2.04	670	1.81	2,990			1.69	3,630
.754	916	.752	962	1.23	3,730				
2.03	897	2.01	966	1.65	3,880				
		.856	1,537						
		1.95	1,560						
		.980	2,270						
		1.88	2,335						

TABLE 2a. - Critical boundary velocity gradients for flashback of two-component fuels (Con.); carbon monoxide-hydrogen mixtures (Con.)

F_F	g_F	F_F	g_F	F_F	g_F	F_F	g_F	F_F	g_F	F_F	g_F
Fuel No. 20 composition, percent: 49.9 CO, 49.5 H_2, 0.3 N_2, 0.3 CO_2; Stoichiometric percentage: 29.6 (Data for figure 30)											
Tube diam. 0.873 cm.		Tube diam. 0.699 cm.		Tube diam. 0.611 cm.		Tube diam. 0.458 cm.		Tube diam. 0.354 cm.		Tube diam. 0.303 cm.	
0.519	296	0.582	586	0.562	476	0.744	1,611	0.933	3,825	1.70	5,220
2.27	280	2.24	714	2.26	502	2.14	1,570	1.89	3,972	1.11	5,480
.572	472	.670	992	.632	888	.940	3,070	1.01	4,550	1.64	5,720
2.25	462	2.10	1,840	2.22	932	1.94	3,023	1.81	5,040	1.20	6,350
.623	826	.841	2,440	.746	1,735	1.11	4,415	1.13	5,780	1.50	7,350
2.21	819	1.90	4,260	2.08	2,098	1.74	5,060	1.71	6,340		
.689	1,320			.943	3,430	1.30	5,570	1.20	6,440		
2.16	1,345			1.96	3,550	1.46	6,030	1.52	7,570		
				1.18	5,870						
				1.72	6,060						
Fuel No. 21 composition, percent: 63.4 H_2, 36.5 CO, 0.1 CO_2; Stoichiometric percentage: 29.5 (Data for figure 30)											
Tube diam. 0.891 cm.		Tube diam. 0.699 cm.		Tube diam. 0.458 cm.		Tube diam. 0.354 cm.		Tube diam. 0.303 cm.			
0.483	284	0.538	568	0.685	1,575	0.820	3,280	0.916	3,930		
2.35	287	2.31	664	2.16	1,447	1.95	3,310	1.83	3,870		
.526	463	.622	1,098	.814	2,770	.951	5,080	1.04	5,690		
2.33	465	2.19	1,105	1.97	2,570	1.81	4,830	1.65	5,600		
.582	820	.718	2,090	.990	4,520	1.19	7,050	1.27	7,540		
2.25	818	2.09	2,100	1.85	4,060	1.65	6,820	1.47	6,940		
				1.19	6,310	1.22	7,510				
				1.65	6,100	1.32	7,900				
				1.30	6,860						
				1.36	7,070						
Fuel No. 22 composition, percent: 85.9 H_2, 14.1 CO; Stoichiometric percentage: 29.5 (Data for figure 30)											
Tube diam. 0.891 cm.		Tube diam. 0.611 cm.		Tube diam. 0.468 cm.		Tube diam. 0.354 cm.		Tube diam. 0.303 cm.			
2.31	243	0.453	427	0.607	1,665	0.722	3,430	0.814	4,730		
.442	304	2.26	539	2.17	1,646	1.97	3,280	1.79	4,630		
2.31	353	.512	818	.664	2,470	.902	5,960	.950	6,900		
.470	434	2.26	803	2.03	2,302	1.70	5,920	1.57	6,750		
.505	719	.563	1,308	.792	4,035	1.01	6,920	1.11	8,900		
2.27	658	2.18	1,266	1.89	3,725	1.52	8,700	1.41	9,200		
.540	1,115	.630	2,050	.873	5,280						
2.18	1,065	2.06	1,886	1.75	5,160						
				1.01	8,180						
				1.58	7,990						
				1.06	8,470						
				1.47	9,000						
Fuel No. 23 composition, percent: 93.0 H_2, 6.6 CO, 0.4 O_2; Stoichiometric percentage: 29.8 (Data for figure 30)											
Tube diam. 1.023 cm.		Tube diam. 0.874 cm.		Tube diam. 0.566 cm.		Tube diam. 0.485 cm.		Tube diam. 0.390 cm.			
0.408	248	0.450	360	0.606	1,570	0.566	1,510	0.854	5,080		
2.27	251	2.25	346	2.13	1,570	2.06	2,110	1.77	4,890		
.455	498	.502	771	.644	2,500	.682	3,400	1.07	8,700		
2.27	538	2.23	778	1.99	2,430	1.91	3,580	1.50	8,620		
.506	1,015	.536	1,740	.724	4,000	.853	5,750				
2.17	978	2.08	1,660	1.87	3,990	1.71	6,080				
				.943	8,390	1.05	8,700				
				1.58	8,600	1.46	8,970				

TABLE 2a. - Critical boundary velocity gradients for flashback of two-component fuels (Con.); methane-carbon monoxide mixtures

Fuel No. 24 composition, percent: 63.1 CH_4, 36.4 CO, 0.4 H_2, 0.1 CO_2
Stoichiometric percentage: 12.6 (Data for figure 32)

F_F	g_F	F_F	g_F	F_F	g_F
Tube diam. 1.058 cm.		Tube diam. 0.891 cm.		Tube diam. 0.776 cm.	
0.696	111	0.732	171	0.810	273
1.37	110	1.32	169	1.26	292
.739	151	.824	249	.883	360
1.33	149	1.27	244	1.20	376
.780	204	.846	348	.998	475
1.30	199	1.23	342	1.15	485
.830	287	.956	455		
1.26	306	1.17	437		
.895	404	1.02	518		
1.21	399	1.12	524		
.950	496				
1.16	506				

Fuel No. 25 composition, percent: 54.0 CO, 46.0 CH_4
Stoichiometric percentage: 15.0 (Data for figure 32)

F_F	g_F	F_F	g_F	F_F	g_F
Tube diam. 0.891 cm.		Tube diam. 0.776 cm.		Tube diam. 0.699 cm.	
0.766	259	0.779	307	0.930	541
1.35	258	1.36	311	1.27	537
.833	358	.859	388	1.00	642
1.35	352	1.30	392	1.22	642
.902	496	.930	541		
1.28	509	1.28	544		
1.06	702	1.03	677		
1.21	706	1.21	674		

Fuel No. 26 composition, percent: 66.6 CO, 32.3 CH_4, 1.0 H_2, 0.1 CO_2
Stoichiometric percentage: 17.5 (Data for figure 32)

F_F	g_F	F_F	g_F	F_F	g_F
Tube diam. 0.891 cm.		Tube diam. 0.776 cm.		Tube diam. 0.699 cm.	
0.771	259	0.771	299	0.854	463
1.42	254	1.44	296	1.33	422
.832	400	.891	510	.894	540
1.39	388	1.35	470	1.30	530
.908	601	.990	706	1.02	742
1.34	576	1.29	672	1.25	716
1.07	874	1.07	828	1.08	820
1.17	893	1.17	847	1.18	838

Fuel No. 8 composition, percent: 88.9 CO, 9.7 CH_4, 1.3 H_2, 0.1 CO_2
Stoichiometric percentage: 24.5 (Data for figure 32)

F_F	g_F	F_F	g_F	F_F	g_F
Tube diam. 0.776 cm.		Tube diam. 0.699 cm.		Tube diam. 0.611 cm.	
0.744	270	0.800	385	1.00	861
1.81	274	1.77	388	1.63	821
.772	316	.914	604	1.07	1,000
1.77	331	1.70	590	1.61	962
.865	471	1.01	861	1.21	1,265
1.74	456	1.66	794	1.56	1,220
.972	718	1.12	1,115		
1.70	712	1.62	1,105		
1.07	962	1.23	1,295		
1.64	968	1.45	1,400		
1.35	1,330				
1.46	1,315				

Fuel No. 27 composition, percent: 93.7 CO, 4.5 CH_4, 1.5 H_2, 0.3 CO_2
Stoichiometric percentage: 27.0 (Data for figure 32)

F_F	g_F	F_F	g_F	F_F	g_F
Tube diam. 0.891 cm.		Tube diam. 0.776 cm.			
0.731	195	1.01	618		
2.01	197	1.88	596		
.838	310	1.09	774		
1.96	325	1.83	828		
.904	437	1.34	1,180		
1.91	497	1.69	1,200		

TABLE 2a. - Critical boundary velocity gradients for flashback of two-component fuels (Con.); propane-hydrogen mixtures

F_F	g_F	F_F	g_F	F_F	g_F	F_F	g_F
Fuel No. 28 composition, percent: 81.6 C_3H_8, 17.4 H_2, 1.0 C_3H_6; Stoichiometric percentage: 4.73 (Data for figure 34)							
Tube diam. 1.023 cm.		Tube diam. 0.891 cm.		Tube diam. 0.776 cm.			
0.754	197	0.776	251	0.856	382		
1.48	200	1.43	251	1.36	380		
.793	299	.842	343	.934	543		
1.47	300	1.39	345	1.30	544		
.854	428	.909	503	.981	654		
1.38	428	1.31	508	1.21	654		
.974	592	1.01	643				
1.26	600	1.23	644				
Fuel No. 29 composition, percent: 55.4 C_3H_8, 44.6 H_2; Stoichiometric percentage: 6.52 (Data for figure 34)							
Tube diam. 0.908 cm.		Tube diam. 0.776 cm.		Tube diam. 0.675 cm.			
0.778	241	0.772	303	0.905	518		
1.49	260	1.41	319	1.32	534		
.814	349	.878	495	1.05	738		
1.43	344	1.34	511	1.22	748		
.870	596	1.02	750				
1.28	613	1.24	760				
1.02	767						
1.21	777						
Fuel No. 30 composition, percent: 74.5 H_2, 25.5 C_3H_8; Stoichiometric percentage: 11.3 (Data for figure 34)							
Tube diam. 0.776 cm.		Tube diam. 0.675 cm.		Tube diam. 0.600 cm.			
0.619	216	0.696	328	0.684	378		
1.52	242	1.49	362	1.47	418		
.700	428	.792	728	.763	586		
1.47	452	1.36	770	1.39	635		
.834	904	1.10	1,520	.950	1,217		
1.34	839	1.14	1,460	1.24	1,263		
1.04	1,374			1.00	1,390		
1.17	1,400			1.23	1,320		
Fuel No. 31 composition, percent: 89.0 H_2, 11.0 C_3H_8; Stoichiometric percentage: 17.4 (Data for figure 34)							
Tube diam. 0.874 cm.		Tube diam. 0.776 cm.		Tube diam. 0.672 cm.		Tube diam. 0.600 cm.	
0.540	204	0.550	246	0.659	877	0.610	475
1.59	199	1.56	275	1.37	983	1.47	570
.562	350	.577	402	.826	1,840	.668	872
1.51	350	1.49	426	1.29	1,810	1.36	1,010
		.633	734	.924	2,360	.756	1,510
		1.43	691	1.19	2,500	1.31	1,480
		.705	1,205			.948	2,400
		1.36	1,180			1.18	2,530
		.904	2,230				
		1.21	2,100				

TABLE 2a. - Critical boundary velocity gradients for flashback of two-component fuels (Con.); ethylene-hydrogen mixtures

F_F	g_F	F_F	g_F	F_F	g_F	F_F	g_F	F_F	g_F
Fuel No. 32 composition, percent: 78.4 C_2H_4, 21.6 H_2; Stoichiometric percentage: 7.83 (Data for figure 36)									
Tube diam. 0.891 cm.		Tube diam. 0.874 cm.		Tube diam. 0.721 cm.		Tube diam. 0.624 cm.		Tube diam. 0.495 cm.	
0.592	215	0.815	926	0.675	383	0.712	571	0.846	1,040
1.61	232	1.33	967	1.49	406	1.45	592	1.29	1,080
.636	292	.954	1,290	.740	676	.774	792	.893	1,210
1.57	316	1.20	1,320	1.42	728	1.37	839	1.26	1,250
.713	496			.923	1,303	1.30	1,156	1.05	1,600
1.49	530			1.27	1,350	1.16	1,470	1.12	1,610
						1.23	1,400		
						.992	1,520		
Fuel No. 33 composition, percent: 55.3 C_2H_4, 44.6 H_2, 0.1 C_3H_6; Stoichiometric percentage: 9.98 (Data for figure 36)									
Tube diam. 0.874 cm.		Tube diam. 0.721 cm.		Tube diam. 0.624 cm.					
0.560	243	0.559	294	0.610	503				
1.57	245	1.49	326	1.41	490				
.602	395	.656	608	.657	720				
1.47	393	1.40	603	1.38	694				
.690	828	.772	1,226	.729	1,024				
1.35	804	1.25	1,274	1.28	1,088				
.745	1,120	1.00	1,850	.781	1,305				
1.27	1,108	1.10	1,763	1.23	1,370				
.845	1,540			.878	1,697				
1.22	1,503			1.08	1,880				
Fuel No. 34 composition, percent: 66.8 H_2, 33.1 C_2H_4, 0.1 C_3H_6; Stoichiometric percentage: 13.6 (Data for figure 36)									
Tube diam. 0.776 cm.		Tube diam. 0.624 cm.		Tube diam. 0.495 cm.					
0.515	245	0.582	446	0.689	1,017				
1.64	257	1.52	518	1.40	952				
.649	794	.740	1,295	.785	1,500				
1.44	785	1.36	1,305	1.34	1,462				
.805	1,780	.952	2,270	.920	2,230				
1.29	1,920	1.22	2,370	1.20	2,330				
				.988	2,480				
				1.15	2,550				
Fuel No. 35 composition, percent: 80.0 H_2, 20.0 C_2H_4; Stoichiometric percentage: 17.3 (Data for figure 36)									
Tube diam. 0.721 cm.		Tube diam. 0.624 cm.		Tube diam. 0.495 cm.					
0.511	290	0.573	550	0.626	858				
1.69	355	1.57	680	1.51	1,037				
.600	798	.665	1,160	.722	1,535				
1.56	708	1.51	1,011	1.46	1,480				
.771	2,155	1.00	3,700	.805	2,270				
1.44	2,140	1.18	3,850	1.35	2,552				
				.907	3,040				
				1.28	3,292				
Fuel No. 36 composition, percent: 91.4 H_2, 8.5 C_2H_4, 0.1 C_2H_6; Stoichiometric percentage: 22.6 (Data for figure 36)									
Tube diam. 0.535 cm.		Tube diam. 0.506 cm.		Tube diam. 0.475 cm.		Tube diam. 0.354 cm.			
0.472	394	1.63	281	0.522	708	0.728	2,575		
		.515	576	1.60	732	1.40	3,140		
		1.65	572	.618	1,410	.856	4,560		
		.582	1,100	1.53	1,400	1.25	5,070		
		1.57	1,014	.697	2,665	.953	5,820		
		.620	1,550	1.41	2,570	1.19	6,240		
		1.46	1,990	.778	3,920				
		.778	3,590	1.33	4,130				
		1.37	3,460	.910	5,960				
		1.32	4,330	1.24	6,080				
		1.01	5,670						
		1.20	5,510						

TABLE 2a. - Critical boundary velocity gradients for flashback of two-component fuels (Con.); nitrogen-hydrogen mixtures

F_F	g_F	F_F	g_F	F_F	g_F	F_F	g_F
Fuel No. 37 composition, percent: 59.8 N_2, 40.1 H_2, 0.1 A; Stoichiometric percentage: 51.0 (Data for figure 38)							
Tube diam. 0.776 cm.		Tube diam. 0.624 cm.		Tube diam. 0.495 cm.			
0.630	336	0.608	260	0.651	417		
1.40	250	1.37	327	.720	678		
.664	505	.713	587	1.35	622		
1.38	446	1.34	626	.856	1,207		
.770	930	.769	642	1.25	1,200		
1.32	744	.836	1,216	.964	1,760		
.863	1,400	1.28	932	1.17	1,730		
1.23	1,460						
Fuel No. 38 composition, percent: 50.1 H_2, 49.6 N_2, 0.3 O_2; Stoichiometric percentage: 45.8 (Data for figure 38)							
Tube diam. 0.874 cm.		Tube diam. 0.721 cm.		Tube diam. 0.624 cm.		Tube diam. 0.495 cm.	
0.491	180	0.530	302	1.50	324	0.694	1,200
.540	362	1.55	258	.572	515	1.37	1,204
.617	740	.564	442	1.51	453	.800	2,000
		1.54	422	.658	917	1.28	2,130
		.632	818	1.41	1,070	.926	2,950
		1.46	743	.747	1,646	1.20	3,060
		.686	1,340	1.34	1,678		
		1.38	1,376	.874	2,660		
		.809	2,230	1.24	2,770		
		1.29	2,340				
Fuel No. 39 composition, percent: 62.4 H_2, 37.3 N_2, 0.1 CH_4, 0.1 CO, 0.1 CO_2; Stoichiometric percentage: 39.9 (Data for figure 38)							
Tube diam. 0.874 cm.		Tube diam. 0.721 cm.		Tube diam. 0.624 cm.		Tube diam. 0.495 cm.	
0.465	173	0.513	315	0.681	1,487	0.658	1,046
1.75	292	1.74	425	1.57	1,450	.780	2,350
.540	455	.570	614	.794	2,670	1.53	1,972
1.72	576	.624	1,033	1.44	2,980	.940	3,970
.593	787	1.67	960	1.01	4,340	1.33	4,020
1.65	1,023	.730	1,964	1.29	4,320		
.629	1,173	1.55	1,890				
1.60	1,400	.840	2,970				
		1.49	2,500				

Other mixtures

F_F	g_F	F_F	g_F	F_F	g_F
Fuel No. 40 composition, percent: 88.5 CH_4, 0.6 C_2H_6, 10.8 N_2, 0.1 CO_2; Stoichiometric percentage: 10.5					
Tube diam. 1.247 cm.		Tube diam. 1.058 cm.		Tube diam. 0.891 cm.	
0.765	115	0.762	112	0.730	129
1.25	122	1.27	119	1.28	137
.742	133	.766	143	.750	159
1.26	141	1.24	154	1.27	169
.814	180	.804	222	.778	201
1.22	189	1.18	228	1.23	212
.858	258	.862	297	.814	240
1.18	268	1.17	308	1.19	251
.943	389	.871	342	.871	317
1.11	397	1.15	353	1.14	327
.956	430	1.14	352	.985	430
1.08	436	.918	369	1.04	432
		1.11	377		
		.944	403		
		1.10	410		
Fuel No. 41 composition, percent: 79.4 CH_4, 20.6 C_2H_4; Stoichiometric percentage: 8.66 (Points for figure 27)					
Tube diam. 1.058 cm.		Tube diam. 0.891 cm.		Tube diam. 0.776 cm.	
0.760	205	0.784	233	1.22	366
1.30	201	1.31	221	.919	493
.776	251	.816	342	1.16	506
1.30	258	1.27	331	1.03	574
.818	303	.892	451	1.13	580
1.28	297	1.20	451		
.866	398	.945	561		
1.24	401	1.14	572		
.922	516				
1.18	522				
Fuel No. 42 composition, percent: 78.6 C_2H_4, 21.4 CH_4; Stoichiometric percentage: 6.98					
Tube diam. 0.874 cm.		Tube diam. 0.776 cm.		Tube diam. 0.624 cm.	
0.687	249	0.683	299	0.746	490
1.52	265	1.45	317	1.37	526
.734	396	.782	505	.804	597
1.43	418	1.38	528	1.34	622
.834	706	.883	788	.878	861
1.31	732	1.30	814	1.25	882
.965	986	.980	1,018	.951	1,030
1.24	896	1.22	994	1.19	1,050

TABLE 2b. - Critical boundary velocity gradients for blowoff of two-component fuels; methane-hydrogen mixtures

Fuel No. 15 composition, percent: 87.4 CH_4, 12.6 H_2
Stoichiometric percentage: 10.4 (Data for figure 29)

Tube diam. 1.058 cm.		Tube diam. 0.873 cm.		Tube diam. 0.600 cm.		Tube diam. 0.468 cm.		Tube diam. 0.294 cm.		Tube diam. 0.170 cm.	
F_B	g_B	F_B	g_B	F_B	g_B	F_B	g_B	F_B	g_B	F_B	g_B
0.682	247	0.706	401	0.816	989	0.941	2,312	1.35	8,230	2.04	20,200
.746	431	.767	584	.890	1,664	1.17	4,790	1.97	19,630	2.48	32,400
.792	702	.866	1,258	.968	2,476	1.39	7,760	2.47	33,200	3.11	50,200
				1.05	3,800	1.60	10,860			3.41	59,200

Fuel No. 10 composition, percent: 74.0 CH_4, 26.0 H_2
Stoichiometric percentage: 11.5 (Data for figure 29)

Tube diam. 1.058 cm.		Tube diam. 0.873 cm.		Tube diam. 0.611 cm.		Tube diam. 0.468 cm.		Tube diam. 0.294 cm.		Tube diam. 0.170 cm.	
F_B	g_B	F_B	g_B	F_B	g_B	F_B	g_B	F_B	g_B	F_B	g_B
0.688	196	0.666	198	0.788	816	0.910	2,034	1.19	7,740	2.08	41,600
.727	371	.714	612	.861	1,607	.989	3,850	1.45	16,550	2.25	52,000
.742	577	.790	984	.913	2,750	1.12	7,230	1.80	31,100	2.60	70,800
.760	740	.820	1,325	.945	3,590	1.27	10,800			2.90	98,100

Fuel No. 11 composition, percent: 53.6 CH_4, 46.4 H_2
Stoichiometric percentage: 13.8 (Data for figure 29)

Tube diam. 1.058 cm.		Tube diam. 0.873 cm.		Tube diam. 0.611 cm.		Tube diam. 0.468 cm.		Tube diam. 0.294 cm.		Tube diam. 0.170 cm.		Tube diam. 0.156 cm.		Tube diam. 0.110 cm.		Tube diam. 0.069 cm.	
F_B	g_B	F_B	g_B	F_B	g_B	F_B	g_B	F_B	g_B	F_B	g_B	F_B	g_B	F_B	g_B	F_B	g_B
0.614	205	0.590	228	0.716	936	0.825	2,940	0.977	7,700	1.31	29,800	1.56	68,800	1.59	70,100	2.17	237,000
.644	410	.660	470	.782	2,250	.892	6,060	1.11	16,100	1.48	50,100	1.80	112,000	1.81	138,000	2.41	396,000
.666	710	.697	936	.840	4,130	.950	8,870	1.18	23,800	1.69	80,900	2.56	1/440,000	2.03	221,000	2.69	694,000
.678	890	.722	1,304					1.34	37,400	2.35	1/344,500	2.55	1/458,000				
										2.56	1/483,500	2.75	1/659,000				

Fuel No. 12 composition, percent: 70.7 H_2, 29.3 CH_4
Stoichiometric percentage: 18.2 (Data for figure 29)

Tube diam. 0.873 cm.		Tube diam. 0.699 cm.		Tube diam. 0.611 cm.		Tube diam. 0.458 cm.		Tube diam. 0.294 cm.		Tube diam. 0.170 cm.		Tube diam. 0.110 cm.	
F_B	g_B	F_B	g_B	F_B	g_B	F_B	g_B	F_B	g_B	F_B	g_B	F_B	g_B
0.493	237	0.582	682	0.592	854	0.601	1,565	0.694	5,460	0.905	27,400	1.24	201,000
.561	577	.593	1,168	.609	1,285	.636	2,050	.778	12,600	1.01	52,800	1.58	1/ 789,000
.574	989			.613	1,680	.692	4,330	.814	18,650	1.13	107,000	1.81	1/1,403,000
				.636	2,650	.732	7,560	.864	31,200	1.43	1/480,000	2.17	1/2,580,000
				.646	3,630								

Fuel No. 13 composition, percent: 84.6 H_2, 15.4 CH_4
Stoichiometric percentage: 22.2 (Data for figure 29)

Tube diam. 0.873 cm.		Tube diam. 0.611 cm.		Tube diam. 0.458 cm.		Tube diam. 0.294 cm.		Tube diam. 0.170 cm.		Tube diam. 0.110 cm.	
F_B	g_B	F_B	g_B	F_B	g_B	F_B	g_B	F_B	g_B	F_B	g_B
0.452	239	0.504	524	0.543	1,930	0.625	8,860	0.743	27,500	0.963	204,000
.492	423	.534	1,445	.582	3,700	.650	16,600	.801	54,000	1.10	1/ 740,000
.488	734	.540	2,450	.600	6,740	.693	31,300	.854	97,800	1.54	1/3,390,000
		.549	3,770	.633	10,130			1.02	1/365,000		
								1.20	1/825,000		

Fuel No. 14 composition, percent: 94.4 H_2, 5.6 CH_4
Stoichiometric percentage: 26.4 (Data for figure 29)

Tube diam. 1.023 cm.		Tube diam. 0.878 cm.		Tube diam. 0.600 cm.		Tube diam. 0.485 cm.		Tube diam. 0.390 cm.		Tube diam. 0.230 cm.	
F_B	g_B	F_B	g_B	F_B	g_B	F_B	g_B	F_B	g_B	F_B	g_B
0.404	294	0.424	416	0.442	1,307	0.461	2,135	0.492	3,880	0.565	16,350
.427	545	.439	848	.467	2,340	.483	3,860	.518	6,070	.578	23,600
		.429	1,765	.469	5,110	.499	6,960	.510	7,940	.612	40,000
								.528	14,100	.748	1/ 232,000
								.536	14,800	.856	1/ 507,000
								.588	1/ 64,000	.944	1/ 754,000
								.620	1/ 87,000	1.03	1/1,045,000
								.652	1/125,400		
								.678	1/167,300		
								.677	1/177,500		
								.691	1/197,200		

1/ Turbulent flow.

TABLE 2b. - Critical boundary velocity gradients for blowoff of two-component fuels (Con.); carbon monoxide-hydrogen mixtures

Fuel No. 16 composition, percent: 85.6 CO, 14.0 H_2, 0.4 CO_2
Stoichiometric percentage: 29.6 (Data for figure 31)

F_B	g_B	F_B	g_B	F_B	g_B	F_B	g_B	F_B	g_B	F_B	g_B	F_B	g_B	F_B	g_B
Tube diam. 0.891 cm.		Tube diam. 0.611 cm.		Tube diam. 0.468 cm.		Tube diam. 0.294 cm.		Tube diam. 0.160 cm.							
0.627	258	0.679	705	0.757	1,670	0.963	6,630	1.36	26,350						
.650	392	.723	1,055	.846	3,140	1.12	12,850	1.51	40,300						
.676	619	.754	1,394	.907	5,110	1.22	20,220	1.62	52,200						
.703	854	.794	2,005	.966	7,800	1.36	30,800	1.74	67,500						
						1.65	1/ 74,400	1.86	85,500						
						1.81	1/104,200	1.91	89,200						
						2.02	1/145,000	2.01	111,500						
								2.28	1/214,000						
								2.45	1/249,000						

Fuel No. 17 composition, percent: 79.3 CO, 19.7 H_2, 0.6 N_2, 0.3 CO_2, 0.1 O_2
Stoichiometric percentage: 29.7 (Data for figure 31)

F_B	g_B	F_B	g_B	F_B	g_B	F_B	g_B	F_B	g_B	F_B	g_B	F_B	g_B	F_B	g_B
Tube diam. 0.873 cm.		Tube diam. 0.699 cm.		Tube diam. 0.611 cm.		Tube diam. 0.458 cm.		Tube diam. 0.294 cm.		Tube diam. 0.170 cm.		Tube diam. 0.156 cm.		Tube diam. 0.110 cm.	
0.582	256	0.588	289	0.628	491	0.687	924	0.835	3,720	1.21	25,700	1.49	68,200	1.47	66,500
.624	473	.640	602	.708	1,580	.823	3,815	.884	5,960	1.37	46,200	1.71	118,200	1.53	83,000
.643	826	.690	1,160	.764	3,210			.909	7,580	1.49	61,100	2.24	1/329,000	1.64	113,000
		.734	2,330					1.00	12,300	1.69	90,000	2.43	1/391,000	1.95	217,000
								1.09	19,300	2.38	1/325,000	2.59	1/458,000		
								1.18	29,900			2.93	1/704,000		

Fuel No. 19 composition, percent: 64.4 CO, 35.5 H_2, 0.1 CO_2
Stoichiometric percentage: 29.5 (Data for figure 31)

F_B	g_B	F_B	g_B	F_B	g_B	F_B	g_B	F_B	g_B	F_B	g_B	F_B	g_B	F_B	g_B
Tube diam. 0.891 cm.		Tube diam. 0.699 cm.		Tube diam. 0.611 cm.		Tube diam. 0.468 cm.		Tube diam. 0.354 cm.		Tube diam. 0.294 cm.		Tube diam. 0.155 cm.			
0.551	292	0.566	355	0.607	804	0.670	1,980	0.698	2,560	0.793	7,970	1.02	25,100		
.567	417	.582	506	.634	1,315	.712	3,220	.722	3,870	.862	12,600	1.08	40,500		
.586	625	.592	682	.670	2,820	.760	4,600	.770	5,800	.942	26,650	1.19	67,200		
.600	913	.604	968	.714	4,310			.808	8,880	1.07	42,900	1.29	98,900		
		.643	1,573					.851	14,800	1.30	1/141,500	1.38	133,500		
		.659	2,300									1.65	1/ 349,000		
												1.73	1/ 439,000		
												1.77	1/ 450,000		
												1.89	1/ 614,000		
												2.06	1/ 877,000		
												2.49	1/1,467,000		
												2.70	1/1,655,000		

Fuel No. 20 composition, percent: 49.9 CO, 49.5 H_2, 0.3 N_2, 0.3 CO_2
Stoichiometric percentage: 29.6 (Data for figure 31)

F_B	g_B	F_B	g_B	F_B	g_B	F_B	g_B	F_B	g_B	F_B	g_B	F_B	g_B	F_B	g_B
Tube diam. 0.873 cm.		Tube diam. 0.611 cm.		Tube diam. 0.458 cm.		Tube diam. 0.354 cm.		Tube diam. 0.170 cm.		Tube diam. 0.156 cm.					
0.498	294	0.518	522	0.578	1,586	0.642	5,810	0.824	22,700	1.33	1/ 462,500				
.514	462	.544	895	.632	3,169	.682	9,880	.909	43,250	1.49	1/ 716,000				
.530	799	.569	1,740	.667	7,030	.714	15,850	.975	65,400	1.73	1/1,234,000				
.547	1,315	.598	3,400			.736	22,670	1.02	98,400						
								1.17	1/241,000						
								1.26	1/285,000						
								1.24	1/288,000						
								1.42	1/471,000						
								1.49	1/589,000						

Fuel No. 21 composition, percent: 63.4 H_2, 36.5 CO, 0.1 CO_2
Stoichiometric percentage: 29.5 (Data for figure 31)

F_B	g_B	F_B	g_B	F_B	g_B	F_B	g_B	F_B	g_B	F_B	g_B	F_B	g_B	F_B	g_B
Tube diam. 0.891 cm.		Tube diam. 0.699 cm.		Tube diam. 0.458 cm.		Tube diam. 0.354 cm.		Tube diam. 0.155 cm.							
0.476	284	0.491	593	0.539	1,640	0.562	3,410	0.736	15,540						
.488	457	.519	1,080	.564	2,720	.580	4,950	.754	24,200						
.500	814	.534	2,125	.587	4,230	.608	8,610	.794	42,300						
				.604	6,500	.637	13,000	.814	61,200						
				.629	9,400	.660	20,100	.892	90,800						
						.715	30,750	.944	143,000						
								1.19	1/ 574,000						
								1.47	1/1,386,000						
								1.69	1/2,210,000						

Fuel No. 22 composition, percent: 85.9 H_2, 14.1 CO
Stoichiometric percentage: 29.5 (Data for figure 31)

F_B	g_B	F_B	g_B	F_B	g_B	F_B	g_B	F_B	g_B	F_B	g_B	F_B	g_B	F_B	g_B
Tube diam. 0.891 cm.		Tube diam. 0.611 cm.		Tube diam. 0.468 cm.		Tube diam. 0.354 cm.		Tube diam. 0.303 cm.		Tube diam. 0.294 cm.		Tube diam. 0.155 cm.			
0.433	303	0.438	424	0.471	1,704	0.497	3,450	0.505	4,670	0.556	14,450	0.637	29,900		
.467	434	.464	862	.483	2,560	.526	6,000	.544	7,180	.563	20,400	.671	49,650		
.438	720	.468	1,365	.483	4,200	.520	8,450	.539	13,300	.596	35,000	.728	92,800		
.446	1,130	.470	2,100	.495	5,320	.546	17,050	.573	23,500	.702	1/109,000	.744	123,000		
				.500	8,040					.746	1/186,000	.878	1/ 403,000		
												.963	1/ 656,000		
												1.22	1/1,666,000		

1/ Turbulent flow.

TABLE 2b. - Critical boundary velocity gradients for blowoff of two-component fuels (Con.); carbon monoxide-hydrogen mixtures (Con.)

F_B	g_B	F_B	g_B	F_B	g_B	F_B	g_B	F_B	g_B	F_B	g_B
Fuel No. 23 composition, percent: 93.0 H_2, 6.6 CO, 0.4 O_2; Stoichiometric percentage: 29.8 (Data for figure 31)											
Tube diam. 1.023 cm.		Tube diam. 0.874 cm.		Tube diam. 0.566 cm.		Tube diam. 0.485 cm.		Tube diam. 0.390 cm.		Tube diam. 0.230 cm.	
0.391	246	0.414	356	0.474	1,500	0.451	1,900	0.493	5,100	0.540	13,500
.424	492	.426	750	.450	2,500	.455	3,490	.506	8,280	.558	24,600
.409	982	.420	1,670	.460	2,520	.471	6,080	.513	9,520	.576	39,800
				.455	4,870	.474	11,180	.487	17,500	.606	54,600
				.459	7,020	.574	1/83,500	.657	1/195,000	.684	1/183,000
										.754	1/339,000
										.849	1/541,000
										.907	1/784,000

methane-carbon monoxide mixtures

F_B	g_B	F_B	g_B	F_B	g_B	F_B	g_B	F_B	g_B	F_B	g_B
Fuel No. 24 composition, percent: 63.1 CH_4, 36.4 CO, 0.4 H_2, 0.1 CO_2; Stoichiometric percentage: 12.6 (Data for figure 33)											
Tube diam. 1.058 cm.		Tube diam. 0.891 cm.		Tube diam. 0.776 cm.		Tube diam. 0.535 cm.		Tube diam. 0.354 cm.		Tube diam. 0.294 cm.	
0.639	110	0.676	169	0.790	483	0.840	1,078	1.05	3,440	1.59	8,720
.676	149	.737	246	.818	656	.917	1,538	1.22	4,950	1.74	10,000
.720	204	.759	344	.844	898	.982	2,170	1.32	6,400	1.95	11,860
.742	309	.784	444	.865	1,200	1.02	2,910	1.49	8,000	2.12	13,950
.754	396					1.10	3,950	1.66	9,370	2.23	14,800
.767	497							1.76	10,450	2.40	17,250
										2.54	19,900
Fuel No. 25 composition, percent: 54.0 CO, 46.0 CH_4; Stoichiometric percentage: 15.0 (Data for figure 33)											
Tube diam. 0.891 cm.		Tube diam. 0.776 cm.		Tube diam. 0.480 cm.		Tube diam. 0.294 cm.		Tube diam. 0.249 cm.			
0.701	256	0.689	302	0.896	1,620	1.54	11,100	1.21	6,860		
.728	352	.728	380	.960	2,300	1.87	17,400	1.41	9,800		
.756	495	.766	544	1.02	3,350	2.31	24,500	1.55	12,430		
.781	702	.797	672	1.09	4,350			1.73	14,850		
		.822	902	1.16	5,800			1.87	17,500		
		.858	1,327	1.28	7,730			2.10	20,800		
		.896	1,812					2.49	26,800		
								2.78	30,800		
Fuel No. 26 composition, percent: 66.6 CO, 32.3 CH_4, 1.0 H_2, 0.1 CO_2; Stoichiometric percentage: 17.5 (Data for figure 33)											
Tube diam. 0.891 cm.		Tube diam. 0.776 cm.		Tube diam. 0.699 cm.		Tube diam. 0.475 cm.		Tube diam. 0.294 cm.		Tube diam. 0.249 cm.	
0.698	255	0.692	294	0.708	450	0.836	1,455	1.18	7,360	2.00	21,900
.733	400	.743	498	.748	542	.934	2,700	1.38	10,400	2.19	26,750
.752	594	.761	684	.796	762	1.02	3,910	1.53	13,450	2.39	29,700
.777	996			.823	900	1.11	5,880	1.70	17,100	2.66	34,600
				.844	1,295	1.20	7,800	1.83	19,800	2.88	37,300
				.873	1,895			2.08	22,900	3.02	43,400

1/ Turbulent flow

TABLE 2b. - Critical boundary velocity gradients for blowoff of two-component fuels (Con.); methane-carbon monoxide mixtures (Con.)

Fuel No. 8 composition, percent: 88.9 CO, 9.7 CH_4, 1.3 H_2, 0.1 CO_2
Stoichiometric percentage: 24.5 (Data for figure 33)

F_B	g_B	F_B	g_B	F_B	g_B	F_B	g_B	F_B	g_B	F_B	g_B
Tube diam. 0.776 cm.		Tube diam. 0.699 cm.		Tube diam. 0.611 cm.		Tube diam. 0.475 cm.		Tube diam. 0.249 cm.		Tube diam. 0.155 cm.	
0.660	263	0.694	395	0.833	1,270	0.950	3,260	1.07	6,020	1.94	36,700
.682	340	.761	616	.869	1,765	1.02	4,890	1.16	8,210	2.40	50,100
.741	496	.794	826	.918	2,700	1.09	6,840	1.28	12,050	2.78	61,200
.774	738	.816	1,130	.972	3,830	1.17	8,890	1.51	17,700	2.74	61,800
.790	974	.839	1,495					1.73	25,500		
.816	1,335							1.88	32,200		
								2.10	41,400		

Fuel No. 27 composition, percent: 93.7 CO, 4.5 CH_4, 1.5 H_2, 0.3 CO_2
Stoichiometric percentage: 27.0 (Data for figure 33)

F_B	g_B	F_B	g_B	F_B	g_B
Tube diam. 0.776 cm.		Tube diam. 0.480 cm.		Tube diam. 0.249 cm.	
0.782	588	0.915	1,850	1.29	8,820
.814	790	1.05	3,430	1.44	13,500
.848	1,274	1.13	5,500	1.70	21,900
				1.97	29,500
				2.30	42,400
				2.62	52,100

propane-hydrogen mixtures

Fuel No. 28 composition, percent: 81.6 C_3H_8, 17.4 H_2, 0.1 C_3H_6
Stoichiometric percentage: 4.73 (Data for figure 35)

F_B	g_B	F_B	g_B	F_B	g_B	F_B	g_B	F_B	g_B	F_B	g_B
Tube diam. 1.023 cm.		Tube diam. 0.891 cm.		Tube diam. 0.776 cm.		Tube diam. 0.535 cm.		Tube diam. 0.354 cm.		Tube diam. 0.249 cm.	
0.685	199	0.683	250	0.736	544	0.840	1,408	1.05	4,308	1.99	12,900
.696	300	.751	345	.782	702	.936	2,495	1.26	6,430	2.27	15,150
.714	427	.738	507	.797	999	1.04	3,684	1.44	8,270	2.86	18,880
.742	599			.864	1,600	1.18	5,190	1.63	9,940		
								1.83	11,840		
								2.05	13,880		

Fuel No. 29 composition, percent: 55.4 C_3H_8, 44.6 H_2
Stoichiometric percentage: 6.52 (Data for figure 35)

F_B	g_B	F_B	g_B	F_B	g_B	F_B	g_B	F_B	g_B	F_B	g_B
Tube diam. 0.908 cm.		Tube diam. 0.776 cm.		Tube diam. 0.675 cm.		Tube diam. 0.413 cm.		Tube diam. 0.300 cm.		Tube diam. 0.230 cm.	
0.716	262	0.684	342	0.776	694	0.905	1,670	1.21	6,870	1.60	13,480
.754	347	.718	490	.801	1,262	.994	3,350	1.44	11,850	1.89	20,900
.730	590	.780	994	.890	2,360	1.10	5,300	1.67	16,850	2.09	25,300
.764	788					1.26	8,500	1.87	22,900	2.24	27,450
.791	1,617							2.29	29,700	2.39	34,000
										2.63	40,000
										2.83	47,600

Fuel No. 30 composition, percent: 74.5 H_2, 25.5 C_3H_8
Stoichiometric percentage: 11.3 (Data for figure 35)

F_B	g_B	F_B	g_B	F_B	g_B	F_B	g_B	F_B	g_B
Tube diam. 0.776 cm.		Tube diam. 0.675 cm.		Tube diam. 0.600 cm.		Tube diam. 0.390 cm.		Tube diam. 0.230 cm.	
0.552	214	0.640	325	0.604	427	0.730	1,740	0.956	8,480
.628	425	.676	718	.652	578	.832	4,200	1.06	13,800
.668	887	.720	2,300	.722	1,182	.883	6,870	1.14	21,000
.686	1,315			.698	1,222	.949	9,500	1.21	28,000
.698	1,600			.768	3,000	1.05	18,150	1.35	44,000
						1.39	1/ 81,000	1.79	1/168,000
						1.53	1/120,000	2.06	1/328,000
						1.65	1/161,000	2.31	1/481,000
						1.87	1/242,000	2.57	1/643,000
								2.86	1/810,000

Fuel No. 31 composition, percent: 89.0 H_2, 11.0 C_3H_8
Stoichiometric percentage: 17.4 (Data for figure 35)

F_B	g_B	F_B	g_B	F_B	g_B	F_B	g_B	F_B	g_B	F_B	g_B	F_B	g_B
Tube diam. 0.874 cm.		Tube diam. 0.776 cm.		Tube diam. 0.672 cm.		Tube diam. 0.600 cm.		Tube diam. 0.485 cm.		Tube diam. 0.315 cm.		Tube diam. 0.230 cm.	
0.506	203	0.514	244	0.561	1,030	0.555	470	0.613	2,970	0.705	7,360	0.827	22,100
.526	373	.534	399	.588	1,755	.562	854	.648	4,960	.738	12,000	.910	44,400
		.548	722			.566	1,455	.668	7,500	.777	18,000	1.08	1/154,800
		.556	1,170			.596	2,240			.821	27,400	1.18	1/263,000
		.587	2,520			.625	3,830			.934	1/ 79,800	1.36	1/484,000
										1.03	1/141,200	1.48	1/650,000
										1.12	1/212,000	1.72	1/957,000

1/ Turbulent flow.

TABLE 2b. - Critical boundary velocity gradients for blowoff of two-component fuels (Con.); ethylene-hydrogen mixtures

Fuel No. 32 composition, percent: 78.4 C_2H_4, 21.6 H_2
Stoichiometric percentage: 7.83 (Data for figure 37)

F_B	g_B	F_B	g_B	F_B	g_B	F_B	g_B	F_B	g_B	F_B	g_B	F_B	g_B	F_B	g_B
Tube diam. 0.891 cm.		Tube diam. 0.874 cm.		Tube diam. 0.721 cm.		Tube diam. 0.624 cm.		Tube diam. 0.495 cm.		Tube diam. 0.313 cm.		Tube diam. 0.267 cm.		Tube diam. 0.155 cm.	
0.540	215	0.622	910	0.590	381	0.594	566	0.646	1,200	0.807	4,960	1.07	14,820	1.42	29,600
.576	290	.650	1,256	.625	670	.625	782	.680	1,550	.925	8,000	1.28	24,500	1.57	43,000
.607	492	.676	1,636	.668	1,276	.652	1,077	.748	2,550	1.05	12,130	1.47	33,600	1.94	64,200
				.687	1.972	.686	1,482	.793	3,970	1.18	18,620			2.22	82,000
						.695	1,785	.852	6,140					2.61	103,800
						.742	2,950								

Fuel No. 33 composition, percent: 55.3 C_2H_4, 44.6 H_2, 0.1 C_3H_6
Stoichiometric percentage: 9.98 (Data for figure 37)

F_B	g_B	F_B	g_B	F_B	g_B	F_B	g_B	F_B	g_B	F_B	g_B
Tube diam. 0.874 cm.		Tube diam. 0.721 cm.		Tube diam. 0.624 cm.		Tube diam. 0.495 cm.		Tube diam. 0.267 cm.		Tube diam. 0.155 cm.	
0.506	242	0.498	295	0.515	498	0.705	4,390	0.803	7,880	1.22	34,300
.541	392	.558	602	.553	713	.790	7,300	.916	14,200	1.37	50,800
.545	815	.594	1,206	.576	998	.885	11,060	1.00	21,700	1.53	67,600
.577	1,100	.615	1,775	.600	1,280	1.11	1/32,000	1.12	30,000	1.75	99,000
.602	1,500			.626	1,652			1.25	39,400	1.91	125,000
				.652	2,545			1.79	1/145,200		
				.681	3,700			2.12	1/239,000		
				.734	5,360			2.52	1/333,300		
								3.06	1/473,000		

Fuel No. 34 composition, percent: 66.8 H_2, 33.1 C_2H_4, 0.1 C_3H_6
Stoichiometric percentage: 13.6 (Data for figure 37)

F_B	g_B	F_B	g_B	F_B	g_B	F_B	g_B	F_B	g_B	F_B	g_B
Tube diam. 0.776 cm.		Tube diam. 0.624 cm.		Tube diam. 0.495 cm.		Tube diam. 0.381 cm.		Tube diam. 0.249 cm.		Tube diam. 0.155 cm.	
0.481	244	0.504	441	0.575	1,000	0.620	1,880	0.764	6,880	1.05	29,400
.528	780	.588	1,266	.612	1,462	.700	4,850	.844	11,070	1.12	43,000
.592	1,720	.645	2,810	.632	2,290	.760	8,060	.928	22,500	1.10	46,400
				.672	4,000	.840	15,320	1.02	35,100	1.25	73,400
				.720	6,070			1.51	1/204,000	1.37	105,700
								1.71	1/319,000		
								1.89	1/426,000		
								2.15	1/574,500		
								2.40	1/731,000		

Fuel No. 35 composition, percent: 80.0 H_2, 20.0 C_2H_4
Stoichiometric percentage: 17.3 (Data for figure 37)

F_B	g_B	F_B	g_B	F_B	g_B	F_B	g_B	F_B	g_B
Tube diam. 0.721 cm.		Tube diam. 0.624 cm.		Tube diam. 0.495 cm.		Tube diam. 0.313 cm.		Tube diam. 0.220 cm.	
0.470	288	0.516	544	0.539	845	0.637	4,760	0.757	23,800
.511	784	.548	1,144	.557	1,487	.700	9,160	.806	39,300
.559	2,070	.588	3,400	.563	2,580	.732	15,950	.894	69,600
				.625	6,500	.774	23,470	1.09	1/ 184,000
						.802	28,300	1.27	1/ 356,500
								1.59	1/ 802,000
								1.83	1/1,029,000
								2.11	1/1,583,000

Fuel No. 36 composition, percent: 91.4 H_2, 8.5 C_2H_4, 0.1 C_2H_6
Stoichiometric percentage: 22.6 (Data for figure 37)

F_B	g_B	F_B	g_B	F_B	g_B	F_B	g_B	F_B	g_B	F_B	g_B	F_B	g_B
Tube diam. 0.535 cm.		Tube diam. 0.506 cm.		Tube diam. 0.475 cm.		Tube diam. 0.354 cm.		Tube diam. 0.299 cm.		Tube diam. 0.249 cm.		Tube diam. 0.220 cm.	
0.450	412	0.472	570	0.485	702	0.536	2,450	0.587	10,000	0.674	36,500	0.638	24,000
		.494	1,075	.512	1,370	.546	4,200	.636	20,300	.791	1/ 133,700	.674	44,700
		.500	2,060	.495	2,530	.556	7,080	.665	29,400	.900	1/ 292,000		
		.505	3,340	.514	4,950	.583	14,850	.760	1/ 95,000	.992	1/ 451,000		
		.536	6,370					.792	1/131,500	1.11	1/ 678,000		
								.831	1/173,000	1.24	1/1,007,000		
								.932	1/295,000				

1/ Turbulent flow.

TABLE 2b. - Critical boundary velocity gradients for blowoff of two-component fuels (Con.); nitrogen-hydrogen mixtures

Fuel No. 37 composition, percent: 59.8 N_2, 40.1 H_2, 0.1 A
Stoichiometric percentage: 51.0 (Data for figure 39)

F_B	g_B	F_B	g_B	F_B	g_B	F_B	g_B	F_B	g_B	F_B	g_B	F_B	g_B
Tube diam. 0.776 cm.		Tube diam. 0.624 cm.		Tube diam. 0.506 cm.		Tube diam. 0.495 cm.		Tube diam. 0.315 cm.		Tube diam. 0.220 cm.			
0.624	334	0.578	254	0.653	1,605	0.629	431	0.738	6,100	0.801	25,500		
.650	500	.678	572	.674	3,000	.654	746	.752	11,680	.828	46,000		
.626	830	.712	612	.681	4,970	.656	1,177	.781	20,000	.870	71,300		
.628	1,453	.644	1,045	.704	8,060	.645	2,100	.804	28,450	1.06	1/274,000		
								.897	1/91,700				

Fuel No. 38 composition, percent: 50.1 H_2, 49.6 N_2, 0.3 O_2
Stoichiometric percentage: 45.8 (Data for figure 39)

F_B	g_B	F_B	g_B	F_B	g_B	F_B	g_B	F_B	g_B	F_B	g_B	F_B	g_B
Tube diam. 0.874 cm.		Tube diam. 0.721 cm.		Tube diam. 0.624 cm.		Tube diam. 0.495 cm.		Tube diam. 0.381 cm.		Tube diam. 0.267 cm.		Tube diam. 0.220 cm.	
0.463	178	0.514	299	0.554	507	0.556	1,100	0.582	3,810	0.630	12,370	0.680	29,400
.524	359	.546	437	.542	852	.546	1,694	.584	7,000	.650	22,500	.700	52,600
.522	698	.534	770	.540	1,695	.554	3,110	.610	12,100	.680	37,650	.726	81,200
		.528	1,390	.540	2,680	.560	4,850	.624	19,000	.762	1/125,700	.815	1/204,500
		.534	2,300									.905	1/313,500

Fuel No. 39 composition, percent: 62.4 H_2, 37.3 N_2, 0.1 CH_4, 0.1 CO, 0.1 CO_2
Stoichiometric percentage: 39.9 (Data for figure 39)

F_B	g_B	F_B	g_B	F_B	g_B	F_B	g_B	F_B	g_B	F_B	g_B	F_B	g_B
Tube diam. 0.874 cm.		Tube diam. 0.721 cm.		Tube diam. 0.624 cm.		Tube diam. 0.495 cm.		Tube diam. 0.381 cm.		Tube diam. 0.267 cm.		Tube diam. 0.220 cm.	
0.453	172	0.485	310	0.506	1,627	0.540	982	0.556	6,500	0.622	16,700	0.631	26,900
.524	451	.511	595	.517	2,960	.536	2,390	.562	9,900	.653	35,300	.678	60,800
.522	460	.510	975			.516	3,930	.600	18,030	.776	1/189,600	.839	1/244,000
.496	750	.513	1,964			.546	7,850			.854	1/334,000	.968	1/519,000
.491	1,110	.524	2,510										

other mixtures

Fuel No. 40 composition, percent: 88.5 CH_4, 0.6 C_2H_6, 10.8 N_2, 0.1 CO_2
Stoichiometric percentage: 10.5

F_B	g_B	F_B	g_B	F_B	g_B	F_B	g_B	F_B	g_B	F_B	g_B	
Tube diam. 1.247 cm.		Tube diam. 1.058 cm.		Tube diam. 0.891 cm.		Tube diam. 0.699 cm.		Tube diam. 0.468 cm.		Tube diam. 0.381 cm.		
0.692	133	0.696	111	0.662	128	0.942	1,300	1.06	2,450	1.19	3,310	
.724	178	.699	141	.696	158	1.10	2,545	1.15	3,180	1.26	4,150	
.762	255	.740	220	.708	199	1.15	3,010	1.32	4,530	1.46	5,130	
.784	382	.763	278	.750	314			1.45	5,500	1.56	5,850	
.762	420	.764	338	.804	462					1.64	6,200	
		.790	484	.831	598					1.77	7,120	
		.796	690	.846	727					2.02	8,410	
		.824	822	.888	980					2.12	9,160	
				.985	1,554					2.22	10,740	
				1.04	2,035					2.52	12,450	
				1.14	2,835					2.56	13,350	
				1.13	2,860					2.72	14,030	

Fuel No. 41 composition, percent: 79.4 CH_4, 20.6 C_2H_4
Stoichiometric percentage: 8.66 (Points for figure 27)

F_B	g_B	F_B	g_B	F_B	g_B	F_B	g_B	F_B	g_B	F_B	g_B	
Tube diam. 1.058 cm.		Tube diam. 0.891 cm.		Tube diam. 0.776 cm.		Tube diam. 0.535 cm.		Tube diam. 0.354 cm.		Tube diam. 0.294 cm.		
0.687	204	0.698	232	0.728	377	0.828	1,220	1.09	3,850	1.92	14,750	
.706	249	.720	339	.768	485	.899	2,035	1.17	6,060	2.36	20,050	
.706	300	.720	444	.774	710	.969	3,020	1.32	8,130	2.60	23,100	
.732	393	.737	550	.802	1,020	1.04	4,700	1.45	9,300	3.08	28,400	
.750	514			.846	1,542			1.62	11,200			
								1.83	13,780			
								2.07	16,650			

Fuel No. 42 composition, percent: 78.6 C_2H_4, 21.4 CH_4
Stoichiometric percentage: 6.98

F_B	g_B	F_B	g_B	F_B	g_B	F_B	g_B	F_B	g_B	F_B	g_B	
Tube diam. 0.874 cm.		Tube diam. 0.776 cm.		Tube diam. 0.624 cm.		Tube diam. 0.381 cm.		Tube diam. 0.267 cm.		Tube diam. 0.155 cm.		
0.618	248	0.602	308	0.641	590	0.810	2,457	0.943	6,360	1.38	20,400	
.629	393	.630	500	.658	848	.864	3,970	1.06	8,930	1.73	30,650	
.658	698	.675	776	.684	1,010	.938	5,500	1.25	14,170	1.99	39,850	
.680	966	.694	996	.756	2,000	1.17	11,670	1.42	19,720	2.32	49,400	
		.714	1,483	.805	3,020			1.61	24,600	2.60	58,000	
										2.97	69,200	

1/ Turbulent flow.

TABLE 3a. - Critical boundary velocity gradients for flashback of multicomponent fuels; mixtures of coke-oven-gas type

F_F	g_F	F_F	g_F	F_F	g_F	F_F	g_F	F_F	g_F
Fuel No. 43 composition, percent: 58.4 H_2, 26.3 CH_4, 10.6 CO, 4.6 N_2, 0.1 CO_2; Stoichiometric percentage: 19.4 (Points for figure 41)									
Tube diam. 0.891 cm.		Tube diam. 0.780 cm.		Tube diam. 0.699 cm.		Tube diam. 0.611 cm.			
0.562	260	0.598	384	0.628	500	0.667	664		
1.48	261	1.43	384	1.41	528	1.39	662		
.586	296	.682	588	.710	758	.744	1,020		
1.46	298	1.39	581	1.38	814	1.27	939		
.652	578	.684	895	.772	1,105	.816	1,320		
1.33	556	1.34	856	1.33	1,180	1.24	1,315		
.708	848	.754	1,175	.820	1,483	.956	1,970		
1.30	839	1.32	1,173	1.27	1,595	1.13	2,055		
		.841	1,660	.954	1,890				
		1.27	1,677	1.14	1,977				
		.921	2,035						
		1.23	2,105						
Fuel No. 44 composition, percent: 38.7 H_2, 31.7 CO, 29.4 CH_4, 0.1 N_2, 0.1 CO_2; Stoichiometric percentage: 18.2									
Tube diam. 0.780 cm.		Tube diam. 0.699 cm.		Tube diam. 0.611 cm.					
0.620	279	0.632	326	0.676	439				
1.41	286	1.40	324	1.36	465				
.672	383	.711	516	.756	698				
1.37	382	1.36	517	1.30	667				
.728	546	.765	735	.842	963				
1.31	576	1.29	741	1.27	967				
.791	758	.858	1,034	.920	1,304				
1.29	772	1.25	1,044	1.19	1,380				
.874	1,130	.940	1,396	.994	1,500				
1.25	1,096	1.19	1,420	1.15	1,505				
1.02	1,583								
1.10	1,610								
Fuel No. 45 composition, percent: 29.6 H_2, 26.2 CO, 23.4 CH_4, 20.8 N_2; Stoichiometric percentage: 21.9									
Tube diam. 0.776 cm.		Tube diam. 0.721 cm.		Tube diam. 0.624 cm.					
0.683	310	0.668	248	0.616	208				
1.31	370	1.35	300	1.33	253				
.746	480	.696	362	.721	407				
1.27	556	1.30	428	.822	677				
.790	607	.775	564	1.21	777				
1.25	690	1.24	643	.950	1,060				
.880	842	.907	984	1.13	1,116				
1.18	918	1.16	1,058						
Fuel No. 46 composition, percent: 55.7 H_2, 34.0 CO, 10.3 CH_4; Stoichiometric percentage: 24.2									
Tube diam. 0.891 cm.		Tube diam. 0.699 cm.		Tube diam. 0.611 cm.		Tube diam. 0.535 cm.		Tube diam. 0.475 cm.	
0.552	273	0.600	514	1.53	918	0.804	1,840	0.764	1,500
1.62	258	1.58	528	.736	1,270	1.45	1,720	1.48	1,460
.588	369	.656	664	1.49	1,510	.899	2,510	.830	1,954
1.62	390	1.56	658	.847	2,010	1.40	2,620	1.41	2,000
.634	584	.711	1,075	1.41	2,430	1.06	3,520	.976	3,000
1.58	603	1.53	1,083	.967	2,770	1.32	3,610	1.35	3,160
.644	773			1.21	3,720			1.09	3,780
1.56	828							1.28	3,765
Fuel No. 47 composition, percent: 53.0 H_2, 33.9 CO, 9.8 CH_4, 3.3 N_2; Stoichiometric percentage: 24.9									
Tube diam. 0.891 cm.		Tube diam. 0.699 cm.		Tube diam. 0.611 cm.		Tube diam. 0.535 cm.			
0.534	252	0.614	534	0.696	897	0.750	1,300		
1.64	246	1.58	542	1.54	938	1.48	1,390		
.593	370	.646	687	.777	1,480	.847	1,990		
1.61	360	1.56	688	1.47	1,435	1.42	2,030		
.612	468	.707	1,105	.924	2,360	.968	2,830		
1.59	570	1.53	1,110	1.40	2,410	1.37	2,770		
.662	789	.803	1,695	1.03	3,220	1.06	3,310		
1.56	794	1.46	1,723	1.29	3,360	1.29	3,520		
		.869	2,200			1.11	3,600		
		1.40	2,250			1.22	3,750		
		.988	2,985						
		1.32	3,100						
		1.27	3,290						
Fuel No. 48 composition, percent: 66.2 CO, 17.5 H_2, 16.3 CH_4; Stoichiometric percentage: 21.9									
Tube diam. 1.023 cm.		Tube diam. 0.776 cm.		Tube diam. 0.624 cm.		Tube diam. 0.495 cm.			
0.649	185	0.742	368	0.846	599	0.964	1,030		
1.59	189	1.54	362	1.48	608	1.36	1,158		
.714	298	.811	535	.928	924	1.15	1,438		
1.55	299	1.50	488	1.43	870	1.24	1,474		
.759	432	1.47	679	1.10	1,402				
1.51	424	.867	712	1.32	1,377				
.860	632	.884	760						
1.46	584	1.39	1,058						
.918	886	1.03	1,164						
1.39	1,017	1.10	1,366						
		1.27	1,435						

TABLE 3a. - Critical boundary velocity gradients for flashback of multicomponent fuels (Con.); mixtures of coke-oven-gas type (Con.)

F_F	g_F	F_F	g_F	F_F	g_F
Fuel No. 49 composition, percent: 52.9 CO, 14.1 H_2, 11.9 CH_4, 21.1 CO_2; Stoichiometric percentage: 26.8					
Tube diam. 0.891 cm.		Tube diam. 0.776 cm.		Tube diam. 0.699 cm.	
0.755	261	0.808	332	0.878	451
1.32	258	1.30	312	1.27	450
.867	405	.890	495	.954	577
1.31	402	1.27	485	1.23	577
1.27	558	1.03	694	1.01	646
.999	638	1.18	718	1.19	688
1.19	688				
Fuel No. 50 composition, percent: 43.0 CO, 11.5 H_2, 10.7 CH_4, 34.8 CO_2; Stoichiometric percentage: 30.0					
Tube diam. 1.058 cm.		Tube diam. 0.891 cm.			
0.713	108	0.800	176		
1.27	109	1.22	169		
.750	149	.887	254		
1.28	146	1.18	255		
.837	213	.970	301		
1.22	215	1.09	317		
.960	300				
1.16	289				
Fuel No. 51 composition, percent: 50.7 CH_4, 24.7 CO, 24.5 H_2, 0.1 CO_2; Stoichiometric percentage: 14.2					
Tube diam. 1.023 cm.		Tube diam. 0.874 cm.		Tube diam. 0.776 cm.	
0.694	205	0.706	238	0.722	265
1.33	228	1.31	261	1.35	294
.736	335	.766	390	.788	465
1.28	366	1.27	424	1.22	500
.826	555	.854	638	.880	712
1.23	594	1.19	674	1.16	745
.938	792				
1.13	816				
Fuel No. 52 composition, percent: 47.6 CH_4, 22.6 CO, 22.6 H_2, 7.1 N_2, 0.1 CO_2; Stoichiometric percentage: 15.1					
Tube diam. 1.023 cm.		Tube diam. 0.874 cm.		Tube diam. 0.776 cm.	
0.685	184	0.740	270	0.793	365
1.35	196	1.30	301	1.28	405
.756	310	.791	364	.825	439
1.31	341	1.27	443	1.26	474
.850	506	.920	658	.948	706
1.25	544	1.20	692	1.17	736
1.01	772				
1.12	787				
Fuel No. 53 composition, percent: 46.1 CH_4, 23.1 CO, 22.9 H_2, 7.9 CO_2; Stoichiometric percentage: 15.4					
Tube diam. 1.023 cm.		Tube diam. 0.874 cm.		Tube diam. 0.776 cm.	
0.676	182	0.746	269	0.774	367
1.32	195	1.31	298	1.23	399
.757	318	.779	370	.810	454
1.25	348	1.24	438	1.21	488
.844	510	.909	660	.952	725
1.20	544	1.14	688	1.12	747
Fuel No. 54 composition, percent: 36.1 CH_4, 17.5 CO, 17.5 H_2, 28.9 CO_2; Stoichiometric percentage: 18.9					
Tube diam. 1.023 cm.		Tube diam. 0.874 cm.		Tube diam. 0.776 cm.	
0.718	140	0.748	200	0.814	270
1.26	146	1.20	214	1.17	257
.832	309	.923	370	.915	382
1.15	295	1.13	345	1.05	394
.898	372				
1.10	390				

TABLE 3a. - Critical boundary velocity gradients for flashback of multicomponent fuels (Con.); mixtures of oil-gas type

Fuel No. 55 composition, percent: 37.4 CH_4, 33.4 C_2H_4, 15.2 H_2, 14.0 N_2
Stoichiometric percentage: 10.3 (Points for figure 43)

F_F	g_F	F_F	g_F	F_F	g_F	F_F	g_F
Tube diam. 0.891 cm.		Tube diam. 0.780 cm.		Tube diam. 0.699 cm.			
0.726	300	0.758	347	0.819	536		
1.45	289	1.41	348	1.35	570		
.778	410	.810	475	.870	668		
1.41	441	.894	696	1.33	704		
.842	630	1.33	676	.996	1,002		
1.33	616	.950	884	1.22	1,027		
.876	842	1.25	912				
1.29	822	1.02	1,036				
1.04	1,030	1.22	1,060				
1.17	1,045						

Fuel No. 56 composition, percent: 29.1 CH_4, 26.2 C_2H_4, 22.1 C_3H_8, 11.8 H_2, 0.2 C_3H_6, 10.6 N_2
Stoichiometric percentage: 7.6

F_F	g_F	F_F	g_F	F_F	g_F	F_F	g_F
Tube diam. 0.891 cm.		Tube diam. 0.780 cm.		Tube diam. 0.699 cm.			
0.731	196	0.778	342	0.800	354		
1.43	208	1.36	359	1.38	370		
.769	287	.830	436	.847	465		
1.38	301	1.32	454	1.30	482		
.810	400	.878	527	.890	572		
1.35	417	1.30	546	1.26	590		
.840	483	.912	612	.956	700		
1.30	501	1.25	629	1.20	714		
.942	654	.966	727	1.05	852		
1.25	672	1.21	742	1.07	854		
.982	756	1.00	814				
1.20	770	1.17	826				

Fuel No. 57 composition, percent: 32.1 CH_4, 28.4 C_2H_4, 12.5 H_2, 27.0 N_2
Stoichiometric percentage: 11.8

F_F	g_F	F_F	g_F	F_F	g_F	F_F	g_F
Tube diam. 0.891 cm.		Tube diam. 0.721 cm.		Tube diam. 0.624 cm.			
0.680	200	0.698	254	0.716	322		
1.40	221	1.39	278	1.35	350		
.706	286	.734	363	.802	506		
1.34	312	1.30	392	1.26	538		
.742	379	.770	451	.881	707		
1.29	415	1.28	484	1.20	738		
.835	562	.866	644	.958	880		
1.26	596	1.23	677	1.13	900		
.906	774	1.00	930				
1.20	805	1.13	947				
.972	856						
1.16	878						

other mixtures

Fuel No. 58 composition, percent: 62.5 CH_4, 22.2 H_2, 15.3 N_2
Stoichiometric percentage: 13.3 (Points for figure 46)

F_F	g_F	F_F	g_F	F_F	g_F	F_F	g_F
Tube diam. 0.891 cm.		Tube diam. 0.699 cm.					
0.721	201	0.754	228				
1.25	218	1.26	245				
.766	285	.793	331				
1.21	307	1.23	354				
.818	389	.857	431				
1.15	408	1.14	451				
.870	485	.933	550				
		1.07	562				
		.954	582				
		1.04	589				

Fuel No. 59 composition, percent: 47.4 CO, 25.9 H_2, 26.5 N_2, 0.2 CO_2
Stoichiometric percentage: 36.3

F_F	g_F	F_F	g_F	F_F	g_F	F_F	g_F
Tube diam. 0.721 cm.		Tube diam. 0.624 cm.		Tube diam. 0.495 cm.		Tube diam. 0.381 cm.	
0.610	204	0.749	558	1.77	572	1.61	1,590
1.81	197	1.79	594	1.75	754	1.05	1,840
1.81	280	.790	709	.932	1,342	1.51	1,981
.681	367	.832	882	1.63	1,357	1.15	2,235
1.80	530	1.70	974	1.49	2,180	1.17	2,327
.771	654	.995	1,588	1.23	2,420	1.41	2,472
		1.58	1,780				
		1.13	2,150				

TABLE 3a. - Critical boundary velocity gradients for flashback of multicomponent fuels (Con.); other mixtures (Con.)

Fuel No. 60 composition, percent: 40.8 CO, 22.1 H_2, 36.9 N_2, 0.2 CO_2
Stoichiometric percentage: 39.9

Tube diam. 0.874 cm.		Tube diam. 0.721 cm.		Tube diam. 0.624 cm.			
F_F	g_F	F_F	g_F	F_F	g_F	F_F	g_F
0.652	248	0.700	351	0.671	300		
1.75	243	1.71	360	1.70	312		
1.67	429	.822	752	.850	848		
.754	505	1.62	702	1.59	848		
1.59	864	1.54	1,063	1.51	1,288		
.893	992	.945	1,197	1.02	1,426		
1.08	1,563	1.08	1,597	1.11	1,700		
1.44	1,616	1.30	1,890	1.42	1,730		

Fuel No. 61 composition, percent: 49.4 CH_4, 22.2 H_2, 16.1 CO, 11.5 CO_2, 0.8 N_2
Stoichiometric percentage: 15.0

Tube diam. 1.023 cm.		Tube diam. 0.874 cm.		Tube diam. 0.776 cm.			
F_F	g_F	F_F	g_F	F_F	g_F	F_F	g_F
0.707	199	1.27	235	1.25	295		
1.29	194	.789	310	.798	372		
.751	249	.841	435	.851	480		
.782	351	1.18	461	1.15	506		
1.22	344	.978	633	1.02	644		
.942	604	1.08	644	1.08	650		
1.15	597						

Fuel No. 62 composition, percent: 65.2 C_2H_4, 18.7 H_2, 16.1 CH_4
Stoichiometric percentage: 8.1

Tube diam. 1.023 cm.		Tube diam. 0.874 cm.		Tube diam. 0.721 cm.		Tube diam. 0.495 cm.	
F_F	g_F	F_F	g_F	F_F	g_F	F_F	g_F
1.51	202	0.597	199	0.679	376	0.834	826
.678	438	1.58	198	1.45	403	1.29	860
.755	743	.674	298	.854	905	.982	1,212
1.34	782	1.48	319	1.30	941	1.19	1,234
		.746	596	.946	1,316		
		1.39	604	1.15	1,340		
		.876	1,020				
		1.27	1,056				

Fuel No. 63 composition, percent: 56.5 C_2H_4, 15.8 H_2, 13.8 CH_4, 0.1 C_3H_6, 13.8 N_2
Stoichiometric percentage: 9.24 (Points for figure 45)

Tube diam. 0.891 cm.		Tube diam. 0.776 cm.		Tube diam. 0.699 cm.			
F_F	g_F	F_F	g_F	F_F	g_F	F_F	g_F
0.640	257	0.704	353	0.754	540		
1.53	260	1.44	348	1.39	552		
.711	405	.738	500	.858	798		
1.46	406	1.42	495	1.33	816		
.773	612	.780	695	.927	1,105		
1.40	612	1.37	700	1.25	1,125		
.876	899	.878	994	1.01	1,240		
1.32	918	1.29	1,000	1.23	1,270		
1.02	1,220	1.00	1,266				
1.20	1,215	1.17	1,290				

Fuel No. 64 composition, percent: 55.1 C_2H_4, 18.8 CH_4, 15.8 H_2, 10.2 CO, 0.1 C_3H_6
Stoichiometric percentage: 8.81

Tube diam. 1.023 cm.		Tube diam. 0.874 cm.		Tube diam. 0.721 cm.		Tube diam. 0.495 cm.	
F_F	g_F	F_F	g_F	F_F	g_F	F_F	g_F
1.63	160	0.636	196	0.689	275	0.833	840
.715	425	1.61	216	1.60	301	1.32	888
1.50	458	.724	394	.795	592	.962	1,170
.735	538	1.48	398	1.46	632	1.27	1,200
1.48	579	.800	788	.887	1,040		
.788	726	1.37	833	1.30	1,080		
1.39	770	.950	1,240	1.02	1,345		
		1.25	1,280	1.18	1,367		

Fuel No. 65 composition, percent: 36.4 H_2, 22.6 CO, 13.3 CH_4, 7.2 C_2H_6, 5.8 C_2H_4, 1.9 C_3H_8, 0.1 C_3H_6, 9.8 N_2, 2.9 CO_2
Stoichiometric percentage: 16.1 (Points for figure 42)

Tube diam. 1.023 cm.		Tube diam. 0.874 cm.		Tube diam. 0.776 cm.			
F_F	g_F	F_F	g_F	F_F	g_F	F_F	g_F
0.633	199	0.681	266	0.756	447		
1.41	205	1.42	249	1.31	498		
.728	380	.796	620	.824	706		
1.36	377	1.32	600	1.28	714		
.887	812	.988	1,033	.909	920		
1.25	806	1.15	1,067	1.23	898		

TABLE 3a. - Critical boundary velocity gradients for flashback of multicomponent fuels (Con.); other mixtures (Con.)

F_F	g_F	F_F	g_F	F_F	g_F
Fuel No. 66 composition, percent: 42.6 CH_4, 18.1 C_2H_4, 17.0 H_2, 9.1 CO, 2.2 C_2H_6, 1.9 C_3H_8, 0.2 C_3H_6, 0.2 C_4H_{10}, 0.1 C_4H_8, 5.2 CO_2, 3.4 N_2; Stoichiometric percentage: 10.8					
Tube diam. 1.023 cm.		Tube diam. 0.908 cm.		Tube diam. 0.776 cm.	
0.766	261	0.790	348	1.32	399
1.40	241	1.34	345	.87	520
.842	445	.850	490	.898	584
1.33	422	1.28	519	1.23	608
1.02	750	.958	670	.960	730
1.06	786	1.23	692	1.20	752
Fuel No. 67 composition, percent: 37.5 CH_4, 20.4 C_2H_4, 17.5 H_2, 3.9 CO, 13.3 N_2, 7.4 CO_2; Stoichiometric percentage: 12.5 (Points for figure 44)					
Tube diam. 0.908 cm.		Tube diam. 0.776 cm.		Tube diam. 0.675 cm.	
1.36	170	0.690	248	0.729	329
.690	203	1.34	268	1.29	357
.724	318	.782	415	1.24	449
1.29	351	1.26	412	.864	643
.776	504	.804	540	1.19	608
1.22	538	1.22	574	.906	765
.904	787	.912	797	1.12	790
1.13	812	1.12	822		

TABLE 3b. - Critical boundary velocity gradients for blowoff of multicomponent fuels; mixtures of coke-oven-gas type

F_B	g_B	F_B	g_B	F_B	g_B	F_B	g_B	F_B	g_B	F_B	g_B
Fuel No. 43 composition, percent: 58.4 H_2, 26.3 CH_4, 10.6 CO, 4.6 N_2, 0.1 CO_2; Stoichiometric percentage: 19.4 (Points for figure 41)											
Tube diam. 0.891 cm.		Tube diam. 0.780 cm.		Tube diam. 0.699 cm.		Tube diam. 0.468 cm.		Tube diam. 0.294 cm.		Tube diam. 0.155 cm.	
0.541	259	0.564	381	0.568	494	0.632	1,685	0.753	6,030	1.01	35,900
.556	295	.602	578	.612	742	.700	3,030	.819	9,920	1.14	60,400
.565	568	.610	880	.620	1,070	.708	4,440	.853	15,900	1.20	92,000
.598	863			.638	1,533	.740	7,010	.914	26,000	1.27	122,500
				.652	2,170			1.16	1/ 98,200	1.63	1/ 433,000
								1.30	1/174,000	1.65	1/ 451,500
								1.41	1/261,000	1.70	1/ 554,000
										1.86	1/ 936,000
										2.05	1/1,018,000
										2.42	1/1,564,000
Fuel No. 44 composition, percent: 38.7 H_2, 31.7 CO, 29.4 CH_4, 0.1 N_2, 0.1 CO_2; Stoichiometric percentage: 18.2											
Tube diam. 0.780 cm.		Tube diam. 0.699 cm.		Tube diam. 0.611 cm.		Tube diam. 0.468 cm.		Tube diam. 0.294 cm.		Tube diam. 0.155 cm.	
0.568	276	0.688	1,037	0.598	451	0.710	1,784	0.846	5,940	1.17	24,250
.610	378	.700	1,404	.654	683	.781	2,930	.950	10,000	1.28	39,500
.642	536	.721	2,080	.680	968	.802	4,380	.989	13,700	1.35	54,300
.666	782			.704	1,384	.856	6,900	1.05	20,200	1.50	75,000
.704	1,090							1.11	27,800	1.65	110,500
.721	1,575									1.76	140,400
										2.30	1/411,000
										2.40	1/483,000
										2.72	1/642,000
Fuel No. 45 composition, percent: 29.6 H_2, 26.2 CO, 23.4 CH_4, 20.8 N_2; Stoichiometric percentage: 21.9											
Tube diam. 0.776 cm.		Tube diam. 0.721 cm.		Tube diam. 0.624 cm.		Tube diam. 0.381 cm.		Tube diam. 0.267 cm.		Tube diam. 0.155 cm.	
0.615	305	0.642	246	0.578	206	0.812	2,610	0.972	7,500	1.37	36,730
.661	470	.629	356	.650	400	.860	4,160	1.08	14,050	1.44	45,500
.677	590	.666	548	.682	672	.906	6,120	1.17	22,100	1.49	52,000
.694	802	.703	932	.713	995	.957	9,150	1.25	30,360	1.62	71,400
.707	1,068	.756	1,682	.738	1,456			1.69	1/119,300	1.79	109,200
				.776	2,150			1.90	1/190,000		
				.802	3,420						

1/ Turbulent flow.

TABLE 3b. - Critical boundary velocity gradients for blowoff of multicomponent fuels (Con.); mixtures of coke-oven-gas type (Con.)

F_B	g_B	F_B	g_B	F_B	g_B	F_B	g_B	F_B	g_B	F_B	g_B	F_B	g_B	F_B	g_B
Fuel No. 46 composition, percent: 55.7 H_2, 34.0 CO, 10.3 CH_4; Stoichiometric percentage: 24.2															
Tube diam. 0.891 cm.		Tube diam. 0.699 cm.		Tube diam. 0.611 cm.		Tube diam. 0.535 cm.		Tube diam. 0.475 cm.		Tube diam. 0.354 cm.		Tube diam. 0.249 cm.		Tube diam. 0.155 cm.	
0.529	271	0.542	505	0.576	859	0.613	1,800	0.638	3,080	0.710	6,100	0.791	13,550	0.958	40,900
.539	381	.564	682	.606	1,980	.620	2,570	.661	4,760	.729	10,080	.843	21,600	1.03	59,900
.554	598	.573	1,124	.630	2,880	.636	3,640	.691	6,620	.775	16,630	.866	27,500	1.10	88,500
.561	806			.640	3,800							.930	46,300	1.15	126,000
												1.05	1/118,000	1.44	1/ 413,000
												1.20	1/211,000	1.52	1/ 568,000
														1.70	1/ 768,000
														2.06	1/1,383,000
Fuel No. 47 composition, percent: 53.0 H_2, 33.9 CO, 9.8 CH_4, 3.3 N_2; Stoichiometric percentage: 24.9															
Tube diam. 0.891 cm.		Tube diam. 0.699 cm.		Tube diam. 0.611 cm.		Tube diam. 0.535 cm.		Tube diam. 0.402 cm.		Tube diam. 0.249 cm.		Tube diam. 0.155 cm.			
0.510	251	0.548	564	0.584	868	0.606	1,306	0.672	3,640	0.783	12,500	0.980	40,400		
.554	366	.572	694	.616	1,445	.634	2,065	.710	6,200	.851	19,900	1.08	69,200		
.551	491	.594	1,126	.626	2,410	.644	2,860	.719	9,080	.902	32,300	1.15	103,000		
.566	806	.604	1,730	.650	3,335	.656	4,440	.763	14,150	.940	45,500	1.35	1/ 322,000		
										1.10	1/136,000	1.49	1/ 441,000		
										1.16	1/183,500	1.60	1/ 561,000		
										1.23	1/244,000	1.66	1/ 687,000		
												1.76	1/ 838,000		
												1.87	1/1,046,000		
												2.14	1/1,360,000		
Fuel No. 48 composition, percent: 66.2 CO, 17.5 H_2, 16.3 CH_4; Stoichiometric percentage: 21.9															
Tube diam. 1.023 cm.		Tube diam. 0.776 cm.		Tube diam. 0.624 cm.		Tube diam. 0.495 cm.		Tube diam. 0.313 cm.		Tube diam. 0.267 cm.		Tube diam. 0.155 cm.			
0.605	183	0.655	360	0.686	574	0.786	1,525	0.920	3,800	1.10	10,030	1.53	37,500		
.632	292	.674	516	.722	874	.840	2,550	.958	5,180	1.18	15,000	1.70	52,600		
.653	420	.694	689	.770	1,385	.896	3,930	1.06	8,150	1.36	27,120	1.87	72,800		
.680	603	.698	722	.812	2,200	.946	5,970	1.10	12,450	1.56	41,200	1.98	96,000		
		.742	1,192	.848	3,355			1.24	18,320	1.60	42,500	2.16	108,000		
		.757	1,520							2.06	1/125,600	2.19	114,300		
										2.27	1/157,200	2.24	118,400		
												2.30	123,600		
												3.15	1/357,000		
												3.49	1/422,500		
												3.81	1/510,000		
Fuel No. 49 composition, percent: 52.9 CO, 14.1 H_2, 11.9 CH_4; 21.1 CO_2; Stoichiometric percentage: 26.8															
Tube diam. 0.891 cm.		Tube diam. 0.776 cm.		Tube diam. 0.699 cm.		Tube diam. 0.475 cm.		Tube diam. 0.354 cm.		Tube diam. 0.249 cm.		Tube diam. 0.155 cm.			
0.680	254	0.685	319	0.743	574	0.888	2,100	1.01	3,890	1.26	9,260	1.85	38,300		
.726	411	.743	514	.822	1,002	.975	3,200	1.19	7,120	1.34	12,700	2.02	51,600		
.752	624	.752	688	.860	1,705	1.04	5,000	1.27	11,120	1.53	20,700	2.27	78,800		
.766	730			.905	2,400					1.68	31,900	2.55	110,500		
										1.80	40,900				
Fuel No. 50 composition, percent: 43.0 CO, 11.5 H_2, 10.7 CH_4, 34.8 CO_2; Stoichiometric percentage: 30.0															
Tube diam. 1.058 cm.		Tube diam. 0.891 cm.		Tube diam. 0.611 cm.		Tube diam. 0.475 cm.		Tube diam. 0.294 cm.		Tube diam. 0.249 cm.		Tube diam. 0.155 cm.			
0.670	107	0.716	173	0.864	612	0.970	1,250	1.42	7,250	1.77	19,350	2.26	37,400		
.710	146	.774	261	.900	892	1.04	2,010	1.51	9,740	2.03	30,300	2.44	49,800		
.746	216	.798	333	1.00	1,410	1.13	2,730	1.61	13,550	2.26	41,500	2.60	63,400		
.788	295	.854	512			1.19	3,980	1.79	23,900						
.826	419	.874	687			1.26	6,000								
						1.35	8,770								
Fuel No. 51 composition, percent: 50.7 CH_4, 24.7 CO, 24.5 H_2, 0.1 CO_2; Stoichiometric percentage: 14.2															
Tube diam. 1.023 cm.		Tube diam. 0.874 cm.		Tube diam. 0.776 cm.		Tube diam. 0.495 cm.		Tube diam. 0.313 cm.		Tube diam. 0.249 cm.		Tube diam. 0.220 cm.			
0.650	202	0.665	236	0.666	263	0.775	1,080	0.971	4,680	1.37	19,250	1.20	15,500		
.666	331	.666	384	.684	458	.847	2,200	1.10	8,500	1.65	39,100	1.44	30,370		
.694	544	.702	622	.720	694	.882	3,290	1.20	12,870	2.47	1/133,400	1.63	47,600		
.717	764			.780	1,478	.939	4,960	1.49	25,800	2.81	1/179,300	1.80	67,800		
						.972	6,230					2.84	1/200,800		

1/ Turbulent flow.

TABLE 3b. - Critical boundary velocity gradients for blowoff of multicomponent fuels (Con.); mixtures of coke-oven-gas type (Con.)

Fuel No. 52 composition, percent: 47.6 CH_4, 22.6 CO, 22.6 H_2, 7.1 N_2, 0.1 CO_2
Stoichiometric percentage: 15.1

F_B	g_B	F_B	g_B	F_B	g_B	F_B	g_B	F_B	g_B	F_B	g_B	F_B	g_B
Tube diam. 1.023 cm.		Tube diam. 0.874 cm.		Tube diam. 0.776 cm.		Tube diam. 0.495 cm.		Tube diam. 0.313 cm.		Tube diam. 0.249 cm.		Tube diam. 0.220 cm.	
0.642	197	0.684	292	0.706	410	0.814	1,367	0.987	4,460	1.40	19,000	1.22	13,300
.685	311	.711	405	.708	444	.859	2,205	1.12	8,300	1.71	37,800	1.52	29,700
.724	502	.735	638	.740	696	.912	3,260	1.24	13,000	1.80	44,200	1.73	47,400
.738	736			.799	1,462	.980	4,960	1.51	25,000	2.51	1/136,400	1.96	68,400
						1.02	6,300			3.13	1/209,400		

Fuel No. 53 composition, percent: 46.1 CH_4, 23.1 CO, 22.9 H_2, 7.9 CO_2
Stoichiometric percentage: 15.4

F_B	g_B	F_B	g_B	F_B	g_B	F_B	g_B	F_B	g_B	F_B	g_B	F_B	g_B
Tube diam. 1.023 cm.		Tube diam. 0.874 cm.		Tube diam. 0.776 cm.		Tube diam. 0.495 cm.		Tube diam. 0.313 cm.		Tube diam. 0.249 cm.		Tube diam. 0.220 cm.	
0.641	192	0.682	294	0.687	413	0.790	1,383	0.974	4,500	1.39	19,500	1.16	13,400
.676	314	.698	397	.692	445	.850	2,220	1.11	8,220	1.67	37,800	1.48	30,200
.704	498	.735	643	.731	698	.896	3,080	1.24	12,750	1.77	43,700	1.70	48,200
.720	729			.796	1,475	.908	3,270	1.50	24,500	2.28	1/130,300	1.90	70,600
						.977	4,950			2.76	1/165,000		
						1.02	6,310						

Fuel No. 54 composition, percent: 36.1 CH_4, 17.5 CO, 17.5 H_2, 28.9 CO_2
Stoichiometric percentage: 18.9

F_B	g_B	F_B	g_B	F_B	g_B	F_B	g_B	F_B	g_B	F_B	g_B
Tube diam. 1.023 cm.		Tube diam. 0.874 cm.		Tube diam. 0.776 cm.		Tube diam. 0.495 cm.		Tube diam. 0.294 cm.		Tube diam. 0.220 cm.	
0.662	140	0.700	213	0.718	306	0.876	1,205	1.18	5,360	1.59	18,550
.725	302	.755	357	.764	403	.982	2,470	1.36	9,700	1.84	31,500
.782	562	.802	493	.824	792	1.10	4,520	1.55	15,250	2.10	50,900
				.902	1,600	1.17	6,310	1.68	21,000	2.27	73,600
										3.02	1/162,500

1/ Turbulent flow.

mixtures of oil-gas type

Fuel No. 55 composition, percent: 37.4 CH_4, 33.4 C_2H_4, 15.2 H_2, 14.0 N_2
Stoichiometric percentage: 10.3 (Points for figure 43)

F_B	g_B	F_B	g_B	F_B	g_B	F_B	g_B	F_B	g_B	F_B	g_B
Tube diam. 0.891 cm.		Tube diam. 0.780 cm.		Tube diam. 0.699 cm.		Tube diam. 0.468 cm.		Tube diam. 0.294 cm.		Tube diam. 0.155 cm.	
0.656	298	0.636	342	0.678	528	0.774	1,693	0.982	5,980	1.59	25,600
.678	405	.716	682	.750	974	.866	2,640	1.08	8,000	1.77	33,650
.700	620	.746	1,070	.814	2,050	.898	3,628	1.31	14,850	1.97	42,600
.726	828					.948	5,000	1.47	22,000	2.27	54,800
.754	1,450					1.06	6,760	1.70	29,300	2.60	69,800
						1.10	10,140			2.84	80,400
										3.01	91,100

Fuel No. 56 composition, percent: 29.1 CH_4, 26.2 C_2H_4, 22.1 C_3H_8, 11.8 H_2, 0.2 C_3H_6, 10.6 N_2
Stoichiometric percentage: 7.6

F_B	g_B	F_B	g_B	F_B	g_B	F_B	g_B	F_B	g_B	F_B	g_B
Tube diam. 0.891 cm.		Tube diam. 0.780 cm.		Tube diam. 0.468 cm.		Tube diam. 0.294 cm.		Tube diam. 0.155 cm.			
0.650	195	0.657	339	0.764	1,303	1.08	6,000	1.54	15,100		
.666	283	.693	431	.830	2,000	1.14	7,460	1.76	20,150		
..690	395	.722	520	.907	2,910	1.26	10,000	1.93	24,100		
.716	478	.727	602	.990	4,460	1.43	12,550	1.96	24,200		
.718	642	.742	714	1.09	6,080	1.62	16,240	2.21	30,000		
.735	741	.754	798	1.19	8,450	1.86	21,650	2.42	34,800		
		.807	1,398			2.27	28,600	2.63	40,000		
								2.91	46,200		
								3.04	50,800		

Fuel No. 57 composition, percent: 32.1 CH_4, 28.4 C_2H_4, 12.5 H_2, 27.0 N_2
Stoichiometric percentage: 11.8

F_B	g_B	F_B	g_B	F_B	g_B	F_B	g_B	F_B	g_B	F_B	g_B
Tube diam. 0.891 cm.		Tube diam. 0.721 cm.		Tube diam. 0.624 cm.		Tube diam. 0.381 cm.		Tube diam. 0.267 cm.		Tube diam. 0.155 cm.	
0.618	199	0.631	251	0.650	319	0.877	3,150	1.28	14,600	1.94	33,450
.636	283	.641	359	.669	498	.938	4,970	1.64	24,100	2.27	43,400
.656	375	.666	445	.693	690	1.07	7,930	1.82	31,100	2.37	48,100
.683	552	.705	630	.706	850	1.22	12,620	1.98	36,400	2.63	59,600
.706	754	.719	932	.757	1,360	1.38	17,830	2.14	39,200	3.03	75,100
.720	828			.822	2,440	1.45	19,200			3.18	87,400
.731	1,050			.900	4,040						

TABLE 3b. - Critical boundary velocity gradients for blowoff of multicomponent fuels (Con.); other mixtures

F_B	g_B	F_B	g_B	F_B	g_B	F_B	g_B	F_B	g_B	F_B	g_B	F_B	g_B
Fuel No. 58 composition, percent: 62.5 CH_4, 22.2 H_2, 15.3 N_2; Stoichiometric percentage: 13.3 (Points for figure 46)													
Tube diam. 0.891 cm.		Tube diam. 0.699 cm.		Tube diam. 0.468 cm.		Tube diam. 0.294 cm.		Tube diam. 0.155 cm.					
0.650	199	0.706	327	0.882	2,340	1.15	7,900	1.80	27,800				
.700	282	.730	423	.962	3,470	1.33	12,500	1.83	28,000				
.724	382	.746	535	1.02	4,515	1.50	17,900	1.86	28,450				
.739	475	.796	802	1.08	6,090	1.50	18,300	2.00	37,100				
		.842	1,300	1.16	8,760	1.76	31,100	2.10	42,900				
		.873	1,965	1.22	9,800	1.79	32,000	2.17	49,600				
		.932	2,960					2.47	74,400				
								2.64	88,200				
								2.74	98,800				
Fuel No. 59 composition, percent: 47.4 CO, 25.9 H_2, 26.5 N_2, 0.2 CO_2; Stoichiometric percentage: 36.3													
Tube diam. 0.721 cm.		Tube diam. 0.624 cm.		Tube diam. 0.495 cm.		Tube diam. 0.381 cm.		Tube diam. 0.267 cm.		Tube diam. 0.155 cm.			
0.572	200	0.648	532	0.695	1,186	0.735	1,895	0.932	10,940	1.10	19,430		
.619	355	.662	666	.740	2,102	.764	2,300	1.02	20,900	1.17	30,700		
.656	618	.669	813	.754	2,460	.768	2,800	1.12	35,250	1.31	59,800		
		.702	1,583	.765	3,253	.813	4,330			1.47	104,000		
				.793	4,870	.872	7,970			1.93	1/414,000		
						.922	13,580						
Fuel No. 60 composition, percent: 40.8 CO, 22.1 H_2, 36.9 N_2, 0.2 CO_2; Stoichiometric percentage: 39.9													
Tube diam. 0.874 cm.		Tube diam. 0.721 cm.		Tube diam. 0.624 cm.		Tube diam. 0.495 cm.		Tube diam. 0.381 cm.		Tube diam. 0.249 cm.		Tube diam. 0.155 cm.	
0.614	243	0.639	339	0.621	292	0.787	2,810	0.896	7,100	1.03	15,080	1.29	40,900
.656	478	.680	706	.683	776	.810	3,763	.957	11,940	1.11	21,880	1.37	56,400
.682	974	.709	1,209	.717	1,414	.859	5,980	1.02	16,930	1.15	29,870	1.41	57,400
.704	1,476	.741	1,970	.732	1,780	.914	9,140			1.21	40,250	1.46	76,000
				.746	2,170					1.47	1/136,300	1.48	76,800
				.811	4,590					1.47	1/140,000	1.53	96,400
												1.54	98,200
												1.62	122,000
												1.62	125,800
												2.07	1/428,300
Fuel No. 61 composition, percent: 49.4 CH_4, 22.2 H_2, 16.1 CO, 11.5 CO_2, 0.8 N_2; Stoichiometric percentage: 15.0													
Tube diam. 1.023 cm.		Tube diam. 0.874 cm.		Tube diam. 0.776 cm.		Tube diam. 0.495 cm.		Tube diam. 0.294 cm.		Tube diam. 0.220 cm.			
0.654	197	0.678	307	0.708	420	0.826	1,380	1.05	5,110	1.33	17,940		
.674	246	.728	426	.714	419	.890	2,290	1.21	8,950	1.58	32,600		
.693	346	.759	760	.775	906	.968	3,780	1.35	14,030	1.75	47,500		
.740	584			.838	1,620	1.08	7,100	1.53	22,400	1.98	69,700		
								2.24	1/ 89,400	2.97	1/203,000		
								2.49	1/117,700				
								2.76	1/151,000				

1/ Turbulent flow.

TABLE 3b. - Critical boundary velocity gradients for blowoff of multicomponent fuels (Con.); other mixtures (Con.)

Fuel No. 62 composition, percent: 65.2 C_2H_4, 18.7 H_2, 16.1 CH_4
Stoichiometric percentage: 8.1

F_B	g_B	F_B	g_B	F_B	g_B	F_B	g_B	F_B	g_B	F_B	g_B	F_B	g_B
Tube diam. 1.023 cm.		Tube diam. 0.874 cm.		Tube diam. 0.721 cm.		Tube diam. 0.495 cm.		Tube diam. 0.381 cm.		Tube diam. 0.249 cm.		Tube diam. 0.155 cm.	
0.604	492	0.560	198	0.594	373	0.726	1,617	0.874	5,040	1.06	10,850	1.55	29,480
.615	734	.604	296	.680	892	.764	2,520	.968	8,760	1.31	20,000	1.69	37,000
		.638	591	.674	1,286	.793	3,835	1.09	14,020	1.47	29,900	1.83	47,700
		.646	1,003	.714	2,032	.887	6,400			1.74	40,700	2.22	61,650
												2.45	76,550
												2.78	92,900
												2.89	103,200

Fuel No. 63 composition, percent: 56.5 C_2H_4, 15.8 H_2, 13.8 CH_4, 0.1 C_3H_6, 13.8 N_2
Stoichiometric percentage: 9.24 (Points for figure 45)

F_B	g_B	F_B	g_B	F_B	g_B	F_B	g_B	F_B	g_B	F_B	g_B	F_B	g_B
Tube diam. 0.891 cm.		Tube diam. 0.776 cm.		Tube diam. 0.699 cm.		Tube diam. 0.475 cm.		Tube diam. 0.294 cm.		Tube diam. 0.249 cm.		Tube diam. 0.155 cm.	
0.577	255	0.614	350	0.686	1,080	0.759	2,030	0.911	5,540	1.58	30,300	2.19	51,400
.617	402	.631	495	.732	1,610	.815	3,270	1.08	10,120	1.90	40,700	2.26	59,600
.643	606	.643	700	.770	2,340	.857	4,580	1.22	15,800			2.75	73,800
.676	909	.676	1,005			.926	7,180	1.46	25,000				
.702	1,240	.704	1,310					1.79	33,100				

Fuel No. 64 composition, percent: 55.1 C_2H_4, 18.8 CH_4, 15.8 H_2, 10.2 CO, 0.1 C_3H_6
Stoichiometric percentage: 8.81

F_B	g_B	F_B	g_B	F_B	g_B	F_B	g_B	F_B	g_B	F_B	g_B	F_B	g_B
Tube diam. 1.023 cm.		Tube diam. 0.874 cm.		Tube diam. 0.721 cm.		Tube diam. 0.495 cm.		Tube diam. 0.313 cm.		Tube diam. 0.249 cm.		Tube diam. 0.155 cm.	
0.618	422	0.581	195	0.632	273	0.732	1,730	0.887	4,960	1.22	16,200	1.64	35,200
.631	534	.628	391	.668	585	.777	2,970	.994	8,030	1.41	24,700	1.94	46,330
.644	716	.645	780	.688	970	.828	3,880	1.09	11,100	1.58	32,000	2.05	53,850
		.677	1,210	.691	1,360	.923	6,800	1.17	15,170	1.78	40,500	2.26	64,800
				.728	2,000			1.32	19,890			2.53	78,800
												2.85	94,800

Fuel No. 65 composition, percent: 36.4 H_2, 22.6 CO, 13.3 CH_4, 7.2 C_2H_6, 5.8 C_2H_4, 1.9 C_3H_8, 0.1 C_3H_6, 9.8 N_2, 2.9 CO_2
Stoichiometric percentage: 16.1 (Points for figure 42)

F_B	g_B	F_B	g_B	F_B	g_B	F_B	g_B	F_B	g_B	F_B	g_B	F_B	g_B
Tube diam. 1.023 cm.		Tube diam. 0.874 cm.		Tube diam. 0.776 cm.		Tube diam. 0.495 cm.		Tube diam. 0.313 cm.		Tube diam. 0.220 cm.			
0.591	198	0.622	292	0.646	438	0.744	1,495	0.919	5,640	1.02	14,000		
.636	374	.674	606	.672	686	.797	2,600	1.05	10,200	1.19	23,800		
.675	786	.719	1,182	.698	884	.845	3,970	1.17	17,100	1.35	44,700		
				.756	1,815	.936	7,220	1.30	27,400	1.51	70,500		
								1.72	1/ 91,000	2.22	1/215,000		
								1.79	1/103,000	2.75	1/326,700		
								1.90	1/129,500				

other mixtures (Con.)

Fuel No. 66 composition, percent: 42.6 CH_4, 18.1 C_2H_4, 17.0 H_2, 9.1 CO, 2.2 C_2H_6, 1.9 C_3H_8, 0.2 C_3H_6, 0.2 C_4H_{10}, 0.1 C_4H_8, 5.2 CO_2, 3.4 N_2
Stoichiometric percentage: 10.8

F_B	g_B	F_B	g_B	F_B	g_B	F_B	g_B	F_B	g_B	F_B	g_B	F_B	g_B	F_B	g_B
Tube diam. 1.023 cm.		Tube diam. 0.908 cm.		Tube diam. 0.776 cm.		Tube diam. 0.600 cm.		Tube diam. 0.475 cm.		Tube diam. 0.315 cm.		Tube diam. 0.294 cm.		Tube diam. 0.249 cm.	
0.690	289	0.706	390	0.736	624	0.812	1,200	0.912	3,010	1.09	6,270	1.15	7,280	1.77	25,250
.701	438	.718	482	.764	996	.881	2,410	1.03	5,500	1.24	10,120	1.34	12,200	2.02	34,800
.744	760	.756	654	.814	1,610	.950	3,810	1.12	8,020	1.37	13,970	1.57	19,570	2.25	42,300
										1.53	17,800	1.66	21,160		
										1.71	22,830	1.80	26,200		
										2.02	28,400	1.93	28,750		
										2.95	1/ 85,700	2.19	33,850		
										3.29	1/102,500				

Fuel No. 67 composition, percent: 37.5 CH_4, 20.4 C_2H_4, 17.5 H_2, 3.9 CO, 13.3 N_2, 7.4 CO_2
Stoichiometric percentage: 12.5 (Points for figure 44)

F_B	g_B	F_B	g_B	F_B	g_B	F_B	g_B	F_B	g_B	F_B	g_B	F_B	g_B	F_B	g_B
Tube diam. 0.908 cm.		Tube diam. 0.776 cm.		Tube diam. 0.675 cm.		Tube diam. 0.413 cm.		Tube diam. 0.300 cm.		Tube diam. 0.230 cm.					
0.633	201	0.612	245	0.642	325	0.828	1,460	1.05	7,460	1.67	26,000				
.655	352	.674	397	.705	595	.851	2,945	1.33	14,950	2.01	37,100				
.667	497	.670	564	.705	788	.960	5,400	1.54	22,200	2.24	46,300				
.697	764	.730	1,107	.796	2,030	1.14	10,270	1.75	28,100	2.45	53,200				

1/ Turbulent flow.

TABLE 4. - Calculation of flame-stability diagram by linear mixture rule; two-component mixture

Fuel No. 40[1/] composition, percent: 88.5 CH_4, 0.6 C_2H_6,[2/] 10.8 N_2, 0.1 CO_2
Stoichiometric percentage: 10.5

Complex for flashback: (100% CH_4)(N_2 and CO_2).

Calc. of complex: Use 100% CH_4 flame-stability diagram.

Total percentage of CH_4 = 89.1.

F_F	A (figure 20) g_F for 100% CH_4	B A × 0.891 g_F for total fuel
0.75	135	120
.8	190	169
.9	330	294
1.0	390	348
1.1	340	303
1.2	180	160
1.25	120	107

Complex for blowoff: (100% CH_4)(N_2 and CO_2).

Calc. of complex: Use 100% CH_4 flame-stability diagram.

Total percentage of CH_4 = 89.1.

F_B	A (figure 20) g_B for 100% CH_4	B A × 0.891 g_B for total fuel
0.7	170	152
.8	530	472
.9	1,100	981
1.0	1,950	1,737
1.2	3,750	3,340
1.4	5,380	4,790
1.8	8,300	7,400
2.2	11,000	9,810
2.6	14,300	12,750
3.0	18,000	16,050

1/ Compare with experimental points (A-T/2a,2b-No./40).
2/ Tally with CH_4.

TABLE 4. - Calculation of flame-stability diagram by linear mixture rule (Con.); two-component mixture (Con.)

Fuel No. 41[1/] composition, percent: 79.4 CH_4, 20.6 C_2H_4
Stoichiometric percentage: 8.66 (Curves for figure 27)

Complexes for flashback: (100% CH_4)(100% C_2H_4)

Calc. of complexes: Use 100% CH_4 flame-stability diagram; use 100% C_2H_4 flame-stability diagram.

Total percentage of CH_4 = 79.4; total percentage of C_2H_4 = 20.6.

F_F	A (figure 20) g_F for 100% CH_4	B A × 0.794	C (figure 22) g_F for 100% C_2H_4	D C × 0.206	B + D g_F for total fuel
0.6			105	22	22
.7			390	80	80
.75	135	107	570	118	225
.8	190	151	760	157	308
.9	330	262	1,050	216	478
1.0	390	310	1,280	264	574
1.1	340	270	1,380	284	554
1.2	180	143	1,300	268	411
1.25	120	95	1,200	247	342
1.3			1,070	220	220
1.4			730	150	150
1.5			390	80	80
1.6			190	39	39

Complexes for blowoff: (100% CH_4)(100% C_2H_4).

Calc. of complexes: Use 100% CH_4 flame-stability diagram; use 100% C_2H_4 flame-stability diagram.

Total percentage of CH_4 = 79.4; total percentage of C_2H_4 = 20.6.

F_B	A (figure 20) g_B for 100% CH_4	B A × 0.794	C (figure 22) g_B for 100% C_2H_4	D C × 0.206	B + D g_B for total fuel
0.6			370	76	76
.7	170	135	1,600	330	465
.8	530	421	3,850	794	1,215
.9	1,100	873	6,700	1,380	2,253
1.0	1,950	1,550	10,000	2,060	3,610
1.2	3,750	2,980	17,000	3,500	6,480
1.4	5,380	4,270	26,000	5,360	9,630
1.8	8,300	6,590	44,000	9,060	15,650
2.2	11,000	8,730	61,500	12,660	21,390
2.6	14,300	11,350	76,000	15,650	27,000
3.0	18,000	14,300	92,000	18,950	33,250

1/ Compare with experimental points (A-T/2a,2b-No./41).

TABLE 4. - Calculation of flame-stability diagram by linear mixture rule (Con.); two-component mixture (Con.)

Fuel No. 42[1/] composition, percent: 78.6 C_2H_4, 21.4 CH_4

Stoichiometric percentage: 6.98

Complexes for flashback: (100% C_2H_4)(100% CH_4).

Calc. of complexes: Use 100% C_2H_4 flame-stability diagram; use 100% CH_4 flame-stability diagram.

Total percentage of C_2H_4 = 78.6; total percentage of CH_4 = 21.4.

F_F	A (figure 22) g_F for 100% C_2H_4	B A × 0.786	C (figure 20) g_F for 100% CH_4	D C × 0.214	B + D g_F for total fuel
0.6	105	83			83
.7	390	307			307
.75	570	448	135	29	477
.8	760	597	190	41	638
.9	1,050	826	330	71	897
1.0	1,280	1,006	390	83	1,089
1.1	1,380	1,085	340	73	1,158
1.2	1,300	1,022	180	39	1,061
1.25	1,200	943	120	26	969
1.3	1,070	841			841
1.4	730	574			574
1.5	390	307			307
1.6	190	149			149

Complexes for blowoff: (100% C_2H_4)(100% CH_4).

Calc. of complexes: Use 100% C_2H_4 flame-stability diagram; use 100% CH_4 flame-stability diagram.

Total percentage of C_2H_4 = 78.6; total percentage of CH_4 = 21.4.

F_B	A (figure 22) g_B for 100% C_2H_4	B A × 0.786	C (figure 20) g_B for 100% CH_4	D C × 0.214	B + D g_B for total fuel
0.6	370	291			291
.7	1,600	1,258	170	36	1,294
.8	3,850	3,030	530	114	3,144
.9	6,700	5,270	1,100	235	5,505
1.0	10,000	7,860	1,950	417	8,277
1.2	17,000	13,360	3,750	802	14,160
1.4	26,000	20,450	5,380	1,150	21,600
1.8	44,000	34,600	8,300	1,775	36,380
2.2	61,500	48,300	11,000	2,350	50,650
2.6	76,000	59,800	14,300	3,060	62,860
3.0	92,000	72,400	18,000	3,850	76,250

1/ Compare with experimental points (A-T/2a,2b-No./42).

TABLE 4. - Calculation of flame-stability diagram by linear mixture rule (Con.); mixture of coke-oven-gas type

Fuel No. 43[1/] composition, percent: 58.4 H_2, 26.3 CH_4, 10.6 CO, 4.6 N_2, 0.1 CO_2
Stoichiometric percentage: 19.4 (Curves for figure 41)

Complexes for flashback: (CH_4 + CO)(CH_4 + H_2)(N_2 and CO_2).

Calc. of complexes: (10.6/10.6 + 58.4) × 26.3 = 4.04 (CH_4 going with CO); CH_4/CO = 4.04/10.6 = 0.381;

(58.4/10.6 + 58.4) × 26.3 = 22.26 (CH_4 going with H_2); CH_4/H_2 = 22.26/58.4 = 0.381.

Total percentage of CH_4/CO = 4.04 + 10.6 = 14.64; total percentage of CH_4/H_2 = 22.26 + 58.4 = 80.66.

F_F	A (figure 32) g_F for CH_4/CO = 0.381	B A × 0.1464	C (figure 28) g_F for CH_4/H_2 = 0.381	D C × 0.8066	B + D g_F for total fuel
0.5			117	94	94
.6			520	420	420
.7	170	25	1,070	864	889
.75	285	42	1,370	1,105	1,147
.8	390	57	1,700	1,370	1,427
.9	605	89	2,160	1,743	1,832
1.0	795	116	2,400	1,935	2,051
1.1	950	139	2,150	1,735	1,874
1.2	910	133	1,530	1,235	1,368
1.25	845	124	1,140	920	1,044
1.3	735	108	765	617	725
1.4	440	64	250	202	266
1.6	190	28	100	81	109

Complexes for blowoff: (CH_4 + H_2)(H_2/CO = 0.20)(N_2 and CO_2).

Calc. of complexes: H_2/CO = 0.20, 0.20×10.6 = 2.12 (H_2 going with CO); H_2/CO = 2.12/10.6 = 0.20;

58.4 - 2.12 = 56.28 (H_2 going with CH_4); CH_4/H_2 = 26.3/56.28 = 0.467.

Total percentage of H_2/CO = 2.12 + 10.6 = 12.72; total percentage of CH_4/H_2 = 26.3 + 56.28 = 82.58.

F_B	A (figure 31) g_B for H_2/CO = 0.20	B A × 0.1272	C (figure 29) g_B for CH_4/H_2 = 0.467	D C × 0.8258	B + D g_B for total fuel
0.5			185	153	153
.6	250	32	1,050	866	898
.7	1,000	127	5,000	4,130	4,257
.8	2,700	343	12,500	10,320	10,660
.9	5,300	674	25,000	20,630	21,300
1.0	9,500	1,208	41,500	34,250	35,460
1.2	22,000	2,800	125,000	103,200	106,000
1.4	41,000	5,220	325,000	268,000	273,200
1.8	111,000	14,120	1,100,000	908,000	922,100
2.2	225,000	28,600	2,150,000	1,775,000	1,804,000
2.6	380,000	48,300	3,260,000	2,690,000	2,738,000
3.0	560,000	71,200	7,150,000	5,900,000	5,971,000

1/ Compare with experimental points (A-T/3a,3b-No./43).

TABLE 4. - Calculation of flame-stability diagram by linear mixture rule (Con.); mixture of coke-oven-gas type (Con.)

Fuel No. 44[1/] composition, percent: 38.7 H_2, 31.7 CO, 29.4 CH_4, 0.1 N_2, 0.1 CO_2

Stoichiometric percentage: 18.2

Complexes for flashback: $(CH_4 + CO)(CH_4 + H_2)(N_2$ and $CO_2)$.

Calc. of complexes: (31.7/31.7 + 38.7) × 29.4 = 13.24 (CH_4 going with CO); CH_4/CO = 13.24/31.7 = 0.418;

(38.7/31.7 + 38.7) × 29.4 = 16.16 (CH_4 going with H_2); CH_4/H_2 = 16.16/38.7 = 0.417.

Total percentage of CH_4/CO = 13.24 + 31.7 = 44.94; total percentage of CH_4/H_2 = 16.16 + 38.7 = 54.86.

	A (figure 32)	B	C (figure 28)	D	B + D
F_F	g_F for CH_4/CO = 0.418	A × 0.4494	g_F for CH_4/H_2 = 0.417	C × 0.5486	g_F for total fuel
0.5			100	55	55
.6			480	263	263
.7	166	75	995	546	621
.75	280	126	1,270	698	824
.8	385	173	1,590	874	1,047
.9	590	265	2,000	1,096	1,361
1.0	780	350	2,100	1,152	1,502
1.1	915	411	1,970	1,080	1,491
1.2	870	391	1,310	720	1,111
1.25	800	360	980	538	898
1.3	675	303	660	362	665
1.4	395	178	200	110	288
1.6	168	75			75

Complexes for blowoff: $(CH_4 + H_2)(H_2/CO = 0.20)(N_2$ and $CO_2)$.

Calc. of complexes: H_2/CO = 0.20, 0.20 × 31.7 = 6.34 (H_2 going with CO); H_2/CO = 6.34/31.7 = 0.20;

38.7 - 6.34 = 32.36 (H_2 going with CH_4); CH_4/H_2 = 29.4/32.36 = 0.909.

Total percentage of H_2/CO = 6.34 + 31.7 = 38.04; total percentage of CH_4/H_2 = 29.4 + 32.36 = 61.76.

	A (figure 31)	B	C (figure 29)	D	B + D
F_B	g_B for H_2/CO = 0.20	A × 0.3804	g_B for CH_4/H_2 = 0.909	C × 0.6176	g_B for total fuel
0.6	250	95	320	198	293
.7	1,000	380	1,510	932	1,312
.8	2,700	1,026	4,650	2,870	3,896
.9	5,300	2,020	9,300	5,740	7,760
1.0	9,500	3,610	15,000	9,260	12,870
1.2	22,000	8,370	35,500	21,900	30,270
1.4	41,000	15,600	72,000	44,500	60,100
1.8	111,000	42,200	220,000	136,000	178,200
2.2	225,000	81,800	495,000	306,000	387,800
2.6	380,000	144,500	900,000	556,000	700,500
3.0	560,000	213,000	1,700,000	1,050,000	1,263,000

1/ Compare with experimental points (A-T/3a,3b-No./44).

TABLE 4. - Calculation of flame-stability diagram by linear mixture rule (Con.); mixture of coke-oven-gas type (Con.)

Fuel No. 45[1] composition, percent: 29.6 H_2, 26.2 CO, 23,4 CH_4, 20.8 N_2

Stoichiometric percentage: 21.9

Complexes for flashback: $(CH_4 + CO)(CH_4 + H_2)(N_2)$.

Calc. of complexes: (26.2/26.2 + 29.6) × 23.4 = 11.0 (CH_4 going with CO); CH_4/CO = 11.0/26.2 = 0.42;

(29.6/26.2 + 29.6) × 23.4 = 12.4 (CH_4 going with H_2); CH_4/H_2 = 12.4/29.6 = 0.419.

Total percentage of CH_4/CO = 11.0 + 26.2 = 37.2; total percentage of CH_4/H_2 = 12.4 + 29.6 = 42.0.

	A (figure 32)	B	C (figure 28)	D	B + D
F_F	g_F for CH_4/CO = 0.42	A × 0.372	g_F for CH_4/H_2 = 0.419	C × 0.42	g_F for total fuel
0.5			100	42	42
.6			480	202	202
.7	166	62	995	418	480
.75	280	104	1,270	534	638
.8	385	143	1,590	668	811
.9	590	219	2,000	840	1,059
1.0	780	290	2,100	882	1,172
1.1	915	340	1,970	827	1,167
1.2	870	324	1,310	550	874
1.25	800	298	980	412	710
1.3	675	251	660	277	528
1.4	395	147	200	84	231
1.6	168	63			63

Complexes for blowoff: $(CH_4 + H_2)(H_2/CO = 0.20)(N_2)$.

Calc. of complexes: H_2/CO = 0.20, 0.20×26.2 = 5.24 (H_2 going with CO); H_2/CO = 5.24/26.2 = 0.20;

29.6 - 5.24 = 24.36 (H_2 going with CH_4); CH_4/H_2 = 23.4/24.36 = 0.961.

Total percentage of H_2/CO = 5.24 + 26.2 = 31.44; total percentage of CH_4/H_2 = 23.4 + 24.36 = 47.76.

	A (figure 31)	B	C (figure 29)	D	B + D
F_B	g_B for H_2/CO = 0.20	A × 0.3144	g_B for CH_4/H_2 = 0.961	C × 0.4776	g_B for total fuel
0.6	250	79	288	138	217
.7	1,000	314	1,340	640	954
.8	2,700	849	4,250	2,030	2,879
.9	5,300	1,665	8,500	4,060	5,725
1.0	9,500	2,990	13,500	6,450	9,440
1.2	22,000	6,920	31,800	15,200	22,120
1.4	41,000	12,900	63,500	30,300	43,200
1.8	111,000	34,900	193,000	92,200	127,100
2.2	225,000	70,800	430,000	205,000	275,800
2.6	380,000	119,500	800,000	382,000	501,500
3.0	560,000	176,000	1,470,000	702,000	878,000

1/ Compare with experimental points (A-T/3a,3b-No./45).

TABLE 4. - Calculation of flame-stability diagram by linear mixture rule (Con.); mixture of coke-oven-gas type (Con.)

Fuel No. 46[1/] composition, percent: 55.7 H_2, 34.0 CO, 10.3 CH_4

Stoichiometric percentage: 24.2

Complexes for flashback: $(CH_4 + CO)(CH_4 + H_2)$.

Calc. of complexes: $(34.0/34.0 + 55.7) \times 10.3 = 3.9$ (CH_4 going with CO); $CH_4/CO = 3.9/34.0 = 0.115$;

$(55.7/34.0 + 55.7) \times 10.3 = 6.4$ (CH_4 going with H_2); $CH_4/H_2 = 6.4/55.7 = 0.115$.

Total percentage of $CH_4/CO = 3.9 + 34.0 = 37.9$; total percentage of $CH_4/H_2 = 6.4 + 55.7 = 62.1$.

F_F	A (figure 32) g_F for $CH_4/CO = 0.115$	B A × 0.379	C (figure 28) g_F for $CH_4/H_2 = 0.115$	D C × 0.621	B + D g_F for total fuel
0.5			515	320	320
.6			1,260	782	782
.7	187	71	2,380	1,480	1,551
.75	284	108	2,950	1,830	1,938
.8	365	138	3,650	2,270	2,408
.9	565	214	4,650	2,890	3,104
1.0	820	311	5,450	3,385	3,696
1.1	1,040	394	5,600	3,480	3,874
1.2	1,220	462	5,450	3,385	3,847
1.25	1,300	493	4,900	3,040	3,533
1.3	1,340	508	4,150	2,580	3,088
1.4	1,360	516	2,600	1,615	2,131
1.6	1,050	398	520	323	721
1.8	253	96			96

Complexes for blowoff: $(CH_4 + H_2)(H_2/CO = 0.20)$.

Calc. of complexes: $H_2/CO = 0.20$, $0.20 \times 34.0 = 6.8$ (H_2 going with CO); $H_2/CO = 6.8/34.0 = 0.20$;

$55.7 - 6.8 = 48.9$ (H_2 going with CH_4); $CH_4/H_2 = 10.3/48.9 = 0.211$.

Total percentage of $H_2/CO = 6.8 + 34.0 = 40.8$; total percentage of $CH_4/H_2 = 10.3 + 48.9 = 59.2$.

F_B	A (figure 31) g_B for $H_2/CO = 0.20$	B A × 0.408	C (figure 29) g_B for $CH_4/H_2 = 0.211$	D C × 0.592	B + D g_B for total fuel
0.5			690	408	408
.6	250	102	4,550	2,690	2,792
.7	1,000	408	19,700	11,650	12,060
.8	2,700	1,100	45,000	26,600	27,700
.9	5,300	2,160	107,000	63,400	65,560
1.0	9,500	3,880	245,000	145,000	148,900
1.2	22,000	8,980	525,000	311,000	320,000
1.4	41,000	16,730	1,180,000	699,000	715,700
1.8	111,000	45,300	3,950,000	2,340,000	2,385,000
2.2	225,000	91,800	7,650,000	4,530,000	4,622,000

1/ Compare with experimental points (A-T/3a,3b-No./46).

TABLE 4. - Calculation of flame-stability diagram by linear mixture rule (Con.); mixture of coke-oven-gas type (Con.)

Fuel No. 47[1] composition, percent: 53.0 H_2, 33.9 CO, 9.8 CH_4, 3.3 N_2

Stoichiometric percentage: 24.9

Complexes for flashback: $(CH_4 + CO)(CH_4 + H_2)(N_2)$.

Calc. of complexes: $(33.9/33.9 + 53.0) \times 9.8 = 3.82$ (CH_4 going with CO); $CH_4/CO = 3.82/33.9 = 0.113$;

$(53.0/33.9 + 53.0) \times 9.8 = 5.98$ (CH_4 going with H_2); $CH_4/H_2 = 5.98/53.0 = 0.113$.

Total percentage of $CH_4/CO = 3.82 + 33.9 = 37.72$; total percentage of $CH_4/H_2 = 5.98 + 53.0 = 58.98$.

F_F	A (figure 32) g_F for $CH_4/CO = 0.113$	B A × 0.3772	C (figure 28) g_F for $CH_4/H_2 = 0.113$	D C × 0.5898	B + D g_F for total fuel
0.5			515	304	304
.6			1,260	743	743
.7	187	71	2,380	1,404	1,475
.75	284	107	2,950	1,740	1,847
.8	365	138	3,650	2,150	2,288
.9	565	213	4,650	2,740	2,953
1.0	820	309	5,450	3,210	3,519
1.1	1,040	392	5,600	3,300	3,692
1.2	1,220	460	5,450	3,210	3,670
1.25	1,300	490	4,900	2,890	3,380
1.3	1,340	506	4,150	2,450	2,956
1.4	1,360	513	2,600	1,532	2,045
1.6	1,050	396	520	306	702
1.8	253	95			95

Complexes for blowoff: $(CH_4 + H_2)(H_2/CO = 0.20)(N_2)$.

Calc. of complexes: $H_2/CO = 0.20$, $0.20 \times 33.9 = 6.78$ (H_2 going with CO); $H_2/CO = 6.78/33.9 = 0.20$;

$53.0 - 6.78 = 46.22$ (H_2 going with CH_4); $CH_4/H_2 = 9.8/46.22 = 0.212$.

Total percentage of $H_2/CO = 6.78 + 33.9 = 40.68$; total percentage of $CH_4/H_2 = 9.8 + 46.22 = 56.02$.

F_B	A (figure 31) g_B for $H_2/CO = 0.20$	B A × 0.4068	C (figure 29) g_B for $CH_4/H_2 = 0.212$	D C × 0.5602	B + D g_B for total fuel
0.5			690	386	386
.6	250	102	4,550	2,550	2,652
.7	1,000	407	19,700	11,040	11,450
.8	2,700	1,100	45,000	25,200	26,300
.9	5,300	2,160	107,000	60,000	62,160
1.0	9,500	3,870	245,000	137,300	141,200
1.2	22,000	8,940	525,000	294,000	302,900
1.4	41,000	16,700	1,180,000	661,000	677,700
1.8	111,000	45,100	3,950,000	2,210,000	2,255,000
2.2	225,000	91,500	7,650,000	4,285,000	4,377,000

1/ Compare with experimental points (A-T/3a,3b-No./47).

TABLE 4. - Calculation of flame-stability diagram by linear mixture rule (Con.); mixture of coke-oven-gas type (Con.)

Fuel No. 48[1] composition, percent: 66.2 CO, 17.5 H_2, 16.3 CH_4

Stoichiometric percentage: 21.9

Complexes for flashback: $(CH_4 + CO)(CH_4 + H_2)$.

Calc. of complexes: $(66.2/66.2 + 17.5) \times 16.3 = 12.9$ (CH_4 going with CO); $CH_4/CO = 12.9/66.2 = 0.195$;

$(17.5/66.2 + 17.5) \times 16.3 = 3.4$ (CH_4 going with H_2); $CH_4/H_2 = 3.4/17.5 = 0.194$.

Total percentage of $CH_4/CO = 12.9 + 66.2 = 79.1$; total percentage of $CH_4/H_2 = 3.4 + 17.5 = 20.9$.

F_F	A (figure 32) g_F for $CH_4/CO = 0.195$	B $A \times 0.791$	C (figure 28) g_F for $CH_4/H_2 = 0.194$	D $C \times 0.209$	B + D g_F for total fuel
0.5			310	65	65
.6			885	185	185
.7	194	154	1,710	357	511
.75	305	241	2,180	456	697
.8	410	324	2,750	574	898
.9	650	514	3,500	732	1,246
1.0	870	688	4,050	846	1,534
1.1	1,100	870	3,800	794	1,664
1.2	1,140	902	3,480	728	1,630
1.25	1,200	950	2,950	616	1,566
1.3	1,210	958	2,200	460	1,418
1.4	965	764	1,100	230	994
1.6	525	415	147	31	446
1.8	133	105			105

Complexes for blowoff: $(CH_4 + H_2)(H_2/CO = 0.20)$.

Calc. of complexes: $H_2/CO = 0.20$, $0.20 \times 66.2 = 13.24$ (H_2 going with CO); $H_2/CO = 13.24/66.2 = 0.20$;

$17.5 - 13.24 = 4.26$ (H_2 going with CH_4); $H_2/CH_4 = 4.26/16.3 = 0.261$.

Total percentage of $H_2/CO = 13.24 + 66.2 = 79.44$; total percentage of $H_2/CH_4 = 4.26 + 16.3 = 20.56$.

F_B	A (figure 31) g_B for $H_2/CO = 0.20$	B $A \times 0.7944$	C (figure 29) g_B for $H_2/CH_4 = 0.261$	D $C \times 0.2056$	B + D g_B for total fuel
0.6	250	199	102	21	220
.7	1,000	794	295	61	855
.8	2,700	2,145	1,020	210	2,355
.9	5,300	4,210	2,050	421	4,631
1.0	9,500	7,540	3,580	736	8,276
1.2	22,000	17,500	7,280	1,495	19,000
1.4	41,000	32,600	11,300	2,320	34,920
1.8	111,000	88,200	23,000	4,730	92,930
2.2	225,000	179,000	37,500	7,710	186,700
2.6	380,000	302,000	55,500	11,400	313,400
3.0	560,000	445,000	83,000	17,050	462,100

1/ Compare with experimental points (A-T/3a,3b-No./48).

TABLE 4. - Calculation of flame-stability diagram by linear mixture rule (Con.); mixture of coke-oven-gas type (Con.)

Fuel No. 49[1/] composition, percent: 52.9 CO, 14.1 H_2, 11.9 CH_4, 21.1 CO_2

Stoichiometric percentage: 26.8

Complexes for flashback: $(CH_4 + CO)(CH_4 + H_2)(CO_2)$.

Calc. of complexes: $(52.9/52.9 + 14.1) \times 11.9 = 9.4$ (CH_4 going with CO); $CH_4/CO = 9.4/52.9 = 0.178$;

$(14.1/52.9 + 14.1) \times 11.9 = 2.5$ (CH_4 going with H_2); $CH_4/H_2 = 2.5/14.1 = 0.177$.

Total percentage of $CH_4/CO = 9.4 + 52.9 = 62.3$; total percentage of $CH_4/H_2 = 2.5 + 14.1 = 16.6$.

F_F	A (figure 32) g_F for CH_4/CO = 0.178	B A × 0.623	C (figure 28) g_F for CH_4/H_2 = 0.177	D C × 0.166	B + D g_F for total fuel
0.5			340	56	56
.6			950	158	158
.7	195	122	1,850	307	429
.75	303	189	2,320	385	574
.8	405	252	2,920	485	737
.9	645	402	3,750	622	1,024
1.0	875	546	4,350	722	1,268
1.1	1,120	698	4,200	697	1,395
1.2	1,160	722	3,850	639	1,361
1.25	1,250	779	3,350	556	1,335
1.3	1,270	791	2,550	423	1,214
1.4	1,070	666	1,330	221	887
1.6	610	380	520	86	466
1.8	150	93	172	29	122

Complexes for blowoff: $(CH_4 + H_2)(H_2/CO = 0.20)(CO_2)$.

Calc. of complexes: $H_2/CO = 0.20$, $0.20 \times 52.9 = 10.58$ (H_2 going with CO); $H_2/CO = 10.58/52.9 = 0.20$;

$14.1 - 10.58 = 3.52$ (H_2 going with CH_4); $H_2/CH_4 = 3.52/11.9 = 0.296$.

Total percentage of $H_2/CO = 10.58 + 52.9 = 63.48$; total percentage of $H_2/CH_4 = 3.52 + 11.9 = 15.42$.

F_B	A (figure 31) g_B for H_2/CO = 0.20	B A × 0.6348	C (figure 29) g_B for H_2/CH_4 = 0.296	D C × 0.1542	B + D g_B for total fuel
0.6	250	159	106	16	175
.7	1,000	635	300	46	681
.8	2,700	1,714	1,100	170	1,884
.9	5,300	3,360	2,200	339	3,699
1.0	9,500	6,030	3,820	589	6,619
1.2	22,000	13,960	7,900	1,220	15,180
1.4	41,000	26,000	12,500	1,930	27,930
1.8	111,000	70,400	26,000	4,010	74,410
2.2	225,000	142,800	43,500	6,710	149,500
2.6	380,000	241,000	65,000	10,000	251,000
3.0	560,000	355,000	96,500	14,880	369,900

1/ Compare with experimental points (A-T/3a,3b-No./49).

TABLE 4. - Calculation of flame-stability diagram by linear mixture rule (Con.); mixture of coke-oven-gas type (Con.)

Fuel No. 50 1/ composition, percent: 43.0 CO, 11.5 H_2, 10.7 CH_4, 34.8 CO_2

Stoichiometric percentage: 30.0

Complexes for flashback: $(CH_4 + CO)(CH_4 + H_2)(CO_2)$.

Calc. of complexes: $(43.0/43.0 + 11.5) \times 10.7 = 8.44$ (CH_4 going with CO); $CH_4/CO = 8.44/43.0 = 0.196$;

$(11.5/43.0 + 11.5) \times 10.7 = 2.26$ (CH_4 going with H_2); $CH_4/H_2 = 2.26/11.5 = 0.197$.

Total percentage of $CH_4/CO = 8.44 + 43.0 = 51.44$; total percentage of $CH_4/H_2 = 2.26 + 11.5 = 13.76$.

F_F	A (figure 32) g_F for $CH_4/CO = 0.196$	B A × 0.5144	C (figure 28) g_F for $CH_4/H_2 = 0.197$	D C × 0.1376	B + D g_F for total fuel
0.5			310	43	43
.6			885	122	122
.7	194	100	1,710	235	335
.75	305	157	2,180	300	457
.8	410	211	2,750	379	590
.9	650	335	3,500	482	817
1.0	870	448	4,050	558	1,006
1.1	1,100	566	3,800	523	1,089
1.2	1,140	587	3,480	479	1,066
1.25	1,200	618	2,950	406	1,024
1.3	1,210	623	2,200	303	926
1.4	965	497	1,100	152	649
1.6	525	270	147	20	290
1.8	133	68			68

Complexes for blowoff: $(CH_4 + H_2)(H_2/CO = 0.20)(CO_2)$.

Calc. of complexes: $H_2/CO = 0.20$, $0.20 \times 43.0 = 8.6$ (H_2 going with CO); $H_2/CO = 8.6/43.0 = 0.20$;

$11.5 - 8.6 = 2.9$ (H_2 going with CH_4); $H_2/CH_4 = 2.9/10.7 = 0.271$.

Total percentage of $H_2/CO = 8.6 + 43.0 = 51.6$; total percentage of $H_2/CH_4 = 2.9 + 10.7 = 13.6$.

F_B	A (figure 31) g_B for $H_2/CO = 0.20$	B A × 0.516	C (figure 29) g_B for $H_2/CH_4 = 0.271$	D C × 0.136	B + D g_B for total fuel
0.6	250	129	103	14	143
.7	1,000	516	295	40	556
.8	2,700	1,394	1,040	142	1,536
.9	5,300	2,735	2,120	288	3,023
1.0	9,500	4,900	3,650	496	5,396
1.2	22,000	11,350	7,500	1,020	12,370
1.4	41,000	21,150	11,600	1,578	22,730
1.8	111,000	57,200	23,800	3,240	60,440
2.2	225,000	116,000	39,500	5,370	121,400
2.6	380,000	196,000	57,000	7,750	203,800
3.0	560,000	289,000	85,000	11,550	300,600

1/ Compare with experimental points (A-T/3a,3b-No./50).

TABLE 4. - Calculation of flame-stability diagram by linear mixture rule (Con.); mixture of coke-oven-gas type (Con.)

Fuel No. 51[1/] composition, percent: 50.7 CH_4, 24.7 CO, 24.5 H_2, 0.1 CO_2

Stoichiometric percentage: 14.2

Complexes for flashback: (CH_4 + CO)(CH_4 + H_2)(CO_2).

Calc. of complexes: (24.7/24.7 + 24.5) × 50.7 = 25.45 (CH_4 going with CO); CO/CH_4 = 24.7/25.45 = 0.971;

(24.5/24.7 + 24.5) × 50.7 = 25.25 (CH_4 going with H_2); H_2/CH_4 = 24.5/25.25 = 0.971.

Total percentage of CO/CH_4 = 24.7 + 25.45 = 50.15; total percentage of H_2/CH_4 = 24.5 + 25.25 = 49.75.

F_F	A (figure 32) g_F for CO/CH_4 = 0.971	B A × 0.5015	C (figure 28) g_F for H_2/CH_4 = 0.971	D C × 0.4975	B + D g_F for total fuel
0.6			102	51	51
.7	122	61	440	219	280
.75	204	102	590	294	396
.8	280	141	725	361	502
.9	440	221	940	468	689
1.0	585	293	1,050	522	815
1.1	645	323	885	440	763
1.2	580	291	570	284	575
1.25	500	251	420	209	460
1.3	370	186	213	106	292

Complexes for blowoff: (CH_4 + H_2)(H_2/CO = 0.20).

Calc. of complexes: H_2/CO = 0.20, 0.20 × 24.7 = 4.94 (H_2 going with CO); H_2/CO = 4.94/24.7 = 0.20;

24.5 - 4.94 = 19.56 (H_2 going with CH_4); H_2/CH_4 = 19.56/50.7 = 0.386.

Total percentage of H_2/CO = 4.94 + 24.7 = 29.64; total percentage of H_2/CH_4 = 19.56 + 50.7 = 70.26.

F_B	A (figure 31) g_B for H_2/CO = 0.20	B A × 0.2964	C (figure 29) g_B for H_2/CH_4 = 0.386	D C × 0.7026	B + D g_B for total fuel
0.6	250	74	119	84	158
.7	1,000	296	325	228	524
.8	2,700	800	1,290	907	1,707
.9	5,300	1,570	2,590	1,820	3,390
1.0	9,500	2,820	4,400	3,090	5,910
1.2	22,000	6,520	9,500	6,680	13,200
1.4	41,000	12,150	15,400	10,820	22,970
1.8	111,000	32,900	34,500	24,200	57,100
2.2	225,000	66,700	58,500	41,100	107,800
2.6	380,000	112,600	90,500	63,600	176,200
3.0	560,000	166,000	135,000	94,900	260,900

1/ Compare with experimental points (A-T/3a,3b-No./51).

TABLE 4. - Calculation of flame-stability diagram by linear mixture rule (Con.); mixture of coke-oven-gas type (Con.)

Fuel No. 52[1/] composition, percent: 47.6 CH_4, 22.6 CO, 22.6 H_2, 7.1 N_2, 0.1 CO_2

Stoichiometric percentage: 15.1

Complexes for flashback: $(CH_4 + CO)(CH_4 + H_2)(N_2$ and $CO_2)$.

Calc. of complexes: $(22.6/22.6 + 22.6) \times 47.6 = 23.8$ (CH_4 going with CO); $CO/CH_4 = 22.6/23.8 = 0.95$;

$(22.6/22.6 + 22.6) \times 47.6 = 23.8$ (CH_4 going with H_2); $H_2/CH_4 = 22.6/23.8 = 0.95$.

Total percentage of $CO/CH_4 = 22.6 + 23.8 = 46.4$; total percentage of $H_2/CH_4 = 22.6 + 23.8 = 46.4$.

F_F	A (figure 32) g_F for $CO/CH_4 = 0.95$	B A × 0.464	C (figure 28) g_F for $H_2/CH_4 = 0.95$	D C × 0.464	B + D g_F for total fuel
0.7	120	56	428	199	255
.75	202	94	575	267	371
.8	277	129	705	327	456
.9	438	203	915	425	628
1.0	580	269	1,040	483	752
1.1	635	295	870	404	699
1.2	568	264	560	260	524
1.25	485	225	415	193	418
1.3	363	169	209	97	266

Complexes for blowoff: $(CH_4 + H_2)(H_2/CO = 0.20)$.

Calc. of complexes: $H_2/CO = 0.20$, $0.20 \times 22.6 = 4.52$ (H_2 going with CO); $H_2/CO = 4.52/22.6 = 0.20$;

$22.6 - 4.52 = 18.08$ (H_2 going with CH_4); $H_2/CH_4 = 18.08/47.6 = 0.38$.

Total percentage of $H_2/CO = 4.52 + 22.6 = 27.12$; total percentage of $H_2/CH_4 = 18.08 + 47.6 = 65.68$.

F_B	A (figure 31) g_B for $H_2/CO = 0.20$	B A × 0.2712	C (figure 29) g_B for $H_2/CH_4 = 0.38$	D C × 0.6568	B + D g_B for total fuel
0.6	250	68	118	78	146
.7	1,000	271	322	212	483
.8	2,700	732	1,280	840	1,572
.9	5,300	1,440	2,570	1,690	3,130
1.0	9,500	2,580	4,350	2,860	5,440
1.2	22,000	5,970	9,300	6,110	12,080
1.4	41,000	11,120	15,400	10,100	21,220
1.8	111,000	30,100	34,000	22,300	52,400
2.2	225,000	61,000	58,500	38,400	99,400
2.6	380,000	103,000	88,500	58,100	161,100
3.0	560,000	152,000	134,000	88,000	240,000

1/ Compare with experimental points (A-T/3a,3b-No./52).

TABLE 4. - Calculation of flame-stability diagram by linear mixture rule (Con.); mixture of coke-oven-gas type (Con.)

Fuel No. 53[1/] composition, percent: 46.1 CH_4, 23.1 CO, 22.9 H_2, 7.9 CO_2

Stoichiometric percentage: 15.4

Complexes for flashback: $(CH_4 + CO)(CH_4 + H_2)(CO_2)$.

Calc. of complexes: $(23.1/23.1 + 22.9) \times 46.1 = 23.15$ (CH_4 going with CO); $CO/CH_4 = 23.1/23.15 = 0.998$;

$(22.9/23.1 + 22.9) \times 46.1 = 22.95$ (CH_4 going with H_2); $H_2/CH_4 = 22.9/22.95 = 0.998$.

Total percentage of CO/CH_4 = 23.1 + 23.15 = 46.25; total percentage of H_2/CH_4 = 22.9 + 22.95 = 45.85.

	A (figure 32)	B	C (figure 28)	D	B + D
F_F	g_F for $CO/CH_4 = 0.998$	A × 0.4625	g_F for $H_2/CH_4 = 0.998$	C × 0.4585	g_F for total fuel
0.6			114	52	52
.7	123	57	455	209	266
.75	208	96	605	277	373
.8	282	131	750	344	475
.9	445	206	960	440	646
1.0	595	275	1,080	495	770
1.1	655	303	920	422	725
1.2	595	275	590	271	546
1.25	515	238	435	200	438
1.3	387	179	220	101	280
1.4	106	49			49

Complexes for blowoff: $(CH_4 + H_2)(H_2/CO = 0.20)(CO_2)$.

Calc. of complexes: $H_2/CO = 0.20$, $0.20 \times 23.1 = 4.62$ (H_2 going with CO); $H_2/CO = 4.62/23.1 = 0.20$;

$22.9 - 4.62 = 18.28$ (H_2 going with CH_4); $H_2/CH_4 = 18.28/46.1 = 0.397$.

Total percentage of H_2/CO = 4.62 + 23.1 = 27.72; total percentage of H_2/CH_4 = 18.28 + 46.1 = 64.38.

	A (figure 31)	B	C (figure 29)	D	B + D
F_B	g_B for $H_2/CO = 0.20$	A × 0.2772	g_B for $H_2/CH_4 = 0.397$	C × 0.6438	g_B for total fuel
0.6	250	69	121	78	147
.7	1,000	277	335	216	493
.8	2,700	748	1,330	856	1,604
.9	5,300	1,470	2,670	1,770	3,240
1.0	9,500	2,630	4,500	2,900	5,530
1.2	22,000	6,100	9,650	6,210	12,310
1.4	41,000	11,360	16,000	10,300	21,660
1.8	111,000	30,800	35,500	22,800	53,600
2.2	225,000	62,400	61,500	39,600	102,000
2.6	380,000	105,400	95,500	61,400	166,800
3.0	560,000	155,400	143,000	92,000	247,400

1/ Compare with experimental points (A-T/3a,3b-No./53).

TABLE 4. - Calculation of flame-stability diagram by linear mixture rule (Con.); mixture of coke-oven-gas type (Con.)

Fuel No. 54[1/] composition, percent: 36.1 CH_4, 17.5 CO, 17.5 H_2, 28.9 CO_2

Stoichiometric percentage: 18.9

Complexes for flashback: $(CH_4 + CO)(CH_4 + H_2)(CO_2)$.

Calc. of complexes: $(17.5/17.5 + 17.5) \times 36.1 = 18.05$ (CH_4 going with CO); $CO/CH_4 = 17.5/18.05 = 0.97$;

$(17.5/17.5 + 17.5) \times 36.1 = 18.05$ (CH_4 going with H_2); $H_2/CH_4 = 17.5/18.05 = 0.97$.

Total percentage of $CO/CH_4 = 17.5 + 18.05 = 35.55$; total percentage of $H_2/CH_4 = 17.5 + 18.05 = 35.55$.

	A (figure 32)	B	C (figure 28)	D	B + D
F_F	g_F for $CO/CH_4 = 0.97$	A × 0.3555	g_F for $H_2/CH_4 = 0.97$	C × 0.3555	g_F for total fuel
0.6			102	36	36
.7	122	43	440	157	200
.75	204	73	590	210	283
.8	280	100	725	258	358
.9	440	157	940	334	491
1.0	585	208	1,050	373	581
1.1	645	229	885	315	544
1.2	580	206	570	203	409
1.25	500	178	420	149	327
1.3	370	132	213	76	208

Complexes for blowoff: $(CH_4 + H_2)(H_2/CO = 0.20)(CO_2)$.

Calc. of complexes: $H_2/CO = 0.20$, $0.20 \times 17.5 = 3.5$ (H_2 going with CO); $H_2/CO = 3.5/17.5 = 0.20$;

$17.5 - 3.5 = 14.0$ (H_2 going with CH_4); $H_2/CH_4 = 14.0/36.1 = 0.388$.

Total percentage of $H_2/CO = 3.5 + 17.5 = 21.0$; total percentage of $H_2/CH_4 = 14.0 + 36.1 = 50.1$.

	A (figure 31)	B	C (figure 29)	D	B + D
F_B	g_B for $H_2/CO = 0.20$	A × 0.21	g_B for $H_2/CH_4 = 0.388$	C × 0.501	g_B for total fuel
0.6	250	53	119	60	113
.7	1,000	210	325	163	373
.8	2,700	567	1,290	646	1,213
.9	5,300	1,114	2,590	1,297	2,411
1.0	9,500	1,995	4,400	2,205	4,200
1.2	22,000	4,620	9,500	4,760	9,380
1.4	41,000	8,610	15,400	7,720	16,330
1.8	111,000	23,300	34,500	17,300	40,600
2.2	225,000	47,200	58,500	29,300	76,500
2.6	380,000	79,800	90,500	45,300	125,100
3.0	560,000	117,500	135,000	67,600	185,100

1/ Compare with experimental points (A-T/3a,3b-No./54).

TABLE 4. - Calculation of flame-stability diagram by linear mixture rule (Con.); mixture of oil-gas type

Fuel No. 55[1/] composition, percent: 37.4 CH_4, 33.4 C_2H_4, 15.2 H_2, 14.0 N_2
Stoichiometric percentage: 10.3 (Curves for figure 43)

Complexes for flashback: $(C_2H_4 + H_2)(CH_4)(N_2)$.

Calc. of complexes: H_2/C_2H_4 = 15.2/33.4 = 0.455; use 100% CH_4 flame-stability diagram.

Total percentage of H_2/C_2H_4 = 15.2 + 33.4 = 48.6; total percentage of CH_4 = 37.4.

	A (figure 36)	B	C (figure 20)	D	B + D
F_F	g_F for H_2/C_2H_4 = 0.455	A × 0.486	g_F for 100% CH_4	C × 0.374	g_F for total fuel
0.6	305	148			148
.7	615	299			299
.75	830	403	135	51	454
.8	1,060	515	190	71	586
.9	1,430	695	330	124	819
1.0	1,680	816	390	146	962
1.1	1,770	860	340	127	987
1.2	1,480	719	180	67	786
1.25	1,300	632	120	45	677
1.3	1,090	530			530
1.4	715	348			348
1.5	413	201			201
1.6	220	107			107

Complexes for blowoff: $(CH_4 + H_2)(C_2H_4)(N_2)$.

Calc. of complexes: H_2/CH_4 = 15.2/37.4 = 0.406; use 100 C_2H_4 flame-stability diagram.

Total percentage of H_2/CH_4 = 15.2 + 37.4 = 52.6; total percentage of C_2H_4 = 33.4.

	A (figure 29)	B	C (figure 22)	D	B + D
F_B	g_B for H_2/CH_4 = 0.406	A × 0.526	g_B for 100% C_2H_4	C × 0.334	g_B for total fuel
0.6	120	63	370	124	187
.7	330	174	1,600	534	708
.8	1,330	700	3,850	1,285	1,985
.9	2,650	1,395	6,700	2,240	3,635
1.0	4,500	2,370	10,000	3,340	5,710
1.2	9,650	5,080	17,000	5,680	10,760
1.4	15,900	8,360	26,000	8,680	17,040
1.8	35,500	18,700	44,000	14,700	33,400
2.2	61,000	32,100	61,500	20,550	52,650
2.6	95,000	50,000	76,000	25,400	75,400
3.0	143,000	75,200	92,000	30,700	105,900

1/ Compare with experimental points (A-T/3a,3b-No./55).

TABLE 4. - Calculation of flame-stability diagram by linear mixture rule (Con.); mixture of oil-gas type (Con.)

Fuel No. 56[1/] composition, percent: 29.1 CH_4, 26.2 C_2H_4, 22.1 C_3H_8, 11.8 H_2, 0.2 C_3H_6,[2/] 10.6 N_2

Stoichiometric percentage: 7.6

Complexes for flashback: $(C_2H_4 + H_2)(CH_4)(C_3H_8)(N_2)$.

Calc. of complexes: $H_2/C_2H_4 = 11.8/26.2 = 0.45$; use 100% CH_4 flame-stability diagram; use 100% C_3H_8 flame-stability diagram .

Total percentage of $H_2/C_2H_4 = 11.8 + 26.2 = 38.0$; total percentage of $CH_4 = 29.1$; total percentage of $C_3H_8 = 22.3$.

F_F	A (figure 36)	B	C (figure 20)	D	E (figure 21)	F	B + D + F
	g_F for $H_2/C_2H_4 = 0.45$	A × 0.38	g_F for 100% CH_4	C × 0.291	g_F for 100% C_3H_8	E × 0.223	g_F for total fuel
0.6	305	117					117
.7	615	234					234
.75	830	315	135	39	155	35	389
.8	1,060	403	190	55	230	51	509
.9	1,430	544	330	96	420	94	734
1.0	1,680	638	390	114	590	132	884
1.1	1,770	672	340	99	640	143	914
1.2	1,480	562	180	52	570	127	741
1.25	1,300	494	120	35	520	116	645
1.3	1,090	414			460	103	517
1.4	715	272			310	69	341
1.5	413	157			170	38	195
1.6	220	84					84

Complexes for blowoff: $(CH_4 + H_2)(C_3H_8 + H_2)(C_2H_4)(N_2)$.

Calc. of complexes: $(29.1/29.1 + 22.3) \times 11.8 = 6.68$ (H_2 going with CH_4); $H_2/CH_4 = 6.68/29.1 = 0.23$;

$(22.3/29.1 + 22.3) \times 11.8 = 5.12$ (H_2 going with C_3H_8); $H_2/C_3H_8 = 5.12/22.3 = 0.23$; use 100% C_2H_4 flame-stability diagram .

Total percentage of $H_2/CH_4 = 6.68 + 29.1 = 35.78$; total percentage of $H_2/C_3H_8 = 5.12 + 22.3 = 27.42$;

total percentage of $C_2H_4 = 26.2$.

F_B	A (figure 29)	B	C (figure 35)	D	E (figure 22)	F	B + D + F
	g_B for $H_2/CH_4 = 0.23$	A × 0.3578	g_B for $H_2/C_3H_8 = 0.23$	C × 0.2742	g_B for 100% C_2H_4	E × 0.262	g_B for total fuel
0.6					370	97	97
.7	290	104	300	82	1,600	419	605
.8	950	340	1,000	274	3,850	1,010	1,624
.9	1,930	690	2,000	548	6,700	1,755	2,993
1.0	3,380	1,210	3,300	905	10,000	2,620	4,735
1.2	6,800	2,430	5,850	1,605	17,000	4,450	8,485
1.4	10,500	3,760	8,050	2,210	26,000	6,810	12,780
1.8	20,800	7,440	13,200	3,620	44,000	11,530	22,590
2.2	33,500	12,000	16,800	4,610	61,500	16,100	32,710
2.6	48,000	17,160	19,700	5,400	76,000	19,900	42,460
3.0	73,000	26,100	23,200	6,360	92,000	24,100	56,560

1/ Compare with experimental points (A-T/3a,3b-No./56).
2/ Tally with propane.

TABLE 4. - Calculation of flame-stability diagram by linear mixture rule (Con.); mixture of oil-gas type (Con.)

Fuel No. 57[1/] composition, percent: 32.1 CH_4, 28.4 C_2H_4, 12.5 H_2, 27.0 N_2

Stoichiometric percentage: 11.8

Complexes for flashback: $(C_2H_4 + H_2)(CH_4)(N_2)$

Calc. of complexes: H_2/C_2H_4 = 12.5/28.4 = 0.44; use 100% CH_4 flame-stability diagram.

Total percentage of H_2/C_2H_4 = 12.5 + 28.4 = 40.9; total percentage of CH_4 = 32.1.

F_F	A (figure 36) g_F for H_2/C_2H_4 = 0.44	B A × 0.409	C (figure 20) g_F for 100% CH_4	D C × 0.321	B + D g_F for total fuel
0.6	300	123			123
.7	605	247			247
.75	820	335	135	43	378
.8	1,050	429	190	61	490
.9	1,420	581	330	106	687
1.0	1,670	683	390	125	808
1.1	1,760	720	340	109	829
1.2	1,480	605	180	58	663
1.25	1,300	532	120	39	571
1.3	1,090	446			446
1.4	715	292			292
1.5	410	168			168
1.6	219	90			90

Complexes for blowoff: $(CH_4 + H_2)(C_2H_4)(N_2)$.

Calc. of complexes: H_2/CH_4 = 12.5/32.1 = 0.39; use 100% C_2H_4 flame-stability diagram.

Total percentage of H_2/CH_4 = 12.5 + 32.1 = 44.6; total percentage of C_2H_4 = 28.4.

F_B	A (figure 29) g_B for H_2/CH_4 = 0.39	B A × 0.446	C (figure 22) g_B for 100% C_2H_4	D C × 0.284	B + D g_B for total fuel
0.6	120	54	370	105	159
.7	327	146	1,600	454	600
.8	1,300	580	3,850	1,094	1,674
.9	2,600	1,160	6,700	1,904	3,064
1.0	4,400	1,963	10,000	2,840	4,803
1.2	9,500	4,240	17,000	4,830	9,070
1.4	15,600	6,960	26,000	7,380	14,340
1.8	35,000	15,600	44,000	12,500	28,100
2.2	60,000	26,800	61,500	17,460	44,260
2.6	92,500	41,200	76,000	21,600	62,800
3.0	139,000	62,000	92,000	26,100	88,100

1/ Compare with experimental points (A-T/3a,3b-No./57).

TABLE 4. - Calculation of flame-stability diagram by linear mixture rule (Con.); other mixture

Fuel No. 58[1/] composition, percent: 62.5 CH_4, 22.2 H_2, 15.3 N_2

Stoichiometric percentage: 13.3 (Curves for figure 46)

Complexes for flashback: $(CH_4 + H_2)(N_2)$.

Calc. of complexes: H_2/CH_4 = 22.2/62.5 = 0.355.

Total percentage of H_2/CH_4 = 22.2 + 62.5 = 84.7.

F_F	A (figure 28) g_F for H_2/CH_4 = 0.355	B A × 0.847 g_F for total fuel
0.7	160	136
.75	230	195
.8	310	263
.9	495	419
1.0	610	516
1.1	490	415
1.2	325	275
1.25	240	203
1.3	130	110

Complexes for blowoff: $(CH_4 + H_2)(N_2)$.

Calc. of complexes: H_2/CH_4 = 22.2/62.5 = 0.355.

Total percentage of H_2/CH_4 = 22.2 + 62.5 = 84.7.

F_B	A (figure 29) g_B for H_2/CH_4 = 0.355	B A × 0.847 g_B for total fuel
0.7	310	263
.8	1,200	1,016
.9	2,350	1,990
1.0	3,950	3,345
1.2	8,700	7,370
1.4	14,500	12,300
1.8	30,500	25,800
2.2	48,500	41,100
2.6	73,000	61,800
3.0	108,000	91,500

1/ Compare with experimental points (A-T/3a,3b-No./58).

TABLE 4. - Calculation of flame-stability diagram by linear mixture rule (Con.); other mixture (Con.)

Fuel No. 59[1/] composition, percent: 47.4 CO, 25.9 H_2, 26.5 N_2, 0.2 CO_2

Stoichiometric percentage: 36.3

Complexes for flashback: (CO + H_2)(N_2 and CO_2).

Calc. of complexes: H_2/CO = 25.9/47.4 = 0.546.

Total percentage of H_2/CO = 25.9 + 47.4 = 73.3.

F_F	A (figure 30) g_F for H_2/CO = 0.546	B A × 0.733 g_F for total fuel
0.6	330	242
.7	690	506
.75	920	674
.8	1,200	870
.9	1,850	1,356
1.0	2,450	1,795
1.1	3,100	2,270
1.2	3,700	2,710
1.25	3,900	2,860
1.3	4,050	2,970
1.4	4,200	2,080
1.6	4,000	2,930
1.8	2,850	3,090
2.0	1,080	792

Complexes for blowoff: (CO + H_2)(N_2 and CO_2).

Calc. of complexes: H_2/CO = 25.9/47.4 = 0.546.

Total percentage of H_2/CO = 25.9 + 47.4 = 73.3.

F_B	A (figure 31) g_B for H_2/CO = 0.546	B A × 0.733 g_B for total fuel
0.6	850	623
.7	3,050	2,235
.8	8,500	6,230
.9	16,500	12,100
1.0	28,500	20,900
1.2	74,000	54,200
1.4	170,000	124,500
1.8	510,000	374,000
2.2	1,070,000	784,000
2.6	1,580,000	1,160,000
3.0	1,800,000	1,320,000

1/ Compare with experimental points (A-T/3a,3b-No./59).

TABLE 4. - Calculation of flame-stability diagram by linear mixture rule (Con.); other mixture (Con.)

Fuel No. 60[1/] composition, percent:	40.8 CO, 22.1 H_2, 36.9 N_2, 0.2 CO_2
Stoichiometric percentage:	39.9

Complexes for flashback: $(CO + H_2)(N_2$ and $CO_2)$.

Calc. of complexes: $H_2/CO = 22.1/40.8 = 0.542$.

Total percentage of $H_2/CO = 22.1 + 40.8 = 62.9$.

F_F	A (figure 30) g_F for $H_2/CO = 0.542$	B A × 0.629 g_F for total fuel
0.6	330	208
.7	690	434
.75	920	578
.8	1,200	754
.9	1,850	1,164
1.0	2,450	1,540
1.1	3,100	1,950
1.2	3,700	2,330
1.25	3,900	2,450
1.3	4,050	2,550
1.4	4,200	2,640
1.6	4,000	2,515
1.8	2,850	1,793
2.0	1,080	680

Complexes for blowoff: $(CO + H_2)(N_2$ and $CO_2)$.

Calc. of complexes: $H_2/CO = 22.1/40.8 = 0.542$.

Total percentage of $H_2/CO = 22.1 + 40.8 = 62.9$.

F_B	A (figure 31) g_B for $H_2/CO = 0.542$	B A × 0.629 g_B for total fuel
0.6	850	534
.7	3,050	1,920
.8	8,500	5,340
.9	16,500	10,380
1.0	28,500	17,930
1.2	74,000	46,500
1.4	170,000	107,000
1.8	510,000	321,000
2.2	1,070,000	673,000
2.6	1,580,000	994,000
3.0	1,800,000	1,133,000

1/ Compare with experimental points (A-T/3a,3b-No./60).

TABLE 4. - Calculation of flame-stability diagram by linear mixture rule (Con.); other mixture (Con.)

Fuel No. 61[1/] composition, percent: 49.4 CH_4, 22.2 H_2, 16.1 CO, 11.5 CO_2, 0.8 N_2

Stoichiometric percentage: 15.0

Complexes for flashback: (CH_4 + CO)(CH_4 + H_2)(N_2 and CO_2).

Calc. of complexes: (16.1/16.1 + 22.2) × 49.4 = 20.8 (CH_4 going with CO); CO/CH_4 = 16.1/20.8 = 0.774;

(22.2/16.1 + 22.2) × 49.4 = 28.6 (CH_4 going with H_2); H_2/CH_4 = 22.2/28.6 = 0.776.

Total percentage of CO/CH_4 = 16.1 + 20.8 = 36.9; total percentage of H_2/CH_4 = 22.2 + 28.6 = 50.8.

	A (figure 32)	B	C (figure 28)	D	B + D
F_F	g_F for CO/CH_4 = 0.774	A × 0.369	g_F for H_2/CH_4 = 0.776	C × 0.508	g_F for total fuel
0.7	111	41	340	173	214
.75	182	67	460	234	301
.8	253	93	565	287	380
.9	413	153	765	389	542
1.0	535	198	880	447	645
1.1	575	212	725	368	580
1.2	485	179	465	236	415
1.25	393	145	345	175	320
1.3	280	103	168	85	188

Complexes for blowoff: (CH_4 + H_2)(H_2/CO = 0.20).

Calc. of complexes: H_2/CO = 0.20, 0.20× 16.1 = 3.22 (H_2 going with CO); H_2/CO = 3.22/16.1 = 0.20;

22.2 - 3.22 = 18.98 (H_2 going with CH_4); H_2/CH_4 = 18.98/49.4 = 0.384.

Total percentage of H_2/CO = 3.22 + 16.1 = 19.32; total percentage of H_2/CH_4 = 18.98 + 49.4 = 68.38.

	A (figure 31)	B	C (figure 29)	D	B + D
F_B	g_B for H_2/CO = 0.20	A × 0.1932	g_B for H_2/CH_4 = 0.384	C × 0.6838	g_B for total fuel
0.6	250	48	118	81	129
.7	1,000	193	321	219	412
.8	2,700	522	1,280	874	1,396
.9	5,300	1,024	2,570	1,760	2,784
1.0	9,500	1,835	4,350	2,970	4,805
1.2	22,000	4,250	9,350	6,390	10,640
1.4	41,000	7,920	15,400	10,530	18,450
1.8	111,000	21,450	34,000	23,200	44,650
2.2	225,000	43,500	58,000	39,600	83,100
2.6	380,000	73,400	88,500	60,500	133,900
3.0	560,000	108,000	134,000	91,600	199,600

1/ Compare with experimental points (A-T/3a,3b-No./61).

TABLE 4. - Calculation of flame-stability diagram by linear mixture rule (Con.); other mixture (Con.)

Fuel No. 62[1/] composition, percent: 65.2 C_2H_4, 18.7 H_2, 16.1 CH_4

Stoichiometric percentage: 8.1

Complexes for flashback: $(C_2H_4 + H_2)(CH_4)$.

Calc. of complexes: H_2/C_2H_4 = 18.7/65.2 = 0.287; use 100% CH_4 flame-stability diagram.

Total percentage of H_2/C_2H_4 = 18.7 + 65.2 = 83.9; total percentage of CH_4 = 16.1.

	A (figure 36)	B	C (figure 20)	D	B + D
F_F	g_F for H_2/C_2H_4 = 0.287	A × 0.839	g_F for 100% CH_4	C × 0.161	g_F for total fuel
0.6	220	185			185
.7	515	432			432
.75	720	604	135	22	626
.8	945	793	190	31	824
.9	1,280	1,075	330	53	1,128
1.0	1,550	1,300	390	63	1,363
1.1	1,700	1,425	340	55	1,480
1.2	1,450	1,216	180	29	1,245
1.25	1,300	1,090	120	19	1,109
1.3	1,100	924			924
1.4	755	634			634
1.5	445	373			373
1.6	230	193			193

Complexes for blowoff: $(C_2H_4 + H_2)(CH_4)$.

Calc. of complexes: H_2/C_2H_4 = 18.7/65.2 = 0.287; use 100% CH_4 flame-stability diagram.

Total percentage of H_2/C_2H_4 = 18.7 + 65.2 = 83.9; total percentage of CH_4 = 16.1.

	A (figure 37)	B	C (figure 20)	D	B + D
F_B	g_B for H_2/C_2H_4 = 0.287	A × 0.839	g_B for 100% CH_4	C × 0.161	g_B for total fuel
0.6	480	403			403
.7	2,030	1,703	170	27	1,730
.8	4,400	3,690	530	85	3,775
.9	7,550	6,340	1,100	177	6,517
1.0	11,000	9,220	1,950	314	9,534
1.2	20,500	17,200	3,750	604	17,800
1.4	31,500	26,400	5,380	866	27,270
1.8	56,500	47,400	8,300	1,336	48,740
2.2	82,000	68,800	11,000	1,770	70,570
2.6	105,000	88,100	14,300	2,300	90,400
3.0	127,000	106,500	18,000	2,900	109,400

1/ Compare with experimental points (A-T/3a,3b-No./62).

TABLE 4. - Calculation of flame-stability diagram by linear mixture rule (Con.); other mixture (Con.)

Fuel No. 63[1/] composition, percent: 56.5 C_2H_4, 15.8 H_2, 13.8 CH_4, 0.1 C_3H_6,[2/] 13.8 N_2
Stoichiometric percentage: 9.24 (Curves for figure 45)

Complexes for flashback: $(C_2H_4 + H_2)(CH_4)$.

Calc. of complexes: H_2/C_2H_4 = 15.8/56.6 = 0.279; use 100% CH_4 **flame-stability diagram**.

Total percentage of H_2/C_2H_4 = 15.8 + 56.6 = 72.4; total percentage of CH_4 = 13.8.

F_F	A (figure 36) g_F for H_2/C_2H_4 = 0.279	B A × 0.724	C (figure 20) g_F for 100% CH_4	D C × 0.138	B + D g_F for total fuel
0.6	215	156			156
.7	510	369			369
.75	715	518	135	19	537
.8	935	677	190	26	703
.9	1,270	919	330	46	965
1.0	1,550	1,122	390	54	1,176
1.1	1,670	1,210	340	47	1,257
1.2	1,440	1,043	180	25	1,068
1.25	1,280	926	120	17	943
1.3	1,100	796			796
1.4	755	546			546
1.5	440	319			319
1.6	228	165			165

Complexes for blowoff: $(C_2H_4 + H_2)(CH_4)$.

Calc. of complexes: H_2/C_2H_4 = 15.8/56.6 = 0.279; use 100% CH_4 **flame-stability diagram**.

Total percentage of H_2/C_2H_4 = 15.8 + 56.6 = 72.4; total percentage of CH_4 = 13.8.

F_B	A (figure 37) g_B for H_2/C_2H_4 = 0.279	B A × 0.724	C (figure 20) g_B for 100% CH_4	D C × 0.138	B + D g_B for total fuel
0.6	475	344			344
.7	2,000	1,450	170	23	1,473
.8	4,350	3,150	530	73	3,223
.9	7,500	5,430	1,100	152	5,582
1.0	11,000	7,960	1,950	269	8,229
1.2	20,300	14,700	3,750	518	15,220
1.4	31,200	22,600	5,380	742	23,340
1.8	56,000	40,600	8,300	1,145	41,750
2.2	81,000	58,600	11,000	1,520	60,120
2.6	105,000	76,000	14,300	1,975	77,980
3.0	125,000	90,400	18,000	2,480	92,880

1/ Compare with experimental points (A-T/3a,3b-No./63).
2/ Tally with C_2H_4.

TABLE 4. - Calculation of flame-stability diagram by linear mixture rule (Con.); other mixture (Con.)

Fuel No. 64[1] composition, percent: 55.1 C_2H_4, 18.8 CH_4, 15.8 H_2, 10.2 CO, 0.1 C_3H_6[2]

Stoichiometric percentage: 8.81

Complexes for flashback: $(C_2H_4 + H_2)(CH_4 + CO)$.

Calc. of complexes: H_2/C_2H_4 = 15.8/55.2 = 0.286; CO/CH_4 = 10.2/18.8 = 0.543.

Total percentage of H_2/C_2H_4 = 15.8 + 55.2 = 71.0; total percentage of CO/CH_4 = 10.2 + 18.8 = 29.0.

F_F	A (figure 36) g_F for H_2/C_2H_4 = 0.286	B A × 0.710	C (figure 32) g_F for CO/CH_4 = 0.543	D C × 0.290	B + D g_F for total fuel
0.6	220	156			156
.7	515	366	104	30	396
.75	720	511	163	47	558
.8	945	671	227	66	737
.9	1,280	909	394	114	1,023
1.0	1,550	1,100	500	145	1,245
1.1	1,700	1,206	503	146	1,352
1.2	1,450	1,030	383	111	1,141
1.25	1,300	923	290	84	1,007
1.3	1,100	781	193	56	837
1.4	755	536			536
1.5	445	316			316
1.6	230	164			164

Complexes for blowoff: $(C_2H_4 + H_2)(CH_4 + CO)$.

Calc. of complexes: H_2/C_2H_4 = 15.8/55.2 = 0.286; CO/CH_4 = 10.2/18.8 = 0.543.

Total percentage of H_2/C_2H_4 = 15.8 + 55.2 = 71.0; total percentage of CO/CH_4 = 10.2 + 18.8 = 29.0.

F_B	A (figure 37) g_B for H_2/C_2H_4 = 0.286	B A × 0.710	C (figure 33) g_B for CO/CH_4 = 0.543	D C × 0.290	B + D g_B for total fuel
0.6	480	341			341
.7	2,030	1,440	206	60	1,500
.8	4,400	3,120	595	173	3,293
.9	7,550	5,360	1,410	409	5,769
1.0	11,000	7,810	2,530	734	8,544
1.2	20,500	14,550	5,000	1,450	16,000
1.4	31,500	22,400	7,050	2,045	24,450
1.8	56,500	40,100	11,300	3,280	43,380
2.2	82,000	58,200	15,000	4,350	62,550
2.6	105,000	74,600	19,700	5,720	80,320
3.0	127,000	90,200	25,500	7,400	97,600

1/ Compare with experimental points (A-T/3a,3b-No./64).
2/ Tally with C_2H_4.

TABLE 4. - Calculation of flame-stability diagram by linear mixture rule (Con.); other mixture (Con.)

Fuel No. 65[1/] composition, percent: 36.4 H_2, 22.6 CO, 13.3 CH_4, 7.2 C_2H_6,[2/] 5.8 C_2H_4,[2/] 1.9 C_3H_8,[2/] 0.1 C_3H_6,[2/] 9.8 N_2, 2.9 CO_2

Stoichiometric percentage: 16.1

Complexes for flashback: (CH_4 + CO)(CH_4 + H_2)(N_2 and CO_2).

Calc. of complexes: (22.6/22.6 + 36.4) × 28.3 = 10.85 (CH_4 going with CO); CH_4/CO = 10.85/22.6 = 0.48;

(36.4/22.6 + 36.4) × 28.3 = 17.45 (CH_4 going with H_2); CH_4/H_2 = 17.45/36.4 = 0.48.

Total percentage of CH_4/CO = 10.85 + 22.6 = 33.45; total percentage of CH_4/H_2 = 17.45 + 36.4 = 53.85.

	A (figure 32)	B	C (figure 28)	D	B + D
F_F	g_F for CH_4/CO = 0.48	A × 0.3345	g_F for CH_4/H_2 = 0.48	C × 0.5385	g_F for total fuel
0.6			430	232	232
.7	160	54	910	490	544
.75	270	90	1,170	630	720
.8	375	126	1,450	781	907
.9	570	191	1,800	970	1,161
1.0	760	254	1,970	1,060	1,314
1.1	860	288	1,750	942	1,230
1.2	820	274	1,230	662	936
1.25	730	244	850	458	702
1.3	610	204	550	296	500
1.4	330	110	143	77	187

Complexes for blowoff: (CH_4 + H_2)(H_2/CO = 0.20)(N_2 and CO_2).

Calc. of complexes: H_2/CO = 0.20, 0.20 × 22.6 = 4.52 (H_2 going with CO); H_2/CO = 4.52/22.6 = 0.20;

36.4 - 4.52 = 31.88 (H_2 going with CH_4); CH_4/H_2 = 28.3/31.88 = 0.888.

Total percentage of H_2/CO = 4.52 + 22.6 = 27.12; total percentage of CH_4/H_2 = 28.3 + 31.88 = 60.18.

	A (figure 31)	B	C (figure 29)	D	B + D
F_B	g_B for H_2/CO = 0.20	A × 0.2712	g_B for CH_4/H_2 = 0.888	C × 0.6018	g_B for total fuel
0.6	250	68	330	199	267
.7	1,000	271	1,570	944	1,215
.8	2,700	733	4,800	2,890	3,623
.9	5,300	1,440	9,650	5,800	7,240
1.0	9,500	2,580	15,500	9,320	11,900
1.2	22,000	5,970	37,000	22,250	28,220
1.4	41,000	11,120	76,000	45,700	56,820
1.8	111,000	30,100	238,000	143,000	173,100
2.2	225,000	61,000	530,000	319,000	380,000
2.6	380,000	103,000	960,000	578,000	681,000
3.0	560,000	152,000	1,800,000	1,083,000	1,235,000

1/ Compare with experimental points (A-T/3a,3b-No./65).
2/ Tally with CH_4.

TABLE 4. - Calculation of flame-stability diagram by linear mixture rule (Con.); other mixture (Con.)

Fuel No. 66[1] composition, percent: 42.6 CH_4, 18.1 C_2H_4, 17.0 H_2, 9.1 CO, 2.2 C_2H_6,[2] 1.9 C_3H_8,[2] 0.2 C_3H_6,[3] 0.2 C_4H_{10},[2] 0.1 C_4H_8,[3] 5.2 CO_2, 3.4 N_2

Stoichiometric percentage: 10.8

Complexes for flashback: $(C_2H_4 + H_2)(CH_4 + CO)(N_2 \text{ and } CO_2)$.

Calc. of complexes: $H_2/C_2H_4 = 17.0/18.4 = 0.924$; $CO/CH_4 = 9.1/46.9 = 0.194$.

Total percentage of $H_2/C_2H_4 = 17.0 + 18.4 = 35.4$; total percentage of $CO/CH_4 = 9.1 + 46.9 = 56.0$.

F_F	A (figure 36) g_F for $H_2/C_2H_4 = 0.924$	B A × 0.354	C (figure 32) g_F for $CO/CH_4 = 0.194$	D C × 0.560	B + D g_F for total fuel
0.5	124	44			44
.6	440	156			156
.7	940	333			333
.75	1,130	400	140	78	478
.8	1,380	489	197	111	600
.9	1,760	623	355	199	822
1.0	1,980	702	428	240	942
1.1	1,880	666	395	221	887
1.2	1,530	542	250	140	682
1.25	1,320	467	175	98	565
1.3	970	343	103	58	401
1.4	595	211			211
1.5	345	122			122
1.6	180	64			64

Complexes for blowoff: $(CH_4 + H_2)(CH_4 + CO)(C_2H_4)(N_2 \text{ and } CO_2)$.

Calc. of complexes: $(17.0/17.0 + 9.1) \times 46.9 = 30.55$ (CH_4 going with H_2); $H_2/CH_4 = 17.0/30.55 = 0.556$;

$(9.1/17.0 + 9.1) \times 46.9 = 16.35$ (CH_4 going with CO); $CO/CH_4 = 9.1/16.35 = 0.556$; use 100% C_2H_4 flame-stability diagram.

Total percentage of $H_2/CH_4 = 17.0 + 30.55 = 47.55$; total percentage of $CO/CH_4 = 9.1 + 16.35 = 25.45$; total percentage of $C_2H_4 = 18.4$.

F_B	A (figure 29) g_B for $H_2/CH_4 = 0.556$	B A × 0.4755	C (figure 33) g_B for $CO/CH_4 = 0.556$	D C × 0.2545	E (figure 22) g_B for 100% C_2H_4	F E × 0.184	B + D + F g_B for total fuel
0.6	150	71			370	68	139
.7	460	219	208	53	1,600	294	566
.8	1,770	842	600	153	3,850	708	1,703
.9	3,500	1,665	1,430	364	6,700	1,233	3,262
1.0	5,850	2,780	2,550	649	10,000	1,840	5,269
1.2	13,000	6,180	5,050	1,285	17,000	3,130	10,600
1.4	22,800	10,850	7,150	1,820	26,000	4,780	17,450
1.8	55,000	26,200	11,400	2,900	44,000	8,100	37,200
2.2	103,000	49,000	15,500	3,820	61,500	11,320	64,140
2.6	172,000	81,800	20,000	5,090	76,000	14,000	100,900
3.0	265,000	126,000	25,700	6,540	92,000	16,920	149,500

1/ Compare with experimental points (A-T/3a,3b-No./66).
2/ Tally with CH_4.
3/ Tally with C_2H_4.

TABLE 4. - Calculation of flame-stability diagram by linear mixture rule (Con.); other mixture (Con.)

Fuel No. 67[1] composition, percent: 37.5 CH_4, 20.4 C_2H_4, 17.5 H_2, 3.9 CO, 13.3 N_2, 7.4 CO_2

Stoichiometric percentage: 12.5 (Curves for figure 44)

Complexes for flashback: $(C_2H_4 + H_2)(CH_4 + CO)(N_2$ and $CO_2)$.

Calc. of complexes: H_2/C_2H_4 = 17.5/20.4 = 0.858; CO/CH_4 = 3.9/37.5 = 0.104.

Total percentage of H_2/C_2H_4 = 17.5 + 20.4 = 37.9; total percentage of CO/CH_4 = 3.9 + 37.5 = 41.4.

F_F	A (figure 36) g_F for H_2/C_2H_4 = 0.858	B A × 0.379	C (figure 32) g_F for CO/CH_4 = 0.104	D C × 0.414	B + D g_F for total fuel
0.5	106	40			40
.6	430	163			163
.7	910	345			345
.75	1,100	416	137	57	473
.8	1,340	507	193	80	587
.9	1,740	659	345	143	802
1.0	1,940	734	410	170	904
1.1	1,850	700	370	153	853
1.2	1,510	572	217	90	662
1.25	1,300	492	150	62	554
1.3	955	362			362
1.4	580	220			220
1.5	337	128			128
1.6	177	67			67

Complexes for blowoff: $(CH_4 + H_2)(CH_4 + CO)(C_2H_4)(N_2$ and $CO_2)$.

Calc. of complexes: (17.5/17.5 + 3.9) × 37.5 = 30.67 (CH_4 going with H_2); H_2/CH_4 = 17.5/30.67 = 0.571;

(3.9/17.5 + 3.9) × 37.5 = 6.83 (CH_4 going with CO); CO/CH_4 = 3.9/6.83 = 0.571; use 100% C_2H_4 flame-stability diagram.

Total percentage of H_2/CH_4 = 17.5 + 30.67 = 48.17; total percentage of CO/CH_4 = 3.9 + 6.83 = 10.73; total percentage of C_2H_4 = 20.4.

F_B	A (figure 29) g_B for H_2/CH_4 = 0.571	B A × 0.4817	C (figure 33) g_B for CO/CH_4 = 0.571	D C × 0.1073	E (figure 22) g_B for 100% C_2H_4	F E × 0.204	B + D + F g_B for total fuel
0.6	152	73			370	76	149
.7	475	229	208	22	1,600	326	577
.8	1,840	886	605	65	3,850	786	1,737
.9	3,620	1,745	1,430	153	6,700	1,366	3,264
1.0	6,000	2,890	2,570	276	10,000	2,040	5,206
1.2	13,400	6,460	5,080	545	17,000	3,470	10,480
1.4	23,800	11,450	7,200	772	26,000	5,300	17,520
1.8	58,000	27,900	11,400	1,224	44,000	8,980	38,100
2.2	111,000	53,400	15,400	1,653	61,500	12,550	67,600
2.6	185,000	89,100	20,200	2,170	76,000	15,500	106,800
3.0	286,000	137,600	25,900	2,780	92,000	18,760	159,100

1/ Compare with experimental points (A-T/3a,3b-No./67).

TABLE 5. - Yellow-tip limits of fuel gases; methane - propane group[1/] - ethylene

Long cylindrical tubes; $g = (32\ V)/(\pi D^3)$

Noncircular and sharp-edged short ports; $g = (\lambda\ V\ Re)/(2\pi D^3)$

Fuel No. 2 composition, percent: 100 CH_4 $F_c = 1.80$

Stoichiometric percentage: 9.46 (Points for figure 49 and data for figures 52-59) C_3H_8 group/CH_4 = 0/100 = 0

Tube diam. 3.78 cm.		Tube diam. 2.47 cm.		Tube diam. 1.914 cm.		Tube diam. 1.503 cm.		Tube diam. 0.776 cm.		Tube diam. 0.413 cm.		Tube diam. 0.294 cm.		Tube diam. 0.195 cm.	
F_y	g_y	F_y	g_y	F_y	g_y	F_y	g_y	F_y	g_y	F_y	g_y	F_y	g_y	F_y	g_y
2.20	11.0	3.12	16.6	3.09	36.3	3.02	72.6	3.06	530	4.46	794	4.52	2,220	4.82	8,000
2.10	14.4	2.79	26.6	2.70	57.5	2.75	119	2.68	854	4.04	1,220	4.18	3,455	4.48	12,430
2.11	23.3	2.54	40.2	2.37	85.3	2.58	181	2.63	1,330	3.74	1,818	3.98	5,260	4.32	18,900
1.87	35.2	2.34	52.5	2.09	181	2.53	307			3.62	2,470	3.87	7,080	4.18	25,400
1.79	62.2	1.99	128	2.14	279	2.39	595			3.48	3,270	3.74	9,410	4.11	33,150
		1.85	227	2.20	515	1.94	1,015			3.41	4,305	3.63	12,300	4.05	38,200
										3.22	6,130	3.53	17,730		
										3.10	9,450				

Fuel No. 68 composition, percent: (Natural gas) 89.5 CH_4, 6.7 C_2H_6, 2.7 C_3H_8, 0.4 C_3H_6, 0.4 C_4H_{10}, 0.3 CO_2 $F_c = 1.78$

Stoichiometric percentage: 8.66 (Points for figure 50 and data for figures 52-56) C_3H_8 group/CH_4 = 10.2/89.5 = 0.114

Tube diam. 5.08 cm.		Tube diam. 3.78 cm.		Tube diam. 3.15 cm.		Tube diam. 2.47 cm.		Tube diam. 2.06 cm.		Tube diam. 1.914 cm.		Tube diam. 1.503 cm.		Tube diam. 1.43 cm.		Tube diam. 1.023 cm.	
F_y	g_y	F_y	g_y	F_y	g_y	F_y	g_y	F_y	g_y	F_y	g_y	F_y	g_y	F_y	g_y	F_y	g_y
1.80	2/ 287	2.27	10.5	1.81	131	2.83	15.4	1.78	610	2.83	33.1	2.77	69.1	1.97	1,320	3.06	221
1.74	2/ 710	2.15	14.1	1.81	266	2.60	25.1	1.85	2/1,800	2.49	53.2	2.56	112	1.88	2/3,590	2.72	356
1.79	2/ 986	1.85	29.1	1.75	2/ 767	2.37	37.8	1.76	2/2,880	2.17	80.2	2.40	167	1.86	2/6,070	2.36	538
1.74	2/1,325	1.79	41.9	1.76	2/1,210	2.24	50.6	1.81	2/4,270	2.00	108	2.23	226	1.83	2/8,930	2.29	721
1.76	2/1,715	1.76	53.2	1.78	2/1,700	2.05	83.3	1.75	2/5,790	2.00	174	2.05	363			2.23	932
1.82	2/2,450	1.76	60.2			1.85	105	1.79	2/7,500	1.87	226	2.00	467			2.36	1,193
1.82	2/3,220					1.84	138			1.91	299	2.03	630			2.29	1,523
						1.80	183			1.88	393					2.23	2,015

Tube diam. 0.776 cm.		Tube diam. 0.535 cm.		Tube diam. 0.413 cm.		Tube diam. 0.354 cm.		Tube diam. 0.294 cm.		Tube diam. 0.249 cm.		Tube diam. 0.195 cm.		Tube diam. 0.155 cm.	
F_y	g_y	F_y	g_y	F_y	g_y	F_y	g_y	F_y	g_y	F_y	g_y	F_y	g_y	F_y	g_y
3.09	509	4.27	333	4.39	719	4.39	1,150	4.43	2,018	4.43	3,372	4.74	7,230	4.71	14,580
2.72	818	3.89	517	3.94	1,132	4.00	1,813	4.09	3,193	4.14	5,450	4.46	11,210	4.48	22,600
2.53	1,245	3.60	767	3.69	1,697	3.71	2,708	3.84	4,770	3.97	7,980	4.19	16,620	4.37	28,000
2.42	1,675	3.35	1,038	3.48	2,315	3.58	3,648	3.6[illegible]	6,420	3.83	10,920	3.98	23,830	4.34	33,150
2.47	2,190	3.20	1,348	3.32	3,013	3.40	4,820	3.60	8,550	3.71	14,280	3.85	30,800		
2.45	2,778	3.06	1,550	3.21	3,770	3.26	6,085	3.55	9,960	3.68	16,480	3.84	35,900		
2.37	3,620	2.88	2,580	3.11	6,000	3.19	9,220	3.48	10,830	3.66	18,100				
		2.83	3,965	2.99	8,630	3.15	14,250	3.38	16,320	3.60	23,000				
		2.83	5,350	2.91	12,060			3.35	19,890						
		2.80	7,060	2.90	15,400										

1/ Propane group is average of (A-T/5-No./73, 3, 5, 74, 75).
2/ Turbulent flow.

TABLE 5. - Yellow-tip limits of fuel gases; methane- propane group[1]- ethylene (Con.)

Long cylindrical tubes; $g = (32\ V)/(\pi D^3)$

Noncircular and sharp-edged short ports; $g = (\lambda V\ Re)/(2\pi D^3)$

Fuel No. 69 composition, percent: 75.2 CH_4, 22.2 C_3H_8, 2.6 C_2H_6 — F_c = 1.76

Stoichiometric percentage: 7.17 — (Data for figures 52-56) — C_3H_8 group/CH_4 = 24.8/75.2 = 0.331

Tube diam. 1.914 cm.		Tube diam. 1.503 cm.		Tube diam. 1.247 cm.		Tube diam. 1.023 cm.		Tube diam. 0.891 cm.		Tube diam. 0.776 cm.	
F_y	g_y	F_y	g_y	F_y	g_y	F_y	g_y	F_y	g_y	F_y	g_y
2.08	38.4	2.30	44.1	3.24	24.5	3.11	46.7	3.11	70.7	3.11	107
1.83	112	2.16	71.6	2.50	60.7	2.37	141	2.40	213	2.40	323
1.79	169	1.86	234	2.31	112	2.26	201	2.26	305	2.26	462
1.79	239	1.77	346	1.88	402	1.86	740	1.92	1,126	1.96	1,714
1.75	317	1.77	485	1.80	603	1.91	1,108	1.99	1,690	2.02	2,560
				1.79	862	1.89	1,537	1.91	2,313	1.96	3,585
				1.75	1,095	1.84	2,073	1.90	3,163		

Tube diam. 0.611 cm.		Tube diam. 0.535 cm.		Tube diam. 0.413 cm.		Tube diam. 0.354 cm.		Tube diam. 0.249 cm.		Tube diam. 0.195 cm.	
F_y	g_y	F_y	g_y	F_y	g_y	F_y	g_y	F_y	g_y	F_y	g_y
3.15	220	3.13	334	3.17	728	3.22	1,163	3.24	3,340	3.37	7,040
2.42	663	2.32	1,453	2.41	3,180	2.43	5,065	2.82	8,080	3.01	17,100
2.31	946	2.11	2,898	2.21	6,345	2.32	10,150	2.67	13,360		
2.02	3,531	2.09	5,990	2.20	10,120						
2.01	5,240	2.02	7,790								
1.98	6,800										

Fuel No. 70 composition, percent: 74.2 CH_4, 13.4 C_3H_6, 9.6 C_3H_8, 2.5 C_2H_6, 0.3 CO_2 — F_c = 1.66

Stoichiometric percentage: 7.30 — (Data for figures 52-56) — C_3H_8 group/CH_4 = 25.5/74.2 = 0.344

Tube diam. 1.914 cm.		Tube diam. 1.503 cm.		Tube diam. 1.247 cm.		Tube diam. 1.023 cm.		Tube diam. 0.891 cm.		Tube diam. 0.776 cm.	
F_y	g_y	F_y	g_y	F_y	g_y	F_y	g_y	F_y	g_y	F_y	g_y
2.39	11.7	2.74	18.5	2.78	30.6	2.93	45.0	2.93	68.0	3.02	99.9
2.21	19.6	2.28	38.4	2.28	69.3	2.27	129	2.30	194	2.32	295
2.00	32.3	2.08	67	2.03	118	2.06	212	2.10	323	2.11	488
1.89	60.6	1.91	125	1.91	219	1.91	382	1.93	602	1.91	908
1.78	119	1.80	245	1.80	430	1.79	775	1.83	1,178	1.83	1,788
1.72	168	1.73	350	1.74	617	1.80	1,118	1.81	1,670	1.86	2,580
1.66	219	1.67	452	1.70	796	1.74	1,448	1.79	2,195	1.79	3,328
1.66	353	1.66	733	1.66	1,267	1.72	2,305				
		1.66	873								

Tube diam. 0.611 cm.		Tube diam. 0.535 cm.		Tube diam. 0.413 cm.		Tube diam. 0.354 cm.		Tube diam. 0.249 cm.		Tube diam. 0.195 cm.	
F_y	g_y	F_y	g_y	F_y	g_y	F_y	g_y	F_y	g_y	F_y	g_y
3.18	179	3.18	266	3.18	579	3.18	920	3.18	2,640	3.21	5,515
2.48	470	2.48	700	2.55	1,532	2.59	2,440	2.79	4,980	2.94	10,500
2.27	754	2.28	1,125	2.34	2,458	2.40	3,925	2.69	7,780	2.84	14,950
2.13	1,005	2.19	1,505	2.21	3,280	2.25	5,225	2.61	9,940		
1.96	1,860	1.99	2,800	2.04	6,115	2.12	9,780	2.53	11,940		
1.84	3,670	1.93	5,505	2.00	8,745						

Fuel No. 71 composition, percent: 62.1 CH_4, 35.5 C_3H_8, 2.4 C_2H_6 — F_c = 1.71

Stoichiometric percentage: 6.31 — (Points for figure 61 and data for figures 52-56) — C_3H_8 group/CH_4 = 37.9/62.1 = 0.61

Tube diam. 1.914 cm.		Tube diam. 1.503 cm.		Tube diam. 1.247 cm.		Tube diam. 1.023 cm.		Tube diam. 0.891 cm.		Tube diam. 0.776 cm.	
F_y	g_y	F_y	g_y	F_y	g_y	F_y	g_y	F_y	g_y	F_y	g_y
2.23	18.0	3.04	14.3	2.93	25.4	2.93	45.9	2.93	69.6	2.93	105
2.03	31.5	2.27	36.3	2.30	65.2	2.32	118	2.32	179	2.32	271
1.77	81.8	2.03	65.2	2.05	114	2.05	206	2.07	313	2.10	474
1.71	164	1.78	169	1.78	296	1.77	534	1.84	811	1.87	1,226
1.71	234	1.70	337	1.72	595	1.74	1,070	1.78	1,625	1.80	2,453
1.70	324	1.71	480	1.71	842	1.76	1,508	1.73	2,280	1.80	3,515
				1.70	1,157	1.72	2,093	1.72	3,140		

Tube diam. 0.611 cm.		Tube diam. 0.535 cm.		Tube diam. 0.413 cm.		Tube diam. 0.354 cm.		Tube diam. 0.249 cm.		Tube diam. 0.195 cm.	
F_y	g_y	F_y	g_y	F_y	g_y	F_y	g_y	F_y	g_y	F_y	g_y
3.20	193	3.17	286	3.17	623	3.17	989	3.17	2,838	3.23	5,940
2.45	504	2.46	752	2.50	1,637	2.52	2,598	2.63	7,520	2.75	15,840
2.12	981	2.12	1,460	2.17	3,185	2.23	5,085	2.51	11,100		
1.88	2,328	1.86	3,810	2.04	7,760	2.07	9,560				
1.82	3,860	1.82	5,725								
1.80	5,120	1.81	7,550								
1.78	6,340										

[1] Propane group is average of (A-T/5-No./73, 3, 5, 74, 75).

TABLE 5. - Yellow-tip limits of fuel gases; methane - propane group[1/] - ethylene (Con.)

Long cylindrical tubes; $g = (32\ V)/(\pi D^3)$

Noncircular and sharp-edged short ports; $g = (\lambda\ V\ Re)/(2\pi D^3)$

Fuel No. 29 composition, percent: 55.4 C_3H_8, 44.6 H_2 — $F_c = 1.76$

Stoichiometric percentage: 6.52 (Data for figures 52-56) — CH_4/C_3H_8 group = 0/55.4 = 0

Tube diam. 1.023 cm.		Tube diam. 0.891 cm.		Port diam. 0.796 cm.[2/]			Tube diam. 0.776 cm.		Tube diam. 0.354 cm.		Tube diam. 0.294 cm.		Tube diam. 0.249 cm.		Port diam. 0.239 cm.[2/]			Tube diam. 0.195 cm.		Tube diam. 0.155 cm.	
F_y	g_y	F_y	g_y	F_y	g_y	λ	F_y	g_y	F_y	g_y	F_y	g_y	F_y	g_y	F_y	g_y	λ	F_y	g_y	F_y	g_y
2.04	214	2.06	303	2.08	461	0.380	2.08	408	2.90	907	2.87	1,575	2.96	2,610	2.99	3,375	0.520	3.05	5,480	3.18	10,870
1.90	333	1.92	456	1.95	715	.273	1.97	618	2.50	2,095	2.35	5,260	2.60	5,800	2.65	7,820	.273	2.80	10,660	2.97	24,950
1.81	560	1.82	759	1.88	1,265	.173	1.83	1,020	2.20	4,480	2.25	8,800	2.45	9,300	2.47	13,100	.178	2.68	18,200	2.90	38,400
1.76	820	1.77	1,170	1.78	2,365	.103	1.79	1,850	2.06	8,500	2.19	15,150	2.38	13,260	2.38	18,330	.136	2.62	25,450	2.88	48,700
1.74	1,000	1.75	1,515	1.78	2,995	.084	1.77	2,300	2.03	16,250	2.19	23,650	2.30	24,900	2.37	22,750	.116	2.59	30,800		
									2.02	20,750	2.19	25,500	2.30	29,350	2.37	29,200	.093				

Fuel No. 28 composition, percent: 81.6 C_3H_8, 17.4 H_2, 1.0 C_3H_6 — $F_c = 1.61$

Stoichiometric percentage: 4.73 (Data for figures 52-56) — CH_4/C_3H_8 group = 0/81.6 = 0

Tube diam. 1.023 cm.		Tube diam. 0.891 cm.		Tube diam. 0.776 cm.		Tube diam. 0.699 cm.		Tube diam. 0.535 cm.		Tube diam. 0.354 cm.		Tube diam. 0.249 cm.	
F_y	g_y	F_y	g_y	F_y	g_y	F_y	g_y	F_y	g_y	F_y	g_y	F_y	g_y
2.03	127	2.05	193	2.04	289	2.02	399	2.04	898	2.11	3,110	2.27	9,000
1.72	358	1.72	543	1.72	778	1.71	1,094	1.76	2,060	1.86	6,750	2.20	12,650
1.65	518	1.64	785	1.65	1,175	1.64	1,675	1.65	3,630	1.79	10,550		
1.60	750	1.61	1,131	1.63	1,527	1.61	2,348	1.65	5,240				
1.61	833	1.61	1,260	1.62	1,716								

Fuel No. 72 composition, percent: 70.1 C_3H_8, 15.7 H_2, 13.7 CO, 0.5 C_3H_6 — $F_c = 1.60$

Stoichiometric percentage: 5.38 (Data for figures 52-56) — CH_4/C_3H_8 group = 0/70.6 = 0

Tube diam. 1.023 cm.		Tube diam. 0.891 cm.		Tube diam. 0.776 cm.		Tube diam. 0.699 cm.		Tube diam. 0.354 cm.		Tube diam. 0.249 cm.	
F_y	g_y	F_y	g_y	F_y	g_y	F_y	g_y	F_y	g_y	F_y	g_y
2.00	159	1.97	240	1.91	362	1.93	503	2.14	2,430	2.35	6,000
1.72	433	1.66	658	1.70	998	1.71	1,376	1.97	5,120	2.26	7,940
1.62	776	1.62	1,175	1.65	1,775	1.65	2,440	1.89	10,650	2.24	13,150
1.60	983	1.59	1,490	1.61	2,260	1.62	3,095				

1/ Propane group is average of (A-T/5-No./73, 3, 5, 74, 75)
2/ 0.635 cm., port depth.
λ = Coefficients of friction (line 13c, figure 75).

TABLE 5. - Yellow-tip limits of fuel gases; methane - propane group[1] - ethylene (Con.)

Long cylindrical tubes; $g = (32\ V)/(\pi D^3)$

Noncircular and sharp-edged short ports; $g = (\lambda\ V\ Re)/(2\pi D^3)$

Fuel No. 73 composition, percent: 97.9 C_2H_6, 2.1 C_3H_6 $F_c = 1.87$

Stoichiometric percentage: 5.60 (Data for figures 52-56) CH_4/C_3H_8 group = 0/100 = 0

Tube diam. 0.891 cm.		Tube diam. 0.776 cm.		Tube diam. 0.699 cm.		Tube diam. 0.611 cm.		Tube diam. 0.354 cm.		Tube diam. 0.249 cm.	
F_y	g_y	F_y	g_y	F_y	g_y	F_y	g_y	F_y	g_y	F_y	g_y
2.11	300	2.14	405	2.11	564	2.17	797	2.38	2,940	2.60	7,320
1.97	495	1.99	683	1.97	1,005	2.05	1,380	2.25	5,990	2.56	9,560
1.92	705	1.89	1,185	1.94	1,703	1.99	2,390	2.21	8,020	2.54	12,100
1.89	1,007	1.87	1,805	1.89	2,650	1.92	3,840	2.20	10,010		
1.84	1,515	1.86	2,290	1.88	3,150	1.89	4,720				

Fuel No. 3 composition, percent: 98.6 C_3H_8, 1.4 C_3H_6 $F_c = 1.61$

Stoichiometric percentage: 4.02 (Points for figure 51 and data for figures 52-56) CH_4/C_3H_8 group = 0/100 = 0

Tube diam. 1.023 cm.		Tube diam. 0.891 cm.		Tube diam. 0.776 cm.		Tube diam. 0.699 cm.		Tube diam. 0.611 cm.		Port diam. 0.595 cm.[2]			Tube diam. 0.413 cm.		Tube diam. 0.354 cm.		Tube diam. 0.249 cm.		Tube diam. 0.195 cm.	
F_y	g_y	F_y	g_y	F_y	g_y	F_y	g_y	F_y	g_y	F_y	g_y	λ	F_y	g_y	F_y	g_y	F_y	g_y	F_y	g_y
1.79	271	1.62	1,240	2.08	271	2.22	330	2.07	507	2.10	548	0.320	2.15	1,835	2.22	3,030	3.04	2,120	5.46	1,168
1.72	363	1.62	1,455	1.97	353	1.93	602	1.85	1,007	2.03	651	.283	2.05	2,519	2.08	4,462	3.04	1,843	5.46	894
1.67	522			1.82	612	1.74	1,209	1.67	2,216	1.86	958	.220	1.98	3,080	2.00	6,140	2.87	2,440	5.07	1,265
1.61	745			1.73	1,015	1.64	2,321	1.60	3,445	1.75	2,340	.123	1.92	4,088	1.97	7,857	2.87	2,113	5.07	949
1.58	959			1.66	1,703	1.63	3,020	1.61	4,520	1.66	4,710	.076	1.91	4,602			2.44	4,575	4.14	1,595
				1.62	2,205								1.89	6,147			2.32	8,210	4.14	1,210
													1.89	7,163			2.30	9,148	3.53	2,543
																			3.53	2,186
																			3.33	2,625
																			3.33	2,254
																			3.20	3,628
																			3.20	2,970
																			2.82	4,302
																			2.82	3,863
																			2.62	5,620
																			2.62	5,361
																			2.47	6,763
																			2.40	9,870

1/ Propane group is average of (A-T/5-No./73, 3, 5, 74, 75).
2/ 0.635 cm., port depth.
λ = Coefficients of friction (line 13d, figure 75).

TABLE 5. - Yellow-tip limits of fuel gases; methane - propane group[1/] - ethylene (Con.)

Long cylindrical tubes; $g = (32\ \bar{V})/(\pi D^3)$

Noncircular and sharp-edged short ports; $g = (\lambda \bar{V}\ Re)/(2 \pi D^3)$

Fuel No. 5 composition, percent: 99.2 C_3H_6, 0.4 C_3H_8, 0.4 C_2H_6 — F_c = 1.44

Stoichiometric percentage: 4.45 (Data for figures 52-56) CH_4/C_3H_8 group = 0/100 = 0

Port diam. 1.114 cm.[2/]			Tube diam. 1.023 cm.		Port diam. 0.952 cm.[2/]			Tube diam. 0.878 cm.		Tube diam. 0.776 cm.		Tube diam. 0.624 cm.		Port diam. 0.595 cm.[2/]			Tube diam. 0.354 cm.		Tube diam. 0.249 cm.	
F_y	g_y	λ[3/]	F_y	g_y	F_y	g_y	λ[3/]	F_y	g_y	F_y	g_y	F_y	g_y	F_y	g_y	λ[3/]	F_y	g_y	F_y	g_y
1.72	208	0.410	1.76	183	1.83	186	0.560	1.86	169	1.77	301	1.81	616	1.80	730	0.410	1.79	2,601	1.79	7,036
1.62	442	.223	1.59	351	1.69	363	.335	1.71	305	1.71	420	1.71	794	1.70	957	.323	1.61	4,959	1.77	9,108
1.45	854	.135	1.45	596	1.62	637	.216	1.63	500	1.66	497	1.58	1,303	1.64	1,665	.213			1.77	10,040
1.43	1,014	.116	1.44	835	1.56	1,050	.145	1.55	795	1.63	602	1.50	2,495	1.54	3,415	.122				
			1.43	959	1.45	1,385	.116	1.47	1,300	1.54	801	1.43	3,580	1.46	5,800	.077				
					1.44	1,643	.100	1.42	1,520	1.47	1,405	1.42	4,220	1.44	7,070	.067				
										1.44	1,935									
										1.43	2,195									

Fuel No. 74 composition, percent: 100 C_4H_{10} — F_c = 1.57

Stoichiometric percentage: 3.12 (Data for figures 52-56) CH_4/C_3H_8 group = 0/100 = 0

Port diam. 0.796 cm.[2/]			Tube diam. 0.776 cm.		Tube diam. 0.699 cm.		Tube diam. 0.611 cm.		Port diam. 0.595 cm.[2/]			Tube diam. 0.354 cm.	
F_y	g_y	λ[4/]	F_y	g_y	F_y	g_y	F_y	g_y	F_y	g_y	λ[4/]	F_y	g_y
1.68	464	0.243	1.72	524	1.64	1,320	1.63	1,480	1.63	1,720	0.148	1.82	6,930
1.59	1,038	.143	1.62	1,020	1.60	1,833	1.63	2,020	1.62	2,520	.116	1.76	8,020
1.56	1,686	.103	1.57	1,525	1.59	2,810	1.60	4,220	1.56	5,000	.073		
1.54	2,390	.082	1.55	2,050									

Fuel No. 75 composition, percent: 94.1 C_4H_8, 2.8 C_2H_4, 2.1 C_3H_6, 1.0 C_4H_{10} — F_c = 1.40

Stoichiometric percentage: 3.43 (Data for figures 52-56) CH_4/C_3H_8 group = 0/100 = 0

Tube diam. 1.023 cm.		Tube diam. 0.891 cm.		Tube diam. 0.776 cm.		Tube diam. 0.611 cm.		Tube diam. 0.402 cm.		Tube diam. 0.354 cm.	
F_y	g_y	F_y	g_y	F_y	g_y	F_y	g_y	F_y	g_y	F_y	g_y
1.55	237	1.53	451	1.53	600	1.54	1,188	1.55	3,920	1.56	5,660
1.49	323	1.47	600	1.47	854	1.50	1,587	1.54	4,940		
1.47	504	1.46	808	1.46	1,330	1.46	2,420	1.51	5,610		
1.43	716	1.43	1,114	1.42	1,725	1.43	3,450				
1.42	938	1.40	1,425	1.41	2,150	1.41	4,410				

1/ Propane group is average of (A-T/5-No./73, 3, 5, 74, 75).
2/ 0.635 cm., port depth.
3/ Coefficients of friction (line 13c, figure 75).
4/ Coefficients of friction (line 13d, figure 75).

TABLE 5. - Yellow-tip limits of fuel gases; methane - propane group[1] - ethylene (Con.)

Long cylindrical tubes; $g = (32\ V)/(\pi D^3)$

Noncircular and sharp-edged short ports; $g = (\lambda\ V\ Re)/(2 \pi D^3)$

Fuel No. 76 composition, percent: 53.1 C_2H_4, 46.9 C_3H_8 — F_c = 1.72

Stoichiometric percentage: 5.04 (Data for figures 52-56) — C_3H_8 group/C_2H_4 = 46.9/53.1 = 0.884

F_y	g_y	F_y	g_y	F_y	g_y	F_y	g_y	F_y	g_y	F_y	g_y	F_y	g_y	F_y	g_y	F_y	g_y	F_y	g_y
Tube diam. 1.023 cm.		Tube diam. 0.891 cm.		Tube diam. 0.776 cm.		Tube diam. 0.354 cm.		Tube diam. 0.294 cm.		Tube diam. 0.249 cm.		Tube diam. 0.195 cm.		Tube diam. 0.155 cm.					
1.97	187	1.98	283	1.98	429	2.78	908	2.80	1,600	2.81	2,575	2.80	7,330	3.01	10,170				
1.78	436	1.78	661	1.78	1,001	2.38	1,828	2.39	3,485	2.47	5,430	2.63	12,080	2.82	21,700				
1.73	635	1.73	962	1.73	1,455	2.24	2,820	2.28	5,120	2.36	8,240	2.55	16,670	2.81	31,500				
1.71	869	1.71	1,317	1.72	1,996	2.11	4,770	2.19	8,380	2.33	11,170	2.50	22,480						
1.71	1,040	1.71	1,575	1.72	2,390	2.03	8,690	2.13	19,700	2.31	13,900	2.48	29,200						
						1.99	12,930			2.29	19,400								
						1.95	17,350												

Fuel No. 77 composition, percent: 74.4 C_2H_4, 25.6 C_3H_8 — F_c = 1.68

Stoichiometric percentage: 5.62 (Data for figures 52-56) — C_3H_8 group/C_2H_4 = 25.6/74.4 = 0.344

F_y	g_y	F_y	g_y	F_y	g_y	F_y	g_y	F_y	g_y	F_y	g_y	F_y	g_y	F_y	g_y	F_y	g_y	F_y	g_y
Tube diam. 1.023 cm.		Tube diam. 0.891 cm.		Tube diam. 0.776 cm.		Tube diam. 0.699 cm.		Tube diam. 0.611 cm.		Tube diam. 0.535 cm.		Tube diam. 0.413 cm.		Tube diam. 0.354 cm.		Tube diam. 0.249 cm.		Tube diam. 0.195 cm.	
2.02	126	2.02	198	2.05	305	2.05	418	2.01	639	2.08	920	2.03	2,040	2.15	3,265	2.52	2,340	2.58	4,980
1.78	317	1.78	480	1.78	726	1.80	996	1.80	1,490	1.80	2,220	1.84	4,870	1.87	7,700	2.26	5,960	2.38	11,900
1.72	495	1.75	751	1.72	1,135	1.75	1,555	1.77	2,330	1.74	3,460	1.77	7,560	1.81	12,050	2.21	8,930	2.33	19,600
1.70	642	1.71	966	1.71	1,463	1.72	2,005	1.71	3,000	1.72	4,470	1.72	9,720	1.81	18,700	2.15	11,800	2.31	24,550
1.69	768	1.69	1,160	1.69	1,760	1.68	2,400	1.69	3,600	1.68	5,360	1.71	11,660			2.12	14,300	2.29	33,900
1.69	838	1.69	1,270	1.69	1,920	1.69	2,635	1.69	4,660	1.69	6,940	1.72	15,150						
1.68	990	1.68	1,503	1.68	2,265	1.68	3,110												

Fuel No. 78 composition, percent: 90.0 C_2H_4, 10.0 C_3H_8 — F_c = 1.78

Stoichiometric percentage: 6.13 (Data for figures 52-56) — C_3H_8 group/C_2H_4 = 10.0/90.0 = 0.111

F_y	g_y	F_y	g_y	F_y	g_y	F_y	g_y	F_y	g_y	F_y	g_y	F_y	g_y	F_y	g_y	F_y	g_y	F_y	g_y
Tube diam. 1.023 cm.		Tube diam. 0.891 cm.		Tube diam. 0.776 cm.		Tube diam. 0.535 cm.		Tube diam. 0.413 cm.		Tube diam. 0.294 cm.									
1.89	300	1.85	454	1.89	690	1.92	2,110	2.00	4,610	2.11	12,950								
1.82	507	1.84	770	1.84	1,165	1.87	3,565	1.95	7,800	2.11	21,900								
1.81	711	1.82	1,073	1.82	1,625	1.85	4,970	1.93	10,870	2.04	30,500								
1.78	1,004	1.79	1,520	1.79	2,305	1.83	7,060	1.87	15,370										

Fuel No. 79 composition, percent: 76.0 C_2H_4, 24.0 H_2 — F_c = 1.90

Stoichiometric percentage: 8.01 (Data for figures 52-56) — C_3H_8 group/C_2H_4 = 0/76.0 = 0

F_y	g_y	F_y	g_y	F_y	g_y	F_y	g_y	F_y	g_y	F_y	g_y	F_y	g_y	F_y	g_y	F_y	g_y	F_y	g_y
Tube diam. 1.023 cm.		Tube diam. 0.891 cm.		Tube diam. 0.776 cm.		Tube diam. 0.354 cm.		Tube diam. 0.294 cm.		Tube diam. 0.249 cm.		Tube diam. 0.195 cm.		Tube diam. 0.155 cm.					
2.03	188	2.03	285	2.03	432	2.75	926	2.78	1,620	2.82	2,680	2.98	5,580	3.08	11,430				
1.94	412	1.94	624	1.95	942	2.41	1,970	2.48	3,460	2.58	5,680	2.67	12,090	2.91	24,400				
1.93	620	1.93	940	1.93	1,423	2.27	3,040	2.37	5,280	2.47	8,780	2.60	18,360	2.82	37,900				
1.91	855	1.91	1,298	1.91	1,960	2.22	4,145	2.31	7,290	2.41	12,130	2.54	25,600	2.77	51,400				
1.89	1,058	1.89	1,605	1.90	2,430	2.21	4,635	2.29	8,100	2.40	13,540	2.54	28,600	2.72	64,000				
						2.19	5,100	2.28	8,960	2.39	14,900	2.52	31,450	2.71	83,800				
						2.12	10,120	2.18	17,760	2.30	29,850	2.48	46,400	2.68	108,700				
						2.10	15,280	2.16	26,980	2.27	44,950	2.45	63,500						
						2.07	20,900	2.10	37,000	2.24	50,800	2.42	82,000						
						2.04	26,050	2.10	40,110										

1/ Propane group is average of (A-T/5-No./73, 3, 5, 74, 75).

TABLE 5. - Yellow-tip limits of fuel gases; methane-propane group 1/ - ethylene (Con.)

Long cylindrical tubes; $g = (32\ V)/(\pi D^3)$

Noncircular and sharp-edged short ports; $g = (\lambda\ V\ Re)/(2\pi D^3)$

Fuel No. 4 composition, percent: 100 C_2H_4 $F_c = 1.88$

Stoichiometric percentage: 6.52 (Data for figures 52-56) C_3H_8 group/C_2H_4 = 0/100 = 0

Tube diam. 1.914 cm.		Port diam. 0.952 cm. 2/			Port diam. 0.796 cm. 2/			Tube diam. 0.776 cm.		Tube diam. 0.699 cm.		Tube diam. 0.611 cm.		Port diam. 0.595 cm. 2/		
F_y	g_y	F_y	g_y	λ 3/	F_y	g_y	λ 3/	F_y	g_y	F_y	g_y	F_y	g_y	F_y	g_y	λ 3/
1.89	88.5	1.89	189	0.595	1.98	205	0.745	1.99	299	2.03	299	2.15	299	2.10	349	0.770
1.87	133	1.92	409	.323	1.93	313	.530	1.91	691	2.00	396	2.03	498	1.99	614	.490
1.87	154	1.86	825	.183	1.90	796	.246	1.93	994	1.99	594	2.03	723	1.95	936	.345
		1.85	1,537	.112	1.88	1,291	.170	1.90	1,510	1.95	798	1.98	900	1.94	1,206	.283
					1.86	2,565	.098			1.91	1,300	1.90	1,490	1.92	2,120	.183
										1.91	1,805	1.93	2,010	1.85	7,440	.067
										1.86	3,130	1.91	4,700			

Tube diam. 0.249 cm.		Port diam. 0.239 cm. 2/			Port dimen. 0.654×3.18 cm. E.H.D.=1.085 cm. 5/			Port dimen. 0.318×2.5 cm. E.H.D.=0.564 cm. 5/			Port dimen. 0.354×1.28 cm. E.H.D.=0.555 cm. 5/			Port dimen. 0.196×1.29 cm. E.H.D.=0.34 cm. 5/		
F_y	g_y	F_y	g_y	λ 3/	F_y	g_y	λ 4/	F_y	g_y	λ 4/	F_y	g_y	λ 4/	F_y	g_y	λ 4/
2.26	6,540	2.27	7,390	0.290	2.03	93.1	0.278	2.07	568	0.125	2.00	594	0.123	1.99	2,290	0.066
2.23	16,840	2.20	27,000	.102	1.96	166	.113	1.85	1,095	.042	1.90	1,056	.048	1.91	4,095	.026
2.17	39,600	2.21	46,600	.066	1.91	225	.066	1.84	1,530	.024	1.86	1,436	.029	1.88	5,740	.016
					1.88	306	.040	1.83	2,120	.015	1.84	1,964	.018			
					1.87	345	.033				1.83	2,214	.015			

1/ Propane group is average of (A-T/5-No./73, 3, 5, 74, 75).
2/ 0.635 cm., port depth.
3/ Coefficients of friction (line 13c, figure 75).
4/ Coefficients of friction (line 13g, figure 75).
5/ E.H.D., equivalent hydraulic diameter.

TABLE 6. - Yellow-tip limits of fuel gases; methane-ethylene

Long cylindrical tubes; $g = (32\ V)/(\pi D^3)$

Noncircular and sharp-edged short ports; $g = (\lambda V\ Re)/(2\pi D^3)$

Fuel No. 2 composition, percent: 100 CH_4 F_c = 1.80

Stoichiometric percentage: 9.46 C_2H_4/CH_4 = 0/100 = 0

(A-T/5-No./2)

Fuel No. 80 composition, percent: 72.5 CH_4, 15.9 C_2H_4, 7.7 H_2, 2.6 C_2H_6, 0.4 C_3H_8, 0.2 C_3H_6, 0.2 C_4H_{10}, 0.5 CO_2 F_c = 1.76

Stoichiometric percentage: 9.07 (Data for figures 57-59) C_2H_4/CH_4 = 19.3/72.5 = 0.266

Tube diam. 2.47 cm.		Tube diam. 1.914 cm.		Tube diam. 1.503 cm.		Tube diam. 1.236 cm.		Tube diam. 1.023 cm.		Tube diam. 0.776 cm.		Tube diam. 0.611 cm.		Tube diam. 0.413 cm.		Tube diam. 0.294 cm.		Tube diam. 0.195 cm.	
F_y	g_y	F_y	g_y	F_y	g_y	F_y	g_y	F_y	g_y	F_y	g_y	F_y	g_y	F_y	g_y	F_y	g_y	F_y	g_y
2.43	10.3	2.60	19.6	2.55	49.2	2.57	85.8	2.68	129	2.80	252	2.92	470	3.00	1,495	3.10	5,100	3.29	20,850
2.20	19.4	2.27	44.8	2.34	98.5	2.30	164	2.47	198	2.34	779	2.53	1,275	2.63	4,610	2.94	9,400	3.15	35,100
2.06	30.6	2.07	79.5	2.14	205	2.07	294	2.17	398	2.27	1,485	2.37	3,140	2.55	7,730	2.89	14,850	3.12	51,800
1.88	79.0	1.85	170	1.92	352	1.93	618	2.11	648	2.22	2,640	2.28	5,460			2.72	27,450		
1.76	154	1.79	331	1.83	670			2.15	1,144										
1.74	207	1.76	457	1.87	943			2.10	2,120										

Fuel No. 81 composition, percent: 67.6 CH_4, 26.8 C_2H_4, 2.3 C_2H_6, 2.2 H_2, 0.4 C_3H_8, 0.2 C_3H_6, 0.1 C_4H_{10}, 0.4 CO_2 F_c = 1.79

Stoichiometric percentage: 8.37 (Data for figures 57-59) C_2H_4/CH_4 = 29.8/67.6 = 0.441

Tube diam. 1.914 cm.		Tube diam. 1.503 cm.		Tube diam. 1.247 cm.		Tube diam. 1.023 cm.		Tube diam. 0.891 cm.		Tube diam. 0.776 cm.		Tube diam. 0.611 cm.		Tube diam. 0.535 cm.		Tube diam. 0.413 cm.		Tube diam. 0.354 cm.		Tube diam. 0.249 cm.		Tube diam. 0.195 cm.	
F_y	g_y	F_y	g_y	F_y	g_y	F_y	g_y	F_y	g_y	F_y	g_y	F_y	g_y	F_y	g_y	F_y	g_y	F_y	g_y	F_y	g_y	F_y	g_y
2.70	10.5	2.79	18.6	2.89	29.9	2.93	53.8	2.92	82.0	2.97	123	3.17	201	3.21	296	3.21	643	3.23	1,023	3.26	2,950	3.40	6,240
2.32	17.2	2.40	35.7	2.45	62.6	2.49	114	2.49	173	2.51	263	2.58	518	2.60	774	2.67	1,695	2.73	2,710	2.87	7,900	3.02	16,780
2.09	33.8	2.15	69.9	2.17	123	2.19	222	2.22	337	2.24	511	2.28	1,054	2.30	1,572	2.40	3,455	2.44	5,510	2.74	15,490	2.98	32,250
1.96	80.3	2.01	168	2.02	294	2.02	528	2.04	805	2.07	1,224	2.14	2,540	2.15	3,790	2.19	8,270	2.25	13,180	2.68	21,390		
1.87	175	1.82	376	1.92	638	2.00	1,156	2.02	1,765	2.02	2,670	2.03	5,465	2.05	8,230	2.06	15,000	2.21	17,540				
1.79	242	1.80	496	1.85	874	1.96	1,614	1.95	2,418	1.99	3,670												
1.79	358	1.79	734	1.84	1,305																		

Fuel No. 57 composition, percent: 32.1 CH_4, 28.4 C_2H_4, 12.5 H_2, 27.0 N_2 F_c = 1.90

Stoichiometric percentage: 11.84 (Points for figure 62 and data for figures 57-59) C_2H_4/CH_4 = 28.4/32.1 = 0.885

Tube diam. 1.247 cm.		Tube diam. 1.023 cm.		Tube diam. 0.891 cm.		Tube diam. 0.776 cm.		Tube diam. 0.354 cm.		Tube diam. 0.294 cm.		Tube diam. 0.249 cm.		Tube diam. 0.195 cm.		Tube diam. 0.155 cm.	
F_y	g_y	F_y	g_y	F_y	g_y	F_y	g_y	F_y	g_y	F_y	g_y	F_y	g_y	F_y	g_y	F_y	g_y
2.12	128	2.23	213	2.22	326	2.25	489	3.05	1,114	3.08	1,983	3.13	3,290	3.34	7,030	3.45	14,300
1.97	284	1.96	528	1.99	804	2.06	1,230	2.64	2,238	2.72	4,175	2.78	7,120	3.05	14,150	3.30	27,100
1.91	421	1.94	768	1.96	1,165	2.00	1,780	2.52	3,605	2.62	6,340	2.70	10,600	2.96	22,850	3.24	40,350
1.89	566	1.92	1,025	1.93	1,564	1.98	2,387	2.44	5,950	2.52	10,650	2.65	18,030	2.90	30,850	3.20	53,200
1.89	667	1.91	1,215	1.92	1,852	1.95	2,810	2.35	11,900	2.44	23,500	2.56	43,400	2.86	39,100	3.18	63,700
								2.32	18,150	2.40	33,850			2.80	61,200		
								2.29	24,650								

TABLE 6. - Yellow-tip limits of fuel gases; methane-ethylene (Con.)

Long cylindrical tubes; $g = (32\ V)/(\pi D^3)$

Noncircular and sharp-edged short ports; $g = (\lambda V\ Re)/(2\pi D^3)$

Fuel No. 55 composition, percent: 37.4 CH_4, 33.4 C_2H_4, 15.2 H_2, 14.0 N_2 — F_c = 1.90

Stoichiometric percentage: 10.27 — (Data for figures 57-59) — C_2H_4/CH_4 = 33.4/37.4 = 0.893

Tube diam. 1.023 cm.		Tube diam. 0.891 cm.		Tube diam. 0.776 cm.		Tube diam. 0.699 cm.		Tube diam. 0.611 cm.		Tube diam. 0.249 cm.		Tube diam. 0.155 cm.	
F_y	g_y	F_y	g_y	F_y	g_y	F_y	g_y	F_y	g_y	F_y	g_y	F_y	g_y
2.06	300	2.11	407	2.15	510	2.19	798	2.21	1,230	2.65	9,560	3.27	15,500
1.97	512	1.98	716	2.06	805	2.04	1,500	2.05	3,050	2.57	17,200	3.17	22,800
1.92	708	1.96	1,015	1.98	1,315	2.00	2,450	2.04	4,150	2.47	29,240	3.03	32,000
1.89	942	1.93	1,330	1.94	2,050	1.95	3,520	2.02	5.310	2.43	44,900	2.99	39,200
1.90	1,110	1.90	1,685	1.93	2,550								

Fuel No. 82 composition, percent: 33.5 CH_4, 30.1 C_2H_4, 13.4 H_2, 12.8 N_2, 10.2 CO_2 — F_c = 1.88

Stoichiometric percentage: 11.30 — (Data for figures 57-59) — C_2H_4/CH_4 = 30.1/33.5 = 0.898

Tube diam. 1.023 cm.		Tube diam. 0.891 cm.		Tube diam. 0.776 cm.		Tube diam. 0.611 cm.		Tube diam. 0.249 cm.		Tube diam. 0.155 cm.	
F_y	g_y	F_y	g_y	F_y	g_y	F_y	g_y	F_y	g_y	F_y	g_y
2.08	297	2.05	446	2.08	681	2.14	1,410	2.63	9,390	3.31	15,100
1.95	508	1.95	770	1.98	1,170	2.05	2,425	2.56	17,550	3.16	22,700
1.89	717	1.92	1,090	1.96	1,660	2.04	3,440	2.49	29,300	3.03	32,230
1.86	960	1.91	1,465	1.94	2,230	2.00	4,610	2.43	45,600	3.00	40,000
1.87	1,140	1.89	1,695	1.92	2,540	1.98	5,060				

Fuel No. 83 composition, percent: 72.5 C_2H_4, 27.5 CH_4 — F_c = 1.85

Stoichiometric percentage: 7.12 — (Data for figures 57-59) — CH_4/C_2H_4 = 27.5/72.5 = 0.38

Tube diam. 1.023 cm.		Tube diam. 0.891 cm.		Tube diam. 0.776 cm.		Tube diam. 0.699 cm.		Tube diam. 0.611 cm.		Tube diam. 0.413 cm.		Tube diam. 0.354 cm.		Tube diam. 0.249 cm.	
F_y	g_y	F_y	g_y	F_y	g_y	F_y	g_y	F_y	g_y	F_y	g_y	F_y	g_y	F_y	g_y
2.12	134	2.20	205	2.19	310	2.14	422	2.20	636	2.24	2,065	2.33	3,305	2.46	9,740
1.94	293	1.98	478	1.99	679	1.99	930	2.03	1,398	2.07	4,170	2.14	6,660	2.29	20,130
1.87	477	1.90	721	1.91	1,095	1.94	1,494	1.96	2,250	2.03	7,190	2.08	11,480	2.22	33,500
1.85	638	1.87	973	1.88	1,470	1.92	2,010	1.94	3,015	1.98	12,180	2.04	19,480	2.22	36,250
1.82	790	1.85	1,200	1.87	1,816	1.89	2,490	1.92	3,740						
1.83	1,023	1.86	1,554			1.87	3,220	1.90	4,840						

Fuel No. 79 composition, percent: 76.0 C_2H_4, 24.0 H_2 — F_c = 1.90

Stoichiometric percentage: 8.01 — CH_4/C_2H_4 = 0/76.0 = 0

(A-T/5-No./79)

Fuel No. 4 composition, percent: 100 C_2H_4 — F_c = 1.88

Stoichiometric percentage: 6.52 — CH_4/C_2H_4 = 0/100 = 0

(A-T/5-No./4)

TABLE 7. - Yellow-tip limits of fuel gases; other fuels

Long cylindrical tubes; $g = (32\ V)/(\pi D^3)$

Noncircular and sharp-edged short ports; $g = (\lambda V\ Re)/(2 \pi D^3)$

Fuel No. 6 composition, percent: 100 C_6H_6 $F_c = 1.18$

Stoichiometric percentage: 2.71 (Points for figure 64)

Tube diam. 1.023 cm.		Tube diam. 0.891 cm.		Tube diam. 0.776 cm.		Tube diam. 0.611 cm.		Tube diam. 0.413 cm.		Tube diam. 0.354 cm.		Tube diam. 0.249 cm.	
F_y	g_y	F_y	g_y	F_y	g_y	F_y	g_y	F_y	g_y	F_y	g_y	F_y	g_y
1.28	607	1.33	732	1.34	665	1.37	758	1.36	1,544	1.35	2,460	1.34	5,080
1.23	917	1.24	1,247	1.24	1,428	1.29	1,551	1.26	2,475	1.30	3,865		
1.19	1,267	1.21	1,755	1.22	2,145	1.22	2,970	1.23	3,390	1.26	5,235		
1.19	1,570	1.19	2,280	1.20	2,925	1.20	4,590	1.20	4,440				
1.18	1,898	1.18	2,875	1.18	3,565			1.21	5,310				

Fuel No. 84 composition, percent: 100 C_7H_8 $F_c = 1.34$

Stoichiometric percentage: 2.27 (Points for figure 65)

Tube diam. 1.023 cm.		Tube diam. 0.891 cm.		Tube diam. 0.776 cm.		Tube diam. 0.611 cm.		Tube diam. 0.413 cm.		Tube diam. 0.354 cm.	
F_y	g_y	F_y	g_y	F_y	g_y	F_y	g_y	F_y	g_y	F_y	g_y
1.55	471	1.69	473	1.62	774	1.69	912	1.61	2,530	1.80	3,760
1.44	740	1.53	818	1.45	1,353	1.47	2,090	1.58	2,920		
1.40	970	1.39	1,330	1.38	2,003	1.44	2,775	1.55	3,190		
1.36	1,200	1.34	2,010	1.35	2,750						
1.36	1,343	1.33	2,468								
1.34	1,934										

Fuel No. 85 composition, percent: 97.3 C_2H_2, 2.7 CH_3COCH_3 $F_c = 2.10$

Stoichiometric percentage: 7.60 (Points for figure 66)

Tube diam. 0.776 cm.		Tube diam. 0.535 cm.		Tube diam. 0.354 cm.		Tube diam. 0.249 cm.		Tube diam. 0.195 cm.	
F_y	g_y	F_y	g_y	F_y	g_y	F_y	g_y	F_y	g_y
2.12	1,408	2.14	1,277	2.17	2,110	2.31	2,995	2.33	5,950
2.12	1,825	2.12	2,240	2.17	4,420	2.25	6,100	2.25	12,710
2.09	2,480	2.11	3,490	2.17	7,560	2.24	12,780	2.18	29,300
		2.11	5,570	2.13	12,160	2.19	21,500	2.20	49,900
		2.08	7,580	2.13	19,270	2.21	35,300		

TABLE 7. - Yellow-tip limits of fuel gases; other fuels (Con.)

Long cylindrical tubes; $g = (32\ V)/(\pi D^3)$

Noncircular and sharp-edged short ports; $g = (\lambda\ V\ Re)/(2\pi D^3)$

Fuel No. 86 composition, percent: 84.2 CH_4, 7.6 C_2H_2, 5.3 C_2H_6, 1.6 C_3H_6, 0.6 C_4H_{10}, 0.3 C_3H_6, 0.4 CO_2

Stoichiometric percentage: 8.70 (Points for figure 67) F_c = 1.77

Tube diam. 2.47 cm.		Tube diam. 1.914 cm.		Tube diam. 1.503 cm.		Tube diam. 0.354 cm.		Tube diam. 0.249 cm.	
F_y	g_y	F_y	g_y	F_y	g_y	F_y	g_y	F_y	g_y
1.85	78.4	1.88	123	1.93	353	2.85	5,130	3.56	3,003
1.76	133	1.86	148	1.77	571	2.58	12,920	3.15	8,700
1.74	217	1.84	174	1.76	961	2.49	17,950	2.97	22,050
		1.73	281						
		1.78	465						

Fuel No. 87 composition, percent: 91.6 CH_4, 4.0 C_7H_8, 3.2 C_2H_6, 0.7 C_3H_8, 0.2 C_3H_6, 0.3 CO_2

Stoichiometric percentage: 8.17 (Points for figure 68) F_c = 1.74

Tube diam. 1.914 cm.		Tube diam. 1.503 cm.		Tube diam. 1.023 cm.		Tube diam. 0.776 cm.		Tube diam. 0.413 cm.		Tube diam. 0.354 cm.		Tube diam. 0.249 cm.	
F_y	g_y	F_y	g_y	F_y	g_y	F_y	g_y	F_y	g_y	F_y	g_y	F_y	g_y
2.27	41.8	2.64	31.3	2.36	111	2.36	254	2.68	1,036	2.77	1,903	2.65	5,360
2.03	62.9	2.05	105	2.07	334	2.02	782	2.53	1,230	2.47	4,180	2.45	8,850
1.93	107	1.98	172	2.02	534	1.95	1,450	2.38	2,405	2.36	6,690	2.37	11,750
1.83	176	1.85	290	1.92	887	1.89	2,555	2.27	3,815	2.32	7,320		
1.81	243	1.78	498	1.79	1,575	1.88	3,470	2.14	5,940	2.23	9,070		
1.77	316	1.74	661	1.78	2,025			2.08	7,860				
1.74	412							2.05	8,850				

Fuel No. 66 composition, percent: 42.6 CH_4, 18.1 C_2H_4, 17.0 H_2, 9.1 CO, 2.2 C_2H_6, 1.9 C_3H_8, 0.2 C_3H_6, 0.2 C_4H_{10}, 0.1 C_4H_8, 5.2 CO_2, 3.4 N_2

Stoichiometric percentage: 10.8 F_c = 1.80

Tube diam. 2.47 cm.		Tube diam. 1.914 cm.		Tube diam. 1.503 cm.		Tube diam. 1.023 cm.		Tube diam. 0.891 cm.		Tube diam. 0.776 cm.		Tube diam. 0.413 cm.		Tube diam. 0.294 cm.		Tube diam. 0.195 cm.	
F_y	g_y	F_y	g_y	F_y	g_y	F_y	g_y	F_y	g_y	F_y	g_y	F_y	g_y	F_y	g_y	F_y	g_y
2.05	14.3	2.36	18.8	2.42	38.9	2.56	119	2.56	167	2.58	253	2.84	1,260	2.85	3,990	3.07	15,880
2.00	28.2	2.22	28.8	2.30	65.6	2.38	210	2.38	319	2.38	489	2.65	2,020	2.69	6,440	2.94	31,500
1.91	60.2	2.09	57.6	2.16	106	2.23	340	2.26	516	2.24	780	2.52	3,590	2.57	14,860	2.86	61,000
1.84	127	2.00	107	1.94	285	2.00	876	2.07	1,290	2.13	1,885	2.41	6,260	2.50	29,700		
1.79	175	1.86	208	1.84	782	2.00	1,913					2.30	11,650				
		1.82	380														

TABLE 7. - Yellow-tip limits of fuel gases; other fuels (Con.)

Long cylindrical tubes; $g = (32\ V)/(\pi D^3)$

Noncircular and sharp-edged short ports; $g = (\lambda\ V\ Re)/(2 \pi D^3)$

Fuel No. 56 composition, percent: 29.1 CH_4, 26.2 C_2H_4, 22.1 C_3H_8, 11.8 H_2, 0.2 C_3H_6, 10.6 N_2

Stoichiometric percentage: 7.60 $F_c = 1.76$

Tube diam. 1.023 cm.		Tube diam. 0.891 cm.		Tube diam. 0.776 cm.		Tube diam. 0.354 cm.		Tube diam. 0.294 cm.		Tube diam. 0.249 cm.		Tube diam. 0.195 cm.		Tube diam. 0.155 cm.	
F_y	g_y	F_y	g_y	F_y	g_y	F_y	g_y	F_y	g_y	F_y	g_y	F_y	g_y	F_y	g_y
2.14	134	2.14	203	2.14	307	2.88	898	2.93	1,570	2.96	2,593	3.01	5,430	3.16	10,450
1.87	332	1.87	504	1.87	762	2.46	2,133	2.49	3,745	2.58	6,220	2.72	13,110	3.00	21,960
1.79	550	1.79	835	1.79	1,265	2.35	3,300	2.35	6,420	2.44	10,520	2.61	22,100	2.90	36,550
1.76	801	1.76	1,213	1.76	1,830	2.07	8,150	2.27	9,220	2.36	15,300	2.52	32,400		
1.75	1,034	1.76	1,560	1.76	2,365	1.99	13,650	2.20	20,600	2.34	24,700				
						1.97	19,400	2.19	23,600						

Port dimen. 1.25x1.25x1.25 cm. E.H.D.=0.722 cm. 1/			Port dimen. 1.2×2.9 cm. E.H.D.=1.698 cm. 1/			Port dimen. 1.068×1.075 cm. E.H.D.=1.072 cm. 1/			Port dimen. 0.354×1.284 cm. E.H.D.=0.555 cm. 1/			Port dimen. 0.196×1.29 cm. E.H.D.=0.34 cm. 1/			
F_y	g_y	λ 2/	F_y	g_y	λ 3/	F_y	g_y	λ 4/	F_y	g_y	λ 3/	F_y	g_y	λ 3/	
2.07	194	0.105	1.82	530	0.153	2.07	98.6	0.255	2.07	610	0.110	2.08	2,290	0.061	
1.84	372	.035	1.72	775	.084	1.83	223	.102	1.79	1,170	.039	1.86	4,475	.022	
1.79	534	.019	1.72	882	.068	1.76	351	.060	1.72	1,740	.022	1.80	6,100	.013	
1.78	627	.016	1.71	1,034	.055	1.75	408	.050	1.72	1,962	.017				
1.76	711	.013				1.74	480	.041	1.70	2,213	.014				

1/ E.H.D., equivalent hydraulic diameter.
2/ Coefficients of friction (line 13h, figure 75).
3/ Coefficients of friction (line 13g, figure 75).
4/ Coefficients of friction (line 13f, figure 75).

TABLE 8a. - Calculation of coefficients of friction, λ, for sharp-edged short ports

$$\lambda = \frac{2\pi g D^3}{V \, Re}$$

Fuel No. 17 composition, percent: 79.7 CO, 20.1 H_2, 0.2 CO_2 — $\lambda = 41.4/Re^{0.89}$

Stoichiometric percentage: 29.5 — (Points for figure 70)

Port diameter 0.952 cm.1/

F_F	g_F 3/	V_F 4/	Re	λ
0.675	370	22.6	180	0.493
2.25	580	21.0	162	.926
.783	680	35.8	285	.362
2.20	850	33.1	255	.546
.950	1,300	60.5	480	.242
2.14	1,200	62.2	480	.219
F_B	g_B 5/	V_B 6/	Re	λ
0.582	240	21.9	174	0.343
.614	400	34.6	277	.228
.639	580	60.1	482	.109

Port diameter 0.650 cm.2/

F_F	g_F 3/	V_F 4/	Re	λ
0.739	540	15.1	177	0.351
2.22	750	15.6	177	.470
.909	1,130	22.5	261	.332
2.10	1,400	23.1	262	.398
1.10	1,950	35.9	415	.225
1.99	2,100	38.7	439	.213
1.32	2,700	46.7	540	.185
1.79	3,000	50.9	580	.175
F_B	g_B 5/	V_B 6/	Re	λ
0.634	520	16.1	188	0.297
.698	1,300	23.7	277	.342
.718	1,500	38.1	443	.153
.787	3,000	61.9	724	.116
.881	5,800	85.7	998	.117

Port diameter 0.595 cm.1/

F_F	g_F 3/	V_F 4/	Re	λ
0.786	680	12.1	154	0.482
2.21	800	12.5	154	.548
.952	1,300	20.2	257	.330
2.13	1,220	19.8	244	.334
1.32	2,750	35.3	443	.232
1.93	2,400	32.6	405	.241
F_B	g_B 5/	V_B 6/	Re	λ
0.640	590	12.4	159	0.397
.641	590	18.0	230	.189
.719	1,550	31.9	404	.159
.758	2,350	45.3	579	.119
.804	3,400	63.5	810	.088

Port diameter 0.476 cm.1/

F_F	g_F 3/	V_F 4/	Re	λ
1.10	1,950	15.0	236	0.374
2.10	1,420	12.7	197	.384
1.33	2,750	20.5	323	.281
1.86	2,750	20.1	310	.298
F_B	g_B 5/	V_B 6/	Re	λ
0.692	1,200	13.9	222	0.265
.728	1,700	20.8	330	.167
.796	3,200	30.4	485	.147

Port diameter 0.476 cm.2/

F_F	g_F 3/	V_F 4/	Re	λ
0.898	1,100	11.9	189	0.331
2.11	1,350	12.6	193	.376
1.10	1,950	17.3	273	.279
1.87	2,700	22.0	340	.243
1.42	3,050	24.2	381	.223
1.73	3,200	25.0	388	.223
F_B	g_B 5/	V_B 6/	Re	λ
0.688	1,100	12.4	198	0.306
.726	1,700	19.9	316	.183
.846	4,800	31.6	501	.206
.905	6,600	49.0	780	.118
.980	10,200	66.1	1,045	.100

Port diameter 0.407 cm.1/

F_F	g_F 3/	V_F 4/	Re	λ
1.25	2,520	12.6	231	0.368
1.97	2,200	11.9	216	.365
1.33	2,800	13.8	254	.340
1.79	3,000	14.8	269	.320
F_B	g_B 5/	V_B 6/	Re	λ
0.726	1,700	11.4	212	0.299
.776	2,800	17.2	320	.215
.858	5,200	27.5	510	.157
.896	6,500	35.4	655	.119
.963	9,400	55.1	1,016	.071
1.10	18,500	76.2	1,405	.073

Port diameter 0.407 cm.2/

F_F	g_F 3/	V_F 4/	Re	λ
1.09	1,900	11.0	203	0.360
1.89	2,600	12.4	224	.397
1.33	2,770	15.5	284	.265
1.86	2,750	15.3	277	.274
F_B	g_B 5/	V_B 6/	Re	λ
0.732	1,800	11.0	205	0.340
.776	2,800	16.9	311	.225
.898	6,400	26.9	498	.203
.980	10,200	45.7	843	.112
1.04	14,000	60.9	1,130	.086

Port diameter 0.245 cm.1/

F_B	g_B 5/	V_B 6/	Re	λ
0.935	8,000	12.3	379	0.160
1.06	15,000	20.5	630	.107
1.18	25,500	29.6	907	.088
1.33	42,000	42.5	1,300	.070

1/ 0.635 cm., port depth.
2/ 0.318 cm., port depth.
3/ g_F, flashback with tubes, figure 69.
4/ V_F, flows at flashback with sharp-edged short ports.
5/ g_B, blowoff with tubes, figure 69.
6/ V_B, flows at blowoff with sharp-edged short ports.

TABLE 8a. - Calculation of coefficients of friction, λ, for sharp-edged short ports (Con.)

$$\lambda = \frac{2 \pi g D^3}{V \ Re}$$

Fuel No. 2 composition, percent: 100 CH_4 — Re = $20.4/Re^{0.80}$

Stoichiometric percentage: 9.46 — (Data for line 13d, figure 75)

Port diameter 1.114 cm.[1]					Port diameter 0.952 cm.[1]					Port diameter 0.796 cm.[1]				
F_F	g_F[2]	V_F[3]	Re	λ	F_F	g_F[2]	V_F[3]	Re	λ	F_F	g_F[2]	V_F[3]	Re	λ
T = 300° K.					T = 300° K.					T = 300° K.				
0.728	110	18.9	131	0.387	0.782	165	17.2	139	0.374	0.946	370	18.3	177	0.361
1.26	105	19.0	131	.368	1.26	105	17.3	139	.236	1.17	240	17.9	173	.247
.744	125	25.6	177	.240	.854	260	25.9	209	.260					
1.27	100	25.6	176	.193	1.19	200	25.3	204	.210					
.864	280	38.4	266	.237	.996	390	32.8	265	.244					
1.19	190	38.0	261	.166	1.11	335	31.6	256	.224					
.984	390	50.3	347	.194										
1.08	365	50.8	349	.179										
T = 348° K.					T = 348° K.					T = 348° K.				
1.30	160	18.5	128	0.586	1.28	195	14.9	120	0.588	0.803	300	15.8	153	0.392
.743	210	28.7	199	.318	.791	290	21.5	174	.420	1.24	260	15.4	148	.361
1.28	200	28.2	194	.315	1.27	200	21.3	171	.298	.911	470	22.2	214	.312
.817	325	40.2	279	.255	.857	410	29.8	241	.309	1.18	360	21.6	208	.254
1.22	280	40.3	278	.216	1.23	260	28.8	232	.211	.944	510	22.8	220	.320
.924	500	54.8	377	.209	.938	506	37.8	304	.238	1.15	410	23.3	225	.246
1.16	380	53.9	371	.164	1.16	390	39.1	314	.172	1.02	520	24.9	241	.273
										1.11	470	25.1	243	.242
T = 423° K.					T = 423° K.					T = 423° K.				
1.42	110	15.1	104	0.602	1.34	220	17.4	140	0.491	0.792	470	22.6	219	0.300
.632	150	26.0	179	.278	.692	260	25.2	204	.274	1.30	290	21.5	208	.204
1.38	150	25.3	175	.294	1.33	240	25.6	206	.247	.882	680	29.4	283	.258
.716	300	35.5	245	.297	.858	640	42.0	339	.243	1.23	440	29.3	283	.166
1.33	230	35.8	246	.225	1.24	400	42.5	343	.149	.970	800	34.5	332	.220
.775	440	53.9	373	.189	.999	810	59.6	482	.153	1.13	680	35.1	338	.181
1.28	310	53.1	367	.137	1.14	650	58.7	472	.127					
.886	690	76.0	524	.149										
1.18	540	74.4	514	.122										
.997	800	85.5	591	.130										
1.09	770	86.3	598	.130										

1/ 0.635 cm., port depth.
2/ g_F, flashback with tubes, figure 20 for 300° K., figure 72 for 348° and 423° K.
3/ V_F, flows at flashback with sharp-edged short ports for 300°, 348° and 423° K.

TABLE 8a. - Calculation of coefficients of friction, λ, for sharp-edged short ports (Con.)

$$\lambda = \frac{2 \pi g D^3}{V\ Re}$$

Fuel No. 2 composition, percent: 100 CH_4

$Re = 20.4/Re^{0.80}$

Stoichiometric percentage: 9.46

(Data for line 13d, figure 75)

Port diameter 1.114 cm. 1/					Port diameter 0.952 cm. 1/				
F_B	g_B 2/	V_B 3/	Re	λ	F_B	g_B 2/	V_B 3/	Re	λ
T = 300° K.					T = 300° K.				
0.685	130	18.8	130	0.461	0.702	165	17.0	138	0.381
.708	170	25.5	177	.328	.755	300	25.6	207	.316
.741	260	38.0	263	.244	.775	400	32.1	260	.261
.760	320	50.1	345	.163					
T = 348° K.					T = 348° K.				
0.689	220	28.6	198	0.336	0.704	270	21.3	172	0.399
.715	310	39.8	275	.244	.733	390	29.4	238	.303
.740	450	53.8	371	.195	.763	600	40.2	324	.249
T = 423° K.					T = 423° K.				
0.616	160	25.9	179	0.298	0.664	320	25.1	203	0.341
.651	280	35.3	243	.282	.711	540	41.4	334	.211
.682	420	53.3	369	.184	.749	760	59.3	478	.145
.724	620	75.4	520	.137					

Port diameter 0.796 cm. 1/					Port diameter 0.595 cm. 1/				
F_B	g_B 2/	V_B 3/	Re	λ	F_B	g_B 2/	V_B 3/	Re	λ
T = 300° K.					T = 300° K.				
0.747	290	18.0	174	0.295	0.911	1,200	26.6	344	0.174
.777	400	25.0	242	.209	1.02	2,050	41.7	540	.120
.836	730	35.0	338	.196	1.16	3,400	59.8	769	.098
.890	1,050	49.8	482	.139	1.36	5,100	83.1	1,070	.076
.972	1,700	75.3	726	.098					
T = 348° K.					T = 348° K.				
0.740	440	21.8	211	0.301	0.877	1,600	25.3	327	0.258
.776	700	29.6	285	.262	.965	2,700	37.3	481	.200
.803	880	37.2	360	.207	1.08	4,000	53.7	692	.143
.853	1,300	51.0	495	.162	1.21	5,900	77.0	995	.103
.920	2,200	74.3	716	.130					
T = 423° K.									
0.722	590	28.9	279	0.232					
.780	960	44.7	432	.156					

Port diameter 0.407 cm. 1/					Port diameter 0.245 cm. 1/				
F_B	g_B 2/	V_B 3/	Re	λ	F_B	g_B 2/	V_B 3/	Re	λ
T = 300° K.					T = 300° K.				
1.23	4,000	24.1	455	0.155	2.16	10,500	18.6	580	0.090
1.46	5,900	34.8	658	.109	2.45	13,000	22.1	692	.078
1.69	7,400	43.9	832	.086	2.73	15,500	26.1	815	.067
1.90	8,900	55.7	1,060	.064					
2.35	12,000	68.4	1,285	.058					
2.80	16,200	72.2	1,350	.070					

1/ 0.635 cm., port depth.
2/ g_B, blowoff with tubes, figure 20 for 300° K., figure 72 for 348° and 423° K.
3/ V_B, flows at blowoff with sharp-edged short ports for 300°, 348°, and 423° K.

TABLE 8b. - Critical boundary velocity gradients using λ for sharp-edged short ports

$$g = \frac{\lambda\ V\ Re}{2 \pi D^3}$$

Fuel No. 17 composition, percent: 79.7 CO, 20.1 H_2, 0.2 CO_2

Stoichiometric percentage: 29.5

(Points for figure 71)

Port diameter 0.952 cm. 1/			Port diameter 0.650 cm. 2/			Port diameter 0.595 cm. 1/			Port diameter 0.476 cm. 1/		
F_F	g_F	λ	F_F	g_F	λ	F_F	g_F	λ	F_F	g_F	λ
0.675	315	0.418	0.739	655	0.425	0.786	677	0.480	1.10	1,710	0.328
2.25	288	.460	2.22	678	.425	2.21	702	.480	2.10	1,425	.385
.783	522	.278	.909	1,020	.300	.952	1,204	.305	1.33	2,430	.248
2.20	474	.305	2.10	1,055	.300	2.13	1,170	.320	1.86	2,390	.258
.950	938	.174	1.10	1,710	.198	1.32	2,220	.188			
2.14	958	.174	1.99	1,870	.190	1.93	2,020	.203			
			1.32	2,310	.158						
			1.79	2,530	.148						
F_B	g_B	λ	F_B	g_B	λ	F_B	g_B	λ	F_B	g_B	λ
0.582	301	0.430	0.634	701	0.400	0.640	694	0.465	0.692	1,575	0.348
.614	499	.283	.698	1,077	.283	.641	1,048	.335	.728	2,480	.243
.639	928	.173	.718	1,840	.188	.719	1,980	.203	.796	3,770	.173
			.787	3,110	.120	.758	2,935	.148			
			.881	4,520	.091	.804	4,230	.109			

Port diameter 0.476 cm. 2/			Port diameter 0.407 cm. 1/			Port diameter 0.407 cm. 2/			Port diameter 0.245 cm. 1/		
F_F	g_F	λ	F_F	g_F	λ	F_F	g_F	λ			
0.898	1,320	0.400	1.25	2,300	0.335	1.09	1,964	0.372			
2.11	1,400	.390	1.33	2,540	.308	1.89	2,230	.342			
1.10	2,010	.288	1.79	2,760	.293	1.33	2,910	.278			
1.87	2,640	.238	1.97	2,160	.358	1.86	2,850	.285			
1.42	2,940	.215									
1.73	3,040	.212									
F_B	g_B	λ	F_B	g_B	λ	F_B	g_B	λ	F_B	g_B	λ
0.688	1,386	0.385	0.726	2,070	0.363	0.732	1,956	0.370	0.935	10,850	0.216
.726	2,380	.255	.776	3,260	.250	.776	3,200	.257	1.06	19,250	.138
.846	3,925	.168	.858	5,460	.165	.898	5,380	.170	1.18	28,700	.099
.905	6,360	.113	.896	7,280	.133	.980	9,570	.105	1.33	42,400	.071
.980	8,880	.087	.963	11,800	.089	1.04	13,150	.081			
			1.10	16,900	.067						

1/ 0.635 cm., port depth.
2/ 0.318 cm., port depth.
λ = Coefficients of friction (figure 70).

TABLE 9. - Critical boundary velocity gradients for long cylindrical tubes at 348° and 423° K.

Fuel No. 2 composition, percent: 100 CH_4

Stoichiometric percentage: 9.46 (Points for figure 72)

Tube diameter 1.257 cm.		Tube diameter 1.058 cm.		Tube diameter 0.944 cm.		Tube diameter 0.511 cm.	
F_F	g_F	F_F	g_F	F_F	g_F		
T = 348° K.							
0.731	168	0.745	203	0.794	266		
1.29	167	1.28	180	1.23	267		
1.25	227	.791	280	.868	403		
.836	366	1.22	275	1.15	398		
1.18	372	.869	403	.963	512		
.906	502	1.16	399	1.06	517		
1.10	512	.916	495				
		1.11	506				
T = 423° K.							
		0.664	249				
		1.33	254				
		.781	405				
		1.23	401				
		.846	602				
		1.16	602				
		.939	782				
		1.08	794				
		F_B	g_B	F_B	g_B	F_B	g_B
T = 348° K.							
		0.690	202	0.686	263	0.857	1,090
		.712	278			.898	1,685
		.736	398			.969	2,480
		.769	604			1.06	3,760
						1.14	5,100
T = 423° K.							
		0.641	248				
		.691	401				
		.732	594				
		.754	804				

TABLE 10a. - Calculation of coefficients of friction, λ, for long square channels

$$\lambda = \frac{2 \pi g D^3}{V \text{ Re}}$$

Fuel No. 2 composition, percent: 100 CH_4
Stoichiometric percentage: 9.46
(Data for line 13f, figure 75) $\lambda = 61.4/Re^{1.09}$

Channel dimensions 1.068 × 1.075 cm. E.H.D. = 1.07 cm.

F_F	g_F 1/	V_F 2/	Re	λ
0.728	115	26.5	191	0.175
1.24	128	26.3	189	.198
.766	150	38.9	279	.106
1.21	160	39.6	284	.109
.794	180	51.9	372	.072
1.18	205	52.3	375	.080
.879	295	77.4	557	.053
1.11	330	78.4	562	.058

F_B	g_B 4/	V_B 5/	Re	λ
0.661	98	17.5	126	0.341
.696	160	26.4	189	.246
.715	190	38.7	278	.136
.738	250	51.6	370	.101
.776	400	78.4	562	.070

Channel dimensions 0.740 × 0.744 cm. E.H.D. = 0.742 cm.

F_F	g_F 1/	V_F 2/	Re	λ
0.879	295	19.9	206	0.185
1.09	345	20.3	210	.208
.944	375	25.3	261	.146
1.04	390	25.5	264	.149

F_B	g_B 4/	V_B 5/	Re	λ
0.766	360	21.5	222	0.194
.775	400	24.9	258	.160
.784	420	29.8	309	.117
.817	600	44.1	458	.076
.863	900	61.2	634	.060
.889	1,050	77.1	798	.044
.900	1,120	92.3	951	.033

Channel dimensions 0.596 × 0.600 cm. E.H.D. = 0.598 cm.

F_B	g_B 4/	V_B 5/	Re	λ
0.833	680	19.1	246	0.194
.877	960	26.9	347	.138
.927	1,400	44.6	575	.073
1.01	2,000	68.1	869	.045
1.07	2,500	91.2	1,170	.031

Fuel No. 17 composition, percent: 79.7 CO, 20.1 H_2, 0.2 CO_2
Stoichiometric percentage: 29.5
(Data for line 13e, figure 75) $\lambda = 156.4/Re^{1.22}$

Channel dimensions 0.596 × 0.600 cm. E.H.D. = 0.598 cm.

F_F	g_F 3/	V_F 2/	Re	λ
0.674	370	11.7	148	0.287
2.23	720	12.5	154	.503
.698	440	16.6	210	.170
2.17	1,000	17.7	217	.349
.806	760	28.1	355	.100
2.07	1,600	31.7	389	.175
.859	940	38.8	491	.066
.938	1,280	49.7	626	.055
2.03	1,900	47.1	578	.094
1.03	1,650	69.4	874	.037
1.94	2,350	72.2	892	.049
1.14	2,100	88.7	1,110	.029
1.82	2,900	95.1	1,180	.035
1.23	2,450	103.1	1,290	.025
1.30	2,700	113.5	1,425	.022
1.32	2,750	117.8	1,475	.021
1.61	3,300	128.5	1,600	.022
1.64	3,300	121.8	1,510	.024

F_B	g_B 6/	V_B 5/	Re	λ
0.618	460	12.4	158	0.317
.617	460	17.6	223	.158
.670	880	30.8	390	.099
.686	1,100	44.3	561	.059
.716	1,400	62.0	785	.039
.741	1,900	88.6	1,124	.026
.766	2,500	118.3	1,500	.019

E.H.D. = Equivalent hydraulic diameter.
1/ g_F, flashback with tubes, figure 20.
2/ V_F, flows at flashback with long square channels.
3/ g_F, flashback with tubes, figure 69.
4/ g_B, blowoff with tubes, figure 20.
5/ V_B, flows at blowoff with long square channels.
6/ g_B, blowoff with tubes, figure 69.

TABLE 10b. - Critical boundary velocity gradients using λ for long square channels

$$g = \frac{\lambda \; V \; Re}{2 \pi D^3}$$

Fuel No. 2 composition, percent: 100 CH_4; Stoichiometric percentage: 9.46									Fuel No. 17 composition, percent: 79.7 CO, 20.1 H_2, 0.2 CO_2; Stoichiometric percentage: 29.5		
Channel dimensions 1.068 × 1.075 cm. E.H.D. = 1.07 cm.			Channel dimensions 0.740 × 0.744 cm. E.H.D. = 0.742 cm.			Channel dimensions 0.596 × 0.600 cm. E.H.D. = 0.598 cm.			Channel dimensions 0.596 × 0.600 cm. E.H.D. = 0.598 cm.		
F_F	g_F	λ 1/	F_F	g_F	λ 1/				F_F	g_F	λ 2/
0.728	135	0.205	0.879	300	0.188				0.674	453	0.352
1.24	134	.208	1.09	307	.185				2.23	486	.340
.766	192	.136	.944	381	.148				.698	596	.230
1.21	198	.135	1.04	378	.144				2.17	636	.222
.794	249	.099							.806	905	.122
1.18	250	.098							2.07	991	.108
.879	359	.064							.859	1,164	.082
1.11	362	.063							.938	1,411	.061
									2.03	1,376	.068
									1.03	1,826	.041
									1.94	1,894	.040
									1.14	2,235	.031
									1.82	2,340	.028
									1.23	2,520	.025
									1.30	2,710	.023
									1.32	2,820	.022
									1.61	3,000	.020
									1.64	2,860	.021
F_B	g_B	λ 1/	F_B	g_B	λ 1/	F_B	g_B	λ 1/	F_B	g_B	λ 2/
0.661	92	0.320	0.766	323	0.174	0.833	550	0.157	0.618	472	0.325
.696	135	.208	.775	371	.148	.877	745	.107	.617	628	.215
.715	193	.138	.784	439	.122	.927	1,185	.062	.670	965	.108
.738	246	.099	.817	629	.080	1.01	1,730	.039	.686	1,295	.070
.776	361	.063	.863	844	.056	1.07	2,260	.029	.716	1,665	.046
			.889	1,030	.043				.741	2,220	.030
			.900	1,215	.036				.766	2,775	.021

E.H.D. = Equivalent hydraulic diameter.
1/ Coefficients of friction (line 13f, figure 75).
2/ Coefficients of friction (line 13e, figure 75).

TABLE 11a.- Calculation of coefficients of friction, λ, for long rectangular channels

$$\lambda = \frac{2\pi g D^3}{V\,Re}$$

Fuel No. 2 composition, percent: 100 CH_4
Stoichiometric percentage: 9.46
(Data for line 13g, figure 75) $\lambda = 125.8/Re^{1.24}$

Channel dimensions 0.634 × 0.968 cm. E.H.D. = 0.766 cm.					Channel dimensions 0.354 × 1.284 cm. E.H.D. = 0.555 cm.				
F_F	g_F 1/	V_F 2/	Re	λ					
0.838	235	18.8	189	0.187					
1.14	270	18.7	187	.218					
.885	310	24.1	242	.150					
1.11	330	23.9	239	.163					
.961	380	31.0	310	.111					
1.06	370	30.8	309	.110					
F_B	g_B 3/	V_B 4/	Re	λ	F_B	g_B 3/	V_B 4/	Re	λ
0.716	190	18.6	187	0.115	0.892	1,050	44.9	624	0.040
.758	310	23.8	238	.154	.941	1,450	65.0	900	.027
.781	400	30.5	305	.111	1.01	1,950	88.3	1,228	.019
					1.05	2,350	107.2	1,490	.016

E.H.D. = Equivalent hydraulic diameter
1/ g_F, flashback with tubes, figure 20.
2/ V_F, flows at flashback with long rectangular channels.
3/ g_B, blowoff with tubes, figure 20.
4/ V_B, flows at blowoff with long rectangular channels.

TABLE 11b. - Critical boundary velocity gradients using λ for long rectangular channels

$$g = \frac{\lambda\,V\,Re}{2\pi D^3}$$

Fuel No. 2 composition, percent: 100 CH_4
Stoichiometric percentage: 9.46

Channel dimensions 0.634 × 0.968 cm. E.H.D. = 0.766 cm.			Channel dimensions 0.354 × 1.284 cm. E.H.D. = 0.555 cm.		
F_F	g_F	λ			
0.838	242	0.193			
1.14	242	.195			
.885	296	.143			
1.11	294	.145			
.961	358	.105			
1.06	354	.105			
F_B	g_B	λ	F_B	g_B	λ
0.716	240	0.195	0.892	1,150	0.044
.758	298	.148	.941	1,525	.028
.781	356	.108	1.01	1,950	.019
			1.05	2,230	.015

E.H.D. = Equivalent hydraulic diameter.
λ = Coefficients of friction (line 13g, figure 75).

TABLE 12a. - Calculation of coefficients of friction, λ, for long triangular channels

$$\lambda = \frac{2\pi g D^3}{V\,Re}$$

Fuel No. 2 composition, percent: 100 CH_4
Stoichiometric percentage: 9.46
(Data for line 13h, figure 75) $\lambda = 90.6/Re^{1.25}$

Channel dimensions 1.25×1.25×1.25 cm. E.H.D. = 0.722 cm.					Channel dimensions 1.75×1.25×1.25 cm. E.H.D. = 0.734 cm.				
F_F	g_F 1/	V_F 2/	Re	λ	F_F	g_F 1/	V_F 2/	Re	λ
0.819	215	20.3	216	0.116	0.807	200	19.6	206	0.123
1.18	210	19.3	204	.126	1.22	150	19.6	206	.092
.845	250	26.6	284	.078	.828	230	29.7	311	.062
1.15	260	26.7	283	.081	1.18	220	30.0	315	.058
.854	260	29.8	317	.065	.862	270	39.7	417	.041
1.13	300	30.7	325	.071	1.14	270	40.3	422	.039
.910	345	39.6	420	.049	.899	330	53.2	558	.028
1.09	370	40.4	429	.051	1.10	350	54.4	572	.028
.967	385	45.5	482	.042	.931	365	61.6	644	.023
1.05	385	45.8	488	.041	1.02	390	62.2	654	.024
F_B	g_B 3/	V_B 4/	Re	λ	F_B	g_B 3/	V_B 4/	Re	λ
0.732	230	20.1	214	0.126	0.732	240	19.4	204	0.150
.751	290	29.8	317	.059	.746	280	29.5	309	.076
.766	350	37.3	397	.056	.756	300	39.3	409	.046
.797	480	49.3	525	.044	.774	380	60.0	624	.025
.814	580	63.0	670	.033	.822	620	91.5	962	.018
.835	720	76.0	808	.028					
.834	720	90.5	962	.020					

E.H.D. = Equivalent hydraulic diameter.
1/ g_F, flashback with tubes, figure 20.
2/ V_F, flows at flashback with long triangular channels.
3/ g_B, blowoff with tubes, figure 20.
4/ V_B, flows at blowoff with long triangular channels.

TABLE 12b.- Critical boundary velocity gradients using λ for long triangular channels

$$g = \frac{\lambda\,V\,Re}{2\pi D^3}$$

Fuel No. 2 composition, percent: 100 CH_4
Stoichiometric percentage: 9.46

Channel dimensions 1.25×1.25×1.25 cm. E.H.D. = 0.722 cm.			Channel dimensions 1.75×1.25×1.25 cm. E.H.D. = 0.734 cm.		
F_F	g_F	λ	F_F	g_F	λ
0.819	204	0.110	0.807	191	0.117
1.18	198	.119	1.22	191	.117
.845	250	.078	.828	260	.070
1.15	250	.078	1.18	264	.069
.854	272	.068	.862	321	.048
1.13	276	.066	1.14	326	.048
.910	338	.048	.899	402	.034
1.09	340	.047	1.10	409	.033
.967	371	.040	.931	446	.028
1.05	377	.040	1.02	452	.028
F_B	g_B	λ	F_B	g_B	λ
0.732	206	0.113	0.732	191	0.119
.751	272	.068	.746	258	.070
.766	319	.051	.756	322	.050
.797	394	.036	.774	439	.029
.814	473	.027	.822	598	.017
.835	546	.021			
.834	619	.017			

E.H.D. = Equivalent hydraulic diameter.
λ = Coefficients of friction (line 13h, figure 75).

TABLE 13. - Critical boundary velocity gradients for sharp-edged short ports at various initial temperatures

$$g = \frac{\lambda \ V \ Re}{2 \pi D^3}$$

Fuel No. 2 composition, percent: 100 CH_4

Stoichiometric percentage: 9.46 (Data for figures 78 and 79)

Initial temperature: 300° K.

Port diameter 1.114 cm.1/			Port diameter 0.952 cm.1/			Port diameter 0.796 cm.1/			Port diameter 0.595 cm.1/			Port diameter 0.407 cm.1/			Port diameter 0.245 cm.1/		
F_F	g_F	λ	F_F	g_F	λ	F_F	g_F	λ									
0.728	117	0.412	0.782	172	0.390	0.946	330	0.322									
1.26	118	.412	1.26	173	.390	1.17	321	.330									
.744	168	.322	.854	283	.283												
1.27	168	.322	1.19	276	.289												
.864	275	.233	.996	377	.235												
1.19	271	.237	1.11	358	.240												
.984	379	.188															
1.08	385	.188															
F_B	g_B	λ	F_B	g_B	λ	F_B	g_B	λ	F_B	g_B	λ	F_B	g_B	λ	F_B	g_B	λ
0.685	117	0.412	0.702	169	0.390	0.747	328	0.330	0.911	1,314	0.190	1.23	3,940	0.152	2.16	14,600	0.125
.708	168	.322	.755	277	.283	.777	478	.250	1.02	2,250	.132	1.46	6,180	.114	2.45	17,900	.108
.741	271	.235	.775	366	.238	.836	720	.193	1.16	3,440	.099	1.69	8,110	.094	2.73	21,900	.095
.760	379	.190				.890	1,096	.145	1.36	5,100	.076	1.90	10,750	.077			
						.972	1,775	.103				2.35	13,700	.066			
												2.80	14,750	.064			

Initial temperature: 348° K.

Port diameter 1.112 cm.1/			Port diameter 0.952 cm.1/			Port diameter 0.795 cm.1/			Port diameter 0.596 cm.1/			Port diameter 0.477 cm.1/			Port diameter 0.407 cm.1/			Port diameter 0.245 cm.1/		
F_F	g_F	λ	F_F	g_F	λ	F_F	g_F	λ												
1.30	115	0.420	1.28	145	0.440	0.803	276	0.360												
.743	196	.297	.791	226	.328	1.24	266	.370												
1.28	191	.300	1.27	221	.330	.911	435	.288												
.817	297	.228	.857	332	.250	1.18	403	.283												
1.22	296	.228	1.23	320	.260	.944	431	.270												
.924	426	.177	.938	445	.210	1.15	445	.267												
1.16	415	.179	1.16	461	.204	1.02	477	.250												
						1.11	485	.250												
F_B	g_b	λ	F_B	g_B	λ	F_B	g_B	λ	F_B	g_B	λ	F_B	g_B	λ	F_B	g_B	λ	F_B	g_B	λ
0.689	194	0.297	0.704	224	0.330	0.740	410	0.280	0.877	1,230	0.198	1.14	3,320	0.138	1.65	8,230	0.093	2.09	12,340	0.140
.715	289	.228	.733	330	.255	.776	588	.220	.965	1,957	.145	1.32	5,500	.098	1.85	10,440	.079	2.38	17,060	.114
.740	413	.179	.763	478	.199	.803	766	.180	1.08	3,020	.108	1.59	8,120	.077	2.34	15,230	.060	2.93	22,400	.093
						.853	1,140	.142	1.21	4,670	.081	1.86	10,170	.066						
						.920	1,790	.106												

1/ 0.635 cm., port depth.
λ = Coefficients of friction (line 13d, figure 75).

TABLE 13. - Critical boundary velocity gradients for sharp-edged short ports at various initial temperatures (Con.)

$$g = \frac{\lambda V Re}{2\pi D^3}$$

Fuel No. 2 composition, percent: 100 CH_4

Stoichiometric percentage: 9.46

Initial temperature: 423° K. (Data for figures 78 and 79)

Port diameter 1.112 cm.1/			Port diameter 0.952 cm.1/			Port diameter 0.795 cm.1/		
F_F	g_F	λ	F_F	g_F	λ	F_F	g_F	λ
1.42	89	0.490	1.34	174	0.388	0.792	427	0.272
.632	172	.320	.692	273	.288	1.30	401	.282
1.38	167	.325	1.33	278	.285	.882	580	.220
.716	252	.250	.858	508	.193	1.23	579	.220
1.33	255	.250	1.24	511	.190	.97	708	.195
.775	415	.178	.999	770	.145	1.13	726	.193
1.28	407	.180	1.14	752	.147			
.886	622	.135						
1.18	612	.138						
.997	720	.123						
1.09	724	.121						

(Port diameters 0.596, 0.477, 0.407 and 0.245 cm.: no F_F data.)

Port diameter 1.112 cm.1/			Port diameter 0.952 cm.1/			Port diameter 0.795 cm.1/			Port diameter 0.596 cm.1/			Port diameter 0.477 cm.1/			Port diameter 0.407 cm.1/			Port diameter 0.245 cm.1/		
F_B	g_B	λ	F_B	g_B	λ	F_B	g_B	λ	F_B	g_B	λ	F_B	g_B	λ	F_B	g_B	λ	F_B	g_B	λ
0.616	172	0.320	0.664	271	0.288	0.722	567	0.222	0.851	1,640	0.163	1.14	4,630	0.110	1.66	9,100	0.086	2.03	12,450	0.155
.651	248	.250	.711	497	.195	.780	968	.158	1.00	2,970	.109	1.32	6,710	.087	1.95	11,700	.073	2.33	16,250	.116
.682	410	.180	.749	758	.145	.839	1,500	.117	1.11	4,240	.087	1.56	8,710	.072	2.14	15,200	.061			
.724	626	.138				.915	2,390	.087	1.28	5,880	.069	1.79	10,850	.063	2.71	18,900	.054			

Initial temperature: 473° K. (Points for figure 77)

Port diameter 1.112 cm.1/			Port diameter 0.952 cm.1/			Port diameter 0.795 cm.1/		
F_F	g_F	λ	F_F	g_F	λ	F_F	g_F	λ
0.590	180	0.310	0.602	268	0.290	0.679	497	0.248
1.42	183	.300	1.37	282	.283	1.30	467	.259
.700	426	.178	.768	549	.180	.742	660	.204
1.33	413	.180	1.29	562	.180	1.27	615	.215
.893	830	.111	.840	849	.137	.943	929	.163
1.21	813	.113	1.23	844	.137	1.13	946	.159
			.948	1,050	.118			
			1.09	1,070	.116			

Port diameter 1.112 cm.1/			Port diameter 0.952 cm.1/			Port diameter 0.795 cm.1/			Port diameter 0.596 cm.1/			Port diameter 0.477 cm.1/			Port diameter 0.407 cm.1/			Port diameter 0.245 cm.1/
F_B	g_B	λ	F_B	g_B	λ	F_B	g_B	λ	F_B	g_B	λ	F_B	g_B	λ	F_B	g_B	λ	
0.571	180	0.310	0.578	267	0.290	0.696	653	0.204	0.872	2,460	0.124	1.71	10,900	0.061	1.21	6,640	0.105	
.647	420	.178	.681	546	.182	.778	1,354	.127	1.04	4,660	.081	2.09	15,360	.050	1.49	9,870	.082	
.728	816	.113	.731	837	.138	.851	2,270	.090	1.21	6,720	.063	2.46	17,900	.044	1.87	13,270	.067	
.750	1,110	.092				.942	3,450	.068	1.38	8,900	.054				2.17	16,560	.057	
															2.41	18,600	.054	
															2.93	24,200	.046	

1/ 0.635 cm., port depth.
λ = Coefficients of friction (line 13d, figure 75).

TABLE 13. - Critical boundary velocity gradients for sharp-edged short ports at various initial temperatures (Con.)

$$g = \frac{\lambda V Re}{2 \pi D^3}$$

Fuel No. 2 composition, percent: 100 CH_4

Stoichiometric percentage: 9.46

Initial temperature: 523° K. (Data for figures 78 and 79)

Port diameter 1.112 cm.1/			Port diameter 0.952 cm.1/			Port diameter 0.795 cm.1/			Port diameter 0.477 cm.1/			Port diameter 0.407 cm.1/		
F_F	g_F	λ	F_F	g_F	λ	F_F	g_F	λ						
0.553	219	0.270	0.559	385	0.228	0.663	674	0.200						
1.47	219	.270	1.44	385	.228	1.31	730	.190						
.566	345	.200	.606	611	.170	.792	1,100	.145						
1.45	360	.198	1.37	612	.170	1.26	1,100	.145						
.621	538	.149	.664	888	.132	.958	1,313	.128						
1.37	532	.152	1.31	886	.132	1.06	1,325	.128						
.712	800	.113	.815	1,280	.102									
1.32	797	.114	1.23	1,293	.101									
.873	1,118	.092												
1.19	1,125	.092												
F_B	g_B	λ	F_B	g_B	λ	F_B	g_B	λ	F_B	g_B	λ	F_B	g_B	λ
0.534	217	0.270	0.547	385	0.228	0.624	670	0.200	0.906	2,770	0.153	1.26	8,820	0.089
.552	344	.200	.594	610	.170	.719	1,080	.145	1.01	4,600	.110	1.56	11,950	.073
.614	538	.149	.658	886	.132	.806	2,280	.089	1.15	7,070	.083	2.12	15,100	.062
.692	1,118	.091	.722	1,310	.100	.909	3,910	.063	1.38	9,560	.067	2.53	20,200	.051
									1.82	14,170	.051	2.80	23,100	.047
									2.28	18,400	.044			

1/ 0.635 cm., port depth.
λ = Coefficients of friction (line 13d, figure 75).

TABLE 14. - Yellow-tip limits for propylene at various initial temperatures

$$g = \frac{\lambda V Re}{2\pi D^3}$$

Fuel No. 5 composition, percent: 99.2 C_3H_6, 0.4 C_3H_8, 0.4 C_2H_6

Stoichiometric percentage: 4.45 (Data for figure 87A)

Port diameter 1.112 cm.1/			Port diameter 0.952 cm.1/			Port diameter 0.795 cm.1/			Port diameter 0.595 cm.1/			Port diameter 0.477 cm.1/			Port diameter 0.407 cm.1/			Port diameter 0.346 cm.1/			Port diameter 0.245 cm.1/		
F_y	g_y	λ	F_y	g_y	λ	F_y	g_y	λ	F_y	g_y	λ	F_y	g_y	λ	F_y	g_y	λ	F_y	g_y	λ	F_y	g_y	λ
Initial temperature: 348° K.																							
1.64	395	0.253	1.75	303	0.400	1.72	520	0.348	1.77	873	0.370	1.83	1,526	0.330	1.83	2,410	0.293	1.87	3,783	0.268	1.94	11,200	0.194
1.52	622	.177	1.61	646	.250	1.60	1,195	.180	1.70	1,106	.305	1.74	1,983	.268	1.76	3,205	.240	1.79	4,900	.218	1.86	14,610	.157
1.47	855	.137	1.53	1,003	.153	1.51	1,797	.129	1.67	1,443	.245	1.72	2,482	.222	1.70	4,010	.198	1.72	6,250	.179			
1.49	1,067	.114	1.50	1,350	.123	1.49	2,373	.102	1.61	2,909	.140	1.68	2,885	.198	1.69	4,720	.170	1.67	7,800	.150			
1.47	1,296	.097	1.49	1,455	.114	1.47	2,945	.086	1.50	4,405	.100	1.60	5,760	.114	1.66	6,980	.127	1.66	11,900	.105			
1.47	1,980	.068	1.47	1,708	.100	1.47	3,720	.072	1.50	5,870	.078	1.57	8,780	.081	1.63	9,320	.099						
1.47	2,535	.056	1.47	2,090	.084	1.47	5,065	.056	1.47	7,470	.065	1.56	9,380	.078									
			1.47	3,200	.061				1.48	8,500	.058												
			1.47	4,165	.050																		
Initial temperature: 423° K.																							
1.53	780	0.147	1.73	375	0.333	1.68	844	0.235	1.75	1,070	0.303	1.81	1,868	0.275	1.81	2,990	0.248	1.86	4,680	0.223	1.94	13,790	0.163
1.50	1,090	.110	1.62	820	.180	1.61	1,504	.150	1.69	1,368	.250	1.75	2,470	.223	1.76	3,930	.198	1.77	6,170	.180	1.87	16,900	.138
1.49	1,306	.096	1.53	1,233	.127	1.52	2,215	.108	1.66	1,786	.205	1.72	3,095	.186	1.70	5,000	.165	1.73	7,720	.150			
1.48	1,628	.082	1.51	1,779	.097	1.47	2,983	.086	1.59	3,675	.115	1.68	3,555	.166	1.68	5,800	.146	1.72	9,730	.125			
1.46	1,900	.070	1.51	2,150	.084	1.47	3,675	.073	1.48	7,360	.066	1.60	7,060	.096	1.66	8,590	.106	1.67	13,250	.098			
1.47	2,475	.058	1.49	2,573	.070	1.47	4,960	.060	1.48	9,300	.054	1.53	11,830	.064	1.62	11,850	.083						
1.49	3,215	.046	1.48	2,730	.068	1.47	6,450	.047	1.47	10,770	.048												
			1.47	3,950	.051																		
			1.47	5,130	.041																		
Initial temperature: 523° K.																							
1.53	994	0.123	1.63	1,023	0.148	1.73	957	0.208	1.70	1,321	0.258	1.74	2,385	0.233	1.79	3,770	0.202	1.86	5,850	0.185	1.98	17,300	0.135
1.49	1,324	.096	1.54	1,570	.105	1.62	1,860	.123	1.65	1,754	.206	1.70	2,993	.190	1.76	5,025	.165	1.80	7,800	.150	1.89	20,500	.118
1.48	1,644	.078	1.52	2,135	.083	1.53	2,665	.082	1.59	2,273	.170	1.67	3,840	.160	1.74	6,250	.136	1.77	9,810	.123			
1.48	2,120	.064	1.49	2,645	.070	1.50	3,700	.070	1.58	4,775	.092	1.63	5,350	.121	1.72	7,450	.120	1.76	12,260	.103			
1.47	3,130	.048	1.47	3,450	.056	1.48	4,685	.059	1.49	6,880	.069	1.63	9,070	.077	1.72	10,810	.086	1.73	16,700	.079			
			1.47	4,975	.042	1.48	5,950	.048	1.48	9,300	.055	1.61	12,600	.060	1.67	14,670	.069						
			1.46	4,980	.042	1.46	7,940	.039	1.48	10,580	.048												
						1.47	7,970	.039	1.47	11,720	.045												

1/ 0.635 cm., port depth.
λ = Coefficients of friction (figure 70).

BIBLIOGRAPHY

1. AMERICAN GAS ASSOCIATION TESTING LABORATORIES. Interchangeability of Other Fuel Gases with Natural Gas. Bulletin 36, February 1946.

2. BLANC, M. V., GUEST, P. G., VON ELBE, G., and LEWIS, B. Ignition of Explosive Gas Mixtures by Electric Sparks. III. Minimum Ignition Energies and Quenching Distances of Mixtures of Hydrocarbons and Ether with Oxygen and Inert Gases. Third Symposium on Combustion, Flame and Explosion Phenomena, Williams & Wilkins Co., Baltimore, Md., 1949, pp. 363-367.
_____ . Ignition of Explosive Gas Mixtures by Electric Sparks. I. Minimum Ignition Energies and Quenching Distances of Mixtures of Methane, Oxygen and Inert Gases. Jour. Chem. Phys., vol. 15, 1947, pp. 798-802.
_____ . Other unpublished data.

3. BOLLINGER, L. M., and Williams, D. T. Experiments on Stability of Bunsen-Burner Flames for Turbulent Flow. Nat. Advisory Comm. Aeronaut. Tech. Note 1234, June 1947.

4. CLARK, T. P. Influence of External Variables on Smoking of Benzene Flames. NACA Research Memorandum E52G24, 1952.

5. DUGGER, G. L. Effect of Initial Mixture Temperature on Flame Speeds and Blow-Off Limits of Propane-Air Flames. Nat. Advisory Comm. Aeronaut. Tech. Note 2170, 1950.

6. DUGGER, G. L., WEAST, C. R., and HEIMEL, S. Flame Velocity and Preflame Reaction in Heated Propane-Air Mixtures. Ind. Eng. Chem., vol. 47, 1955, pp. 114-116.

7. EDSE, R. Studies on Burner Flames of Hydrogen-Oxygen Mixtures at High Pressures. Wright Air Development Center (WADC) Tech. Rept. 52-59, April 1952.

8. FRIEDMAN, R. Measurement of the Temperature Profile in a Laminar Flame. Fourth Symposium (International) on Combustion, Williams & Wilkins Co., Baltimore, Md., 1953, pp. 259-263.

9. FRISTROM, R. M., PRESCOTT, R., NEUMANN, R. K., and AVERY, W. H., Temperature Profiles in Propane-Air Flame Fronts. Fourth Symposium (International) on Combustion, Williams & Wilkins Co., Baltimore, Md., 1953, pp. 267-274.

10. GRUMER, J. Study of Combustion Characteristics of Fuel Gases. Am. Gas Assoc., Interim Rept. 1, Project PDC-3-GU, October 1951.

11. GRUMER, J., and HARRIS, M. E. Temperature Dependence of Stability Limits of Burner Flames. Ind. Eng. Chem., vol. 46, 1954, pp. 2424-2430.

12. GRUMER, J., HARRIS, M. E., and SCHULTZ, H. Flame Stabilization on Burners With Short Ports or Noncircular Ports. Fourth Symposium (International) on Combustion, Williams & Wilkins Co., Baltimore, Md., 1953, pp. 695-701.

13. GRUMER, J., SCHULTZ, H., and HARRIS, M. E. Calibration of Glass-Wool Flowmeters. Anal. Chem., vol. 25, 1953, p. 840.

14. GUEST, P. G., SIKORA, V. W., and LEWIS, B. Static Electricity in Hospital Operating Suites: Direct and Related Hazards and Pertinent Remedies. Bureau of Mines Bull. 520, 1953, fig. 8.

15. HARRIS, M. E., GRUMER, J., VON ELBE, G., and LEWIS, B. Burning Velocities, Quenching and Stability Data on Nonturbulent Flames of Methane and Propane With Oxygen and Nitrogen. Application of the Theory of Ignition, Quenching and Stabilization to Flames of Propane and Air. Third Symposium on Combustion, Flame, and Explosion Phenomena, Williams & Wilkins Co., Baltimore, Md., 1949, pp. 80-89.

16. IBERALL, A. S. Permeability of Glass Wool and Other Highly Porous Media. Nat. Bureau of Standards Jour. Res., vol. 45, 1950, pp. 398-406.

17. LEWIS, B., and VON ELBE, G. Combustion, Flames and Explosions of Gases. Academic Press, New York, N. Y., 1951, p. 280.

18. _____ . Ignition and Flame Stabilization in Gases. Trans. Am. Soc. Mech. Eng., vol. 4, 1948, pp. 307-316.

19. _____ . Stability and Structure of Burner Flames. Jour. Chem. Phys., vol. 11, 1943, pp. 75-97.

20. MANTON, J., VON ELBE, G., and LEWIS, B. Nonisotropic Propagation of Combustion Waves in Explosive Gas Mixtures and the Development of Cellular Flames. Jour. Chem. Phys., vol. 20, 1952, pp. 153-157.

21. NATIONAL BUREAU OF STANDARDS. Linear Pressure Drop Flowmeters for Oxygen Regulator Test Stands. Report 6.2/6211-2885, Sept. 25, 1947.

22. PRANDTL, L., and TIETZJENS, O. G. Applied Hydro and Aerodynamics. Vol. 2, McGraw-Hill Book Co., New York, N. Y., 1934, pp. 14-57.

23. SHNIDMAN, L. Gaseous Fuels. 2nd ed., Mack Printing Co., Easton, Md., 1954, p. 187.

24. _____ . Work cited in ref. 23, p. 200.

25. SMITH, R. W., JR., EDWARDS, H. E., and BRINKLEY, S. R., JR. Tables of Velocity of Steady Laminar Flow in Channels of Rectangular Cross Section. Bureau of Mines Rept. of Investigations 4885, 1952, pp. 1-41.

26. _____ . The Thermodynamics of Combustion Gases: Temperatures of Methane-Air and Propane-Air Flames at Atmospheric Pressure. Bureau of Mines Rept. of Investigations 4938, 1953, pp. 1-3.

27. STREET, J. C., and THOMAS, A. Carbon Formation in Pre-Mixed Flames. Fuel, vol. 34, 1955, pp. 4-36.

28. VON ELBE, G., and MENTSER, M. Further Studies on the Structure and Stability of Burner Flames. Jour. Chem. Phys., vol. 13, 1945, pp. 89-100.

29. WEBER, E. J. Study of Burner Flexibility on Base and Peak Load Gases. American Gas Association Research Rept. 1192, August 1952.

30. WILSON, C. W. Lifting and Blowoff of Flames from Short Cylindrical Burner Ports. Ind. Eng. Chem., vol. 44, 1952, pp. 2937-2942.

31. WOHL, K. Quenching, Flash-Back, Blow-Off - Theory and Experiment. Fourth Symposium (International) on Combustion, Williams & Wilkins Co., Baltimore, Md., 1953, pp. 68-89.

32. WOHL, K., KAPP, N. M., and GAZLEY, C. The Stability of Open Flames. Third Symposium on Combustion, Flame and Explosion Phenomena, Williams & Wilkins Co., Baltimore, Md., 1949, pp. 3-21.